THE UNIVERSITY *of* EDINBURGH

Murine gammaherpesvirus mediated splenic fibrosis

Shuo Li

PhD

University of Edinburgh

2012

Declaration

I declare that this thesis has been composed by myself and has not been submitted for any other degree. The work described herein is my own except where otherwise indicated and all other authors are duly acknowledged.

Shuo Li

September, 2012

The Roslin Institute and Royal (Dick) School of Veterinary Studies

University of Edinburgh

Easter Bush

EH25 9RG

Acknowledgements

I would like to thank my supervisors, Professor Tony Nash and Dr. Bernadette Dutia for their support and guidance throughout my study. Tony has inspired this project and supported me through my PhD. Bernadette has provided endless help and support in every aspects of my work, from experimental design to results analysing, even driving me home in midnight when I had to work late. Also I would like to thank Babunilayam Gangadharan, the former PhD student in the Nahs/Dutia lab, for my project is largely based on his previous work. Other member's from Nash/Dutia lab also offered great help, and I cannot finish this work without their help. Ian Bennet offered invaluable help and assistance in molecular experiments; Yvonne Ligertwood helped me with animal experiments and all lab matters; Gillian Campbell kindly provided qPCR reagents; Marlynne Quigg-Nicol and Keran Bryson kindly shared their lab experience and encouraged me to work hard; Xuan Wang helped with FACS and discussed the results with me (in my first language). All members from Nash/Dutia lab have helped me throughout my study with great patience and kindness and I have learnt so much from them. Also, I would like to thank Dr. Martin Waterfall and Bob Fleming offered great help in FACS and confocal microscopy.

I would not enjoy my time in Edinburgh so much without the support from my dearest friends. Shoko, Ayeshaa, Yoshi and Gigi, have provided an escape from lab work, by warm chat and endless laughter. Xiaolu and Mengmeng offered a warm home when I was down. Jun and Meng, helped me in every way. Finally, I would like to give the biggest thank you to the most important people to me in this world, my dearest Dad and Mom who supported me even I am thousands miles away.

Summary

Infection of IFNγ receptor knockout (IFNγ $R^{-/-}$) mice with murine gammaherpesvirus-68 (MHV-68) results in fibrosis in the lung, spleen, liver and lymph nodes. In the spleen, pathology involves an increase in the number of latently infected B cells that corresponds with a Th2 biased immune response, in which germinal centres become walled off and fibrosis dominates the splenic architecture. Remarkably, the spleen recovers from this pathology, and the starting point for this process is a loss of latently infected B cells. The aim of this project is to gain further understanding of the control of MHV-68 latent infection in the absence of IFNγ response. This project investigates: (1) the mechanisms that result in the loss of splenocytes, in particular the reduction of latently infected B cells; (2) the dynamics of macrophages in the induction, expression and recovery of fibrosis.

Several approaches were employed to examine the hypothesis that the massive cell loss in IFNγ$R^{-/-}$ spleen is caused by apoptosis. However, there was no evidence for excessive apoptosis throughout the development of fibrosis. Moreover, RT-PCR analysis showed that there was no significant increase in expression of viral genes associated with lytic infection. Hence it is unlikely that viral reactivation and subsequent lytic infection occurs. These data suggest apoptosis and viral reactivation are not the main mechanisms that cause splenic cell loss. Furthermore, B cell subpopulations and cells that express viral ORF73 in IFNγ$R^{-/-}$ mice were examined using a recombinant virus. The ORF73-expressing cells are mainly germinal centre B cells and memory B cells. These two subpopulations undergo a drastic decrease in numbers during fibrosis, whereas naïve B cells, which are less susceptible to infection, maintain a relatively stable population. Therefore, the significant reduction of latently infected B cells appears to be related to the removal of germinal center B cells and memory B cells.

Macrophages induced by Th2 cytokines are considered to be pro-fibrotic, and they are reported to have the potential to differentiate into myofibroblasts. In order to determine the role played by macrophages in MHV-68 induced fibrosis, transgenic mice with eGFP constitutively expressed in macrophages and dendritic cells were used. A different pattern of macrophage distribution in IFNγR-/- mice was observed compared to that in wild type mice. Moreover, the number of splenic macrophages changed dramatically in the spleen at different stages of fibrosis. The possibility that alternatively activated macrophages differentiate into myofibroblasts was investigated by co-staining with α-SMA antibody. However, no evidence was found that macrophages are one of the origins of myofibroblasts. This suggests macrophages may play other roles in regulating fibrosis rather than contributing directly to the formation of fibrosis.

Contents

List of figures

List of tables

Abbreviations

AIDS	Acquired immunodeficiency syndrome
AAMφ	Alternatively activated Macrophage
BCR	B cell receptor
BHK	Baby hamster kidney
BL	Burkitt's lymphoma
BMDC	Bone marrow derived cells
bp	Base pair
CD	Cluster of differentiation
cDNA	Complementary DNA
CPE	Cytopathic effect
CTL	Cytoroxic T lymphocytes
DAB	3,3- diaminobenzidine
DEPC	Diethyl pyrpcarbonate
DNA	Deoxyribonucleic acid
dNTP	Deoxynucleoside triphosphate
DNApol	DNA polymerase
ds DNA	Double stranded Deoxyribonucleic acid
EBNA	EBV nuclear associated antigen
EBV	Epstein-Barr virus
ECM	Extra cellular matrix
EDTA	Ethylene diamine tetra acetic acid
EGFP	Enhance green fluorescent protein
EMT	Epithelial mesenchymal transition
FCS	Foetal calf serum
FDC	Folliculate dendritic cells
FLICE	FADD-like interleukin-1β converting enzyme
FLIP	FLICE inhibitory enzyme
g/gp	Glycoprotein
GC	Germinal centre
GFP	Green fluorescent protein
GM-CSF	Granulocyte macrophage colony stimulating factor
GMEM	Glasgow modified eagle's medium
GPCR	G-protein coupled receptor
HBV	Hepatitis B virus
HCMV	Human cytomegalovirus
HCV	Hepatitis C virus

HD	Hodgkin's disease
HHV	Human herpesvirus
HIV	Human immunodeficiency virus
HLA	Human leukocyte antigen
HSC	Hepatic stellate cells
HSV	Herpes simplex virus
IE	Immediate-early
IF	Immuno-fluorescence
IFNγ	Gamma interferon
Ig	Immunoglobulin
IHC	Immunohistochemistry
IL	Interleukin
IM	Infectious mononucleosis
IP	IFNγ inducible protein
IPF	Interstitial pulmonary fibrosis
IR	Internal repeats
IRF	Interferon regulatory factor
JaK	Janus kinase
kbp	Kilo base pair
kDa	Kilo Dalton
KS	Kaposi's sarcoma
KSHV	Kaposi's sarcoma associated herpesvirus
LANA	Latency associated nuclear antigen
LCL	Lymphoblastoid cell lines
LMP	Latent membrane protein
LPS	Lipopolysaccharide
LTa	Lymphotoxin-alpha
MCD	Multicentric Castelman's disease
MCF	Malignant Catarrhal fever
MCMV	Murid Cytomegalovirus
MHC	Major histocompatibility complex
MHV-68	Murine gammaherpesvirus-68
MIP	Macrophage inflammatory protein
mM	Milli Molar
MMP	Matrix metalloproteinase
MOI	Multiplicity of infection
mRNA	Messenger RNA
MT	Masson's trichrome

MZ	Marginal zone
NBCS	New bone calf serum
NF-κB	Nuclear factor-κB
ORF	Open reading frame
p.i.	Post infection
PALS	Peri-arteriolar lymphoid sheath
PBS	Phosphate buffered saline
PCR	Polymerase chain reaction
PDGF	Platelet derived growth factor
PEC	Peritoneal elucidated cells
PFU	Plaque forming unit
RP	Red pulp
RNA	Ribo nucleic acid
Rta	Reactivation and transcriptional activator
SMA	Smooth muscle actin
ssDNA	Single-stranded DNA
TBM	Tingible body macrophages
TBS	Tris buffered saline
TCR	T cell receptor
TGF	Transforming growth factor
TNF	Tumour necrosis factor
TPB	Tryptose phosphate broth
TR	Terminal repeats
tRNA	Transfer RNA
TUNEL	Terminal deoxynucleotide transferase-mediated dUTP nick end labelling
µg	microgram
µl	microlitre
WP	While pulp
WT	Wild type

Chapter 1 Introduction

1.1 Herpesviruses

There are more than 130 herpesviruses which can infect a broad range of hosts, from human to animals. All herpesviruses share the abilities to (1) encode enzymes related to nucleic acid synthesis and metabolism such as viral DNA polymerase and protein processing proteins such as protein kinase; (2) synthesise viral DNA and assemble capsids in the nucleus of an infected cell; (3) conduct productive replication and produce infective progeny with host cell lysis; and (4) establish latent infection in natural hosts (Roizman and Pellett, 2001). The virus particles of all herpesviruses vary from 120 to 300 nm in diameter, and contain double-stranded, linear DNA genomes of which sizes range from about 120 to 250 kilo base pairs. The viral genome is packed within an icosahedral protein capsid, forming a core which is about 100 nm in diameter and consists of 162 capsomeres. Outside of the capsid lies the tegument, which is mainly a proteinaceous matrix, and then the virion is wrapped by a lipid bilayer envelope. The envelope is initially formed while the virion particle is budding from the host membrane, and contains glycoproteins whose functions include mediating attachment to the host cell and viral entry (Roizman and Pellett, 2001; Ackermann, 2004).

1.1.1 Classification

Based on the virion morphology and biological characteristics such as cell tropism, *Herpesviridae* was classified into 3 subfamilies: the *Alphaherpesvirinae*, the *Betaherpesvirinae* and the *Gammaherpesvirinae*. The development of modern sequencing technology refined the classification of subfamilies and has now becomes the main approach for viral genetic studies. Therefore recently, herpesviridae has been re-named as new order *Herpesvirales,* which is divided into 3 families: *Herpesviridae, Alloherpesviridae*, and *Malacoherpesviridae*. The new family *Alloherpesviridae* includes which viruses that infect fish and frogs, while the only invertebrate herpesvirus is assigned to family *Malacoherpesviridae*. Most members of the family of *Herpesviridae* remain unchanged,

incorporating viruses which infect mammals, birds and reptiles. Within *Herpesviridae*, 3 new genera have been created. *Proboscivirus* was added in the *Betaherpseviridae* subfamily, while *Macavirus* and *Percavirus* were created within *Gammaherpesviridae* (Davison et al., 2009). Despite the newly updated taxonomy of herpesviruses, the classification of the most important herpesviruses has not been changed. Therefore this introduction follows the traditional classification.

Alphaherpesviruses have a relatively wide range of hosts, and are characterised by a rapid, lytic proliferative infection. Members of this subfamily include herpes simplex virus 1 and 2 (HSV-1 and HSV-2), which have the ability of establishing latency in neurons, such as sensory ganglion (Whitley and Roizman, 2001). While a chicken alphaherpesvirus, Marek's disease virus (MDV), establishes latency in CD4+ T cells (Osterrieder et al., 2006).

Betaherpesviruses have a narrower range of hosts. This subfamily has the lowest reproductive rate among the three, and mainly establishes latency in leukocytes. This subfamily includes Human cytomegalovirus (CMV), Human herpesvirus-6 and 7 (HHV-6 and -7), and Murine cytomegalovirus (MCMV) (Griffiths et al., 2000).

Gammaherpesviruses undergo productive infection in lymphoid cells, as well as fibroblastic cell lines and epithelial cell lines *in vitro*. Compared with the other two subfamilies, the gammaherpesviruses have the strictest host specificity, in which infection is often limited to the family or order of the natural host. Generally, latency is established in lymphoid cells and macrophages within lymphoid tissue. Traditionally the subfamily is divided into two main genera: *Lymphocryptovirus* (e.g., EBV) and *Rhadinovirus* (e.g., KSHV and MHV-68) (Ackermann, 2006). A detailed introduction of gammaherpesviruses occurs in section 1.2. A selection of important members from the herpesvirus family and the diseases in which they involved are listed in Table 1.1.

Table 1.1 Classification of Herpesviruses and related diseases

Subfamily and genus		Name	Host	Related diseases
Alpha	Simplex	Herpes Simplex virus-1 (HHV-1/HSV1) and Herpes Simplex virus-2 (HHV-1/HSV2)	Human	Cold sores, keratitis,
	Varicellovirus	Varicella-zoster virus (HHV-3/VZV)	Human	Chicken pox in children and shingles in adults
	Mardivirus	Gallid Herpesvirus-2 (Marek's disease, herpesvirus-1/GsHV-2)	Chicken	Marek's disease (T cell lymphoma)
	Iltovirus	Gallid Herpesvirus-1	Chicken	Infectious Laryngotracheitis (ILT)
Beta	Cytomegalovirus	Human cytomegalovirus (HCMV/HHV-5)	Human	Mononuclesis, multi-system disease in immunocompromised patients
	Muromegalovirus	Murid cytomegalovirus-1 (MCMV-1)	Mouse	Cyto-megalic inclusion disease
	Resolarvirus	Human herpes virus-6 (HHV-6)	Human	Fever and rash in children, mononucleosis in adults
Gamma	Lymphocryptovirus	Epstein-Barr virus (EBV/HHV-4)	Human	Infectious monoculeosis, Burkitt's lymphoma, post-transplantation lymphproliferative disorder, Hodgkin's lymphoma
	Rhadinovirus	Kaposi's sarcoma-associated herpesvirus (KSHV/HHV-8)	Human	Kaposi's sarcoma in AIDS patients

1.1.2 Herpesvirus life cycle—Productive infection

The studies of productive infection of herpesviruses mainly focused on herpes simplex virus by describing lytic gene functions. This is because HSV lytic infection can be maintained in tissue culture system which allows gene function studies. On the other hand, it is very difficult to study lytic infection of EBV and KSHV, for they are mostly latent in tissue culture. Considering the virus genes which are involved in viral replication are highly conservative, it is very likely that herpesviruses share similar mechanisms of productive infection. Moreover, our work is mainly concentrated on latent infection. Therefore, despite the fact that every member of the herpesvirus family has its own cell tropism during productive infection, we discuss HSV productive infection within a single cell as a representative of all herpesviruses as below. The unique mechanisms utilised by important gammaherpesviruses are discussed later on.

1.1.2.1 Attachment and entry

Glycoproteins (gB, gC, gD, gH and gL) on the envelope layer of the virion facilitate the primary attachment of the virus to the cell. In the case of HSV, the initial attachment (Figure 1.1 (1)) is mediated by gB and gC binding to cell heparan sulphate proteoglycans (Laquerre et al., 1998; Shukla and Spear, 2001). Following first binding, the virus penetrates into host cells which involve gB, gD, gH, and gL. Among the four, gD and gH are essential fusion proteins (Campadelli-Fiume et al., 2007; Heldwein et al., 2006). gD can bind to a number of cellular receptors, including nectin-1 and -2 (members of the immunoglobulin superfamily), herpesvirus entry mediator (HVEM, a member of TNF receptor family) and 3-O sulphated heparin sulphate (3-O-S HS) (Shukla et al., 1999; Spear, 2004). Binding of gD with cellular receptor facilitates and activates the glycoprotein complex of gB, gD, gH, and gL, which mediates the virion envelope fusion with cell membrane and nucleocapsid and tegument proteins are released into the cytoplasm (Atanasiu et al., 2007).

1.1.2.2 Transportation of viral DNA to cell nucleus and viral gene expression

The viral DNA is transported into the nucleus through capsid proteins binding to microtubules through the nuclear pore, where it undergoes circularisation. Meanwhile, tegument proteins play important roles in shutting off host gene expression by RNA degradation (Vhs) (Elgadi et al., 1999) (Figure 1.1 (5c)), or by interacting with host transcription pathways to initiate the expression of viral immediate-early genes utilising host machinery (VP16) (Campbell and Preston, 1987; Goding and O'Hare, 1989) (Figure 1.1 (5b)) . Immediate-early proteins are mainly transcription factors, which are necessary for the transcription of the second cascade of viral genes expression. The early genes contain those required for viral nucleic acid metabolism (e.g., TK gene) and DNA replication (e.g., viral DNA polymerase). The late genes can be divided into two groups according to their different roles in viral replication, as well as the order of their expression: the early-late genes are expressed while viral DNA replication occurs, and their replication is enhanced by viral DNA replication. The true late genes are mainly viral structural proteins and their expression depends strictly on the on-going viral DNA replication (Figure 1.1 (14) to (18)) (reviewed in Taylor et al., 2002).

1.1.2.3 Viral DNA replication, assembly, and wrapping with envelope

Herpesvirus DNA replication begins when early genes are expressed. At least 7 gene products are necessary for replication, including DNA polymerase, single stranded DNA binding protein, origin binding protein, and proteins which form a helicase-primase complex. Viral DNA replication is carried out by a rolling circle mechanism. As a result, a concatemer which contains several copies of whole viral DNA sequences linked in series is produced and later on cleaved into single genomes. The viral genome is then packed into capsid the components of which are translated from a subset of late genes (Figure 1.1 (18)). Newly formed nucleocapsid, along with some tegument proteins, then bud from the nuclear

membrane from inside into the perinuclear lumen, releasing the nucleocapsid into cytoplasm, while the virus leaves this initial envelop in the perinuclear lumen (Figure 1.1 (20 a-c)). The nucleocapsid with tegument proteins then are transported into a Golgi compartment (Figure 1.1 (21)), in which the viral tegument and mature envelope is acquired (Figure 1.1 (22)), and the virion is completed for release by exocytosis (Figure 1.1 (23)). Although it is possible to interrupt productive infection by raising the temperature or applying chemicals which target certain key proteins in viral replication, it is generally believed that the lytic replication of most herpesviruses causes cell death (Reviewed by Longnecker and Neipel, 2007).

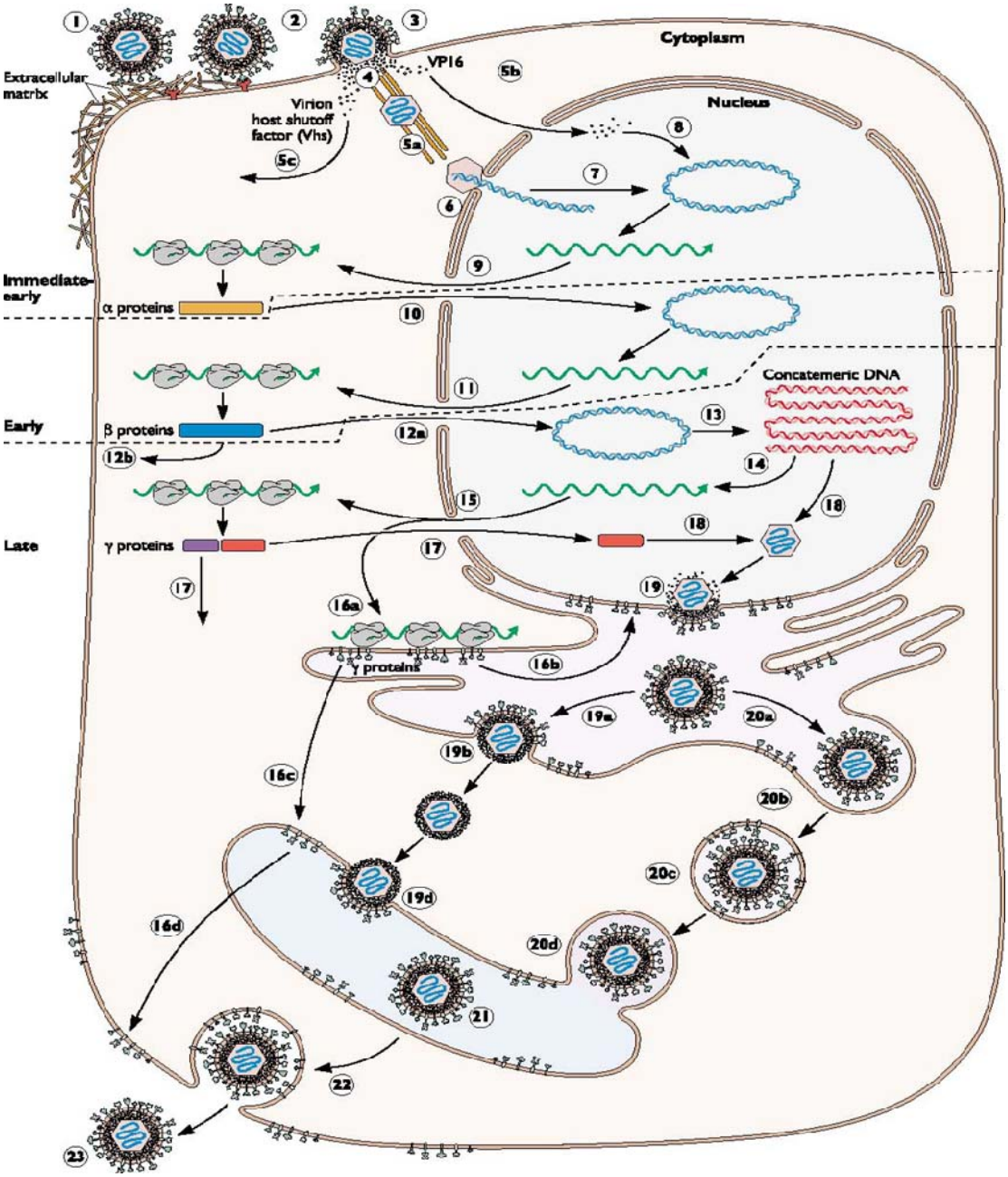

Figure 1.1 Herpes simplex virus type 1 productive infection on a single –cell.

(Figure resource: Flint et al., *Principles of virology*, 3rd ed., vol. 1)

1.1.3 Latent infection

Establishment of latent infection is a key feature of herpesviruses which allows the virus to evade the host immune system to achieve long-term latency. Latent infection of herpesviruses usually has strict specificity on cell type (e.g., HSV establish latency in neurons, while gamma herpesviruses preferentially establish latency in lymphocytes), and is characterised by the shutting off of most of the viral genes expression which are important in lytic infection and activation of latent transcripts. During latent infection, the viral genome forms a circular episome and is maintained in the nucleus. Under certain circumstances, the latent virus undergoes a productive cycle and the infection becomes lytic, which is called reactivation. In the case of HSV, cell stress, tissue damage, and immunosuppression are factors which may trigger reactivation from latent infection. HSV only produces latent associated transcripts (LATs), which are about 1.5 to 2 kb and located in the repeats flanking the U_L region of the genome. LATs play important roles in both establishing and maintaining latency. The function of these viral-encoded RNAs include down-regulating productive-cycle genes expression (Garber et al., 1997) and inhibiting host cell apoptosis (Perng et al., 2000). The mechanisms of the switch between lytic and latent transcriptional programs are poorly understood. The research on EBV, KSHV, and MHV-68 latency is discussed in further detail in sections 1.2 and 1.3 respectively.

1.2 Important human and veterinary gammaherpesviruses

The gammaherpesvirus subfamily was first distinguished by cellular tropism for lymphocytes. Later, molecular phylogenetic analysis confirmed the close relationship among these viruses which is distinct from alpha- and beta-herpesviruses. There are now 4 genera within this family: Lymphocryptovirus, Rhadinovirus, and the newly created genera Macavirus (e.g., Bovine herpesvirus 6 (BoHV6) and Ovine herpesvirus 2 (OvHV2)) and Percavirus (e.g., Equine herpesvirus 2 and 5 (EHV2 and EHV5)). Lymphocryptoviruses are represented by the famous Epstein-Barr virus (EBV), which leads to lymphoproliferative disorders in immune compromised patients. Rhadinoviruses are represented by Kaposi's sarcoma-associated herpesvirus (KSHV), which causes Kaposi's sarcoma, primary effusion lymphoma, and multicentric Castleman's disease in immunosuppressed hosts. Although EBV and KSHV are the most intensively -studied within the subfamily, as they infect humans, there are gammaherpesvirus members which infect cows (e.g., Bovine herpesvirus 4 (BoHV-4)), horses (e.g., Equid herpesvirus 2 (EHV-2)), and mice (Murid herpesvirus 4 (MHV-68)). Also, Alcelaphine herpesvirus 1 (AIHV-1) and Ovine herpesvirus-2(OvHV-2), which cause no syndromes in their natural hosts, lead to malignant catarrhal fever when they infect cattle (Ensser et al., 1997).

1.2.1 Epstein-Barr virus (EBV)

As the first virus discovered related to tumourigenesis, EBV was found to be the aetiological agent of Burkitt's lymphoma (Epstein et al., 1964). By analysing antibodies in the peripheral blood, it was found that EBV was widespread in the human population. The antibody against EBV was found not only in patients with Burkitt's lymphoma but also in healthy children from all over the world (Henle et al., 1969). Furthermore, serological investigations showed that more than 90% of adults in the world were seropositive for EBV (Rickinson, 2002). These results suggest the infection of EBV is common in the world. Although EBV can

infect several cell types, such as T cells and NK cells, B cells and epithelial cells are the major infection sites. *In vitro*, EBV has the ability to immortalise primary B cells in cell culture (Henle et al., 1967), and the cell lines carrying the viral genome are lymphoblastoid cell lines (LCLs). These cells express limited viral genes and offer an important tool for studying EBV latent infection.

1.2.1.1 EBV genome

The EBV strain B95-8 genome was the first herpesvirus genome sequenced (Baer et al., 1984) and this sequence was later completed by adding the 11kb sequence provided by the strain Raji (Parker et al., 1990). The size of the EBV genome is about 172 kb and contains at least 86 ORFs. A long unique region is separated by 4 major internal repeats (IR1 to IR4) and flanked by terminal repeats (TR) at both sides.

1.2.1.2 Lytic infection of EBV

Treatment with phorbol ester can induce viral reactivation from latently infected B cell lines, which is the common approach to study lytic infection of EBV. EBV gp350/220 is a homologue of gC in HSV, which has a similar function in facilitating first attachment. It binds to complement receptor 2 (CR2) on the B cell surface (Prota et al., 2002). Glycoproteins gB, gH, gL, and gp42 are required for viral fusion (Molesworth et al., 2000). Gp42 can bind HLA class II efficiently (Spriggs et al., 1996) and it is also associated with gHgL, forming a three-part complex, which is considered to initiate the B cell fusion (Hutt-Fletcher, 2007).

1.2.1.3 Latent infection of EBV

During EBV latency the viral gene expression is highly restricted, and there are different patterns of EBV latent gene expression in different states of B cells (e.g., proliferating and non-proliferating, healthy or malignant B cells). There are now mainly 4 types of latency which have been defined in lymphomas and LCLs: Latency I, II, III, and 0, based on the

expression of EBNAs and LMPs. These are also called latency programmes, respectively: 'EBNA 1-only', default programme, growth program, and latency program.

The demonstration that EBV transformed B cells into LCLs is crucial not only because it directly links EBV infection to Burkitt's lymphoma, but also because it provides a tool to study viral gene expression, especially the essential genes required in immortalised B cells. The viral proteins expressed in LCLs include 6 Epstein-Barr nuclear antigens (EBNA1, EBNA2, EBNA3A, EBNA3B, EBNA3C, EBNA-LP) and 3 membrane proteins, latency-associated membrane proteins 1, 2A, 2B (LMP1, -2A, -2B) (Rowe et al., 1992). This pattern is termed type III. By expressing these products, the virus can drive resting B cells which appear to be 'activated' and undergo proliferation and differentiation. It is most likely a virus strategy which exploits host B cell germinal centre proliferation in order to enlarge the pool of latent infected cells (Reviewed in Barton et al., 2011). It was surprising when EBV gene expression was found to be very much different in B cells from most of the cases of Burkitt's lymphoma: only EBNA1 is expressed in Burkitt's lymphoma cells, while other genes are perfectly silenced. It was called latency I since only EBNA1 is expressed (Rowe et al., 1986; Masucci et al., 1987). Latency II was found first in undifferentiated nasopharyngeal carcinoma (NPC) (Young et al., 1988; Fahraeus et al., 1988), and later in Hodgkin's lymphoma (Niedobitek et al., 1991; Pallesen et al., 1991) and NK/T cell lymphomas (Chiang et al., 1996). This type of latency is like an intermediate state between latency III and latency I: along with EBNA1, transcripts of LMPs are expressed, while other EBNAs are not expressed. However, the level of each gene expression differs among B cells from different origins. The role of EBNA1 is to maintain and help replication of the latent viral episome during cell replication. Therefore, it is essential for the survival of the latent virus. However, in B cells which are not dividing (memory B cells in periphery circulation), EBNA1 is not required, as there is no viral antigen expressed (latency 0). This state of latency may refer to long-term latency in immune competent hosts (Rowe et al., 2009).

Different transcriptional programs are the basis of latency states, and accumulating evidence suggests that the 'switch' among latency types is programmed and coordinates with host B cell proliferation and differentiation. EBNAs' expression in Latency I is driven by promoter Qp (Schaefer et al., 1995), while latency III is driven by promoter Wp/Cp (Woisetschlaeger et al., 1990). Studies of the viral transcripts in a subset of Burkitt's lymphoma cells infected with EBV that lacking EBNA2 suggest that the expression of EBNA2 is essential for the expression of LMPs in latency III (Wang et al., 1990). However, only EBNA1 and LMPs are expressed in Latency II, which means the expression of LMPs is independent of EBNA2 in this type of latency (Johannsen et al., 1995). EBNA2 is the transcription activator which activates promoters Wp and Cp (promoter next to Wp) and it controls expression of Latency III transcripts (Tempera and Lieberman, 2010). It has also been shown to interact with cellular factors so that it can regulate the Notch pathway. However, the role of this regulation in the latent infection is not yet clear (Reviewed in Barton et al., 2011). Among LMPs, LMP1 is able to transform mouse fibroblast on its own, while it can only transform human B cells with the help of EBNAs. LMP1 belongs to TNF receptor superfamily and may possibly mimic the reactivated state of the CD40 receptor which is expressed on B cells facilitating the interaction with T cells during B cell differentiation from germinal centre B cells to either memory B cells or plasma cells (Reviewed in Barton et al., 2011). The control of latent types' transcription, especially the mechanisms of how EBV switches between Qp and Cp, is under intensive investigation and still not clear.

As discussed above, EBNA1 is the only viral protein expressed during latency I, which suggests it is the only viral protein required for viral episome replication in dividing memory B cells. Moreover, it is the EBV homologue of MHV-68 ORF73 (mLANA), so here we pay special attention to the introduction of EBNA1 in latent infection. EBNA is expressed in all latency types but latency type 0. EBNA1 binds to *OriP* at both functional elements FR and DS of the plasmid-like viral latent genome. The binding with dyad symmetry (DS) is

important for viral DNA replication in a way similar to SV40 DNA replication using the host cell machinery (Gahn and Schildkraut, 1989; Yates et al., 1984). On the other hand, binding with family of repeats (FR) is important in mitotic segregation of EBV epitome during host cell division. There is evidence showing that EBNA1 tethers the EBV episome with chromosomes in mitosis, in which the interaction between EBNA1 and human cellular protein EBP2 maintains the attachment of EBNA1 with chromosomes in the mid and late stage of mitosis (Kapoor and Frappier, 2003, 2005; Nayyar et al., 2009; Shire et al., 1999; Wu et al., 2000). This mechanism is so sophisticated that the replication happens only once every cell cycle, and eventually the viral genomes are segregated evenly; therefore there is no net increase in either of the daughter cells after mitosis. Also, EBNA1 can enhance Cp transcription in type III latency by up-regulating EBNA2 expression, so that it controls the initiation of the Cp transcription and LMPs expression in latency III (Altmann et al., 2006; Gahn and Sugden, 1995), EBNA1 can also self-limit its expression in order to evade from host immune recognition (Yin et al., 2003).

1.2.1.4 EBV associated diseases

In the majority of cases, the first exposure to EBV occurs in childhood and is followed by a symptom-free viral latency throughout the whole lifetime. The spread of EBV might be through saliva. If the first exposure occurs in adulthood, the infection lead to a syndrome termed infectious mononucleosis (IM). IM was first reported in a scientist who was studying EBV. The clinical signs of IM, such as fever and sore throat, can last for weeks (Henle et al., 1968). The infection induces B cells to undergo proliferation, which consequently activates the CD8 T cells. These cytotoxic CD8 T cells which specifically target infected B cells, undergo significant proliferation. Therefore, the lymph cell proliferation in lymph organs which is induced by EBV infection causes swelling of glands, splenomegaly, and tonsillitis, and mononucleosis in peripheral blood.

EBV is famous for its association with many tumourigeneic diseases, such as Burkitt's lymphoma in African children, Hodgkin's lymphoma, nasopharyngeal carcinoma, and post-transplantation lympho-proliferative disorder (Tanner and Alfieri, 2001). Burkitt's lymphoma (BL) is endemic in equatorial Africa, and may develop in the jaw, ovary, mammary gland, liver, intestine, and kidney. BL is either composed of rapidly proliferating small B cells or germinal centre B cells. In other areas, BL occurrence is less related with EBV; for example, EBV is only present in 20% of BL patients in Europe and North America.

1.2.2 Kaposi's sarcoma-associated herpes virus

Kaposi's sarcoma (KS) was first described by Miriz Kaposi in 1872 and was not noticed until the 1980s, when a dramatic increase of KS in AIDS patients was observed following the outbreak of HIV infection. As a pathogen of KS, KSHV was first identified by Chang in 1994 (Chang et al., 1994). Despite the fact that KSHV was discovered 30 years later than EBV, the discovery and association with human diseases for both of them is very similar. Like EBV, transmission of KSHV requires intimate contact, through saliva, for example (Martro et al., 2004). Also, infection with KSHV in immune competent individuals shows no symptoms, while primary infection with KSHV in children can cause a skin rash. However, in contrast to the wide prevalence of EBV, serological studies show that the percentage of KSHV positive persons in the human population is highly variable. For example, in 1996, the infection rate was over 50% in Africa, whereas it was 1 to 6% in northern Europe and the USA (Gao et al., 1996; Kedes et al., 1996; Simpson et al., 1996). Due to the difficulties in detecting viral DNA in KSHV carriers, who show no symptoms, the site of KSHV latency in healthy humans is poorly understood at this time.

1.2.2.1 KSHV genome

The size of the KSHV genome varies from 165 to 170Kbp depending on the strains (Neipel et al., 1998; Renne et al., 1996b), and it shares a common structure with other

Rhadinoviruses in that the linear double stranded DNA has a long unique region of low GC DNA flanked by multi-repetitive high GC terminal repeats (Bornkamm et al., 1976; Russo et al., 1996). This feature leads to the tendency of the viral genome to break apart when it is isolated by density centrifugation (Roizman et al., 1981). Referring to this feature of the genome, the genera's name comes from the Greek word 'rhadino', which means fragile. For different strains, the number of terminal repeats varies but their function remains. The long unique region of the KSHV genome contains at least 89 ORFs, of which 62 have homologues or encode proteins which have similar functions in other herpesviruses. These homologue genes are primarily limited to genes required for cleavage and packaging of the viral DNA and infection of susceptible host cells, for example, those which encode enzymes involved in DNA replication, regular gene expression, and glycoproteins (Longnecker and Neipel, 2007). Apart from the conserved genes, ORFs which are unique to KSHV are named from K1 to K15.

1.2.2.2 Lytic infection of KSHV

In vitro, the lytic cycle can be induced using chemical treatment such as TPA on latently infected cells. Strictly speaking, it is a model of lytic replication following reactivation. The key feature of the lytic lifecycle is the production of linearised viral DNA. As found in lytic infection of other herpesviruses, three classes of viral genes (immediate-early, early, and late) are expressed in strict order. In KSHV, the master controller for initiating lytic replication is Rta, which is encoded by ORF50. Rta activates viral promoters for lytic gene expression by direct binding or interaction with cellular gene RBPJk. The mechanism of productive infection of KSHV is very similar to other herpes family members.

1.2.2.3 Latent infection of KSHV

Using B cell lines derived from primary effusion lymphoma (PEL) and epithelial cells, the latent gene expression of KSHV has been intensively studied, as has the role of latency-associated KSHV antigens and non-coding RNAs (Wen and Damania, 2010). Latent-

associated genes are mainly located in the same region, such as latent-associated nuclear antigen (LANA), cyclin D homolog (v-cyclin), and FLICE inhibitory protein homologue (v-FLIP). Here we mainly introduce LANA, which is the homologue of the viral protein encoded by MHV-68 ORF73 (mLANA) and has a function very similar to that of EBNA1 of EBV, followed by a short introduction of other important viral genes.

The function of LANA in maintaining the latent genome is similar to EBNA1; it tethers the episome onto the host chromosome while the host cell undergoes mitosis. It binds the TR region of the KSHV genome with its C terminus while binding host nucleosomes with its N terminus (Schwam et al., 2000). Moreover, LANA is essential in latent viral genome replication like EBNA1 in EBV latency. Besides, LANA also has multiple functions in regulating both viral activity and host cell status. Apart from maintaining the viral genome during mitosis, LANA is a main controller of the viral life cycle by inhibiting Rta function. It inhibits Rta expression both by direct binding to the Rta protein and by down-regulating the activity of the Rta promoter, therefore inhibiting reactivation so that the latency can be maintained (Lan et al., 2004). Overexpression of Rta leads to a significant up-regulation of the mRNA transcripts of LANA, which suggest LANA expression may change as a response to viral reactivation (Nakamura et al., 2003). Transient transfection experiments show that Rta elevates LANA expression by interacting with the LANA promoter (Lan et al., 2005). Therefore, LANA, along with Rta, may act as a switch between the two important viral lifestyles: latency and productive infection (Verma et al., 2007). Similar mechanisms were also found in HVS (Schafer et al., 2003) and MHV-68 (Hair et al., 2007). Moreover, LANA regulates many cellular factors and pathways whose functions involve the cell cycle, namely proliferation (e.g., inhibits functions of p53, GSK-3β, and β-catenin) and differentiation (e.g. induces expression of Id proteins), host immunity (e.g., binds to IFN-induced protein MNDA), tumour suppression, and apoptosis (Verma et al., 2007). Cellular protein p53 functions as a tumour suppressor by suppressing cell proliferation and initiating apoptosis

(Levine, 1997). LANA has been shown to interact with p53 and inhibit its functions, as well as to down-regulate the level of p53 expression (Friborg et al., 1999). Later studies suggest a repressive function of LANA on p53 which promotes the stability of the host chromosome and facilitates the formation of KSHV-associated tumours (Si and Robertson, 2006).

Besides LANA, important viral genes encoded by KSHV also include v-FLIP, an anti-apoptotic protein which inhibits Fas-mediated apoptosis. LANA2, also known as v-IRF3, is a member of the interferon regulatory factor family which modulates host immunity. In addition, this part of the KSHV genome also encodes 12 pre-micro RNAs and subsequently generates 18 miRNAs. Moreover, at the left end of the genome, a membrane protein K1 is encoded, which is a constitutively signalling B cell receptor and may shares as similar function with LMP2a of EBV. Ten of 12 miRNAs are located in the non-coding region between K12 and K13 ORFs, and the other 2 are located within ORF K12 (Cai et al., 2005; Pearce et al., 2005; Pfeffer et al., 2005; Samols et al., 2005). All of the KSHV miRNAs are expressed during latency (Cai and Cullen, 2006; Murphy et al., 2008; Pearce et al., 2005; Samols et al., 2007) and a subset of them are expressed in lytic cycle as well (Wen and Damania, 2010).

1.2.2.4 KSHV associated diseases

Kaposi's sarcoma is a highly vascular tumour, which is characterised by spindle shaped, poorly differentiated but rapidly proliferating cells with endothelial lymphatic origin (Wang et al., 2004; Beckstead et al., 1985; Dupin et al., 1999). Histologically, KS also shows extravasation of red blood cells, along with inflammatory infiltration and neo-angiogenesis (Gessain and Duprez, 2005). KSHV was found in more than 95% of KS lesions. Clinically, there are 4 types of KS: classic KS, African endemic KS, epidemic (AIDS-associated) KS, and post-transplant KS. The classic Kaposi's sarcoma predominantly occurs in elderly male patients who are HIV-negative in Mediterranean countries. It is characterised by multiple reddish-brown patches on the lower extremities. Cases of endemic KS are mostly found in

HIV-negative patients in Africa, and show different clinical signs to classic KS: they can either present as a benign nodular cutaneous disease in young individuals, or as a fatal aggressive localised cutaneous disease affecting connective tissue and bone. In addition, there are other clinical types of African endemic KS, as mucocutaneous and visceral disease in adults, or lymphadenopathic disease in children. In AIDS patients, KS arises more quickly and presents as multifocal and symmetrical. Although advanced therapies have been developed and the mortality and incidence of AIDS-associated KS has significantly dropped (Eltom et al., 2002; Tam et al., 2002), KS remains the most common tumour associated with HIV- infection (Casper and Wald, 2007). In immune suppressed cases such as patients who have had organ transplantation, the infection may trigger bone marrow failure, splenomegaly, and fever (Luppi et al., 2002). Moreover, KSHV may be transmitted during organ transplantation from the donor, which causes KS to break out in the organ recipient (Barozzi et al., 2003; Marcelin et al., 2004).

KSHV also causes other types of tumour: primary effusion lymphoma (PEL) and multicentric Castleman's disease (MCD). PEL was initially called body cavity based lymphoma (BCBL) and was first reported by Chang and Moore as a rare B cell lymphoma in AIDS patients (Cesarman et al., 1995b). PEL is different from KS in many different ways. The cell origin of PEL is clonally expanding malignant B cells and the tumours are usually effusive and occur in body cavities. However, PEL is also reported to present as a solid mass in lymph nodes (Arvanitakis et al., 1996). Cells in PEL are mainly red blood cells and tumour cells which are morphologically larger than normal lymphocytes, and they express CD45, activation-associated antigens, clonal immunoglobulin rearrangements, but not B cell associated antigens (Nador et al., 1996). The progression of PEL is quicker and more aggressive than KS, and most patients die within 6 months. PELs can be KSHV positive only, or positive for both KSHV and HIV, in which the KSHV viral genome copy number

can be 50 to 150 copies per cell (Renne et al., 1996a; Cesarman et al., 1995a; Staudt et al., 2004).

Multicentric Castleman's disease (MCD) is a lympho-proliferative disorder symptoms of which include lymphadenopathy, fever, and infiltration in the spleen (Castleman et al., 1956). However there is another type of MCD, the hyaline variant, which is not associated with KSHV. MCD is more a rare polyclonal lympho-proliferative disease rather than a cancer (Dupin et al., 2000). Histological study shows there are germinal centre reactions and vascular endothelial proliferation within the lymph node where MCD occurs. A key factor in triggering this disorder is thought to be KSHV encoded v-IL-6 and inflammation. (Soulier et al., 1995).

1.2.3 Gammaherpesviruses of veterinary importance

Apart from EBV and KSHV which infect humans, there are important gamma-herpesviruses infecting animals, especially livestock. In this section we introduce gammaherpesviruses of veterinary importance.

1.2.3.1 Alcelaphine herpesvirus 1 (AlHV-1) and Ovine herpesvirus-2(OvHV-2)

Malignant catarrhal fever (MCF) mainly occurs in cattle, deer, other ruminants, and occasionally pigs. It is a fatal disease which is caused by either Alcelaphine herpesvirus 1 (AIHV-1) or Ovine herpesvirus-2 (OvHV-2). However, some cases of animals with mild symptoms and chronic infection are reported. Although there have been reports of outbreaks in a large population of animals within a herd, this disease is generally sporadic. The clinical signs include fluctuating fever, nasal discharge, corneal ulceration, and lymphadenopathy. MCF is characterised by enlarged lymph organs, infiltration of $CD8^+$ T cells in multiple organs, and vasculitis. These pathological changes occur with or without detection of viral replication (Coulter et al., 2001). Small animal models for studying AIHV-1 and OvHV-2 infection have been reported. Since lab mice are not infected by neither of the viruses,

experimental infection has been established in hamsters (both), rats (AIHV-1), guinea pigs (AIHV-1), and rabbits (OvHV-2) (Buxton et al., 1988; Jacoby et al., 1988a; Jacoby et al., 1988b). Although causing the same disease, the two viruses show different features in cell culture: OvHV-2 mainly establishes latent infection in bovine T cell lines, while AIHV-1 can grow in tissue culture (Rosbottom, 2003)

1.2.3.2 Equid herpesvirus 2(EHV-2)

Equid herpesvirus 2 (EHV-2) and Equid herpesvirus 5 (EHV-5) were originally classified as betaherpesviruses; however, they were later re-classified as gammaherpesviruses based on results of sequencing analysis (Telford et al., 1995). Epidemiological study shows that EHV-2 infection is ubiquitous. A study in horses in Sweden shows 56 to 68% of the horse population tested positive, whereas 71% of horses tested in England were infected. The infection sites include respiratory mucosa, conjunctiva, and WBC of normal horses of all ages. It is believed to be associated with immunosuppression diseases; however, the pathogenesis and clinical significance is obscure.

1.2.3.3 Bovine herpesvirus 4 (BoHV-4)

BoHV-4 infection is wide-spread. The virus can be isolated both from cattle with clinical diseases as well as healthy cattle. Potential clinical diseases associated with BoHV-4 include respiratory and ocular disease, abortion, metritis, pneumonia, diarrhea, and mammary pustular dermatitis. *In vitro*, BoHV-4 is capable of infecting many cell lines such as B cells, T cells, macrophages, endothelial cells and mammary gland cells (Ackermann, 2006).

1.2.4 Animal model for gammaherpesvirus infection

It is very difficult to study the nature of viral pathogenesis especially primary productive infection due to lack of subjects as the primary infection with both EBV and KSHV is asymptomatic. Moreover, an *in vivo* system which would allow clinical trials for potential therapies and vaccinations is also required. Therefore, for decades there have been attempts

to establish suitable animal models for viral infection. In the case of EBV, the first idea was to infect primates. EBV was able to establish B cell proliferative disorder in New World primates, cotton-top tamarins, and this animal model supported studies on lymphoproliferative disorder and potential vaccines (Epstein et al., 1985). However, so many symptoms developed in cotton-top tamarins which were obviously different from those in humans that this model cannot reflect the lytic infection of EBV. The common marmoset inoculated with EBV shows an IM-like syndrome (Wedderburn et al., 1984), but shows no signs of B cell proliferative disorder (Emini et al., 1986). Moreover, the expression of EBNA1 in the common marmoset is shown to be aborted in late time points (Farrell et al., 1997). Therefore this animal model is not successful either. On the other hand, inoculation shows that EBV fails to infect Old World primates (Moghaddam et al., 1998; Wang et al., 2001).

In the case of KSHV, several rhadinoviruses which are closely related to KSHV have been found in primates. Therefore the infection of these viruses in primates became potential animal models. For example, herpesvirus saimiri (HVS) isolated from the squirrel monkey (Saimiri sciureus) is asymptomatic when infecting natural hosts, while it causes T cell lymphoma in New World primates. HVS was made popular as a model for gammaherpesviruses oncogenesis, for it consistently produces T lymphoma and is easy to grow *in vitro*. Homologues of KSHV and EBV have been found in HVS, which is involved in transforming and proliferating tumour cells, as well as viral latency (Damania, 2004).

Although several animal models have been established in primates, small animal models such as rodents are increasingly used because of the privileges they offer: relatively low cost, easy to generate transgenic strains, and easy to keep. Murine models were established for both EBV and KSHV infection, not in normal mice, but in immune deficient mice. EBV-positive B cell lymophoproliferative disease was developed in severe combined immunodeficiency (SCID) mice injected with peripheral blood mononuclear cells (PBMC)

from EBV positive humans (Johannessen and Crawford, 1999). In the case of KSHV, following implantation of infected human tissue, primary lytic infection and latency in B cells were established in SCID mice (Dittmer et al., 1999). However, It seems none of the murine models inoculated using human tissue or cells is good enough to reflect the pathogenesis of gammaherpesvirus and viral/host interaction. Instead of inoculating mice with EBV or KSHV infected human tissue, murine viruses are also used to develop a mouse model for gammaherpesvirus infection. MHV-68 (murine gammaherpesvirus-68, murid herpesvirus 4) infection of laboratory mice has provided a widely used small animal model for gammaherpesvirus pathogeneses and host immune response. In the next sections we introduce this virus in detail and review the knowledge gained from this valuable small animal model.

1.3 Murine gammaherpesvirus-68 (MHV-68)

Murine gammaherpesvirus 68 (MHV-68) was initially isolated from the bank vole in 1980 (Blaskovic et al., 1980). Genetically, MHV-68 is relatively close to KSHV and EBV (Nash et al., 2001; Virgin et al., 1997). MHV-68 latent infection shows multiple cell tropisms in mice, including B cells, macrophages, dendritic cells, and lung epithelial cells, which is also found in human gammaherpesviruses (Flano et al., 2000; Stewart et al., 1998). The MHV-68 infection causes an infectious mononucleosis-like syndrome and establishes life-long viral persistency, which are analogous to features of EBV infection (Reviewed in Doherty et al., 1997; Simas and Efstathiou, 1998). Moreover, MHV-68 is easily grown in many tissue culture systems, and with its known genome sequence and structure it is relatively easy to make a mutant virus. MHV-68 not only shows remarkable similarities with EBV and KSHV in *in vivo* infection, but also has features which benefit *in vitro* study and genome manipulation. Hence, with MHV-68, a small animal model of gammaherpesviruses has been established to reveal the mechanism of infection.

1.3.1 Structure and genome

MHV-68 shares general characterisation of rhadinoviruses in genome structure: it has a unique region of 118.2 kbp flanked by a variable number of 1.23 kbp repeat units at both ends (Efstathiou et al., 1990a; Efstathiou et al., 1990b). In the same work of Efstathiou et al., MHV-68 was reclassified as a gammaherpesvirus based on sequence analysis on 9 genes which had high homology within EBV. Two independent groups have published the complete genome of MHV-68; their results are similar except for a few differences (Nash et al., 2001; Virgin et al., 1997). The unique region of MHV-68 is largely collinear with KSHV and HVS, which contains 73 open reading frames, along with 8 viral tRNA-like molecules and 15 microRNAs (Bowden et al., 1997; Pfeffer et al., 2005; Virgin et al., 1997; Zhu et al., 2010). The organisation of gammaherpesviruses genomes, the conserved genes shared

among them, and the unique genes for each member are illustrated in Figure 1.2. Most of the genes which relate to viral DNA replication and virion structure are conserved between MHV-68 and other gammaherpesviruses. Rhadinoviruses also share some genes which are important for latent infection, such as LANA, v-Cyclin, and vGPCR. Transposon mutagenesis shows that the unique genes of MHV-68 compared to KSHV are not required in lytic infection but are related to latent infection (Moorman et al., 2004; Song et al., 2005). Important MHV-68 genes which are associated with latent infection are introduced in detail in section 1.3.3.

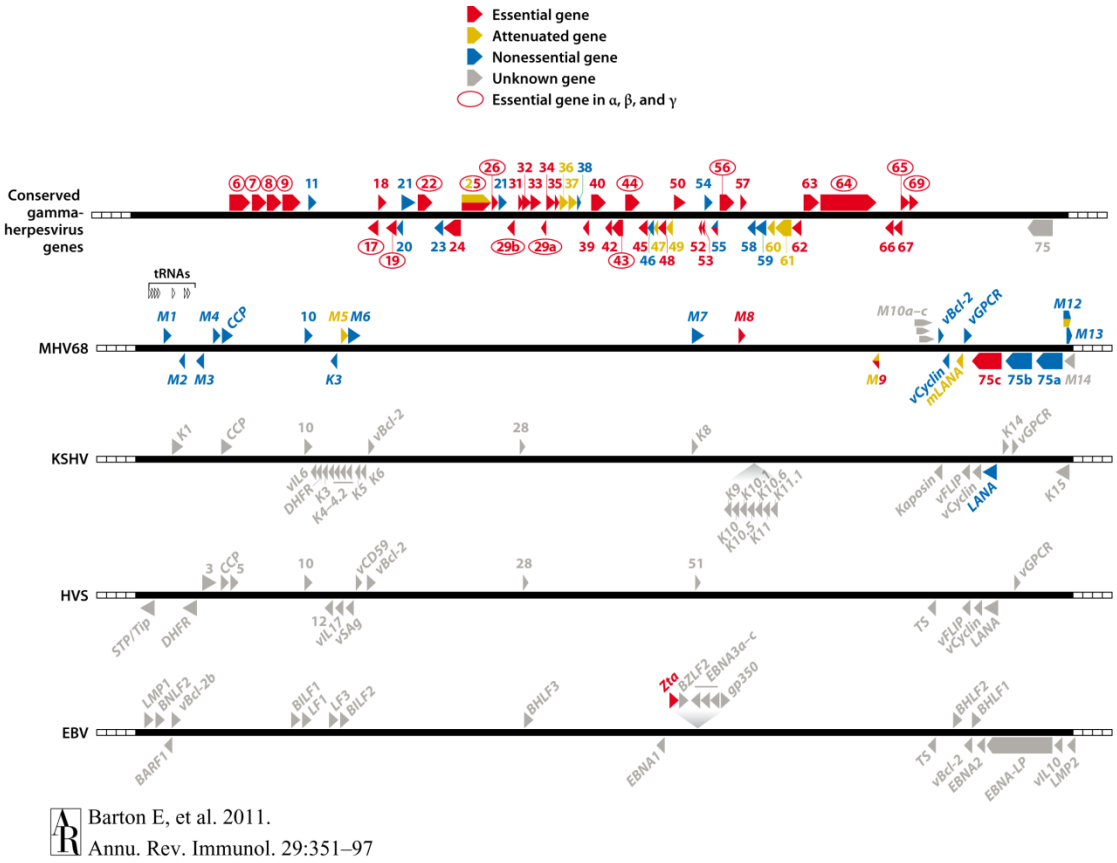

Figure 1.2 Genome map of important gammaherpesviruses showing their conserved and unique genes (Figure source: Barton et al., 2011). Genes present in all gammaherpesviruses are shown at the top. In addition, viral genes which either are essential or play an important role in MHV-68 replication in permissive fibroblasts in tissue culture are indicated (Moorman et al., 2004; Song et al., 2005).

1.3.2 *In vitro* infection of MHV-68

In vitro, MHV-68 is able to infect and replicate in many epithelial and fibroblast cell lines (Svobodova et al., 1982). However, persistent infection is established only in limitedlymphoid cell lines. Unlike KSHV, MHV-68 seems not to infect T cells and the existing cell lines are restricted B cell lines. NS0 cell line is derived from mouse myeloma B cells (Sunil-Chandra et al., 1993). The infection of NS0 is persistent; namely, there are both latent and lytic infections. The virus is mainly maintained as latent, while 5% of infected cells are under reactivation. The first B cell line of MHV-68, S11, is derived from B cell lymphoma developed in MHV-68 infected mice (Usherwood et al., 1996b). Both linear and episomal forms of viral genome were found in the S11 cell line, and an inoculation to nude mice led to tumour development (Usherwood et al., 1996b). The feature of the S11 cell line suggests it is more analogous to Burkitt's lymphoma cells in the case of EBV rather than LCLs. However, attempts to establish KSHV and MHV-68 transformed B cell lines were unsuccessful (Dutia et al., 1999; Jarousse et al., 2008). Recently, Liang et al. found that MHV-68 is able to infect murine foetal liver progenitor B cells, which results in immortalisation and differentiation into B plasmablasts (Liang et al., 2011), which may indicate a similarity to KSHV.

1.3.3 Viral Gene expression in pathogenesis

1.3.3.1 Genes expressed in productive infection in vitro

Ebrahimi et al. have profiled the viral RNA expression in the 3 stages of productive infection using oligonucleotide-based microarray (Ebrahimi et al., 2003). In this study, viral genes which expressed despite the cycloheximide treatment which inhibits cell de novo protein synthesis are defined as immediate early genes. This class of genes include: M4, K3, ORF38 (tegument-associated membrane protein), ORF50 (Rta), ORF57 and ORF73

(mLANA). Early genes were defined as those are sensitive to protein synthesis inhibitor, but expressed despite the treatment of DNA polymerase inhibitor, phosphoroacetic acid, which include: ORF24, ORF29a, ORF36, ORF54, ORF63, ORF64, ORF68, ORF75b and M12. Following the early genes, early-late, and late genes are detected around 12 hours post infection, which are mainly structural proteins ORF19 (tegument protein), ORF65 (capsid protein) and ORF66 (capsid protein).

Recently, signature- tagged transposon mutagenesis has identified the genes which are essential for lytic infection, along with a number of dispensable genes which can significantly enhance the viral replication (Moorman et al., 2004; Song et al., 2005). At present, 41 genes have been identified as essential for MHV-68 replication, of which 17 genes are highly conservative among all herpesviruses.

Within the stage of early-late gene expression, some cellular homologues are expressed, such as a Bcl-2 homologue (M11) (Wang et al., 1999), a cyclin D homologue (ORF72) (van Dyk et al., 1999), and a G-protein coupled receptor (ORF74) (Wakeling et al., 2001). There are generally two routes for viral transmission from one cell to another, the newly formed virion either entering extracellular space and attaching to and entering another cell, or transmitting to an adjacent cell through a cell-to-cell route. Two glycoproteins are related to these routes respectively. Glycoprotein 150 is encoded by the M7 gene, which is required for virion egress into extracellular space (de Lima et al., 2004; Stewart et al., 2004). In contrast, gp48 is encoded by the ORF27 gene which is localised at the plasma membrane to assist the virion's egress into the adjacent cell (May et al., 2005b). This process also requires a gene product encoded by ORF58 (May et al., 2005a).

1.3.3.2 Genes associated to latent infection

Unlike the conservation found in lytic genes among herpesviruses, the viral genes which are employed in latent infection are surprisingly different. Lymphocrytoviruses and rhadinoviruses have very few homologues of latent genes, and even among rhadinoviruses

there are still great differences of gene expression in latent infection. Generally, MHV-68 genes which are associated with latent infection include M1 to M4, vBcl-2 (M11), K3 (ORF12), v-Cyclin (ORF72), mLANA (ORF73), and vGPCR (ORF74). Among them, M1 to M4 are unique to MHV-68; vBcl-2 shares similar functions with some proteins expressed by other gammaherpesviruses; and K3, v-Cyclin (ORF72), mLANA, and vGPCR are shared by all rhadinoviruses. A bacterial artificial chromosome which contains the MHV-68 genome has provided a great tool to manipulate the viral genome (Adler et al., 2000). The role of a latent gene is mainly investigated by generating a recombinant virus which lacks a specific gene product. MHV-76 is a natural deletion mutant of MHV-68, which lacks the unique region at the left end of the genome. Studies with MHV-76 indicated an important role of the genes encoded by the unique genome in MHV-68 latent infections (Dutia et al., 2004; Macrae et al., 2001). Furthermore, it was used to generate 'knock in' mutants with specific genes in order to study their functions (Townsley et al., 2004). There are 4 genes located at the left end of the genome which are unique to MHV-68: M1 to M4. M1, M3, and M4 are secreted proteins, whereas M2 is expressed specifically in B cells. At present, the functions of M1 to M3 have been intensively studied, whereas that of M4 remains unclear.

M1

Disruption of M1 expression does not affect the establishment of latency, whereas an enhanced reactivation was observed in an M1-null virus compared to the wild type (WT) virus (Clambey et al., 2000). Interestingly, the virus lacking M1 expression was shown to be less virulent in IFNγR$^{-/-}$ mice: it does not induce fibrosis in the lung and spleen in IFNγR$^{-/-}$ mice (Evans et al., 2008). M1 is also essential to raise an expansion of Vβ4 CD8+ T cells in peripheral blood around 3 to 4 weeks post infection (p.i.), and this population of T cells is not strictly viral-antigen specific and expresses IFNγ and IL-2. IFNγ and IL-2 can suppress viral reactivation from latency; therefore this observation explains the hyper-reactivation observed in the absence of M1 (Evans et al., 2008). One possibility is that M1 drives Vβ4

CD8+ T cells' expansion as a superantigen (Evans et al., 2008). However, the mechanism underlying this is still unclear. Similar superantigen activations have been observed in EBV and HVS, but with obvious differences. EBV can induce the expression of a human endogenous retroviral super antigen –HERV-K18 in the host cell (Sutkowski et al., 2001), whereas the HVS superantigen is encoded by viral ORF14 which binds to MHC class II directly (Yao et al., 1996).

M2

The role of M2 was first studied by transcription profile of latent genes in an MHV-68 infected S11 B cell line (Husain et al., 1999). M2 plays a critical role in both latency establishment and reactivation from latency. Deletion of M2 did not affect viral replication. However, it shows dose- dependent defect in establishing latency on day 16 p.i. and a profound deficiency in reactivation (Jacoby et al., 2002; Macrae et al., 2003). In the spleen, the M2 deficient virus showed no differences from the WT virus in inducing splenomegaly and occurrence of IM-like syndrome. However, it failed to increase the latent viral load during the acute latent infection (Macrae et al., 2003). In addition, M2 was shown to be essential for latently infected germinal centre B cells to transit to memory B cells. This indicates M2 is involved in manipulating B cell differentiation to establish latency in long-lived memory B cells (Simas et al., 2004; Herskowitz et al., 2005). The molecular basis of this function of M2 is unknown; some studies have addressed its binding ability, suggesting that it may function as a molecular scaffold which modulates specific signal transduction pathways (Herskowitz et al., 2008; Pires de Miranda et al., 2008). Liang et al. has demonstrated that M2 may also suppress STAT-1 and STAT-2 in a cell-type dependent manner, therefore inhibiting IFN response, including apoptosis (Liang et al., 2004).

Moreover, M2 was shown to induce IL-10 expression both *in vitro* and *in vivo*. The elevated IL-10 was predicted to inhibit the host's immunity. Indeed, a CTL response against MHV-68 was enhanced in the absence of M2. In addition, M2 suppressed the expression of MHC

II, b220, and IgD in B cells, while germinal centre B cell markers and IgG expression were up-regulated. These results indicate that M2 drives B cell differentiation (Siegel et al., 2008). Recent studies show that the fluorophore-labeled M2-null virus is observed in germinal centre B cells, but is completely absent from the plasma cells. Moreover, viral reactivation is associated with plasma cell differentiation, thus explaining the essential role of M2 facilitating viral reactivation (Liang et al., 2009).

M3

M3 is highly secreted in both lytic and latent infection and is a broad-spectrum chemokine binding protein encoded by MHV-68 (Simas et al., 1999; van Berkel et al., 1999). All classes of chemokines (CC, CXC, C, and CX3X) can bind to M3, although the binding with CXC chemokine is quite limited (Parry et al., 2000; van Berkel et al., 2000). Disruption of the M3 gene by inserting a β-galactosidase expression cassette did not affect the lytic replication in the lung or the initial spread to lymph organs. However, it caused a significant defect in the establishment of latency in the spleen (Bridgeman et al., 2001). Another study using the M3-stop virus which has an insertion of a translational stop and a frameshift mutation, showed normal establishment and reactivation in the spleen, while the mutant virus showed 100-fold less virulence than the rescued virus after intracerebral inoculation (van Berkel et al., 2002). In the same study, the M3 expressing virus induced meningeal infiltration of neutrophils, whereas the M3-stop virus induced inflammatory infiltration was mainly composed of macrophages and lymphocytes. This result suggests that M3 has a function in the modulation of the immune response. Interestingly, a recent study demonstrated that wood mice infected with the M3-stop virus showed impaired germinal centre reaction in the spleen (Hughes et al., 2011), which is the evidence that the virus may drive the spleen B cell life cycle to expand the pool of latently infected cells.

M4

M4 is a glycosylated protein and its function is still unclear (Evans et al., 2006; Geere et al., 2006). It is dispensable for *in vitro* replication and is known to contribute to viral expansion during acute-latent infection in the spleen.

K3 (ORF12)

K3 is the homologue of KSHV K3 and K5 proteins (Virgin et al., 1997). It is expressed in lytic infection in the lung and in splenic germinal centre B cells at the peak of latency. In the absence of K3, MHV-68 had a normal lytic infection in the lung, but exhibited a decreased frequency of latently infected splenocytes and enhanced viral-specific CTL response. Moreover, the K3 protein is shown to inhibit antigen presentation of MHC class I molecules (Stevenson et al., 2002a; Stevenson et al., 2002b). With its RING domain, K3 can react with the MHC class I heavy chain and initiate ubiquitination which leads to proteasome-dependent degradation (Boname and Stevenson, 2001). In addition, recent research showed that K3 impaired the assembly of MHC class I heavy chain with β2-microgloblin, resulting in MHC class I molecules unable to assemble with high-affinity peptides. These findings imply that K3 may prevent MHC class I molecule assembly by blocking its binding with chaperones (Yu et al., 2002). Altogether, K3 plays an important role in latent infection by suppressing the expression of the MHC class I molecule.

M11 (vBcl-2)

vBcl-2 is encoded by the MHV-68 M11 gene and is a homologue of cellular protein Bcl-2. All gammaherpesviruses encode at least one Bcl-2 homologue. Sequencing of vBcl-2 encoded by MHV-68 shows it has a BH-1 domain but no BH-2 domain, which is different from homologues encoded by other gammaherpesviruses. Given the known function of cellular Bcl-2, vBcl-2 is involved in preventing the host cell undergoing apoptosis in chronic infection (Wang et al., 1999). Studies showed that vBcl-2 encoded by MHV-68 could inhibit apoptosis by blocking the signaling induced by anti-Fas antibody or TNF-α. The M11 gene is expressed in both lytic and latent infection, which suggests that the inhibition of caspase-

dependent apoptosis is required for both viral replication and also latency in the lung and spleen (Roy et al., 2000). By inserting stop codons in the coding region of the gene, a vBcl-2-stop virus was generated and utilised to study the role of M11 *in vivo*. The depletion of vBcl-2 did not significantly affect latency establishment, but it diminished the viral reactivation from latency (Gangappa et al., 2002). More recently, a surface binding groove of vBcl-2, BH-3 domain, was identified, which is important to anti-apoptotic function (Loh et al., 2005). This domain was later shown to inhibit autophagy more efficiently than cellular Bcl-2 (Ku et al., 2008). Subsequent study using a virus which had a mutation in the M11 gene suggested vBcl-2 inhibition of autophagy is important during MHV-68 persistent infection (E et al., 2009). The role of vBcl-2 in spleen latent infection is under debate: vBcl-2 deficiency was found to have no effect in spleen latency following intraperitoneal inoculation (Gangappa et al., 2002), while in an independent study using a different mutant virus a role was found for vBcl-2 in establishing latency in the spleen after intranasal inoculation (de Lima et al., 2005). The conflicting results may have arisen because of the different mutant viruses used and the different route of inoculation applied (intraperitoneal versus intranasal).

v-Cyclin (ORF72)

MHV-68 v-Cyclin is encoded by ORF72. It is a homologue of cellular cyclin D and is shared among rhadinoviruses. In a study using transgenic mice in which v-Cyclin was expressed under the control of proximal promoter LCK, expression of v-Cyclin led to the growth of T cell lymphoma (van Dyk et al., 1999). Crystal structure analysis shows that it binds to both CDK1 (Cyclin-dependent kinase) and CDK2, in which CDK1 regulates the cell cycle through S phase, while CDK2 controls the transition from G1 phase to S phase. Moreover, it was shown to be resistant to inhibition from CDK inhibitor $CKIp27^{Kip1}$ (Card et al., 2000; Swanton et al., 1999).

A recombinant virus marked by a reporter gene as well as knock-out of ORF72 exhibited defects in both acute viral replication and reactivation from latency (Hoge et al., 2000). Another study showed that in B cell knockout mice, maintenance of latent infection also required v-Cyclin (van Dyk et al., 2003). *In vivo* study using a v-Cyclin-null virus showed an impaired acute replication in the lung and failure to induce splenomegaly. The same changes were also observed when using v-Cyclin-CDK binding deficient mutants. However, following intraperitoneal infection, the reactivation was suppressed in peritoneal elucidate cells when infected with the v-Cyclin-null virus but not the v-Cyclin-CDK binding deficient mutants. This suggests that v-Cyclin has a function in peritoneal macrophage infection which is independent from binding with CDKs (Reviewed by Upton and Speck, 2006). Therefore, v-Cyclin may functions in lytic infection as well as in reactivation in a cell type-specific manner.

mLANA (ORF73)

ORF73 encoded latency associated nuclear antigen (LANA) is conserved among rhadinoviruses. Moreover, EBNA1 of EBV has a function similar to that of LANA (Lee et al., 1999). In the absence of mLANA, mutant MHV-68 is severely impaired in latency establishment in the spleen and this finding agrees with the predicted function of EBNA1 in EBV and LANA in KSHV, which is maintaining the viral genome as an episome during latency (Fowler et al., 2003). The mLANA null virus also exhibited a defect in lytic infection in the lung following intranasal inoculation (Moorman et al., 2003b). Using the same virus, however, *in vitro* experiments indicated that there was a more rapid and higher level of viral gene expression, as well as p53 activity, corresponding with accelerated cell death which may impair virion production. This suggests that mLANA may function as a suppressor of lytic gene expression and, moreover, may inhibit cellular apoptosis (Forrest et al., 2007). Interestingly, LANA homologues in RRV and KSHV were observed to have a similar role in enhancing viral gene expression (Wen et al., 2009; Li et al., 2008). Recent

research showed the mLANA-null virus could infect spleen cells in immune-compromised mice which lacked IFNαβ response. However, although the viral genome was maintained and carried for months post infection, it was not maintained in the form of episome and was unable to reactivate from latent infected spleen B cells, which confirms the essential role of mLANA in maintaining latent infection (Paden et al., 2010).

v-GPCR (ORF74)

ORF74 is a homologue of mammalian G protein coupled receptors (GPCR) and its homologue is also expressed by KSHV. It is expressed in both viral replication *in vitro* and latent infection *in vivo* in the lung and the spleen. Like KSHV, vGPCR can transform NIH 3T3 fibroblasts (Wakeling et al., 2001). A study using a mutant virus in which ORF74 was partially deleted showed the dysfunction of vGPCR had no effect on viral replication but was less efficient in reactivation in long-term persistency (day42 p.i.) (Moorman et al., 2003a). In another study, MHV-68 with deletion of ORF74 replicated similarly to WT, and was impaired in reactivation from spleen cells. It was also demonstrated that chemokines KC and MIP-2, but not IP-10, enhanced lytic infection in the WT virus infection but not the in vGPCR knockout virus. This suggests that vGPCR can enhance replication and reactivation by modulating host immune response (Lee et al., 2003). While another chemokine binding protein, M3, binds to all kinds of chemokines, vGPCR seems to bind preferentially to CXC chemokines. Moreover, Verzijil et al. showed that chemokines such as KC and MIP-2 may function as agonists of vGPCR, whereas the vGPCR binds IFNγ inducible IP-10 as an antagonist (Verzijl et al., 2004). These studies suggest that vGPCR modulates the immune system by limiting the activity of these chemokines, which contributes to the maintenance of latency.

1.3.4 MHV-68 infection in immune competent mice following intranasal inoculation

Although there are many data generated from studies using intraperitoneal and intracerebral inoculation, the intranasal route is considered the likely natural route of MHV-68 infection. Therefore here we introduce the events which occur following intranasal inoculation. There are generally 4 distinguishable stages:

1. **Productive (lytic) infection**: A productive infection first occurs in the lung, which is characterised by viral replication within epithelial cells and profound expression of viral proteins. It occurs within days after inoculation and is followed by latency establishment in specific cell reservoirs such as lung epithelial cells, macrophages, dendritic cells, and B cells in secondary lymph organs.
2. **Acute phase of latent infection**: This stage is also termed latency expansion, in which key features include viral gene driven proliferation and differentiation of latently infected B cells. From 2 to 3 weeks post infection, the secondary lymph organs, such as the spleen, shows significant enlargement while the latent viral load is increasing. The virus only expresses a number of latent-associated genes which regulate cell cycle and signaling pathways, as well as those which facilitate immune evasion.
3. **Long-term latency**: This is a state of life-long carriage. The viral gene expression is switched off except for a few proteins essential for viral episome maintenance. Most likely memory B cells are the main site of long-term latency, while macrophages, DCs, and epithelial cells can also be latently infected; however, the role of the latter in long-term latency is not clear.
4. **Reactivation**: Reactivation occurs in both acute and long-term latency: there is a relatively high level of reactivation during latency expansion which rapidly diminishes to a low but detectable level in long-term latency.

Infection in the long-term can be considered a balance between latency and reactivation. Infection studies using peritoneal inoculation show that a reservoir of persistent, low-level productive infection may exist in peritoneal macrophages during long-term MHV-68 infection (Flano et al., 2000; Weck et al., 1999). However, the nature of this type of infection remains unknown.

1.3.4.1 Lytic infection in the lung and viral dissemination to lymph organs

Following intranasal inoculation of immune competent mice with MHV-68, an acute respiratory infection occurs in which the virus replicates rapidly in lung epithelium. In the lung, the virus can be detected in the first 24 hours post infection, and the replication peaks at 3 to 5 days p.i., and the virus is not detectable by plaque assay by 10 days p.i. but still show positive in PCR. Both lung epithelial cells and mononuclear cells are infected (Sunil-Chandra et al., 1992a). Stewart et al. have shown that lung epithelium is one of the sites for MHV-68 persistency (Stewart et al., 1998). The virus enters the mediastinal lymph node (MLN) where dendritic cells, macrophages, and B cells are infected (Nash et al., 2001). The transmission of the virus from lung to lymph node has been intensively studied. It is already known that there are no detectable cell-free viraemia formed in MHV-68 infection (Sunil-Chandra et al., 1992a). Moreover, disruption of essential proteins in virion binding or release does not prevent the establishment of latency (de Lima et al., 2004; Gillet et al., 2007), while deficiency in gp48 which is important cell-to-cell transmission, significantly affects long-term persistency (May et al., 2005b). The studies above suggest a cell-associated route for MHV-68 to traffic to lymph nodes from lung epithelial cells. Therefore it is generally believed that the dendritic cells are responsible for initially transporting the virus to the draining lymph node and colonising B cells. Studies using GFP label MHV-68 infecting normal mice and B cell deficient mice (uMT) reveal DCs and macrophages in MLN were infected no matter whether B cells were present or not, whereas in the absence of B cells the infection appeared to be transient (Selvarajah, unpublished data). More recently, by tracking

a DC-specific virus using cre-lox system, Gaspar et al. showed a great proportion of the latent virus in B cells were passed from DC. They also showed that a virus which only underwent genome deletion in DCs was impaired in its ability to infect B cells (Gaspar et al., 2011). The above results support the conclusion that MHV-68 colonises B cells through dendritic cells. However, this was only observed in superficial cervical lymph nodes (SCLN), which collect lymph from the upper respiratory tract, and seemed not to be the case in MLN, which collect the lymph from the lung (Gaspar et al., 2011).

1.3.4.2 Latent infection in the spleen

MHV-68 establishes latent infection in lymph follicles after reaching the spleen. In the absence of B cells, MHV-68 can reach MLN but not spleen, which suggests that B cells carry the virus to the spleen (Selvarajah, 2001). The viral titre is detectable in the spleen as early as day 5 p.i.(Sunil-Chandra et al., 1992a), whereas the first detection of infection by *in situ* hybridisation appears on day 10 (Gangadharan, 2006). The virus can be recovered consistently from spleen B cells (Sunil-Chandra et al., 1992b); coupled with its cell tropism which showed *in vitro* infections on different cell lines (Sunil-Chandra et al., 1993), this indicates that spleen B cells are a major site of MHV-68 latent infection.

Compared with asymptomatic long-term latency, the acute phase of latent infection features a rapid proliferation of B cells by 2-3 weeks p.i., corresponding with a rapid increase in the number of latently infected B cells. During the acute phase, pathologically the host shows splenomegaly, and the latently infected B cells appear to be located within the germinal centres, which increase both in number and size of germinal centres (Gangadharan, 2006; Nash et al., 2001). As in the MLN, the high viral load in the spleen seems to be transient: the frequency of latently infected cells increases from 1 in 10^7 splenocytes up to 1 in 10^4 splenocytes within days and then drops to 1 in 10^6 splenocytes by week 4 p.i.(Sunil-Chandra et al., 1992a; Usherwood et al., 1996a). Usherwood et al. have shown that the splenomegaly is controlled by $CD4^+$ T cells. In the absence of $CD4^+$ T cells, neither splenomegaly nor a

rapid increase of infected cells was observed, but the virus could still infect B cells and establish latency in the spleen. These findings also suggest that the establishment of latency in the spleen does not require $CD4^+$ T cells. (Usherwood et al., 1996a). On the other hand, the viral latency in the spleen appears to rely on the presence of B cells. Mice lacking mature B cells (uMT mice) showed no infection in the spleen following intranasal inoculation of MHV-68. Moreover, B cells/latently infected B cells were required to develop splenomegaly (Usherwood et al., 1996c). These data indicate that MHV-68 may manipulate the B cell proliferation and differentiation to establish latent infection. However, the work of another group using intra-peritoneal infection showed that in uMT mice the latency was established at a level of 100-fold higher than in normal mice (Weck et al., 1996), which suggests the impact of the different route of infection. Despite these contradictory results, more recently, accumulating evidence has shown that in the acute phase of latency, MHV-68 can activate the infected B cells, drive its proliferation, and utilise the germinal centre reactivation to expand the pool of infected B cells. Eventually, these latently infected germinal centre B cells undergo differentiation and become either memory B cells or plasma cells (reviewed in Barton et al., 2011). The detail of MHV-68 utilising germinal centre reaction in the spleen is discussed in the introduction of Chapter 4.

1.3.4.3 Reactivation from latency

Although they both lead to cell death and virion production, reactivation from latency is different from primary lytic infection in the lung in many respects. First, the immune environment in the host is changed after productive infection. The lytic infection generally occurs in the lung epithelium whereas reactivation mostly takes place in secondary lymph organs, in which an abundance of antibodies and effector cells have been generated or recruited. Moreover, the initiation of reactivation is from inside latently infected cells; therefore the molecular basis involved in reactivation is different from lytic infection, for the

latter requires the process of attachment and entry into the cell (reviewed in Barton et al., 2011).

Reactivation was measured by detecting the infectious virus using the method of modified plaque assay (Sunil-Chandra et al., 1992a). In another study, a subpopulation of activated CD8+ T cells which is specific for epitopes generated from lytic infection were still present in latent infection, which provides evidence for a low level of reactivation or productive infection during long-term latency (Liu et al., 1999). Steed et al. showed that IFNγ significantly suppressed reactivation from latency in PEC and spleen cells from B cell deficient mice (Steed et al., 2006); however, the same group found later on that in wild type mice, reactivation from spleen cells could not be controlled by the same mechanism, which suggests IFNγ can only control reactivation from latently infected macrophages but not from B cells (Steed et al., 2007). Viral gene transcription profiling shows that apart from latent genes, the key gene for lytic infection, ORF50, as well as other lytic-associated genes are expressed in macrophages and dendritic cells, but not B cells at day 14 post infection (Marques et al., 2003). Moreover, Fowler et al showed that an essential gene for latent infection, ORF73, was not transcribed in latent infected macrophages, or possibly the transcription was too low to be detected (Fowler et al., 2003). These findings indicate that the mechanism of reactivation from latency and its control vary according to cell type.

1.3.4.4 Infectious mononucleosis-like syndrome in periphery

Another characteristic feature of MHV-68 infection is the massive expansion of CD8+ T cells in peripheral blood around 3 weeks post infection. The expanded population is dominated by $V\beta4^+$ T–cell receptor expressing cells, which suggests the possibility of a response against a superantigen (Flano et al., 2004; Hardy et al., 2000; Tripp et al., 1997). This infectious mononucleosis-like syndrome appears after the resolution of the acute phase of infection and persists for more than a month, which is comparable with the infectious mononucleosis in EBV primary infection in adults (reviewed in Nash et al., 2001). However,

the expanded CD8+ T cells induced by EBV are largely viral-specific MHC-I restricted T cells, while MHV-68 induced CD8+ T cell are not viral-antigen specific. Previous research shows that the expression of M1 is essential for the expansion of a specific subset of T cells (Evans et al., 2008).

1.3.5 Immune responses involved in MHV-68 infection and pathologies

As discussed above, there are different components of MHV-68 infection: productive infection, acute latency, long-term latency, and reactivation from latency. The pattern of viral gene expression and protein production in each stage is distinct. Therefore, the host response generated against the present stage of infection may be inadequate to control the next phase of infection. Moreover, the genes expressed during latency establishment and reactivation in each type of cells that is infected are different; therefore the immune response against the infection of each reservoir is also likely to be distinct (Tibbetts et al., 2002). To investigate the immune responses against MHV-68 and the role of host immunity in the subsequent pathologies, transgenic mice with a specific deficiency in their immune system are widely utilised.

1.3.5.1 Adaptive immune responses

Numerous studies show that the lytic MHV-68 infection in the lung is well controlled by the host's immunity, in which CD4+ T cells (Stevenson et al., 1999b) and CD8+T cells (Ehtisham et al., 1993) may contribute against viral infection, while the control from antibodies is relatively inefficient (Usherwood et al., 1996c). However, the host immune system fails to completely clear the long-term latency, which is facilitated by viral immune-evasion mechanisms such as viral protein K3 (Stevenson, 2004).

B cells and antibodies

The antibody response against MHV-68 appears to be slow and established only after acute infection has been controlled. MHV-68 specific antibodies are dominated by IgM, produced in the first week post infection, followed by production of IgG2a and IgG2b, in the second week post infection (Sangster et al., 2000; Stevenson and Doherty, 1998). Compared to wild type mice, infected uMT mice which lack B cells and have no antibody production show little difference in lung pathology, which indicates that the antibodies are unlikely to control the lytic infection in the lung (Usherwood et al., 1996c). Moreover, a recent study shows that *in vitro*, using cells expressing IgG Fc receptors, such as macrophages and dendritic cells, specific antibodies failed to block and even enhanced MHV-68 infection (Rosa et al., 2007). On the other hand, studies in which antibodies are introduced before infection indicate important functions of MHV-68 specific antibodies. It has been shown that MHV-68 specific antibodies can control the number of latently infected cells as well as reactivation from latency (Kim et al., 2002; Tibbetts et al., 2003). However, the immunity of vaccinated mice may not reflect the actual host immune environment in the natural infection of gammaherpesviruses.

CD4+T cells

CD4+ T cells specific for MHV-68 are activated and remain so during chronic infection (Christensen and Doherty, 1999). Control of MHV-68 infection in B cell deficient mice appears to be mediated by CD4+ T cells, largely through the function of IFNγ (Christensen et al., 1999). These cells appear to undergo activation and proliferation, as well as IFNγ production (Stuller et al., 2010). IFNγ supresses viral reactivation *ex vivo* (Steed et al., 2007; Steed et al., 2006) by directly inhibiting the transcription of viral ORF50 (Goodwin et al., 2010). Moreover, IFNγ may enhance the immune function of CD4+ and CD8+ T cells (Badovinac et al., 2000; Whitmire et al., 2007). CD4+ T cell depleted mice infected with MHV-68 exhibit no defects in controlling lung and spleen infection by day 12 post infection, and develop neither splenomegaly nor lympho-proliferative disorder (Ehtisham et al., 1993).

Moreover, depletion of CD4+ T cells during acute infection leads to a reduced viral load in the spleen but no effect on latent infection level at day 30 (Usherwood et al., 1996a). MHC class II deficient mice (I-Ab$^{-/-}$ mice) are also used to study CD4+ T cell function. CD4+ T cell depleted mice fail to develop splenomegaly, as well as viral specific antibodies. However, a progressive loss of control in long-term MHV-68 infection which is mediated by CD8+ T cells is observed in mice that have CD4+ deficiency, indicating a crucial role of CD4+ T cells (Cardin et al., 1996). Interestingly, the absence of MHC class II molecules leads to elevated reactivation and chronic disease in the lung (Cardin et al., 1996). This lung disorder is not protected against but partially improved by vaccination using protective T cell epitopes (Belz et al., 2000), whereas CD4+ T cells function can be restored by the stimulation of CD40, which is expressed on B cells and professional APCs (Sarawar et al., 2001).

CD8+T cells

The absence of CD8+ T cells leads to exacerbation of MHV-68 infection in the lung and spleen. Moreover, CD8+ T cells deficient mice also show pathology in the liver and adrenal gland, which suggests a major role of CD8+ T cells in controlling productive infection (Ehtisham et al., 1993). Several studies indicated that the role of CD8+ T cells largely depends on the functions of perforin, granzyme, and Fas induced cell death (Loh et al., 2004; Topham et al., 2001). Perforin-mediated mechanisms suppress the latent viral load in spleen B cells, but not macrophages. Perforin-knockout mice do not show significant defects in either lytic infection in the lung or latent infection in the spleen (Usherwood et al., 1997), which indicates an alternative protection. Mice with double knockout of perforin and the IFNγ receptor showed much higher mortality than mice with either single knockout following MHV-68 infection, indicating an important role of perforin-mediated cytotoxicity which is independent of the IFNγ signal (Tsai et al., 2011). CD8+ T cells raised specifically against the lytic viral gene products (ORF6 and ORF61) were detected in the lung up to 22

days p.i. (Stevenson et al., 1999a), and the presence of these subpopulations is independent from CD4+ T cells and MHC class II molecules (Stevenson and Doherty, 1998). It was thought that CD8+ T cells which control all phases of MHV-68 infection are MHC class Ia restricted. However, knocking out MHC class Ia led to the development of a large number of β2M-dependent CD8+ T cells which control both lytic and latent infection. Moreover, this subpopulation, which appears to be class Ib MHC restricted, is independent of CD1d and it is not clear what antigen induced the activation and proliferation of these CD8+ T cells (Braaten et al., 2006). Part of these T cells are Vβ4 CD8+ T cells which may be related to the M1-induced Vβ4 CD8+ T cell expansion in peripheral blood around 2 weeks post infection (Evans et al., 2008). The expanded Vβ4 CD8+ T cells express IFNγ and TNFα, but it remains unknown whether they can trigger cell death.

1.3.5.2 Cell intrinsic responses and Innate immune responses

Although adaptive immunity against MHV-68 has been investigated intensively, the importance of cell intrinsic response and innate immunity in controlling MHV-68 infection is now receiving great attention. Most cells' intrinsic response is modulated by at least one viral gene product. It has been reported that the host cell responds to viral infection through apoptosis and autophagy, and the latter has recently been shown to be well inhibited by v-Bcl2, suggesting autophagy has an important role in the MHV-68 lifecycle. NF-κB, which is involved in regulation of both innate and adaptive immunity, has been shown to be inhibited by mLANA. Moreover, NF-κB family member p50 has been shown to be essential in controlling the acute phase of latency in the spleen: mice which lack p50 failed to control viral replication in the lung (Krug et al., 2009).

1.3.6 Role of IFNγ in murine gammaherpesvirus infection: MHV-68 infection in the absence of IFNγ response

1.3.6.1 IFNγ *and its receptor*

IFNγ is the only member of type 2 interferon, and it is structurally different from type 1 interferon but shares some functional similarities with the later. So far, all mammals examined have an IFNγ gene. Mouse IFNγ has about 40% protein homologue with human IFN ɣ . It is a poly-peptide with 136 amino acids and approximately 17 kDa in molecular mass (Gray and Goeddel, 1983). In early studies, T cells were considered to be the major source of IFNγ, which includes the population of Th1, Th0, and CTL. The production from CD4+ T cells is primarily stimulated by MHC class II molecules binding with antigens, whereas MHC class I molecules bind to CD8+ T cells. NK cells are another important source for IFNγ, which require stimulation from TNFα and macrophages (Vilcek et al., 1985; Farrar et al., 1986; Johnson et al., 1986; Johnson and Torres, 1984). Nowadays, evidence shows that B cells, dendritic cells, and macrophages also secret IFNγ (reviewed in Schroder et al., 2004). Most likely the production of IFNγ from NK cells, and APCs is important in innate immunity and the early adaptive immunity against infection, whereas that of CD4+ T cells and CTL is a part of the antigen-specific adaptive immune response (Frucht et al., 2001; Sen, 2001). Generally, the production of IFNγ is enhanced by APC-secreted cytokines such as IL-12 and IL-18, whereas the cytokines related to Th2 and T_{reg} types of immunity such as IL-4, IL-10, and TGF-β down-regulate IFNγ production (Schoenborn and Wilson, 2007).

The IFNγ receptor is comprised of two ligand-binding IFNγ R1 chains and two signal-transducing IFNγ R2 chains. Both chains are of the class II cytokine receptor family and IFNγ R2 is considered the limiting factor of IFNγ signaling since IFNγ R1 is expressed constitutively (Bach et al., 1997; Bernabei et al., 2001). The level of IFNγ R2 expression depends on the cell states, such as differentiation or activation (Bach et al., 1997). IFNγ

signaling transduction is carried out by IFNγR1 binding to Jak 1 and IFN ɣ R2 to Jak 2, which subsequently lead to the activation and translocation of STAT1 molecules which initiate certain transcription of interferon-regulated genes (reviewed in Schroder et al., 2004). Interferon regulatory factors (IRFs) such as IRF-1, IRF-2, and IRF-9 are involved in the regulation of IFNγ signaling (Darnell et al., 1994; Mahboubi and Pober, 2002; Rouyez et al., 2005). The negative regulation of IFNγ signaling also involves specific feedback inhibitor SOCS-1, which inhibits IFNγ signaling by interacting with Jak 1or Jak 2 and regulating tyrosine kinase activity. Transgenic mice in which SOCS-1 is over-expressed exhibited deficient IFNγ responses (Sakamoto et al., 1998; Fujimoto et al., 2000).

1.3.6.2 Antiviral activities of IFNγ *response*

The IFNγ system can act directly against infection within infected cells, and functions as a secondary mediator to other immune cells. Therefore it plays antiviral roles in intrinsic cell response, as well as innate and adaptive immunity. IFNγ can induce key antiviral enzymes including double-stranded RNA activated protein kinase PKR, 2'-5' oligoadenylate sythetase, and double-stranded RNA-specific adenosine deaminase (Hovanessian, 1991; Patterson et al., 1995; Meurs et al., 1990). For example, PKR is a serine/threorine kinase which is induced by interferon and its activation requires dsRNA which is produced by RNA viruses (Hovanessian and Galabru, 1987). Activated PKR can prompt phosphorylation of cellular substrate eIF-2α, and subsequently inhibit viral and cellular protein synthesis (Meurs et al., 1990). Moreover, IFNγ also shows pro-apoptotic functions. After IFNγ treatment, cells which over-express IFNγ receptor undergo apoptosis through activated STAT1 in an IRF-1-dependent manner (Chin et al., 1997). The IFNγ system also facilitates apoptosis by up-regulating the expression of the Fas/Fas ligand and TNF-α receptor (Deiss et al., 1995; Deiss et al., 1996; Xu et al., 1998).

As one major product of Th1 cells, IFNγ enhances the activity of CTL and skews the host's immunity to Th1 phenotype by promoting the differentiation of Th0 cells into Th1 cells,

regulating the activities of APCs, and limiting the Th2 cell population. IFNγ can up-regulate the expression of MHC class I (Wenner et al., 1996) and class II molecules (Chang and Flavell, 1995), therefore elevating both antigen-presentation pathways, by which IFNγ contributes to host immunity against intracellular pathogens.

1.3.6.3 Dysfunction of IFN γ *signaling:* IFNγ *receptor knockout mice*

IFNγ-knockout mice, as well as mice with deficiency in either chain of IFNγ receptor, have been generated. All these mice show immune deficiency against viral, bacterial, and parasitic infections (Huang et al., 1993; Pearl et al., 2001; van den Broek et al., 1995). IFNγR$^{-/-}$ mice with a disrupted IFNγR1 chain were widely used to study the role of IFNγ signaling in a variety of viral infections. Studies on the effect of viral infection on IFNγR$^{-/-}$ mice are summarised by Tau and Rothman (Tau and Rothman, 1999): see Table 1.2. Notably, the outcome of these studies reflects partial redundancy of the antiviral function if IFNγ, possibly because of the similarities between the function of IFNγ and Type 1 interferon (Muller et al., 1994). The studies using IFN γ R$^{-/-}$ mice also emphasise another important function of IFNγ: tumour surveillance. IFNγR$^{-/-}$ mice, as well as cells treated with IFNγ-neutralising antibodies, and cells with IFNγR1 mutations, exhibit compromised tumour resistance (Kaplan et al., 1998; Dighe et al., 1994; Tannenbaum and Hamilton, 2000).

1.3.6.4 Model of MHV-68 infection in IFNγ *R$^{-/-}$ mice*

A cytokine profile of MHV-68 infected C57BL/6J mice shows that IFNγ is largely produced during acute viral infection. High levels of IFNγ and IL-6 and lower levels of IL-2 and IL-10 are expressed in the cells obtained from spleen and lymph nodes, whereas IL-4 and IL-5 are barely detected (Sarawar et al., 1996). Moreover, the peak of IL-6 and IFNγ detected corresponds with the clearance of acute infection in the lung on day 10 p.i.. Surprisingly, mice with the IFNγ gene deficiency (IFNγ $^{-/-}$ mice) show clearance of lung infection in

kinetics similar to that in wild type mice, which suggests IFNγ is not essential for clearance of lytic infection in the lung (Sarawar et al., 1997).

Following intranasal inoculation of interferon gamma receptor deficiency (IFNγ $R^{-/-}$ mice) mice on a background of 129Sv/Ev strain with MHV-68, the lytic infection in the lung showed no differences in the viral titers of infectious virus throughout the lung infection, which is consistent with Sarawar's finding in IFNγ $R^{-/-}$ mice under the background of C57BL/6J strain (Dutia et al., 1997). A series of distinctive pathologies have been observed, which include inflammatory disorders consisting of lymphocytic infiltrations in multiple organs and fibrosis in the spleen, lymph nodes, liver, and lung (Ebrahimi et al., 2001). The lack of interferon gamma provides a Th2-dominated host environment which is marked by elevated expression of IL-4, IL-13, IL-21, and IL-5 (Gangadharan et al., 2008). MHV-68 infection leads to atrophy and fibrosis in the spleen of IFNγ $R^{-/-}$ mice by day 20 post infection (Dutia et al., 1997). Significant loss of spleen cells, which was mostly evident on day 23 post infection, is concomitant with the peak of leucocytosis on day 23 p.i.. This suggests the trafficking of peripheral blood cells into the spleen is blocked by fibrosis developed around spleen follicles where the latently infected B cells mainly existed (Ebrahimi et al., 2001). During the same time period post infection, *in situ* hybridisation for infected cells in the spleens of IFNγ $R^{-/-}$ mice shows that the number of these cells decreases dramatically. This result suggests the loss of viral latency in fibrotic spleen (Gangadharan et al., 2008). Interestingly, the spleen of IFNγ $R^{-/-}$ mice at a later time point shows recovery from fibrosis which appears to be a resolution of MHV-68 latency. However, the infectious centre assay for the latent virus shows there are still latent virus still in those spleen tissues in a very low frequency (Dutia, personal communication). It is clear that the CD8+ T cells mediate fibrosis in IFNγ $R^{-/-}$ spleens. But the mechanism of the fibrosis in MHV-68 infected IFNγ $R^{-/-}$ mice is still unclear. It has been observed that CD4+ T cells and CD8+ T cells infiltrate germinal centres around day 12 post infection. Also, in the very early days of the

infection (before extensive fibrosis developed) macrophages are detected in the spleen germinal centres and then become alternatively activated. The RT-qPCR assay shows that the level of Arginase 1 gene expression in the spleen of IFNγ$^{-/-}$ mice is obviously higher than that in wild type mice (Gangadharan et al., 2008). The above observation suggests a complex interaction involving host B cells, T cells, and macrophages. Importantly, Dutia et al have demonstrated that the infection of IFNγR$^{-/-}$ mice with MHV-76 which lacks unique region at the left end (encoding M1-M4 and vtRNA like molecules) does not lead to spleen pathology (Dutia et al., 2004). Moreover, M1, not only is required for Vβ4+ CD8+ T cell expansion in natural infection, but also plays an important role as an activator in the formation of fibrosis in IFNγ R$^{-/-}$ spleens (Clambey et al., 2000; Evans et al., 2008). The mechanisms of M1 mediating Vβ4+ CD8+ T cell expansion and activating fibrosis within IFNγ R$^{-/-}$ spleens are still uncertain, although it is supposed that it works as a super antigen (Evans et al., 2008). On the contrary, mice infected with a virus which has disrupted vtRNA3 but still can encodes M1 to M4 in vitro, shows no splenic pathology (Dutia et al., 2004). However, this result may be caused by the insertion disrupting the transcription of mRNA which is involved in triggering splenic pathology in vivo (Dutia et al., 2004). So far, the role of viral activity in MHV-68 mediated splenic pathology is still unclear.

1.3.7 Strain-dependent variation in MHV-68 infection

Recent studies of MHV-68 infection in IFNγ deficient mice on the BALB/c background showed surprising variations caused by different mouse strains. IFNγ deficient mice on BALB/c background show high mortality during day 9 to 14 post infection. These mice display poor control of acute productive infection and die from acute pneumonia, which is dependent not only on the viral dose, but also on the expression of v-Cyclin and v-Bcl2 (Lee et al., 2009). Interestingly, M1-null virus infection of IFNγ deficient mice on BALB/c background shows no difference compared to wild type virus in developing lethal pneumonia, except an elevated reactivation rate. These results show that the control of lytic

infection in the lung of BALB/c mice is highly dependent on IFNγ response, which is different from C57BL/6 mice and 129Sv mice. One possible explanations is that BALB/c mice have a different cytokine response against MHV-68 in comparison with C57BL/6 mice, which involves a significantly higher expression of CC and CXC chemokines (Weinberg et al., 2004). Similar studies from an independent group also show the requirement of IFNγ in controlling lytic infection in the lung following intranasal inoculation is strain-dependent (Tsai et al., 2011).

These findings raise interest to investigate the difference between natural hosts and strains of laboratory mice in immune responses against MHV-68 infection. In fact, common laboratory strains of mice such as 129Sv/Ev and C57BL/6 have been widely used to study MHV-68. Studies on Sv129 and C57BL/6 showed little differences in pathogeneses and host response (Brownstein, 1998). Hughes et al. compared MHV-68 infection in immune-competent wood mice and BALB/c mice following intranasal infection, finding that BALB/c mice have higher viral replication in the lung and develop pneumonitis. Moreover, MHV-68 established spleen latency in both strains of mice, with significant germinal centre reactions observed in wood mice but not BALB/c mice, and subsequently a higher production of specific antibodies was observed in wood mice in comparison with BALB/c mice (Hughes et al., 2010). However, another group concluded that the replication and the latency site of MHV-68 are comparable in bank voles and laboratory mice (Francois et al., 2010). The author further argues that the wood mice may not be the true natural host of MHV-68 and therefore cannot reflect the pathogenesis as well as bank voles. Hence, although being questioned, laboratory mice are still considered as suitable model to study MHV-68 pathogenesis so far.

Pathogen	*Phenotype in wild type mice*	*Phenotype in IFNγR$^{-/-}$ mice*
MHV-68	*Resistant to multi-organ fibrosis and arteritis*	*Multi-organ fibrosis and arteritis*
Pseudorabies virus	*Vaccine effective; resistant to re-challenge*	*Vaccine failed; susceptible to re-challenge*
Sendai virus	*Infection cleared*	*Infection cleared*
LCMV	*Transient immunodeficiency*	*No transient immunodeficiency; failed in viral clearance; persistent infection*
Vaccinia virus	*Resistant*	*Increased susceptibility; normal TCL response*
Vesicular stomatitis virus	*Mount CTL response*	*Normal CTL response*
Theiler's virus	*Resistant*	*Chronic disease*
Coronavirus	*Hepatitis*	*Severe hepatitis with increased mortality*
Murine cytomegalovirus	*Infection cleared*	*Failed to clear infection; chronic arteritis*
MMTV		*Same clinical phenotype as normal mice with increased Th2 parameters*

Table 1.2 Summary of phenotype of IFN γ *R$^{-/-}$ mice in comparison with wild type mice in different models of virus infection* (adapted from Tau and Rothman, 1999)

1.4 Fibrosis

Fibrosis is characterised by disordered accumulation of extracellular matrix in and around inflammatory or damaged tissue, and leads to scarring and loss of function (Wynn and Ramalingam, 2012). It was reported in the USA that 45% of human mortality is associated with fibrosis (Wynn, 2004). Fibrosis can be induced by many factors, and the site of occurrence varies according to the situation. In humans, the major fibrotic diseases include cirrhosis, idiopathic pulmonary fibrosis (IPF), systemic sclerosis (SS), atherosclerosis, pancreatic fibrosis, rheumatoid arthritis, and glomerulonephritis. Fibrosis was once considered to be irreversible, and there is currently no effective cure for fibrosis. However, recent studies suggest that fibrosis can be reversed to a great extent. This has been confirmed in several studies on fibrosis diseases under different circumstances and in different organs including kidney (Eddy, 2005), lung (Mizuno et al., 2005), and liver (Iredale et al., 1998). The multi-organ fibrosis observed in IFNγR$^{-/-}$ mice induced by MHV-68 infection, including lung, liver, and spleen, shows pathological similarities with human fibrosis (Ebrahimi et al., 2001). Especially, it raises the possibility to generate small animal models to study viral infection associated fibrosis. Therefore in this section, we first introduce the general mechanism of fibrosis, then discuss virus–associated human fibrosis in the lung and liver, and finally discuss the study based on the fibrosis model in MHV-68 infected IFNγR$^{-/-}$ mice.

1.4.1 Mechanisms of fibrosis

Although the origin of collagen-producing myofibroblasts varies in different organs (e.g., in the liver HSC cells are the main origin of myofibroblasts, whereas in lung fibrosis resident mesenchymal cells and epithelial cells are the main origin), fibrosis in different organs generally shares a common cellular and molecular basis (Wynn, 2008). As a response to the various stimuli, inflammatory infiltrates, including platelets, macrophages, neutrophils, eosinophils, plasma cells and T cells, accumulate at the site of tissue damage. These cells

generate a series of pro-fibrotic factors such as platelet-derived growth factor (PDGF), tumour necrosis factor-α (TNF-α), IL-1β, and TGF-β. A Th2 immune response which is dominated by production of cytokines IL-4 and IL-13 is crucial for the development of fibrosis (Wynn, 2004).

1.4.1.1 The key mediator: Transforming growth factor (TGF-β)

As one of the key regulators of the development of fibrosis, TGF-β has been intensively studied. There are 3 isoforms of TGF-β found in mammals, TGF-β1 to 3, and their functions appear to be very similar (Gorelik and Flavell, 2002). Among them, TGF-β1, which is mainly produced by circulating monocytes and tissue macrophages, is most involved in fibrosis. TGF-β1 is produced as an inactive form and stored inside the cell. Its activation and binding to its receptor requires cleavage of the latent form, which involves disassociation of latent associated protein (LAP). Several agents, such as macrophage derived plasminogenactivator, matrix metalloproteinase (MMP), cathepsins, alpain, thrombospondin, and integrin-αvβ6, participate in the activation of TGF-β1, and many of them make potential targets for anti-fibrosis drugs (Gorelik and Flavell, 2002; Letterio and Roberts, 1998; Munger et al., 1999). Activated TGF-β1 is secreted into the intracellular environment, binds to target cells, and regulates the transcription of many important genes, such as procollagen I and III, through transmembrane receptor signaling and intermediate functions of Smad proteins (Roberts et al., 2003). Generally, TGF-β1 directly activates local mesenchymal cells and epithelial cells which undergo epithelial- mesenchymal transition (EMT), and then these cells differentiate into collagen-producing myofibroblasts. However, fibrosis can be induced by other mediators such as Th2 cytokines IL-13 in a TGF-β independent pattern (Kaviratne et al., 2004). Therefore, Th2 cytokines mediate fibrosis by either an independent mechanism, or by triggering TGF-β1 production and activation in macrophages (reviewed inWynn, 2008).

1.4.1.2 The platelet –derived growth factor (PDGF)

The PDGF family of proteins plays an important role in fibrosis as a major mitogen and chemoattractant for mesenchymal cells (Yi et al., 1996). It is produced by many types of cells including activated macrophages, smooth muscle cells, and endothelial cells (Shimokado et al., 1985). There are 4 isoforms of PDGF (PDGF-A, -B, -C, -D); in fact, they are dimeric glycoproteins and form dimers in the form of -AA, -BB, -CC, -DD chains, or a heterodimeric isoform of -AB. Many types of cells, including fibroblasts and smooth muscle cells, express PDGF receptors on the cell surface. There are two types of PDGF receptors, PDGF-α and –β (Matsui et al., 1989); the alpha type binds to PDGF-AA, PDGF-BB, and PDGF-AB, while the beta type PDGFR binds to PDGF-BB and PDGF-AB (Heidaran et al., 1991). The ligand binding activates the receptor, leading to auto-phosphorylation and subsequent signal transduction (e.g., PI3K and JAK/STAT pathway) (reviewed in Ostendorf et al., 2012). Downstream effects include regulation of gene expression and the cell cycle. The smooth muscle cells and fibroblasts which respond to PDGFs may lead to vascular pathologies and fibrotic scarring (Andrae et al., 2008). PDGF has been linked to pulmonary, hepatic, cardiac, and dermal fibrosis, and functions as mitogen for myofibroblast-phenotype cells (Bonner, 2004).

1.4.1.3 The roles of Th2/Th1 immunity in fibrosis

Pro-fibrotic functions of Th2 immunity

The Th2 cytokines such as IL-4, IL-5, and IL13 are considered the key driving force of the development of fibrosis. IL-4 has been found to be elevated in patients with IPF (Emura et al., 1990). Many human and murine fibroblastic cells have the IL-4 receptor (Sempowski et al., 1994; Doucet et al., 1998). One of the functions of IL-4 is inducing collagen synthesis in fibroblasts (Fertin et al., 1991). *In vitro*, IL-4 treatment elevates production of collagen I and III and fibronectin in human lung fibroblasts (Doucet et al., 1998). *In vivo* experiments show that neutralising IL-4 diminishes the development of liver fibrosis (Cheever et al., 1994). A

similar study in a skin model found that IL-4 inhibition reduces fibrosis (Ong et al., 1998). IL-13 shares similar functions and even part of the signaling pathway with IL-4 (Zurawski et al., 1993), and accumulating evidence suggests a role of IL-13 as dominant cytokine in the development of fibrosis (Chiaramonte et al., 1999). The mechanism by which IL-13 induces fibrosis is still under debate: some studies show that IL-13 regulates production of TGF-β (Lee et al., 2001a), while others show that the function of IL-13 is independent of TGF-β (Liu et al., 2011), and it may directly regulate the activity of fibroblasts, epithelial cells, and smooth muscle cells (Lee et al., 2001b). IL-5 is shown to be associated with the differentiation, activation and circulation of eosinophils which produce a series of profibrotic cytokines including TGF-β and IL-13. *In vivo* study using bleomycin-induced fibrosis in IL-$5^{-/-}$ mice shows that IL-5 may not be a direct mediator of fibrosis in this particular fibrosis model, but most likely is an enhancer which exacerbates the disease (Huaux et al., 2003).

Anti-fibrotic functions of Th1 immunity

It has been demonstrated that Th1 immunity has anti-fibrotic activity, which is mainly related to the production of IFNγ (Baroni et al., 1996; Oldroyd et al., 1999). IFNγ producing NK cells have a similar anti-fibrotic function (Kim et al., 2005; Jeong et al., 2008). Th1 cytokine IL12 also shows anti-fibrotic functions by enhancing the expression of IFNγ. One of the important roles of IFNγ is limiting the Th2 cell population and therefore the production of Th2 cytokines (discussed above). Furthermore, IFNγ inhibits the function of TGF-β1by down-regulating the phosphorylation of the signal transducer Smad3 and, as a consequence, suppressing the downstream expression of pro-collagens I and III. IFNγ also induces production of Smad7, which suppresses interactions between Smad3 and TGF-β receptors. Moreover, IFNγ directly inhibits fibroblast proliferation, as well as down-regulates collagen production in myofibroblasts (reviewed in Gurujeyalakshmi and Giri,

1995). There is also evidence that IFNγ prevents circulating monocytes differentiating into fibrocytes, one of the cell origins of myofibroblasts in organ fibrosis (Shao et al., 2008).

Apart from Th1/Th2, which has long been discussed as a paradigm in the formation of fibrosis, Th17 and Treg immunity have been recently associated with fibrosis. A subset of Th17 CD4+ T cells which express IL-17A, which is a pro-inflammatory cytokine, have been shown to play an important role in fibrosis. IL-17A has been related to fibrosis in the lung (Wilson et al., 2010), liver (Wang et al., 2011), and heart (Feng et al., 2009). Moreover, it is already known that T_{reg} cells are also induced in many fibrotic diseases; however, the function of T_{reg} cells associated with fibrosis is still unclear.

1.4.1.4 Cell origins for fibrosis

The key cell in fibrosis is the myofibroblasts, which produces collagen once activated. The known cell origins of myofibroblasts include local resident mesenchymal cells such as fibroblasts, epithelial and endothelial cells which undergo epithelial/endothelial-mesenchymal transition, and fibrocytes which are circulating cells derived from bone-marrow stem cells (reviewed in Wynn, 2008). Epithelial cells can differentiate into myofibroblasts through a process termed epithelial- mesenchymal transition (EMT) (Willis et al., 2006), while endothelial cells undergo a similar process termed endothelial-mesenchymal transition (EndMT) (Zeisberg et al., 2007). Bone marrow derived fibroblastic-like cells are also identified as another origin of myofibroblasts (Bucala et al., 1994), and these cells circulate and contribute to fibrosis in multiple-organs (Direkze et al., 2003; Forbes et al., 2004). The origin of myofibroblasts may vary according to the site of fibrosis: fibroblast is generally the main origin of myofibroblast in kidney fibrosis; in the liver, one type of mesenchymal cell, the hepatic stellate cells (HSC), is considered to be one of the main sources of myofibroblasts, while circulating fibrocytes also contribute (Forbes et al., 2004; Russo et al., 2006). The function of circulating fibrocytes raises a question: what is the driving force for these cells to travel to the injured location? Studies have suggested that

chemokines play an important part in the development and recruitment of myofibroblasts. For example, chemokine CCL3 is mainly produced by macrophages and epithelial cells, and anti-CCL3 antibodies can reduce the pulmonary fibrosis induced by bleomycin (Smith et al., 1995).

1.4.1.5 Alternative regulatory functions of macrophages in fibrosis

Generally, macrophages are considered as the master controller of fibrosis. Accumulating evidence indicates that macrophages play an important role in both induction and resolution of fibrosis.

The pro-fibrotic mediators produced by macrophages TGF-β and PDGF directly activate differentiation into myofibroblasts from different cell origins. As discussed above, TGF-β is an important inducer of fibrosis in multiple-organs. Take liver fibrosis as an example: TGF-β mediates fibrosis by: (1) up-regulating the differentiation from HSC into myofibroblasts, (2) increasing the expression of tissue inhibitors of metalloproteases (TIMP) which inhibit MMPs the functions of which include degrading ECM, and (3) directly up-regulating collagen-related genes through the Smad pathway (reviewed in Bataller and Brenner, 2005). PDGF functions as a mitogen to promote proliferation of myofibroblasts (Friedman and Arthur, 1989). Previous research shows that macrophages are critical producers of pro-fibrotic factors in both the liver (Wahl et al., 1990) and the lung (Bonner et al., 1991). In fibrosis which involves infection, macrophages function as APCs presenting antigens to activate T-cell response, which in turn, may enhance fibrosis by triggering cell death (e.g., CTL targeting infected cells) or producing pro-fibrotic cytokines such as IL-4 and IL-13. Moreover, chemokines produced by macrophages can attract fibroblasts, circulating bone-marrow derived fibrocytes and other inflammatory cells.

On the other hand, previous studies have shown that macrophages also have anti-fibrotic functions. For example, in a study of carbon tetrachloride-induced liver fibrosis in transgenic mice in which macrophages could be selectively deleted, removal of macrophages during

advanced fibrosis led to reduced scarring and fewer myofibroblasts, whereas by contrast macrophage depletion during the recovery phase led to a failure of matrix degradation (Duffield et al., 2005). This result suggests the existence of subpopulations of macrophages with distinct functions in the same tissue and that these macrophages play critical roles in both the injury and recovery phases of inflammatory scarring (Duffield et al., 2005; also reviewed in Wynn and Barron, 2010). Macrophages can regulate the progress of fibrosis by controlling production of both MMPs and TIMPs (Tissue inhibiters of MMPs). The function of MMPs was thought to be degrading extracellular matrix proteins. For example, MMP9 degrades the basement membrane so that the inflammatory cells can be easily recruited (Wynn, 2008). However, recent studies suggest multiple modulatory roles performed by MMPs (and therefore macrophages) during fibrosis can be much more complicated than expected. Some of the MMPs are required in the activation of TGF-β (discussed above). However, recent research has shown that MMP12 produced by macrophages enhances fibrosis by inhibiting the expression of other ECM-degrading MMPs such as MMP2 and MMP13 (Madala et al., 2010). The alternative functions found in MMPs reflect multiple roles of macrophages in fibrosis.

For their close association to Th2 type immunity and the fact that they are commonly observed in the lesion of advanced fibrosis, alternatively activated macrophages, also called M2 macrophages, have long been indicated to be pro-fibrotic. Compared with classically activated macrophages (M1) induced by IFNγ, M2 macrophages are activated by Th2 cytokines such as IL-4 and IL-13 and have distinct functions (Gordon and Taylor, 2005). This phenotype expresses a series of factors such as CD206 (mannose receptor), chitinase-3-like protein-3 (Ym1), resistin-like molecule-α (FIZZ-1), MHC II, and arginase-1 (Arg 1). Arginase 1 is an enzyme which controls L-proline production, and the latter is necessary for collagen synthesis in myofibroblasts (Hesse et al., 2001). Therefore M2 cells have long been indicated to be pro-fibrotic by their response to Th2 signals, suppression of Th1 type

immunity, attraction of fibroblasts, and direct production of fibrosis mediators (Song et al., 2000). However, more recently, emerging evidence has shown that alternatively activated macrophages may pay an important role of suppressing fibrosis. Mice with cre-lox recombination which results in IL4R-α depletion show that the Th2 immune response and the formation of liver fibrosis induced by *Schistosoma mansoni* infection do not require M2 cells (Herbert et al., 2004), which suggests that IL-13 activated HSC is more likely to be the main cause of fibrosis. More interestingly, the function of Arginase 1-expressing macrophages is shown to be the suppression rather than promotion of Th2 immunity and pathology in the liver (Pesce et al., 2009a). One possible mechanism of this suppressive function is that macrophage-specific Arginase 1 competes for L-arginine (L-arginine is required for the production of L-proline and polyamines) with fibroblasts and Th2 cells and subsequently inhibits the function of Th2 cells and the development of fibrosis (Pesce et al., 2009a). However, whether this unexpected role of alternatively activated macrophages is consistent in fibrosis of other organs remains unclear.

1.4.2 Idiopathic pulmonary fibrosis (IPF)

Idiopathic pulmonary fibrosis (IPF), also called cryptogenic fibrostic alveolitis (CFA), is a progressive fibrotic lung disease with no known cause. It is characterised by fibroblast hyperplasia and excess collagen disposition, leading to loss of lung function. Forty-two per cent of patients die within 5 years and there is no existing method to cure IPF or improve the quality of life of patients except lung transplant (Lok et al., 1998; Nonn and Garrity, 1998). Risk factors associated to IPF include age, smoking, occupational dust exposure, genetic factors, and viral infection.

1.4.2.1 Viral aetiology of IPF

Previous studies suggested a viral aetiology of IPF, and the possible mechanisms include viral induced lung injury or exacerbating fibrosis. HCV, adenovirus, human

cytomegalovirus, and EBV are reported to be linked with IPF (Borchers et al., 2011). The link between herpesviruses and IPF was first found in EBV, when elevated levels of EBV-specific IgG and IgA antibodies in IPF patients were detected, compared to patients with known fibrotic diseases (Vergnon et al., 1984). In addition, EBV was found to actively replicate within alveolar epithelial cells in IPF patients (Egan et al., 1995). *In vitro,* EBV infection results in an increase in the activated fibrosis mediator TGF-β in type 2 human alveolar epithelial cells (Malizia et al., 2008). In addition to EBV, HCV is shown to be associated with IPF. The proportion of IPF patients who are seropositive for HCV is higher than in control groups (Meliconi et al., 1996; Ueda et al., 1992). Moreover, 15 out of 6,150 HCV patients developed IPF during 8 years' observation, while none of the 2,050 patients with HBV developed IPF (Arase et al., 2008). Thus, these data indicate the possibility that apart from inducing liver fibrosis and cirrhosis, HCV infection in the long term may also contribute to lung fibrosis. However these investigations are controversial: a study in the UK failed to link HCV to IPF, which may reflect regional differences (Irving et al., 1993).

1.4.2.2 Pathogenesis of IPF

The pathogenesis of IPF has been studied intensively although there are major questions yet to be answered. Recent hypothesis involves repeated epithelial injury which leads to alveolar epithelial cells being activated. Subsequently, fibroblasts are attracted and activated at the site or around the injury, where they differentiate into myofibroblasts (reviewed in Borchers et al., 2011). These cells in IPF lungs are highly responsive to pro-fibrotic mediators including growth factors (TGFβ), chemokines (CCL2 and CCL21), and cytokines (IL-13) (Hetzel et al., 2005; Murray et al., 2008; Pierce et al., 2007).

The number of myofibroblasts is remarkably increased in IPF lungs. Alveolar epithelial cells overlying the fibroblastic foci express CXCL12, which binds to CXCR4 on fibrocytes (Mehrad et al., 2007). The number of these bone marrow-derived circulating collagen producing cells is significantly increased in the peripheral blood of IPF patients (Moeller et

al., 2009). These results suggest that circulating fibrocytes contribute to IPF, and alveolar epithelial cells at certain stage can recruit fibrocytes into the site of pathology. Furthermore, some alveolar epithelial cells undergo epithelial-mesenchymal transition (EMT) and contribute to the myofibroblast population in IPF lungs (Larsson et al., 2008).

Immunohistochemical study shows that there are more apoptosis in IPF lungs (Plataki et al., 2005). Interestingly, however, cultured fibroblasts from IPF lungs are resistant to apoptosis which induced by Fas (Moodley et al., 2004) or plasminogen (Chang et al., 2010). This suggests the fibrosis-associated cells can survive with specific anti-apoptosis strategies, while fibrosis leads to apoptosis of functional cell in the lung during IPF. The structure of lung epithelium is severely destroyed in IPF lungs. In some cases, the epithelium completely disappeared, while in others, cuboidal type 2 cells replaced squamous type 1 cells (reviewed in Borchers et al., 2011). Although several studies have shown that alveolar epithelial cells may undergo excessive apoptosis (Lepparanta et al., 2010; Tzouvelekis et al., 2007; Uhal et al., 1998), it is still under debate in which type of cells the first injury occurs. Morphological studies suggest that type 2 alveolar epithelial cells in the unaffected area in IPF lungs undergo apoptosis is detected in this type of cells (Barbas-Filho et al., 2001; Waisberg et al., 2010). However, in other studies, apoptosis was observed in both alveolar and bronchiolar epithelial cells, which is associated with elevated expression of apoptotic factors (e.g p53, p21, bax, and caspase-3) and inhibition of the expression of anti-apoptotic factors (e.g bcl-2) (Plataki et al., 2005). Fas-mediated pathway of apoptosis and perforin/granzyme B mediated apoptosis may contribute to the cell death of epithelial cells (Kuwano et al., 1999; Maeyama et al., 2001; Miyazaki et al., 2004).

1.4.3 Liver fibrosis

Liver fibrosis, also including biliary fibrosis, is a sequel of chronic liver disease. As IPF, liver fibrosis occurs as an abnormal response to persistent injury. Wound healing process initiates after the injury occurs, in which parenchymal cells replace damaged liver cells and

rebuild the ECM while inflammatory cells clean the debris of the dead cells. However, in the presence of persistent injury, a disordered wound healing process may lead to over production of ECM and disrupt the liver architecture. There are multi aetiologies of liver fibrosis which include viral hepatitis, alcohol, and non-alcoholic fatty liver disease (reviewed in Hayashi and Sakai, 2011).

1.4.3.1 Viral hepatitis fibrosis

Chronic infection of hepatitis B, C or D can lead to liver fibrosis. Every year, there are 170 million people affected by HCV infection and 300,000 deaths due to the subsequent cirrhosis and hepatocellular carcinoma in the world (Poynard et al., 2003). Pathologically, viral hepatitis fibrosis is characterized by lymphocytes infiltration, piecemeal necrosis of hepatocytes, and fibrosis in the periportal areas (reviewed in Hayashi and Sakai, 2011).

1.4.3.2 Recent studies on liver fibrosis

Unlike lung fibrosis, in the liver quiescent hepatic stellate cells (HSCs) are one of the major cell origins of fibrogenic myofibroblasts in the liver (reviewed in Wallace et al., 2008). Current studies have made great progress in studying pathogenesis and searching for potential mechanism leading to the reversal of liver fibrosis, with special attention on HSCs. In a mouse model of liver fibrosis induced by CCl4, some resolution was observed in 4-6 weeks after stop of dosing (Iredale et al., 1998), which is due to a rapid loss of myofibroblasts by apoptosis (Friedman, 2008). This result is confirmed in another mouse model (Issa et al., 2001). Interestingly, the survival of myofibroblasts depends on local ECM. The contact between myofibroblasts and collagen 1can increases cell survival and pro-fibrotic activity (Zhou et al., 2004). In addition, MMPs-TIMPs regulation is also shown to be important in the reversal of fibrosis. A rapid decrease of TIMPs during resolution, suggests an enhanced function of MMPs which is degrading the ECM (Iredale et al., 1998; Issa et al., 2004). Overexpression of TIMP-1 exacerbates liver fibrosis and leads to failure of resolution (Yoshiji et al., 2002). Moreover, TIMP-1 shows a function of preventing

myofibroblasts undergo fibrosis (Elsharkawy et al., 2005). These studies suggest that TIMPs-MMPs regulation is a key factor in liver fibrosis and inhibiting TIMPs may promote resolution of fibrosis.

1.4.4 Animal models for studying virus induced fibrosis

To overcome the limitations of studying viral- associated IPF in humans, animal models were developed to study the pathogenesis and test potential therapies. Bleomycin and FITC have been widely utilised to establish mouse models for pulmonary fibrosis (Moore and Hogaboam, 2008). A murine model for viral-induced fibrosis has been established using MHV-68, which is very close to EBV in humans. In immune-competent mice, MHV-68 infection can exacerbate existing fibrosis (McMillan et al., 2008), as well as augment fibrosis induced by other factors such as FITC (Vannella et al., 2010).

Research on transgenic mice which lack IFNγR$^{-/-}$ mice shows MHV-68 infection alone can trigger pulmonary fibrosis (Ebrahimi et al., 2001). This then becomes a good animal model for viral- induced IPF, because some IPF patients show a Th2-dominated immune response (Wallace et al., 1995). Generally, the development of lung fibrosis in IFNγR$^{-/-}$ mice shows similarities to human IPF, including collagen deposition, increased TGF-β, and viral persistency in type 2 epithelial cells, which suggest the tissue damage caused by infection in these cells may be the cause of fibrosis (Mora et al., 2005). Moreover, the Th2 induced alternatively activated macrophages have been reported to be important in promoting MHV-68 infection induced lung fibrosis in IFNγR$^{-/-}$ mice (Gangadharan et al., 2008; Mora et al., 2006).

1.5 Project outline

The project aims to extend the investigation on the nature of MHV-68 infection in an environment dominated by an extensive tissue fibrosis. The research involves a detailed

understanding of host and virus mechanisms operating in the spleen of MHV-68 infected IFNγR$^{-/-}$ mice and particularly focusing on the viral latency in the spleen.

First, we confirm and extend the previous study on pathological changes and viral infection during latent infection.

Second, we investigate the mechanisms which result in the loss of splenocytes, in particular the reduction of latently infected B cells. The possible mechanisms investigated include excessive apoptosis and viral reactivation. We also examine the infection in each B cell subpopulations to explore the possible link between virus-manipulated germinal centre reaction and fibrosis.

Third, we investigate the dynamics of macrophages in the induction, expression, and recovery of fibrosis.

Chapter 2 Methods and materials

2.1 Mice

Wild type 129Sv mice and interferon gamma receptor knockout (IFNγR$^{-/-}$) mice (Huang et al., 1993) on the 129Sv background were purchased from B&K Universal (Hull, UK) and were bred at the University of Edinburgh Animal Facility.

Transgenic C57BL/6 mice (Macgreen mice) with insertion of a 7.2 kb promoter element of the c-fms gene with EGFP gene show green fluorescence in macrophage, trophoblast, and granulocyte lineages (Sasmono et al., 2003; Sasmono et al., 2007). Macgreen mice were obtained from Prof. David Hume of the Roslin Institute. In order to produce Macgreen IFNγR$^{-/-}$ and wild type mice on 129Sv background, Macgreen mice on C57BL/6 background were crossed with IFNγR$^{-/-}$ mice on 129Sv background. Heterozygotes of F1 generation were crossed to produce IFNγR$^{-/-}$ Macgreen mice and wild type Macgreen mice on a mixed background of 129Sv and C57BL/6. Mice were genotyped by PCR to identify Macgreen IFNγR$^{-/-}$, Macgreen wild type (IFNγR+/+), and Macgreen wildtype / IFNγR+/- (appear as IFNγR+/+), littermates matched as pairs. The work of cross-breeding and typing the mice was done by Dr B. M. Dutia and Mr Ian Bennet using the animal facility of Hugh Robson Building and Royal (Dick) School of Veterinary Medicine. All mice were housed under specific pathogen-free conditions, and mostly used in experiments at 8 to 12 weeks of age (unless otherwise stated).

2.2 Cell culture

Baby hamster kidney 21 (BHK-21) cells (Macpherson and Stoker, 1962) are a continuous fibroblastoid cell line which were cultured in Glasgow modified eagle's medium (GMEM, Invitrogen, UK) with 10% NBCS, 10% tryptose phosphate broth (TPB, Invitrogen, UK), 100u/ml Penicillin streptomycin (Pen-strep, Invitrogen, UK), and 2mM L-glutamine (L-G, Invitrogen, UK).

Master stocks of cells were stored in FCS (with 10% DMSO) in liquid nitrogen. When required for working stocks, the cells were thawed rapidly at 37ºC. Pre-warmed media was added slowly to the cells followed by centrifuging at 1500rpm for 5 minutes. Cell pellets were re-suspended in 5–10ml of media and cultured in sterile plastic-ware (Nunc, UK) and incubated at 37ºC with humidified 5% CO_2. Cells were sub-cultured when they reached 80% confluent growth by incubating in 0.25% trypsin (Invitrogen, UK) until the cells could be removed from the surface of the flask by gentle tapping. The trypsin was then diluted by adding an equal volume of medium, and cells with diluted medium were collected in plastic universals in medium and centrifuged at 1200rpm for 5 minutes. The cell pellets were re-suspended in growth medium. The number of cells was determined by mixing them 1:1 with 0.1% Trypan Blue, then counting using a haemocytometer and optical microscope. Approximately 5×10^6 cells were reseeded into a T175 flask in 40ml of medium.

2.3 Viral stock preparation, titration, and infection of mice

2.3.1 Viral stock preparation

Working stocks of MHV-68 were prepared by infection of BHK-21 cells in GMEM (Invitrogen, UK) with 10% NBCS, 10% TPB, 100u/ml Pen-strep, and 2mM L-G. The virus was added to cells at a multiplicity of infection (MOI) of 0.001 plaque forming unit per cell, followed by incubation at 37ºC for 90 minutes. Then 3×10^6 cells were plated into each T175 flask. Infected cells were incubated at 37ºC until plaques had formed and the cell monolayer started to fall off (about 6 days). Cells carrying the virus were made pellets by centrifugation at 1300 x g for 20 minutes at 4ºC. The pellets were homogenised by grounding in a sterile dounce homogeniser and then sonicating in an ice bath for 15 minutes. The homogenised mixture was then centrifuged at 1300 x g for 20 minutes at 4ºC. The supernatant was collected and the remaining was re-suspended. Homogenisation was repeated once followed by centrifugation at 1300 x g for 20 minutes at 4ºC. Supernatant were pooled together with

the lysate collected from the last step, which carried the majority of the virus. The viral stock then was aliquoted and titrated. All viral stocks were stored at -80ºC.

Genetically modified virus mLANA-MHV68 (Nealy et al., 2010) working stock was obtained from Scott Tibbetts's lab (Louisiana State University, USA) and was cultured as the same as wild type MHV68.

2.3.2 Titration

The virus was serially diluted in complete GMEM from 10^{-2} to 10^{-9} pfu/ml, 4ml each. To each dilution of virus were added 2×10^6 BHK cells, followed by incubation at 37ºC while shaking for 1 hour. For each dilution, 2 Petri dishes were set up by adding 2ml of infected cells to each. Two uninfected controls were set up at the same time. After incubation at 37ºC for 4 days, the medium was removed and the cells were fixed with 10% Neutral Buffered Formaldehyde and stained with 0.1% Toluidine blue. The number of plaques was counted for 3 dilutions and the titre was calculated by the equation below:

Titre = (number of plaques × dilution 1) + (number of plaques × dilution 2) + … / the lowest dilution × number of petri-dishes counted × final volume of each dish (2ml)

2.3.3 Infection of mice

Age-matched mice were anaesthetised using either Halothane or Isoflurane (Merial) and inoculated intranasally with either 4×10^5 or 4×10^3 pfu of virus in 40µl of sterile PBS. The infection was done by dropping the viral solution onto the mouse's nostrils. Mice were sacrificed by CO_2 asphyxiation on day 12, 16, 20, 24, 28, 32, 35, 48, and 60 post infection.

2.4 Spleen cell harvesting

Spleens were teased out of the capsule with a scalpel blade into RPMI medium (with 10% FCS, 2mM L-G, and 100µg/ml Pen-strep). Red blood cells were lysed by a quick mixing 2–

3ml of ddH_2O for 10–15 seconds, followed by rapid addition of 10–12ml of PBS or RPMI media to prevent destruction of the lymphocytes. The cells were pelleted by centrifugation at 1500rpm for 5 minutes and re-suspended in fresh medium. In certain circumstances, collagenase digestion was applied to release cells from fibrotic spleens using Liberase TL research grade (Roche) (alternative: Collagenase 4). Spleen tissue was finely chopped with a scalpel in a small amount (1–2.5ml for each spleen) of digestion buffer (PBS with 5% Pen-strep, 1.8mM $CaCl_2$, and 1mM $MgCl_2$). Liberase and DNase solution were added and followed by an incubation of 20 minutes at 37ºC with horizontal shaking. The digestion was stopped by adding 1ml of EDTA stop solution (0.1M EDTA pH7.3) and mixing. Cells were washed and re-suspended for the next step. The number of splenocytes was determined by mixing them 1:1 with 0.1% Trypan Blue, then counting using a haemocytometer under optical microscope.

2.5 Cell selection by magnetic beads (MACS)

CD19 Microbeads (mouse, Miltenyi, 130-052-201) were used to select spleen B cells from the spleen cell suspension. For each sample, the total cell number and the proper amount of suspension for selection was determined. Before selection, cells were suspended in 90 µl MACS buffer (which contains PBS pH7.2, bovine serum albumin 0.5% [w/v] and EDTA 2mM within a total volume of 1.5L) per 10^7 total cells, and 10µl CD19 Microbeads were added per 10^7 total cells. The mixture was incubated for 15 minutes at 4–8ºC, after which the cells were washed with MACS buffer and re-suspended in 500µl of MACS buffer. Then samples were applied to the top of prepared MACS columns which were set up on a magnetic cell selector. The columns were then removed from the magnet and selected cells were collected by adding 1ml MACS buffer and flushing through with a plunger. The cell number after selection was determined and 10,000 selected cells were preserved for flow cytometry. Selected cells were then pelleted by centrifugation and stored at -70ºC. CD11b

Microbeads (mouse/human, Miltenyi, Germany) were used to select macrophages by the same method described above.

The purity of selected cells was tested by flow cytometry. Cells from CD19 Microbeads positive selection were stained using CD 45R (B220)-FITC antibody (mouse, Miltenyi, Germany). Cells were then fixed with 2% (v/v) formaldehyde and stored in the dark at 4ºC before FACS analysis. Selected macrophages were tested using CD11b-APC Antibody (mouse/human, Miltenyi, Germany).

2.6 DNA extraction

2.6.1 DNA extraction from spleen tissue using DNeasy tissue kit

RNAlater treated spleen tissues (up to 30mg) were stored at -70ºC and were defrosted on ice, and then roughly disrupted into small pieces. The purpose of RNAlater treatment was to prevent RNA degradation for other experiments, and according to the manufacturer, RNAlater does not affect DNA extraction. Total DNA was extracted using a DNeasy tissue kit (Qiagen) following the manufacturer's instructions. First, buffer ATL with Proteinase K was added, and samples were incubated overnight at 55ºC to disrupt the cells. Then 200µl of Buffer AL was added, and samples were incubated at 70ºC for 10 minutes. To precipitate DNA 200µl ethanol was added and the mixture was loaded onto the spin column, followed by centrifugation at 11300 x g for 1 minute. The column was washed once with buffer AW1, and washed again with buffer AW2. Finally, DNA was eluted within 100µl buffer AE. The concentration of DNA extracted was then tested by Nanodrop spectrophotometer.

2.6.2 DNA extraction from 96-well microtiter plates

This method is adopted from *Molecular Cloning: A Laboratory Manual*, third edition, chapter 6.19, protocol 4: isolation of DNA from mammalian cells grown in 96-well microtiter plates. Briefly, the correct amount of cells was added into each well, the plates

were first centrifuged and then the supernatant was removed by pipetting, followed by 2 washes in PBS. Then 100µl cell lysis buffer (10mM NaCl, 10mM Tris-Cl pH7.5, and 10 mM EDTA Ph8.0, 0.5% SDS, Proteinase K 100µg/ml) was added into each well, followed by overnight incubation at 60ºC in an oven or water bath in a sealed humid box. After cooling down to room temperature, 100µl of NaCl/ethanol solution (add 100µl of 5M NaCl per 10ml of absolute ethanol; store at -20ºC) was added. Plates were then left on the bench without mixing for 30 minutes at room temperature until a stringy precipitate of nuclear acid was formed. The solution was then decanted by slowly inverting each plate over a sink or towel papers while the precipitate remained in the wells. The remaining ethanol was drained by placing the plates upside down on a bed of dry towels for a short time. To wash the precipitates, 150µl of 70% ethanol was slowly added to each well, and drained in the same way as described above (repeat 3 times). The plates were dried at room temperature until the rest of the ethanol had evaporated. Total DNA was eventually dissolved in 50µl of TE (pH8.0) buffer by gentle rocking for 12–16 hours at room temperature. The concentration of DNA extracted was tested by Nanodrop spectrophotometer.

2.7 Extraction and quantification of total RNA

2.7.1 Total RNA extraction from spleen tissue or cell pellet

Spleen tissue was preserved in RNAlater at 4ºC overnight, then removed from RNAlater and stored at -70ºC until use. Cells were made pelleted by centrifugation. Supernatant was decanted and stored at -70ºC. Total RNA was extracted using RNeasy mini kit (Qiagen) following the manufacturer's instructions. For samples less than 10^6 cells, RNeasy micro kit (Qiagen) were used to extract total RNA. Spleen tissue (around 30mg) was disrupted and homogenised using a blue pestle (Sigma) in 600µl buffer RLT with 1/100 volume of β-Mercaptoethanol, followed by centrifugation passing though Qiashredder homogeniser (Qiagen). The clear lysate was centrifuged at the speed of 11300 x g for 3 minutes, and then

the supernatant was transferred into a 1.5 centrifuge tube. For extraction from cells, buffer RLT was added directly to re-suspend and make cell lysate. Then 600 µl of 70% ethanol was added and mixed immediately. The mixture was loaded into an RNeasy spin column, and then centrifuged for 15 seconds at 11300 x g, and flow-through liquid was discarded after centrifugation. The rest of the sample was loaded onto the same column by repeating the last step. The column was washed by adding buffer RW1. DNA contamination was eliminated by on-column DNase digestion (Qiagen), followed by washing twice in Buffer RPE. Total RNA bound on the silicon net was eluted by adding 30µl to 50µl (varies according to starting materials) RNase free water then spinning down.

2.7.2 RNA quality test and quantification

For reverse transcription, RNA quality and concentration were tested by both nanodrop spectrometer (Thermal) and Agilent nano/pico RNA microchip (Agilent).

2.8 Reverse transcription

SuperScript III Reverse Transcriptase Kit (Invitrogen, UK) and Random Primers (500µg/ml, Promega) were used in first-strand cDNA synthesis. For each 20µl reaction, 500ng to 1ul of RNA, 1ul of random primers (500µg/ml), and 1ul of dNTPs (10mM) were added first, and incubated at 65ºC for 5 minutes and 1 minute on ice. Then the following reaction components were added:

5×first strand buffer	*4ul*
0.1M DTT (0.1M)	*1ul*
RNase OUT (40 U/ µl)	*1ul*
Superscript III (200 U/ µl)	*1ul*

Samples were left at room temperature for 5 minutes, 50ºC for 60 minutes, and 70ºC for 15 minutes. The cDNA were aliquoted and were kept at 4ºC for immediate use, or at -20ºC for long-term storage.

2.9 Determination of suitable housekeeping genes in spleen B cells

Twelve candidates for reference gene(s) were tested to find the most stably expressed gene(s) in spleen B cells in wild type and IFN-γ $R^{-/-}$ mice in different stages of MHV-68 infection. Mouse Normalisation Gene Panel (Quantace) and standard curve materials (PCR product with known copy number) for 12 housekeeping genes were adopted from Gillian Campbell from Nash/Dutia lab. Groups of cDNA samples were tested as follows:

	Uninfected	Day 12 post infection	Day 20 post infection
Wild type	3	3	3
γ-129 (IFN-γ $R^{-/-}$)	n/a	3	3

Table 2.1 The numbers of mice in each group tested

Real time PCR were carried out for 9 housekeeping genes using qPCR reagents from Roche Company.

	For 20μl reaction (ul)
Water	10.95
10×Buffer	2
dNTPs (10mM each)	0.4
$MgCl_2$ (2.5mM)	0.4
Primer pair (concentration varies depending on different targets)	0.4
Sybr Green	0.7
Faststart Taq (5U/ μl)	0.15

Table 2.2 Components of real time PCR reaction

GACTINE	Gamma actin, cytoplasmic
YWHAZ	Tyrosine 3-monooxygenase, zeta polypeptide
GAPDH	Glyceraldehyde-3-phosphate dehydrogenase
B2MG	B-2 microglobulin
RPL13A	Ribosomal protein L13a
PGK	Phosphoglycerate kinase 1
BACTIN	B actin cytoplasmic
RN18S	18S rRNA Genbank
UBQC	Ubiquitin

Table 2.3 Housekeeping candidates for real time PCR

Results analysis was performed using the software GeneX (Multi D).

2.10 PCR

Conventional polymerase chain reactions (PCR) to amplify housekeeping genes were performed to test the cDNA product. For each 50µl reaction, the PCR reagents included 5µl of 10×PCR buffer, 3 µl of 50mM magnesium chloride, 1 µl of 10mM dNTP mixture, 1ul of 10µM primer forward, 1 µl of 10uM primer reverse, 37 µl of water, 1 µl of cDNA, and 1 µl of Taq (5U/ µl storage concentration at 1:3 dilution for reaction). A hot start protocol was carried out as follows: 94ºC for 5 minutes, 80ºC hold (Taq added during holding), then denature at 94ºC for 45 seconds, anneal at 55ºC for 45 seconds, extend at 72ºC for 1 minute for 35 cycles, and the last extension under 72ºC for 7 minutes.

2.11 Quantitative PCR

qPCR were performed to test viral gene expression. The genes tested and primers' sequences are listed in appendix 2. qPCR for M1 and housekeeping gene YWHAZ were set up for this

project. qPCR for DNA polymerase, RTA, ORF73, and M11 were set up by Mr Ian Bennet in the Nash/Dutia lab.

2.11.1 Generating standard material for qPCR

Amplification using proofreading DNA polymerase

DNA segments were amplified using PfuTurbo DNA polymerase (Promega). A polymerase chain reaction was performed in a 50µl system. The components and reaction programme of a PCR reaction is listed in appendix 1. The PCR product was analysed by gel electrophoresis.

The addition of 3' adenine post-amplification

As amplification with Pfu will not result in the 3' A-overhang which is necessary for cloning using the pCR4-TOPO vector, it is essential to add 3' A-overhang to the amplified product. 1U of Taq polymerase was added into each PCR reaction, followed by incubation at 72ºC for 8–10 minutes. A sufficient number of PCR products with additional 3' adenine were generated for the next step. The products were placed on ice and were used in the cloning reaction immediately.

Cloning reaction and transformation

Cloning was performed using a TOPO TA Cloning Kit for Sequencing (Invitrogen) according to the manufacturer's instructions. The components are as follows:

Fresh PCR product *1ul*

Salt solution *1ul*

Water *3ul*

Topo vector *1ul*

The components were added and mixed gently, then incubated for 5 minutes at room temperature. The mixture was immediately used in transformation.

The ligated vector with DNA insertion was then transformed in One Shot TOP 10 chemically competent cells (Invitrogen) according to the manufacturer's instructions. For each reaction, one vial of competent cells was thawed slowly on ice before the addition of the cloning reaction product. Cells were incubated on ice for 30 minutes, followed by a 30-second heat shock at 42ºC.

The sample was immediately placed on ice. SOC medium was added, followed by incubation at 37ºC for 1 hour while horizontally shaking. LB plates with kanamycin (50µl/ml) were used to culture the transformed *E. coli* cells selectively, followed by incubation at 37ºC for 12–16 hours. At least 4 colonies were picked from each plate, and they were cultured in medium containing kanamycin (50µl/ml). Plasmids were extracted using a mini prep kit (Qiagen) and were first analysed by restriction endonuclease digestion (EcroRI, Promega) and gel electrophoresis. Sequencing of the inserted DNA segments was performed using M13 reverse and M13 forward primers. The sequencing reaction was performed as follows:

Big dye 1ul

5x sequencing buffer 1.5ul

Primer 3.2ul (1 pmol/ul)

Template DNA 1 ul

Water 3.3ul

The components were added and the reaction was performed:

1. 94ºC for 2 minutes

2. 96ºC for 10 seconds

3. 50ºC for 5 seconds

4. 60ºC for 2 minutes (30 cycles, step 2 to step 4)

5. 72ºC for 5 minutes

Sequencing was carried out by the SBS sequencing service (Ashworth Labs, Kings Buildings, University of Edinburgh).

Restriction endonuclease digestions using either NotI or SpeI (Promega) were carried out to linearise the circulated plasmid. The linearised PCR product was used as the standard material for qPCR.

Quantification of plasmid copy number

The concentration of DNA of extracted plasmids was determined by Nanodrop spetrophotometry (Thermal). The number of copies of plasmid was calculated using the following equation:

Copy number (/ul) = 6.032×10^{23} (copies/mol) × plasmid concentration (g/ul) / MW of whole plasmid (g/mol)

MW of whole plasmid (g/mol) = (Bp (insert) + Bp (vector)) × 660 dalton/bp

According to the copy number calculated, standard materials were aliquot and diluted into 10^9 copies/ul and stored at -20ºC until use.

Optimisation of qPCR

qPCR was performed in a Rotorgene 3000 qPCR machine (Qiagen) using the SYBR green method. SYBR green is an intercalating dye which generates green fluorescence when bound to double-strand DNA. Therefore, the levels of dsDNA amplified during PCR reaction are reflected by the level of fluorescence generated. Reactions were performed in a 20µl system in 0.1ml strip tubes (Qiagen), and consisted of the following:

PCR reaction buffer with 20mM $MgCl_2$

dNTPs (10mM each)

0.75U of Faststart Taq DNA polymerase (Roche)

0.7ul of SYBR green (1/5000 dilution in DMSO, Biogen Ltd)

5ul of DNA template (standard material or cDNA/DNA sample); concentration of DNA template added varies according to experiments.

In order to rule out the possibilities that the reaction system was contaminated or the florescent signal was generated by by-products such as dimers, 2 to 3 repeats of no-template controls were performed in each run. Instead of template DNA, 5μl of water was added.

The starting qPCR program is as follows:

95ºC for 5 minutes

94ºC for 20 seconds, 62ºC for 20 seconds (anneal temperature may vary), 72ºC for 20 seconds (repeat 45 cycles), acquire after each cycle.

Hold at 94ºC for 20 seconds.

Melt from 65ºC to 94ºC, rising by 1ºC for each step, wait for 45 seconds on first step, then wait for 5 seconds for each step afterwards, acquire in each step.

For each pair of specific primers, it is necessary to optimise the conditions of reaction, including primer concentration, Mg^{2+} concentration, and anneal temperature.

Primers at different final concentration, from 200nM to 600nM, were added into reactions, and the concentration in which the reaction amplified the most efficiently and generated the least primer dimmer was chosen. Similarly, different final concentrations of $MgCl_2$ (from 2.0 to 5.0) were tested. For the qPCR buffer, which already contained 2.0mM $MgCl_2$, the variable tested was the amount of additional MgCl2 needed for each reaction. Annealing temperature was originally set as 62ºC and was adjusted up or down within a range of 2ºC according to the primers used.

2.11.2 Absolute Quantification

Standard curves are required in absolute quantification. To generate a standard curve, standard material was diluted into 10^5 copies /μl and then serially diluted 10 times until 100 copies /μl in Tris buffer (1mM). There were 3 repeats for each dilution, and 5μl of DNA

template was added in each reaction. The qPCR was performed in the optimised condition, and standard curves were generated as in the example in Figure 2.1. A tolerance range of 0.93 to 1.05 was selected for efficiency of qPCR, and the R and R^2 values should be close to 1. The products were analysed by gel electrophoresis and sequencing.

Normalisation

According to the result of housekeeping genes selection, one of the cellular genes, YWHAZ, was selected. Normalisation with housekeeping gene was performed in order to eliminate the effect of starting material and the efficiency of reverse transcription. Considering the possibility that one cell may carry multiple viral genomes, the viral DNA was also used as a factor to normalise the viral gene expression, in addition to housekeeping gene normalisation. For each spleen sample, both total RNA and DNA were extracted (for method see DNA extraction). Reverse transcribed cDNA and total DNA extracted were both tested using the same pair of primers in qPCR. The data generated from total DNA represent the amount of viral genome in the same amount of spleen cells, and it was used to normalise the copy number of viral genes transcribed into total RNA.

Results analysis

Data processing and statistical analysis were carried out using Rotorgen 6 software (Invitrogen), GenEX (MultiD), and Excel (Microsoft).

2.11.3 Comparative quantification (ΔΔCt method)

Standard curve material is not required in the method of comparative quantification (ΔΔCt method). Instead, a mix of all cDNA samples was used as an inter-plate calibrator. The qPCR assays were optimised as absolute quantification, and the components and programming of the reaction was mostly similar to absolute quantification. The validation of the housekeeping gene is shown in Figure 2.2. Data processing and statistical analysis were carried out using Rotergen 6 software (Invitrogen), GenEX (MultiD), and Excel (Microsoft).

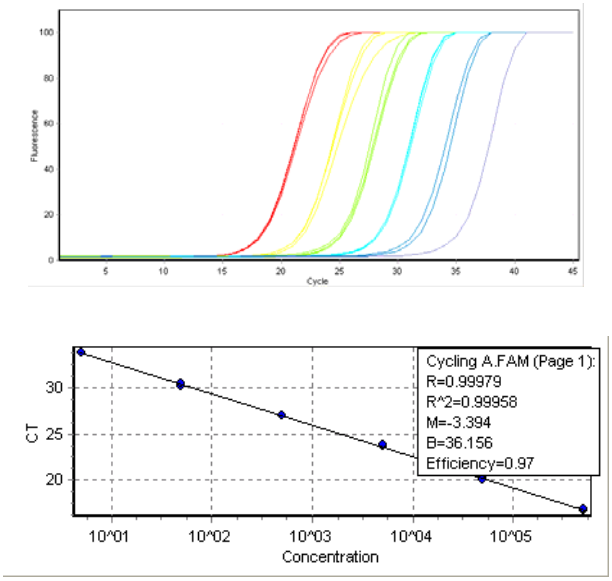

Figure 2.1 An example of a standard curve generated from qPCR assay for M1

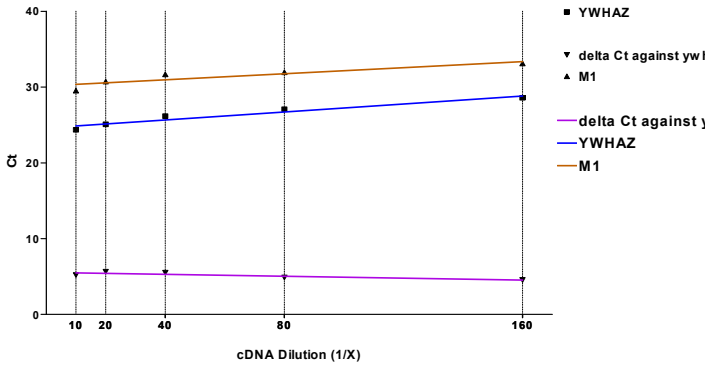

Figure 2.2 Validation of comparative quantification: comparison of qPCR efficiency of target gene and housekeeping gene. The calibrator (mixed cDNA sample) was serially diluted two-fold from 1/10 dilution to 1/160 dilution, similar to standard curves. qPCR was performed using both the gene of interest (GOI) and the housekeeping gene (HKG). The ΔCt value for each dilution was recorded and the ΔΔCt = ΔCtGOI – ΔCtHKG calculated. The purple line represents the linear regression of ΔΔCt changing according to the concentration of starting material cDNA. The slope of this line is close to 0, which means the efficiency of both primers is similar within the range of concentration of starting material tested. The housekeeping gene can only be used when the slope of ΔΔCt linear regression is less than 0.098.

2.12 Limiting dilution assay

IFNγR$^{-/-}$ and 129Sv mice were infected intranasaly with 4000pfu MHV-68 and spleens were harvested on day 28, day 40, and day 68 post infection. For each spleen sample, red blood cells were lysed by quick mixing with 3ml of sterile water, followed by the addition of sterile PBS up to 15ml in total, and whole-spleen cell suspension was prepared and the cell number was determined. For each spleen, in a 96-well plate, 10^6 spleen cells were added in the first row as positive control; 2×10^5 spleen cells were serial diluted twofold 10 times (8 wells/replicates for each dilution). As background, 9×10^5 BHK21 cells were added to each well. Cell mixtures were lysed and digested by proteinase K overnight and total DNA was extracted in each well according to the protocol described in section 2.6.2. For DNA samples from each well, PCR was performed using primers for MHV-68 ORF73 on Rotor-Gene 3000 thermal cycler (Qiagene), with positive and no-template controls for each run. Realtime PCR products were confirmed using melt curve analysis using Rotor-Gene 6 software (Qiagen).

Data were analysed using GraphPad Prism software. The frequencies of viral genome-positive cells were determined from nonlinear regression analysis of sigmoidal dose-response best-fit curve data. Based on Poisson distribution, the frequency at which at least one event in a given population is present occurs at the point where the regression analysis line intersects 63.2% (Nealy *et al.,* 2010).

2.13 Flow cytometry

2.13.1 Sample preparation

Spleen cell suspensions were prepared by scraping using a scalpel blade. For each spleen sample, red blood cells were lysed by quick mixing with 3ml of sterile water, followed by addition of sterile PBS up to 15ml in total. Pelleted spleen cells were adjusted to a

concentration of 2×10^7 cells/ml in FACS buffer (PBS, pH7.2, 1% FCS). For each sample, 2×10^6 cells/ml to 4×10^6 cells/ml (depending on cell number recovered from fibrotic spleens) cell suspension was preserved for FACS analysis and the rest were loaded with β-lactamase substrate for sorting. Spleen cells for analysis were first blocked by adding anti-mouse CD16/CD32 Fc block reagent (Stratagene), followed by incubation at 4ºC for 5 minutes. After blocking, the samples directly proceeded to the staining steps without a washing step in between.

2.13.2 Immunostaining

Florescence conjugated antibodies were added, then incubated for 30 minutes on ice in the dark. B-cell subsets used these antibodies: APC/Cy7-conjugated anti mouse CD19 (Clone 1D3, made in rat, Biolegend), APC-conjugated anti mouse CD38 (clone 90, made in rat, Biolegend), and biotin-conjugated anti mouse IgD (clone 11-26c, made in rat, Biolegend). For monocyte/macrophages and granulocytes labelling, APC conjugated anti-mouse CD11b (made in rat, Miltenyi) and PE conjugated anti mouse Ly-6G (made in rat, Biolegend) were used. After incubation on ice in a darkroom for 20 minutes, cells were washed by adding FACS buffer and mixing, then spinning down 3 times. PE conjugated streptavidin (Biolegend) were used as a secondary reagent to detect biotinlated anti IgD antibody and washed. Unstained control and single-stain controls were performed in each experiment.

2.13.3 Detecting β-lactamase

Cells were adjusted at a concentration of 1×10^7 cells/ml in FACS buffer. The CCF2/AM β-lactamase substrate loading kit (Invitrogen) was used according to the manufacturer's suggestions, as well as a published protocol (Nealy et al., 2010), and adapted as needed for our facilities and practical reasons. Freshly prepared CCF2/AM substrate (for CCF2/AM substrate 100µl 0.6 A +6 B mix and votex, then +93.4ºC, then votex again) was added for 5

minutes at room temperature. Cells were then washed in FACS buffer 3 times. Unstained and uninfected controls were performed in each experiment.

2.13.4 Analysis on flow cytometer

Flow cytometry was performed on FACS Aria III sorter (BD Biosciences) and the results were analysed using either Flowjo (Treestar) or FACS Diva (BD) software. For each spleen, 10^6 cells were used for B-cell staining and analysing, and another 10^6 cells were used for macrophage/granulocytes-staining and analysing. The rest of cells were loaded with substrate and both ORF73-β-lactamase positive and negative cells were sorted into RNAlater. Data were then analysed using GraphPad Prisim software (GraphPad software).

2.14 TUNEL Assay

Spleen tissue paraffin sections were deparaffinised in 2 changes of xylene for 5 minutes each, and hydrated with 2 changes of 100% ethanol for 3 minutes each and 95% ethanol for 1 minute. After rinsing sections and pre-treatment by proteinase K, endogenous peroxidase was blocked by incubating sections in 3% hydrogen peroxide decomposition in PBS for 10 minutes. After pre-incubation in reaction buffer for 10 minutes, a mixture of terminal transferase (New England BioLabs) and Biotin-16-dUTP (Roche Diagnostic) was applied for 2 hours at 37°C. The reaction was stopped by adding stop washing buffer (300mM NaCl, 30mM Sodium Citrate). Positive staining was then detected by streptavidin-POD (Roche, 1/1000 dilution) and DAB (Sigma). All slides were counterstained with hematoxylin to locate the cell nucleus, then re-dehydrated using 95% ethanol for 5 minutes and then 100% ethanol for 3 minutes two times, and cleared twice in xylene for 5 minutes before being covered with mounting medium and a coverslip. Slides were observed under an optical microscope and 10 pictures of continuous views were taken for each spleen. There were at least 3 mice in each group. The number of brown stained cells was counted to measure the level of cell death in the spleen.

2.15 Immunohistochemistry

2.15.1 Immunohistochemistry on paraffin embedded spleen sections

Paraffin sections were deparaffinised and rehydrated, and endogenous peroxidase was quenched as described in TUNEL assay. Antigen unmasking was carried out (according to primary antibody used) by bringing the slides to a boil in sodium citrate buffer (10mM, pH6.0); sub-boiling temperature was maintained for 10 minutes, then the slides were cooled down to room temperature. After blocking non-specific binding (Casblock or normal serum according to the secondary antibodies used, 1 hour), the primary antibody was applied at optimised concentration overnight at 4ºC. Biotin conjugated secondary antibodies were applied at optimised concentration for 1.5 hours at room temperature. Enzyme conjugate and substrate (DAB, Sigma) were applied, counterstained, and dehydrated as in the TUNEL assay.

Target	Pre-treatment	1st Antibody	2nd Antibody
B cells	Block with casblock	CD45R/B220 (rat IgG2a 1/300 diluted)	Rabbit anti-rat biotin conjugated (BA4000, 1/300 diluted)
Caspase 3	Antigen retrieval, block with casblock	Cleaved Caspase3 (cell signalling Rabbit mono IgG)	Goat anti-rabbit biotin conjugated (1/300 diluted)

Table 2.4 Reagents used in immunohistochemistry on paraffin sections

2.15.2 Immunohistochemistry on frozen spleen sections expressing EGFP

Tissue processing and sectioning

Spleens were harvested and fixed for 2 hours in 4% paraformaldehyde, followed by 18% (w/v) sucrose and 30% (w/v) sucrose until they sank to the bottom of the container. Fixed tissues were washed in PBS and embedded in OCT compound (Sakura Finetek). The

embedded tissues were quickly frozen by immersing the specimens in liquid nitrogen and kept at -70° C until sectioned. To protect the EGFP, all the processing and staining were carried out in the dark as much as possible.

The samples were sectioned using a Cryostat sectioning machine (Leica). Sections 10μm thick were cut and collected on poly-L-lysine pre-treated microscope slides (VWR). During sectioning, the material was kept at -16ºC and thawing was avoided. The sections were dried completely at room temperature before being stored at -70ºC.

Staining

After blocking non-specific binding (Casblock or normal serum according to the secondary antibodies used, 1 hour), primary antibody was applied at optimised concentration overnight at 4ºC. Isotype matched control antibodies were applied to show the possible unspecific binding of the primary antibody. Either a biotin conjugated or fluorophore conjugated secondary antibody was applied at optimised concentration for 1.5 hours at room temperature. Fluorophore conjugated streptavidin was used with the biotin conjugated sencondary antibody. Before applying any reagents, the slides were washed in the dark at room temperature 3 times for 5 minutes. DAPI (common nuclear dye, applied by Nash/Dutia lab, 1/10,000 dilution) was applied to counterstain cell nuclei for 3 minutes at room temperature in the dark.

Target	Pre-treatment	1st Antibody	2nd Antibody
B cell	Block with normal rabbit serum 5%	Anti-mouse CD45R/b220 (rat IgG2a 1/300 diluted)	Rabbit anti rat biotin conjugated (BA4000, 1/300 diluted)
T cell	Block with casblock or 5% normal goal serum	CD3 (1/150 Rabbit, monoclonal)	Goat anti-rabbit biotin conjugated (1/300 diluted)
α- smooth muscle actin	Block with casblock or 5% normal goal serum	Anti α-smooth muscle actin (rabbit, polyclonal)	Goat anti-rabbit biotin conjugated

Table 2.5 Reagents used in immunohistochemistry on frozen spleen sections expressing EGFP

2.15.3 Observation and image processing

Slides without fluorescence were observed under an optical microscope (Nikon E800). Slides with fluorescence were observed and scanned using a Confocal Microscope (710, Zeiss). Pictures were taken and analysed by Zen software (Zeiss) and Image J.

Chapter 3 Characterising virus-mediated fibrosis in the spleen

3.1 Introduction

Previous works in the Nash/Dutia lab investigated the role of IFNγ in MHV-68 latency by infecting IFNγ receptor deficient mice (IFNγ $R^{-/-}$ mice), in which distinctive pathological changes were observed. These changes were characterised by severe fibrosis in multiple organs, including lung, liver, and lymphoid tissue (Dutia et al., 1997; Ebrahimi et al., 2001). The fibrosis triggered by viral infection showed similarities to the chronic human diseases idiopathic pulmonary fibrosis (IPF) (Mora et al., 2005) and sclerosing cholangitis (SC) (Gangadharan et al., 2009). IPF has been linked with the presence of EBV, whereas SC is of unknown etiology (reviewed in Moore and Hogaboam, 2008; Vannella et al., 2010).

In contrast to the pathology of the lung and liver, a more dramatic fibrosis was observed in the lymphoid system. The spleen and the mediastinal lymph nodes which collect the lymph from the lung underwent large-scale destruction of tissue architecture, which most likely was the result of persistent tissue damage caused by lytic infection, or host immune response in which T cells and macrophages targeted latently infected cells. Macrophages exhibited an alternate activation phenotype characteristic of an immune response dominated by Th2 cytokines (Gangadharan et al., 2008). Collagen production was evident around day 16 post infection and played an important role in clustering fragmented germinal centres and walling off latently infected B cells. By day 20 post infection, fibrosis was at its most intense, with fibroblasts dominating the splenic architecture. There was a dramatic decline in the number of splenocytes and any further uptake of cells from the vascular system was inhibited. Morphologically, the spleen appeared anemic and shrunken. Remarkably, as the virus was reduced the host began to repair the damage and by day 35 post infection, reformation of follicles and a return of cell numbers were observed.

In this chapter, we extended the previous work in the Nash/Dutia lab to address key questions relating to the distribution and the fate of latently infected B cells at different

phases of the splenic pathology. In this respect we were particularly interested in what happens during the loss of latently infected B cells between day 20 and day 28. We confirmed previous observations of the development and resolution of splenic fibrosis around lymphoid follicles by Masson's trichrome staining. Furthermore, we investigated the distribution of B cells, focusing on late time points between day 16 and day 35 post infection, which have not been investigated thoroughly. The study by Gangadharan used *in situ* hybridisation for vtRNAs to detect latent virus in the spleen. This led to the conclusion that events in the fibrotic spleen lead to a clearance of latent virus around day 26 post infection (Gangadharan, 2006). This surprising observation was further investigated using limiting dilution assays and qPCR, which data is contradictory to the previous finding. Finally, we investigated the mechanism which may result in the massive loss of splenocytes in IFN-γ $R^{-/-}$ mice during fibrosis by looking at excessive apoptosis.

3.2 General pathological studies

3.2.1 Distribution of fibrosis in the spleen of IFNγ $R^{-/-}$ mice

IFNγ $R^{-/-}$ mice and 129Sv (WT) mice were infected with $4x10^3$ pfu (if not specified) in 40µl sterile PBS intranasally. Generally the dose used in our lab is $4x10^5$ pfu; however, there was considerable variation in the development of splenic fibrosis among IFNγ$R^{-/-}$ mice even within littermates of similar age and same sex. In addition, some mice also died unexpectedly. We hypothesized that infection with high doses might cause more variation in the acute immune response as small changes in inoculum reaching the lungs would have a larger effect on the dose. This would therefore affect the speed of fibrosis development. To address this possibility and to prevent the mortality observed at the high inoculum we decreased the dose to $4x10^3$ pfu and observed less mortality in IFNγ$R^{-/-}$ mice. The development of splenic pathological changes occurs one or two days later than that observed

with the high dose, but development and recovery from fibrosis remained. There were four mice in each group, and the spleens were harvested and processed for paraffin sections and embedded and stained with Masson's trichrome, in which collagen and bone are stained as blue/green, cells plasma is red and cell nuclear is black.

By day 16 post infection, fibroblast proliferation and collagen deposition was observed around the germinal centres in IFNγ $R^{-/-}$ mice (Figure 3.1A), while there were no significant extra cellular matrix accumulation in wild type spleen (Figure 3.1B). IFNγ$R^{-/-}$ spleens also show collapsed red pulp in IFNγ $R^{-/-}$ mice (Figure 3.1A and 3.2C), while in wild type spleen the red pulp was congested due to splenomegaly (Figure 3.1B and 3.2D). The peak of fibrosis was observed at around day 26 to day 28 post infection (Figure 3.1C). The spleens of IFNγ $R^{-/-}$ mice were severely fibrotic with a thickened capsule, completely collapsed red pulp and destruction of lymphoid follicles. In wild type spleens, the red pulp had become less congested as the splenomegaly had resolved (Figure 3.1D). From day 32 post infection the spleen of IFNγ$R^{-/-}$ mice showed recovery from fibrosis and there was rebuilding of splenic follicle structure. The red pulp was reformed and the level of fibrosis was significantly reduced (Figure 3.1E). In comparison, the wild type spleen on day 32 post infection showed no significant changes in tissue architecture (Figure 3.1F).

These results extend the observations made by Gangadharan who investigated spleen morphology in IFNγ $R^{-/-}$ mice on day 20. Here we have chosen 3 time points covered from day 16 to day 32 post infection and carried out a comparison with wild type mice. We show that fibrosis begins from day 16, followed by a much more severe accumulation of collagen on day 26, and a reduction of ECM on day 32 post infection. Using this approach we demonstrated a gradual increase followed by a rapid decrease of the amount of collagen in the spleen of IFNγ$R^{-/-}$ mice.

3.2.2 The distribution of B cells in the spleen of IFNγ R-/- mice

To examine changes in B cell distribution in IFNγ$R^{-/-}$ mice, immunohistochemistry staining was carried out using a pan B cell marker CD45 R (B220). The positive cells were stained brown (Figure 3.2). In each group, there were 3 mice aged 8 to 10 weeks. The spleen sample was harvested at 6 time points from day16 to day 32 covering the development and recovery from fibrosis. Confirming the results of previous work which used FACS analysis, the spleen had undergone a massive loss of B cells during fibrosis, and the number of B cells recovered following the resolution of fibrosis. To build a more complete picture of the pathological events in our study we characterized the pathology in IFNγ $R^{-/-}$ spleen by dividing the whole process into 3 phases:

Splenomegaly: This occurred from day 14 to 18 post infection (Figure 3.2, A and B). During this time, collagen started to accumulate around the follicles, germinal centres developed and the B cell zone expanded.

Fibrosis: This occurred from day 20 to 28 post infection (Figure 3.2, C and D). Over this period the fibrosis became severe, the red pulp disappeared, the follicle was highly compact and the B cell zone shrunk. Very few B cells were observed outside of the white pulp. As a result of fibrosis, the B cells areas were greatly reduced at day 28 post infection and the structure of peri-arteriolar lymph sheath (PALS) had disappeared. Although the development of fibrosis varied among the individuals, the most severe fibrosis was usually observed around day 28 post infection. A massive cell loss occurred in the spleen at this stage.

Resolution/recovery: This occurred from day 31 to 40 post infection (Figure 3.2, E and F). During this period, extra cellular materials around the follicles became significantly reduced. Follicle structure was rebuilt, which was characterized by the reappearance of the peri-arteriolar lymph sheath (PALS) and the increased area of B cell zone. The red pulp at this stage was also partially recovered.

In this experiment, day28 post infection was identified as the key time point when the fibrosis was most severe and the B cell number in the spleen reaches the lowest (Figure 3.2, D). Our observation identified day 28 as a crucial time point marking the switch from fibrosis to recovery phase. The pathological changes in wild type spleen infected with MHV-68 are shown for comparison (Figure 3.3). On day 20 post infection, expanded germinal centers were observed, suggesting an on-going splenomegaly (Figure 3.3A), which was resolved by day 24 and 28 post infection (Figure 3.3B and C).

Interestingly, the recovered spleen structure of IFNγR$^{-/-}$ mice on day 30 and 32 post infection (figure 3.2 E and F, arrows) is very much like that of wild type spleen (Figure 3.3 B and C, arrows).

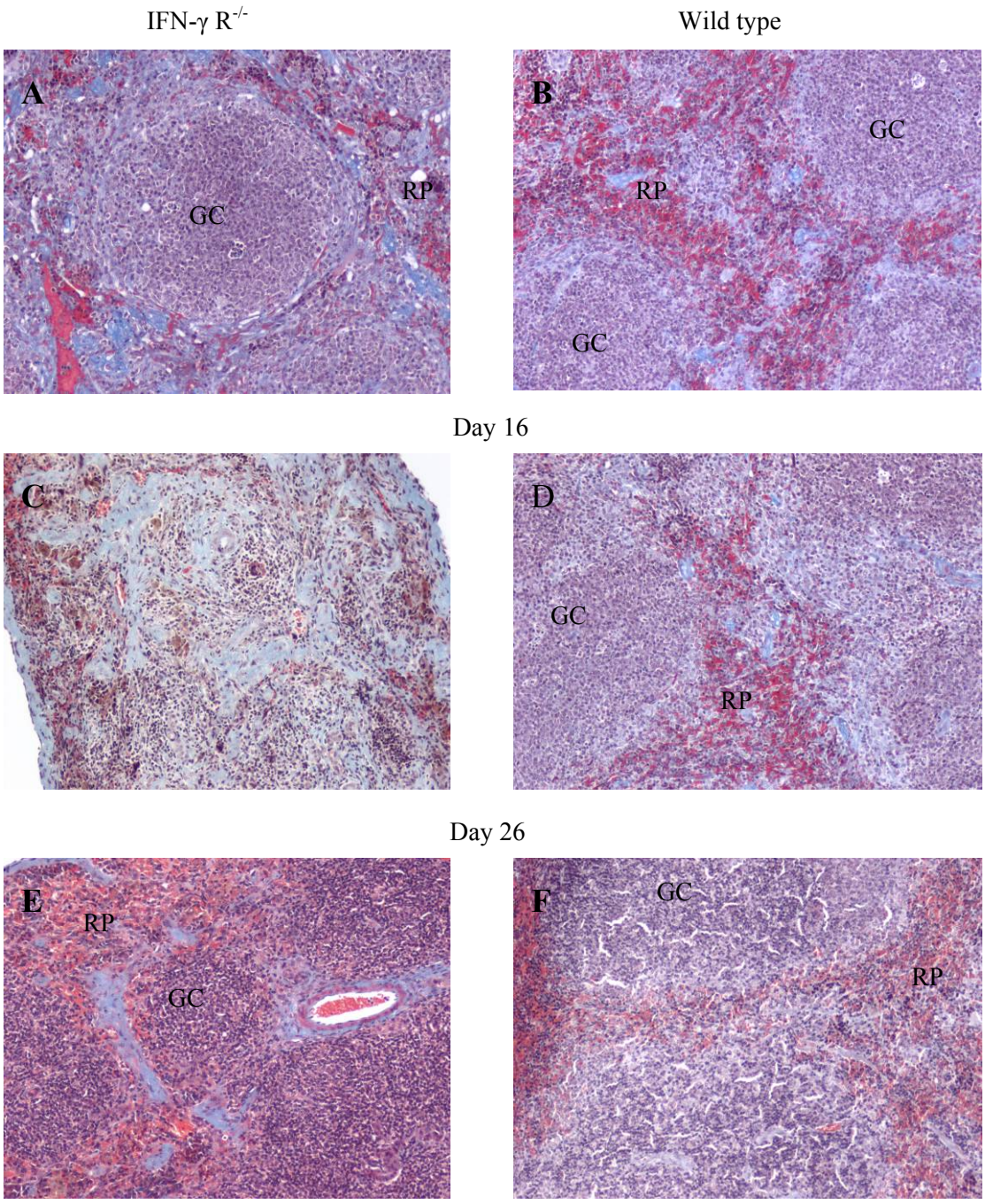

Figure 3.1 Characterisation of fibrosis in the spleen by histopathological technique. IFNγ $R^{-/-}$ mice and 129Sv (WT) mice were infected with 4×10^5 pfu in 40µl sterile PBS intranasally. Formalin fixed paraffin embedded tissue section of spleen from IFNγ $R^{-/-}$ mice and wild-type mice (129Sv) infected with MHV-68 at day 16, 26, and 32 post infection were stained with Masson's trichrome. The collagen of fibrous tissue was stained blue. Pictures were taken under 10 x magnification. (GC: germinal centre; RP: red pulp)

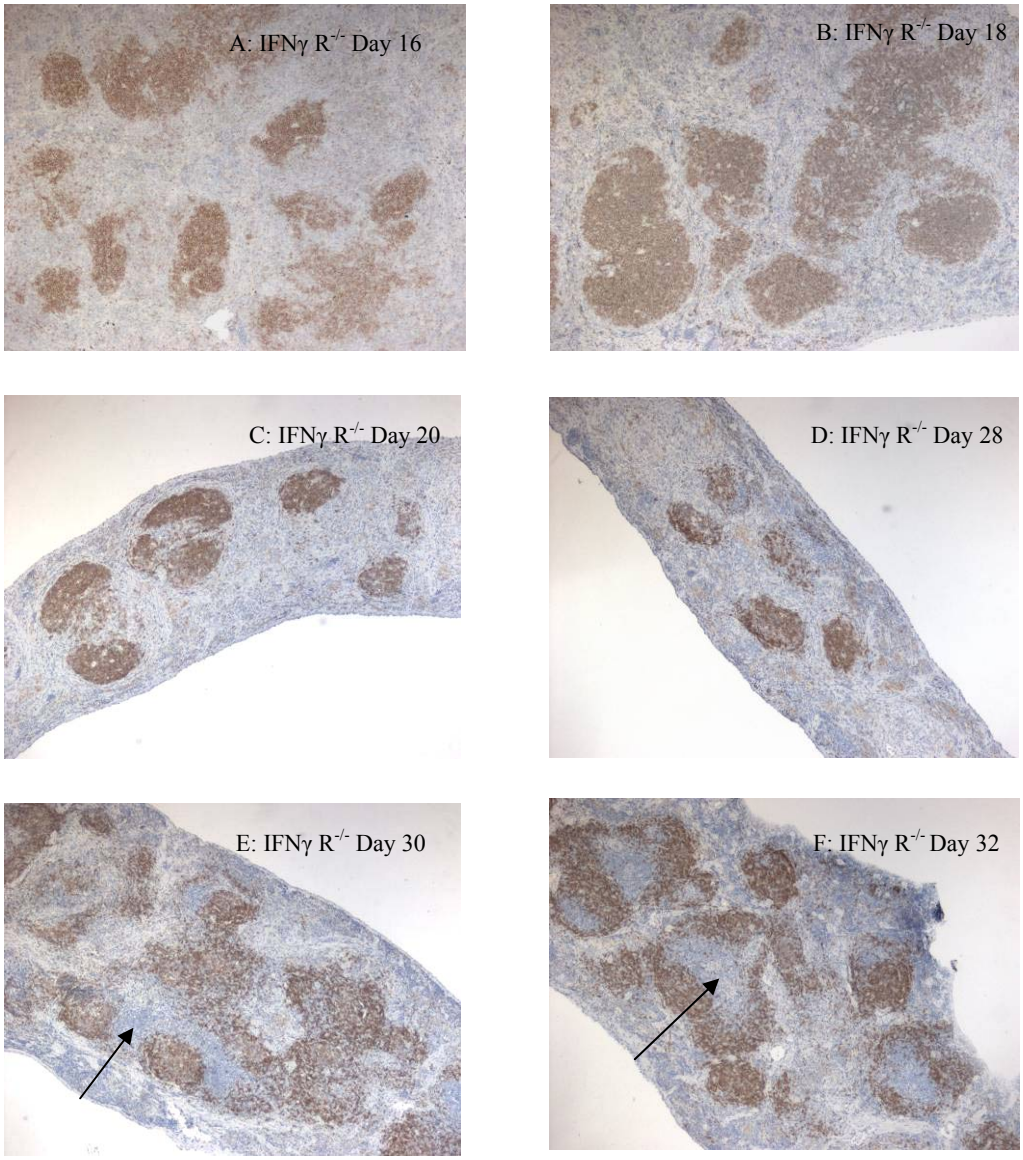

Figure 3.2 IHC stains for B cells (brown) in the spleen of IFNγ $R^{-/-}$ mice from day 16 to day 32 post infection showing the change of B cells and the size of germinal centres. IFNγ $R^{-/-}$ mice were infected with 4×10^5pfu in 40μl sterile PBS intranasally. CD45R(B220) was used to detect B cells. Pictures were taken under 10 × amplification. Note the significant reductions of the areas of B-cell zones through the time course. The structure of PALS disappeared from day 20 to day 28. However, PALS was observed again (arrows) on day 30 and 32 post infection, when the spleen was recovering from fibrosis.

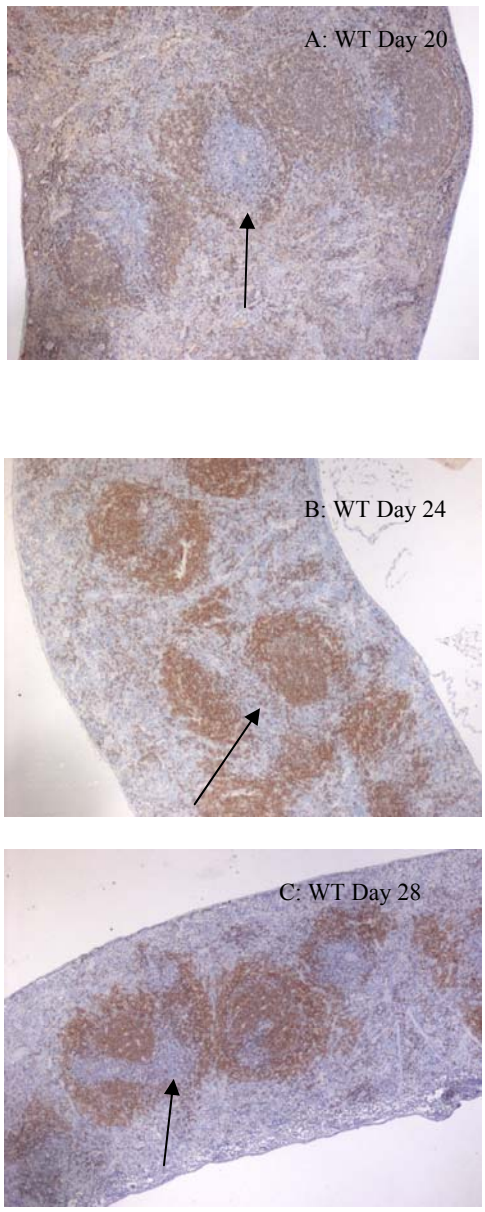

Figure 3.3 IHC stain for B cells (brown) in the spleen of wild-type mice from day 20 to day 28 post infection. 129Sv (WT) mice were infected with 4×10^5 pfu in 40µl sterile PBS intranasally. CD45R-B220 was used to detect B cells. Pictures were taken under 10× magnification. An elevated lymphocyte proliferation was observed on day 20 post infection (A) compared to the later time points (B and C). No collagen accumulation was observed through the time course. Note the PALS area (arrows) was always present in wild-type mice through the course of time.

Charaterisation of infection during fibrosis

In order to investigate the MHV-68 viral load carried by spleen cells in IFNγ $R^{-/-}$ mice using a sensitive method, the frequencies of viral genome carrying cells were determined in limiting dilution-qPCR assay at 4 selected time points. There were 5 mice in each group aged 8 to 12 weeks (Figure 3.4).

There were 8 replicates for each dilution, and the percentage positive for viral genome at each dilution was calculated (for example, if 3 out of 8 samples tested positive in PCR reaction for viral DNA, the percentage was 37.5%). The frequencies of viral genome-positive cells were determined based on the Poisson distribution. The possibility of no infected cells ($\kappa=0$) detected within a certain period of time was nearly 36.8%; therefore the frequency of at least one infected cell within a given number of splenocytes (n) can be determined as where the regression curve intersects 63.2%. Table 3.1 shows the calculated number of spleen cells carrying the MHV-68 genome (positive in real-time PCR reaction for viral genome) at each time point. The comparison between the viral load in IFNγ $R^{-/-}$ mice and in wild-type mice is shown in Figure 3.5.

At the beginning of fibrosis, on day 20 post infection, there was a much higher level of latent infection in knockout mice (about 1 in 400 spleen cells) than in wild-type mice (about 1 in 20,000). During severe fibrosis, the number of latently infected cells in IFNγ $R^{-/-}$ spleen was significantly reduced, falling to a level similar to that in wild-type spleen, as shown in Figure 3.4 on day 28. In the recovery phase, the number of infected cells in the spleen from IFNγ $R^{-/-}$ mice was less than in wild-type mice. However, the difference between the two mouse strains is not statistically significant ($p>0.05$). This experiment also shows that on day 68 post infection, the number of infected cells in both types of mice was reduced (about 1 in 20,000 in IFNγ$R^{-/-}$ mice, and 1 in 13,000 in wild-type mice).

The change of viral load is a result of interactions between virus activity and the host immune response: the high viral load in the spleen on days 14 to 16 post infection suggests

that the control of the expansion of latent infected cells in the spleen is reduced in IFNγR$^{-/-}$ mice. Both latent and lytic infections were elevated at this time post infection: *in situ* hybridisation identified large numbers of infected germinal centres. Although the vast majority of infected cells were latent, during days 14 to 16 post infection, productively infected cells were also detected, presumably the result of virus reactivation from latent infection. Therefore in limiting dilution assay both latent and lytic infections contribute to the increased viral DNA load tested: the latent infected cells replicate viral DNA during mitosis, whereas infectious virus are produced and released to infect healthy cells. However, considering the number of latently infected cells was much greater than lytic cells, along with the fact that the lytic virus was not significantly elevated in the lung (Dutia et al., 1997), it is most likely that the proliferation of latently infected B cells is the main reason for the high viral load in IFNγR$^{-/-}$ spleen. It is also possible that other cell types, such as macrophages and dendritic cells, are infected in IFNγR$^{-/-}$ mice, and these cells can also pass the virus to B cells. The infection of macrophages (CD11b+ cells) is discussed in Chapter 4. Eventually, the viral load in the spleen is controlled under mechanisms which involve the development of severe fibrosis around infected follicles and massive cell loss.

As expected, there was a significant reduction in viral load from day 20 to day 28 post infection, corresponding with the development of fibrosis and massive cell loss. The viral load of IFNγR$^{-/-}$ mice dropped as low as that of WT mice and the viral load remained at a similar level up to day 68 post infection. A certain level of viral DNA was always detected in IFNγR$^{-/-}$ mice, suggesting that although the viral load is controlled, the viral DNA still remains in the spleen. This result disagrees with previous study on infected cells using *in situ* hybridisation, in which the infected cells were not detectable in IFNγR$^{-/-}$ spleen after day 30 post infection (Gangadharan, 2006). The comparison among different methods to detect viral infection and the interpretation of the results are discussed in section 3.5.

Figure 3.4 (next page) Limiting-dilution qPCR on viral genomic DNA analyses of whole spleen cells. IFNγ $R^{-/-}$ mice and 129Sv mice were infected with 4×10^5 pfu in 40μl sterile PBS intranasally. Spleen cells were harvested and limiting diluted-qPCR was performed as described in Chapter 2. Single copy sensitive qPCR analysis was performed on splenocytes harvested at day 20, 28, 40, and 68 post infection. Spleen cells were serially diluted twofold 10 times in 96-well plates. There were 8 replicates for each dilution. The percentages of wells that were positive for the viral genome were calculated and the frequency of cells harbouring viral DNA was determined to be 63.2% according to Poisson distribution. (Legend: gamma- IFNγ $R^{-/-}$ mice;WT-129 Sv)

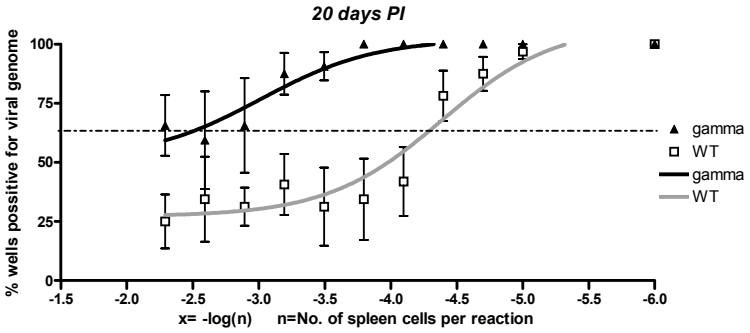
20 days PI
% wells possitive for viral genome
100
75
50
25
0
-1.5
-2.0
-2.5
-3.0
-3.5
-4.0
-4.5
-5.0
-5.5
-6.0
x= -log(n) n=No. of spleen cells per reaction
gamma
WT
gamma
WT

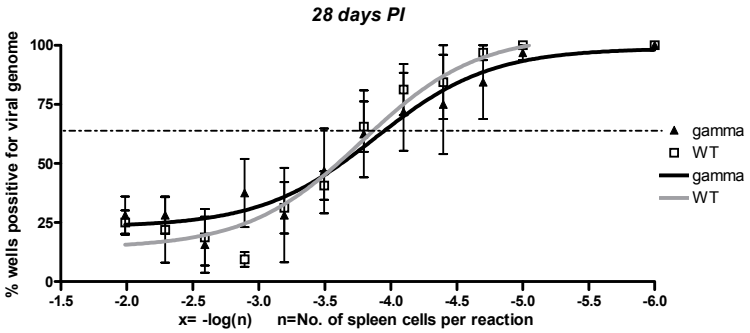
28 days PI
% wells possitive for viral genome
100
75
50
25
0
-1.5
-2.0
-2.5
-3.0
-3.5
-4.0
-4.5
-5.0
-5.5
-6.0
x= -log(n) n=No. of spleen cells per reaction
gamma
WT
gamma
WT

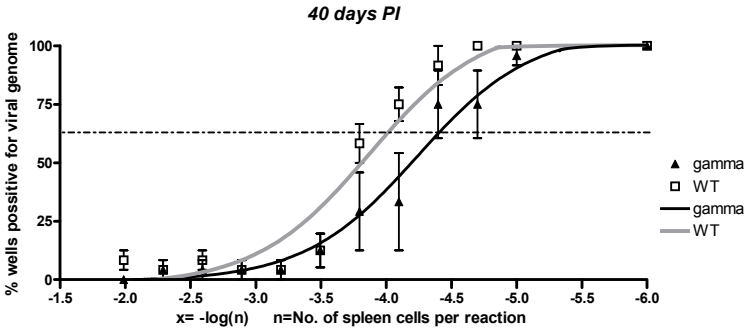
40 days PI
% wells possitive for viral genome
100
75
50
25
0
-1.5
-2.0
-2.5
-3.0
-3.5
-4.0
-4.5
-5.0
-5.5
-6.0
x= -log(n) n=No. of spleen cells per reaction
gamma
WT
gamma
WT

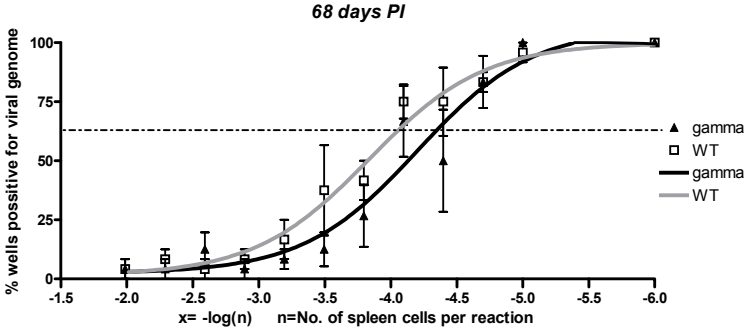
68 days PI
% wells possitive for viral genome
100
75
50
25
0
-1.5
-2.0
-2.5
-3.0
-3.5
-4.0
-4.5
-5.0
-5.5
-6.0
x= -log(n) n=No. of spleen cells per reaction
gamma
WT
gamma
WT

Date p.i./Strain	Log(n)	1 in (n) spleen cells infected	Infected cells%
20/ IFNγ R-/-	2.5	316	0.316
20/ WT	4.3	19,953	0.005
28/ IFNγ $R^{-/-}$	3.9	7,943	0.013
28/ WT	4	10,000	0.010
40/ IFNγ $R^{-/-}$	4.4	25,119	0.004
40/ WT	4	10,000	0.010
68/ IFNγ $R^{-/-}$	4.3	19,953	0.005
68/ WT	4.1	12,589	0.008

Table 3.1 the frequencies of infected cells in the spleen of IFNγ $R^{-/-}$ mice (gamma) and 129Sv (WT). The absolute number of the frequency of cells harbouring the viral genome was calculated from the results shown in figure 3.4.

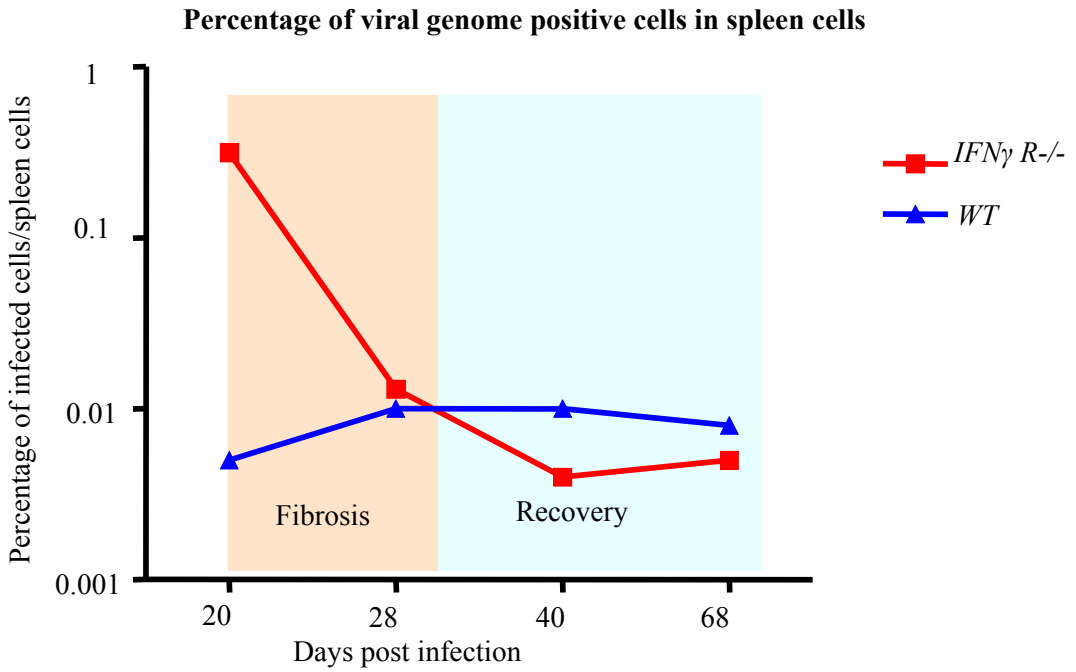

Figure 3.5 the percentage of viral genome positive cells in the spleen of IFNγ $R^{-/-}$ mice (KO) and 129Sv wild-type (WT) mice.

3.3 Looking for apoptosis during latency (day 16 to day 32)

A high viral load in the spleen on day 14 to 16 post infection suggests the control of viral load in the spleen is reduced. However, the viral DNA in the spleen dropped significantly while severe fibrosis developed around infected follicles and a massive cell loss occurred at the same time. The pathology observed in IFNγR$^{-/-}$ spleen may be a Th2 biased host immune response which somehow controlled the number of latently infected cells. Therefore, we carried out further investigations on the fate of infected B cells during fibrosis.

There are several possible mechanisms which may lead to B cell loss. First, the persistence of fibrosis blocks the blood supply as well as cell recruitment from peripheral blood. Second, B-cell survival requires persistence of cell signals, as well as cytokines and chemokines, which may be affected by the pathology. Third, perforin, which is related to CD8 T cells' function, is important for the survival of IFNγR$^{-/-}$ mice from MHV-68 infection (Tsai et al., 2011), so these B cells may also die through CD8+ T-cell triggered cell death. Therefore, we carried out several experiments to investigate whether there was more cell death in the spleen of IFNγR$^{-/-}$ mice.

3.3.1 Detecting damaged DNA by TUNEL assay

TUNEL assay was carried out to detect cell death in the spleen of IFNγ R$^{-/-}$ mice. The protocol we used was optimised to minimise the background staining. However, in the cases of highly fibrotic spleens, there was still non-specific staining as shown in Figure 3.6. Such background staining was not observed in wild-type spleens with the same treatment. The high background colour may affect microscope reading and lead to misinterpretation of results, which suggests that this method may not be ideal for evaluating the level of cell death in highly fibrotic tissue. Therefore we were not able to apply TUNEL assay on all samples.

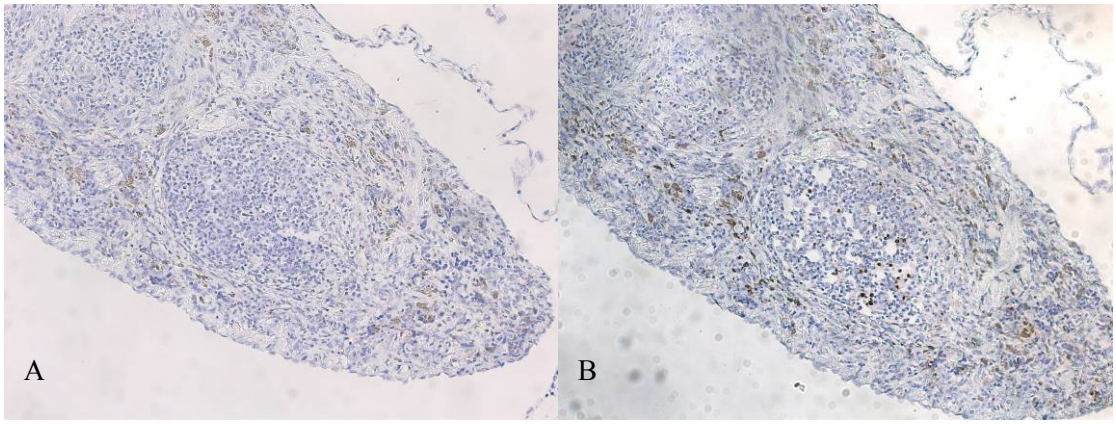

Figure 3.6 TUNEL staining on paraffin embedded spleen sections from an IFNγR$^{-/-}$ mice on day 20 post infection. IFNγ R$^{-/-}$ mice and 129Sv (WT) mice were infected with 4×10^{5}pfu in 40µl sterile PBS intranasally. (B)The positive stained cells (brown). (A) shows the control in which TdT solution was not added. As shown in this figure, there is a background staining in the area of fibrosis. Pictures were taken under 10 × magnification.

3.3.2 Detecting apoptotic cells by IHC staining for cleaved Caspase3

Anti-cleaved caspase 3 antibody was used to compare the apoptosis in IFNγR$^{-/-}$ spleen to that in wild-type mice. Figure 3.7 shows a selection of figures showing distribution of apoptotic cells, in which positive cells are stained brown. Three time points were chosen (days 16, 18, and 20) to cover the period of time when the massive loss of cells occurred in IFNγR$^{-/-}$ spleen. Generally, the patterns of the distribution of apoptotic cells in both mice were similar; apoptosis mainly occurred in the germinal centre, where tingible body macrophages were also observed (Figure 3.7, arrow). However, there were more positive cells observed outside of the follicle in IFNγR$^{-/-}$ mice compared with wild-type mice. The number of positive cells within 10 continuous views at 40 times magnification was counted for each sample. The comparison between IFNγR$^{-/-}$ mice and wild-type mice at each time point is shown in Figure 3.8. There was no significant difference in the number of apoptotic cells in the spleen between IFNγR$^{-/-}$ mice and wild-type mice from day 16 to day 20. The result suggests there is no evidence for excessive apoptosis within the spleen of IFNγR$^{-/-}$ mice during the development of fibrosis.

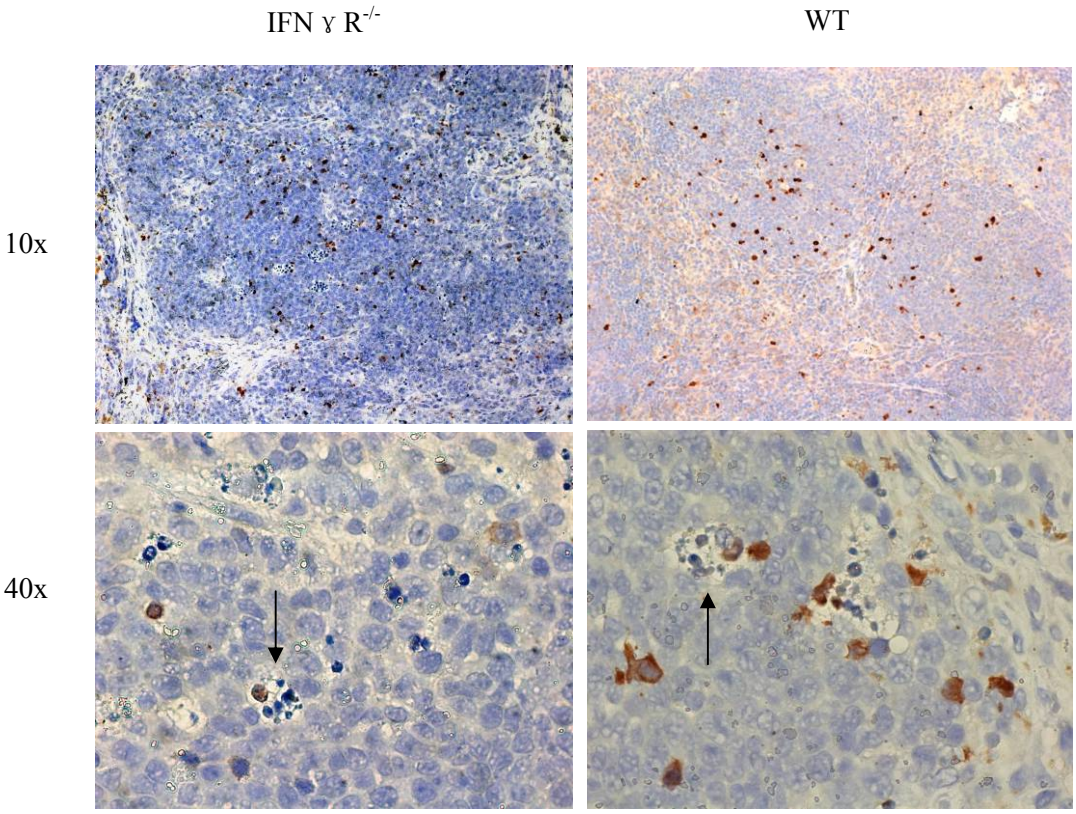

Figure 3.7 A selection of pictures showing the result of immunohistochemistry staining for cleaved Caspase-3 on paraffin embedded spleen sections (18 dpi). IFNγ $R^{-/-}$ mice and 129Sv (WT) mice were infected with 4×10^5pfu in 40µl sterile PBS intranasally. Apoptotic cells are shown as brown (3, 3'-Diaminobenzidine, DAB*). Cell nucleus were counterstained with Hematoxylin . The arrows show the tingible body macrophages within germinal centres engulfing apoptotic/dead cells. Magnifications are noted at the left.*

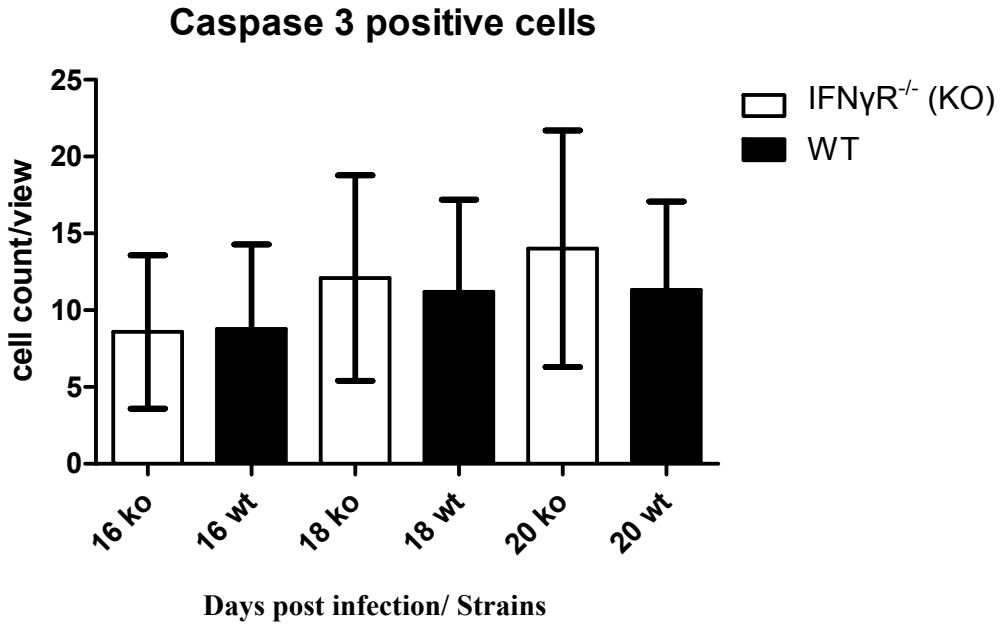

Figure 3.8 Quantification of apoptosis through Caspase-3 pathway in the spleen. IFNγ $R^{-/-}$ mice (KO) and 129Sv (WT) mice were infected with 4×10^5pfu MHV-68 in 40μl sterile PBS intranasally. For each group, there are 3 to 5 mice; for each section the caspase-3 positive cells within 10 continuous views were counted under 40 times magnification.

3.3.3 Flow cytometry confirming cell death

Based on the result of Caspase3 staining, along with previous research based on the TUNEL assay, there is no evidence showing that cell death is responsible for the dramatic cell loss in IFNγR$^{-/-}$ spleen. However, these experiments were carried out on very thin sections of the spleen and may not represent the level of cell death within the whole spleen. Therefore, we used a nuclear dye DRAQ7 as a Life/Death indicator in flow cytometry (Figure 3.9). Due to a financial limitation and the need to complete the PhD thesis, a 'look see' experiment was carried out using a pooled sample from 4 mice for each group and the time points chosen were days 25 and 33 for the benefit of another experiment. The result showed 15% of cells in IFNγR$^{-/-}$ spleen were dead or dying, while only 7% were dying in wild-type mice (Figure 3.9B). This result shows that more cells where membrane was compromised in IFNγR$^{-/-}$ spleen than in wild-type spleen.

However, other factors may be responsible for this result. For instance, the preparation of a single-cell suspension from a fibrotic spleen may cause more cell death. Also, the latent virus carried by spleen cells may undergo reactivation which leads to cell death. Moreover, individual variation was not considered due to the lack of a repeat experiment. Hence, further experiments are needed to validate this result. Nevertheless, it does suggest that the loss of B cells may be the result of cell death.

A

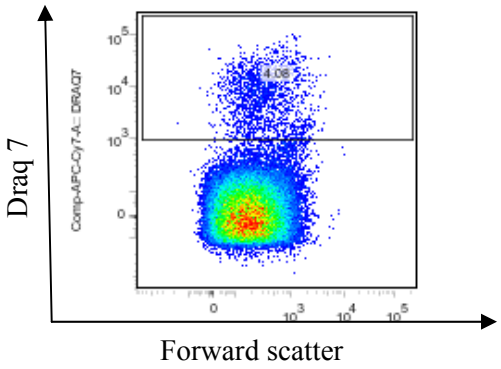

B

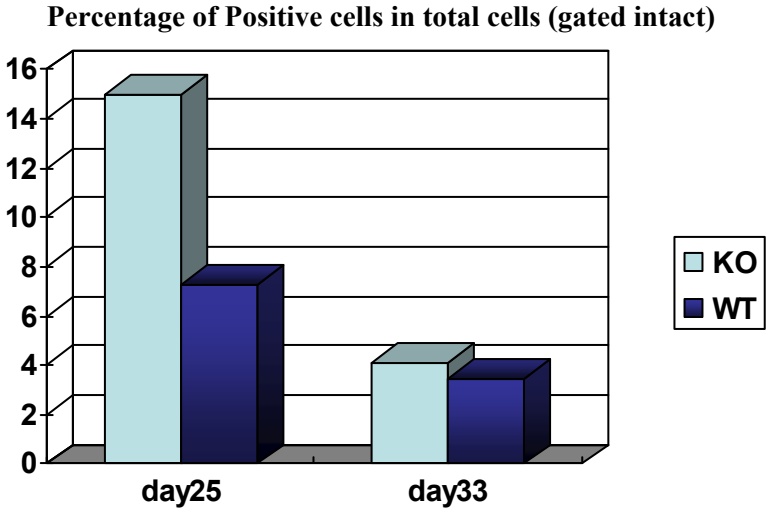

Figure 3.9 IFNγ $R^{-/-}$ mice (KO) and 129Sv (WT) mice were infected with 4×10^3pfu MHV-68 in 40μl sterile PBS intranasally. For each group, spleen cells were harvested and pooled together, and then stained with Draq7 at room temperature for 5 minutes. The stained cell were then analysed by FACS. (A) an example of FACS dot plot shows whole spleen cells treated with Draq7. Cells which had leaking cell membrane were stained (shown in rectancular). (B) Percentage of Draq7 positive cells within total spleen cells (gated as intact single cells) on day 25 and day 33 post infection.

3.4 Discussion

In this chapter, the early observations of Gangadharan were confirmed using histo-pathological approaches, which also enhanced understanding of the pathological changes during fibrosis. Moreover, we investigated the mechanisms leading to rapid loss of B cells carrying latent MHV-68 virus. This objective was based on the observations made by Gangadharan using *in situ* hybridisation to viral tRNA-like molecules, a marker for both lytic and latent virus, which showed that the loss of germinal centres was accompanied by the loss of vtRNA positive cells (Gangadharan, 2006). We hypothesised that the rapid loss of B cells occurs as a result of cell death, which was measured by several approaches. In this chapter, 3 major experiments are included: first, morphological studies on collagen deposition and B cell distribution; second, detection of viral DNA load based on PCR; and third, detection of cell death as a potential mechanism of significant cell loss in IFNγR$^{-/-}$ spleen.

1. Morphological studies on collagen and B cell

The pathological changes in IFNγ R$^{-/-}$ spleens following an intranasal inoculation of MHV-68 in the IFNγ R$^{-/-}$ spleen included a severe fibrosis, along with massive cell loss and dramatic reduction of viral load, followed by recovery from fibrosis. Firstly, we focused on time points between day 16 and day 35, as the fibrosis developed and started to resolve during this period of time. Based on the MT staining for collagen and immune staining for B cells, an important time point, day 28, has been identified: it represents the highest level of fibrosis and the lowest spleen B-cell number. It appears to be a crucial point at which the pathology changes from fibrosis to recovery.

Interestingly, a return of spleen structure was observed during the resolution of fibrosis: areas among B-cell zones, presumably PALS which is occupied by T cells and dendritic cells, disappeared during fibrosis (Figure 3.2 C and D), but, surprisingly, reappeared after

day 30 post infection (Figure 3.2 E and F). The 'recovered' spleen structure in IFNγR$^{-/-}$ mice (Figure 3.2 E and F, black arrows) was very similar to that of wild-type mice which was consistently observed from day 20 to day 28 post infection (Figure 3.3, black arrows). This observation suggests that the rebuilding of PALS is an important part of the splenic recovery, and it also indicate a potential role of the loss of PALS in the destruction of spleen structures during the formation of fibrosis.

However, it is also possible that the 'spaces' observed among patches of B cells were not only PALS, but also the light zones of germinal centres. The light zone is where the B cells (centrocytes) are selected, under the control of T cells and dendritic cells. These B cells are derived from centroblasts in the dark zone of the germinal centre. Infected B cells may reseed the spleen along with uninfected naïve B cells once the fibrosis has resolved and naïve B cells may become activated and form new germinal centres. The proliferating B cells may be activated by viral antigens and proliferate in order to control infection. On the other hand, B cells may be latently infected and proliferate under the driving force of latent virus so that the pool of infected spleen B cells can be recreated. The B cell development and proliferation can be measured by staining with CD38, and immunoglobulins (IgD, IgM, and IgG) and cell proliferation markers such as BrdU.

2. Detection of total viral DNA load based on PCR

The limiting dilution-PCR assay shows that on day 20 post infection, the number of latently infected cells in the spleen of IFNγR$^{-/-}$ mice was much higher than in wild-type mice. This reflects an inefficient control of the expansion of MHV-68 infection in the spleen due to the lack of IFNγ responses. Moreover, the Th2 biased immune response of IFNγR$^{-/-}$ mice may contribute to the dramatic increase of latently infected B cells by enhancing B-cell proliferation and differentiation. One of the important functions of IFNγ is to limit the population of Th2 cells. For example, in the absence of IFNγ responses, elevated Th2 cytokine IL-4 enhances the proliferation of developing B cells and subsequently increases

the production of specific antibodies. Indeed, the absence of IFNγ was shown to have profound influence on antibody production against MHV-68. It has been reported that in IFNγ$^{-/-}$ mice, there were significantly increased frequencies of IgA, IgG1, and IgG2b in lymph nodes than in wild-type mice, and a remarkable increase of IgG2b in the serum (Sangster et al., 2000). During latent infection, the viral genome persists as an episome in the host cell nucleus, and replicates while the host cell undergoes mitosis. This process is facilitated by viral gene ORF73 encoded mLANA. Therefore, it is possible that the dramatic increase in the number of latently infected B cells is due to the enhanced proliferation of spleen B cells responding to the infection. However, the elevated level of antibody may also be due to the lytic infection which is less controlled in IFNγR$^{-/-}$ mice (Christensen et al., 1999; Sarawar et al., 1997), resulting in a greater stimulation of antibody production.

So far, three approaches have been applied to look at latent virus load in the spleen: *in situ* hybridisation, reactivation assay, and detection of viral DNA by PCR. However, none of them can differentiate lytic virus from latent virus, and each method has its own drawbacks.

In situ hybridisation has a sensitivity issue: Gangadharan investigated the presence of latently infected cells in the spleen by *in situ* hybridisation for MHV-68 vtRNAs 1-4. He found that the positive cells for vtRNA 1-4 gradually disappeared over a time course, with complete absence at day 30 post infection; so it seemed that the latent infection was cleared (Gangadharan, 2006). However the limiting dilution-PCR assay and reactivation assay disagree with this result. It was found that up to day 68 post infection, there was a certain amount (approximately 1 in 20,000 spleen cells) of spleen cells positive for viral DNA, and although the number of infected cells in IFNγR$^{-/-}$ mice was lower than that in wild-type mice, there was no statistically significant difference between the two groups (p>0.05). Also, reactivation assays have been carried out previously and showed that on day 90 post infection, the latent virus could still be reactivated from IFNγR$^{-/-}$ spleen cells and cause plaques in cell culture (Dutia et al, unpublished data). Previous research has shown that there

is a close link between plasma cell differentiation and viral reactivation, and it is suggested that a large proportion of cells which react from latency are plasma cells (Collins et al., 2009; Liang et al., 2009; Siegel et al., 2010). In the reactivation assay, some of the latent virus cannot react from latency, which leads to the results of reactivation assay lower than the true value. Therefore the qPCR based limiting dilution assay is considered to be the most sensitive way of detecting infected cells. Here we conclude that in the spleen of IFNγR$^{-/-}$ mice, the viral load is greatly reduced but not cleared. The limiting dilution-PCR assay also confirmed that day 28 was a very important time point. It seems that after the significant reduction, the infection in IFNγR$^{-/-}$ mice reached a level similar to that of wild-type mice, and remained at such low level of infection thereafter.

3. Detection of cell death

Recent study suggests it is most likely that MHV-68 utilises germinal centre proliferation to increase the pool of latently infected B cells, and eventually persists in the memory B-cell reservoir (Collins et al., 2009; Collins and Speck, 2012; Flano et al., 2002; Nealy et al., 2010; Willer and Speck, 2003). This mechanism is shared by human gammaherpesvirus EBV (Babcock et al., 1998; Barton et al., 2011). During fibrosis, from day 20 to day 28 post infection, there is a remarkable contraction of both B cells and latent virus in IFNγR$^{-/-}$ mice. In wild-type mice, a similar contraction of latently infected B cells was also observed around day 16 to day 20 post infection, whereas no massive cell loss was observed (Collins and Speck, 2012). This may be because the cell loss was immediately replaced in the spleen of wild-type mice while the recruitment from circulation was blocked in IFNγR$^{-/-}$ mice due to fibrosis (Ebrahimi et al., 2001). Therefore the IFNγR$^{-/-}$ mice may be a model which reflects the mechanism of the reduction of latent infected cells in wild-type mice.

In the IFNγR$^{-/-}$ mouse model the reduction of spleen B-cell numbers corresponded to the drop in viral load during fibrosis. Therefore the fate of B cells in the MHV-68 infected IFNγR$^{-/-}$ spleen during fibrosis became one of the main questions we addressed in this

project. In this chapter, we have examined cell death during fibrosis. The most likely explanation for the drop in B-cell numbers is cell death, especially apoptosis. Therefore we were expecting a significantly higher portion of cells undergoing apoptosis or other forms of cell death before and during fibrosis in IFNγ $R^{-/-}$ spleens compared to WT spleens. However, although we tried different approaches to detect cell death in the spleen, we found no concrete evidence for excessive apoptosis throughout the infection.

Previous research using TUNEL assay showed that the number and location of TUNEL positive cells were similar in IFNγ$R^{-/-}$ mice and wild-type mice over the course of infection (Ebrahimi et al., 2001). To confirm and to extend the time course, we carried out TUNEL assay, but found it not suitable for detecting cell death in highly fibrotic tissue in our case, due to high background staining caused by unspecific binding. Also, there was no evidence of increased numbers or boosted activity of tingible body macrophages which remove dead cells from the tissue over the course of infection (Gangadharan et al., 2008). Immunohistochemistry for cleaved Caspase3 showed there was no significant difference between IFNγ$R^{-/-}$ mice and wild-type mice during the development of fibrosis. This result shows that excessive loss of splenic cells is not due to apoptosis via the caspase-3 pathway. However, spleen sections can only show a thin layer of tissue in a snapshot, so they may not represent the overall level of apoptosis within the whole spleen. It is also possible that the activated Caspase3 is only elevated for a very short period of time so that we missed it in our assay. On the other hand, flow cytometry offers a more thorough way of analysing cell death though the viral reactivation during cell preparation which may increase the rate of dead cells. It might also be interesting to double stain these dead cells with an apoptosis marker such as Caspase3 to confirm the role of apoptosis. Moreover, FACS analysis also makes it possible to type these dead cells using specific cell markers. Our results, using a stain for 'leaking' cells, show an increased number of dead cells in IFNγ $R^{-/-}$ spleens. However, this was not the result of excessive apoptosis. Moreover, the flow cytometry data suggest an

elevated ratio of spleen cells with a damaged cell membrane. Therefore it would be very interesting to further examine cell death, as well as apoptosis, by flow cytometry.

Although apoptosis is the most recognised cause of programmed cell death, there are other possible mechanisms which are not dependent on Caspase3. For example, pryoptosis, also termed Caspase1-dependent cell death, has been observed causing cell death during inflammation. Autophagy has also been studied as an intrinsic pathway against MHV-68 infection, especially in the maintenance of latently infected cells (Reviewed by Barton et al., 2011). Therefore autophagy may be involved in the host cell response under the stress of fibrosis and contribute to cell loss. The possibility of pryoptosis and autophagy leading to cell loss are discussed in detail in Chapter 6. Furthermore, there is another possibility that viral reactivation from latency kills the infected B cells. In order to answer this question we have investigated the expression of viral genes which are essential for reactivation and lytic infection. This is discussed in Chapter 4.

Moreover, it is possible that cell death is not the only fate of these spleen cells. One possibility is that B cells exit the spleen due to the high tension of the tissue during fibrosis and/or the lack of survival signals. One finding which may support this assumption is that an elevated numbers of lymphocytes in the peripheral blood were observed, corresponding to the peak of fibrosis in IFN$\gamma R^{-/-}$ mice infected with MHV-68 (Ebrahimi et al., 2001). In the same publication, green fluorescent labelled B cells from peripheral blood were shown unable to travel into a fibrotic spleen, which may also impair the recruitment of splenic B cells. The mechanisms which may be responsible for the reduction of infected B cells in the spleen of IFN$\gamma R^{-/-}$ mice are discussed further in Chapter 6.

We paid special attention to the great reduction of spleen B cells for they are the main site of infection during latency and long term persistency. However, it is important to note that not only B cells, but all spleen cells, including T cells and macrophages (and also presumably dendritic cells), were reduced; the reduction of these cell types is illustrated in Chapter 4.

Among these cell types, T cells are not susceptible of infection, whereas peritoneal macrophages are considered another site of latent infection when infecting the mice following peritoneal cavity injection (Weck et al., 1999). This fact suggests that the fibrosis in the spleen is not specifically directed against the infected cells. However, the mechanisms by which these cells are erased from the spleen as well as their influence on latent infection are still poorly understood.

Chapter 4 Characterisation of latent infection in the spleen of IFN-γ receptor knockout mice

4.1 Introduction

4.1.1 Germinal centres

Germinal centres are the sites where B cells are activated and undergo somatic hypermutation and affinity maturation, and subsequently generate antigen specific plasma cells and memory B cells. In mice which have not been exposed to any pathogen, lymphoid follicles in secondary lymph organs are composed of naïve B lymphocytes and no germinal centres are formed. Once the host is infected, germinal centres develop in B-cell zones, and the rest of the naïve B cells are pushed aside and become the so-called B cell mantel (MacLennan, 1994). Each germinal centre can be divided into two parts based on the cell types and functions. The dark zone, located close to PALS, contains mainly B cells (centroblasts) with a high ability of proliferate, and tingible body macrophages (TBMs) among them. The light zone consists of B cells (centrocytes), T cells, TBMs, and some naïve B cells scattered within a follicular dendritic cells network (FDCs). Compared to naïve B cells, which rarely proliferate, germinal centre B cells divide rapidly (reviewed by Victora and Nussenzweig, 2012). Recent studies show that germinal centre B cells in both the dark zone and the light zone can proliferate, and have an irregular and changing morphology (Hauser et al., 2007). Moreover, they migrate frequently within either zone, as well as migrate between the two zones (Schwickert et al., 2007). Also, a certain number of naïve B cells constantly move from the mantle area into the light zone (Schwickert et al., 2007). For decades, centroblasts and cetrocytes were considered two distinct stages of differentiation, but recently it has been demonstrated that the dark zone and light zone B cells are one type of cell in alternating states (Victora et al., 2012).

4.1.2 MHV-68 infection in B cells

Following intranasal inoculation, MHV-68 is able to establish latency in a variety of cell populations (14 days post infection), including naïve B cells, germinal centre B cells, memory B cells, macrophages, and dendritic cells in the spleen (Willer and Speck, 2003). However, results from two independent groups have shown that MHV-68 latency is preferentially established in germinal centre B cells and memory B cells, which are surface IgD negative subsets during long-term latency (Flano et al., 2002; Willer and Speck, 2003). However, how the viruses gain access to mature B cells and how the infected population is maintained are still under investigation.

As found for EBV, research has suggested that MHV-68 may exploit the germinal centre reaction in secondary lymph organs by driving B-cell proliferation and differentiation. However, attempts to immortalize B cell lines for MHV-68 and KSHV have failed, which may be due to the cell surface of primary B cells making it difficult for viral entry (Jarousse et al., 2008). Recently, Liang et al. have demonstrated that MHV-68 is able to immortalise foetal liver-derived B cell progenitors, and this process requires ORF72 (v-Cyclin) and ORF73 (mLANA), in which cells eventually differentiate into B plasmablasts (Liang et al., 2011). Moreover, Coleman et al. have shown that in acute-latent infection, immature B cells in bone marrow as well as transitional B cells in the spleen are infected in long-term latency (Coleman et al., 2010). This suggests that the virus may use immature B cells within primary lymph organs as a reservoir which may keep circulating till they develop in secondary lymph organs such as lymph nodes and the spleen, and differentiate into long-lived mature B cells. Using YFP labelled MHV-68, Collins et al. found that the frequency of virus infected plasma cells accounted for the majority of viral reactivation from spleen cells *ex vivo* (Collins et al., 2009). The MHV-68 unique gene M2 has been shown to be necessary in manipulating the processes of developing B cells differentiating into plasma cells. Infecting mice with M2-null virus leads to the absence of viral infected plasma cell population in the

spleen. In the absence of all other viral gene products, transfection of M2 can drive B lymphoma cells to differentiate into plasma cells (Liang et al., 2009). Moreover, Blimp-1, an essential cellular transcriptional regulator of plasma differentiation, plays an important role in the establishment of latency and reactivation from latency (Siegel et al., 2010). In the absence of plasma cells, both B-cell and CD4+ T-cell responses are reduced, and germinal centre reaction in the spleen is diminished and fewer germinal centre B cells are infected. This result indicates that reactivation from plasma cells may play an important role in the establishment and maintenance of latency (Siegel et al., 2010).

4.1.3 Pathogenesis study using recombinant MHV-68

Several approaches have been developed to investigate the dynamics of a latent herpesvirus infection *in vivo*. Most groups have looked to modify the relevant herpesvirus through introduction of a marker gene under the control of latent gene promoters. However, this has met with mixed results mainly due to the stability of the marker gene and the reduced efficiency of transmission to various cells *in vivo*. To overcome these difficulties in the study of MHV-68 latency, Nealy et al. generated a virus encoding a modified β-lactamase molecule at the C-terminus of the ORF73 (mLANA) encoding sequences. They reported that this virus could be detected in a stable fraction of B cells throughout latent infection until at least day 90 post infection. As a reporter molecule, β-lactamase can cleave the β-lactam ring of a passively-diffusing, membrane-permeating flourogenic substrate, allowing versatile and sensitive means to detect mLANA expression in living cells. It has been demonstrated by limiting dilution reactivation assay that this recombinant virus undergoes normal lytic and latent infection compared with wild type MHV-68 (Nealy et al., 2010).

Recombinant MHV-68 has been widely utilised to study the pathogenesis of gammaherpesviruses. However, although the lytic infection was not affected by the insertion of the foreign gene, most of the recombinant viruses were attenuated in latent infection, which makes it very difficult to track infection at later time points (Milho et al., 2009).

mLANA-MHV-68 is still detectable as late as day 90 post infection, and provides a sensitive system to identify the infected cells expressing mLANA (ORF73). Therefore it is one of the best recombinant viruses available so far for the study of MHV-68 long-term latency.

Based on this system, Nealy et al. have examined the infection in B-cell subsets, whereas the infection in IFNγR$^{-/-}$ spleen B-cell subsets during fibrosis is yet to be studied. In this chapter, our aim was to understand how fibrosis generated by a Th2 biased immune system influences the infection in B-cell subsets in the spleen using the mLANA-MHV-68 virus. First, we investigated the proportion of each B-cell population (naïve B cells, germinal centre B cells, and memory B cells) in total splenocytes, as well as the level of infection within each population at crucial time points. Then we collected these infected cells for further study. To profile the viral activity during infection in IFN γ R$^{-/-}$ mice, we investigated selected viral genes expression profiles within infected cells by reverse transcription quantitative PCR.

4.1.4 Profile of selected viral gene expression in spleen

Previous research has shown that at least one viral gene, M1, is essential for inducing fibrosis (Evans et al., 2008). Therefore, we were very interested in finding out if an IFNγ receptor deficiency affects important viral gene expression, especially that of the M1 gene. As discussed in Chapter 3, there is a possibility that viral reactivation from latency may contribute to cell loss occurring during fibrosis. Therefore, we examined the transcripts of important lytic viral genes. Massive research has been done in analysing important viral genes; for example, Marques et al examined viral gene expression in B cell subsets, macrophages and dendritic cells (Marques et al., 2003). However, the studies so far cover only a short period of time and very little work has been done using IFNγR$^{-/-}$ mice. In the second part of this chapter, we investigate 5 viral genes (M1, ORF73, RTA, viral DNA polymerase, and M11) by reverse-transcription-quantitative PCR, and discuss the possible

viral activities in IFNγR$^{-/-}$ mice during fibrosis. It is the first time that these genes have been tested in IFNγR$^{-/-}$ mice over the period from day 16 to day 60 post infection.

4.2 mLANA-MHV-68 provides a reliable reporting system of infection in the spleen of IFNγR$^{-/-}$ mice and 129Sv mice

4.2.1 Detection of β-lactamase

The pathogenesis of mLANA-MHV-68 recombinant virus in immune competent mice is very similar to that of wild type MHV-68 (Nealy et al., 2010). We first checked the pathology caused by recombinant virus in IFNγR$^{-/-}$ mice compared with wild type MHV-68: following intranasal inoculation ($4x10^3$pfu), the IFNγR$^{-/-}$ mice infected with mLANA-MHV-68 virus developed fibrosis to the same extent as those infected with the wild type virus on day 20 post infection. Then we moved on to looking at whether the detection system works in the IFNγR$^{-/-}$ splenocytes: FACS analysis showed β-lactamase mLANA expression was not affected by the IFNγ receptor deficiency (Figure 4.1). The FACS system successfully detected the transformation of fluorescence from green to blue (Figure 4.1 right). The non-infected control shows (Figure 4.1 left) that all cells were loaded with CCF2/AM and no background colour change was detected. Therefore we have confirmed that β-lactamase works well as a reporting system in live cell flow cytometry and this system is suitable to study MHV-68 latency in the spleen of IFNγR$^{-/-}$ mice.

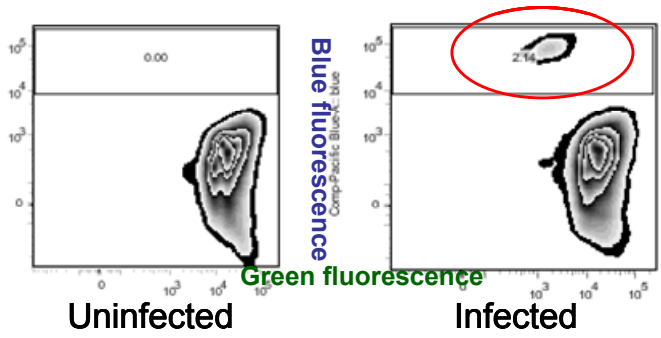

Figure 4.1 Detection of spleen cells which express mLANA by flow cytometry. IFNγ $R^{-/-}$ mice (KO) and 129Sv (WT) mice were infected with 4×10^3pfu mLANA MHV-68 in 40μl sterile PBS intranasally. Infected IFNγ$R^{-/-}$ spleens were harvested on day 16 post infection (i.n.); uninfected spleens were harvested on the same day as control. Single-cell suspensions were loaded with substrate CCF4/AM for β-lactamase reaction and subjected to FACS analysis. For both figures the x *axis shows the green fluorescence signal excited by 488nm laser, and the* y *axis shows the blue fluorescence signal exited by 405nm laser. The left figure shows FACS analysis of uninfected spleen loaded with substrate: the substrate with green fluorescence (at 520nm) has penetrated into every live cell and there is no β-lactamase reaction in uninfected cells (gated). The right figure shows the infected population (red circle) in which the green fluorescence signal has been transformed into blue due to β-lactamase reaction with substrate CCF4/AM.*

4.2.2 Change of viral load in spleen

Although the nature of infection of this recombinant virus in normal mice has been thoroughly investigated, infection of IFNγR$^{-/-}$ mice has not been studied. Due to the limitation of animals and time, plaque assays were not carried out. Instead, we analysed the infection rate of mLANA-MHV-68, and compared it with the result of limiting dilution assay. The change of viral load in the spleen of mLANA MHV68 infected mice (Figure 4.2 A) followed a trend very similar to that of wild type virus in IFNγR$^{-/-}$ mice and 129Sv mice (Figure 4.2 B). Figure 4.2 B summarises the results from a limiting dilution assay (Chapter 3), showing that the spleens of IFNγR$^{-/-}$ mice carried more virus than that of wild type mice in the phase of acute latency (day 16 post infection). The viral load was greatly reduced during fibrosis during the recovery phase. The same trend was also found when using the mLANA-MHV-68 virus. At different time points, the percentage of mLANA β-lactamase positive cells within spleen cells determined by flow cytometry in IFNγR$^{-/-}$ mice was compared with that in wild type mice. Flow cytometry to detect mLANA-MHV-68 showed that 0.5% of total spleen cells were infected in wild type spleens, while in the limiting dilution-qPCR assay for MHV-68 infection, 0.01% was infected. This difference in numbers may be caused by the different experiment methods: the result of FACS analysis was calculated based on the live-gated cells (in order to rule out debris and clumps by looking at the size and shape of each particle) which led to a relatively higher percentage of positive cells than the true value. Also, in a limiting dilution assay, samples were incubated overnight during DNA extraction, which may have caused the loss of viral DNA.

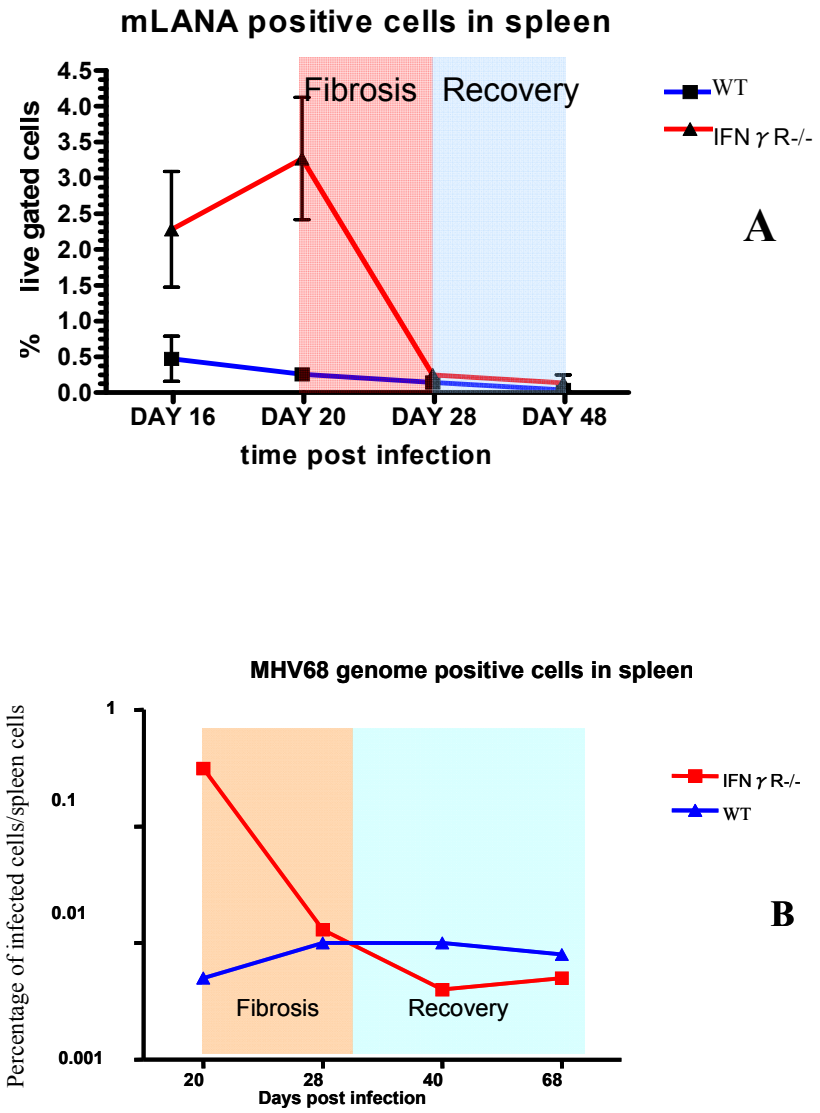

Figure 4.2 Comparison of mLANA-recombinant virus and MHV-68 viral load in the spleen: the behaviour of the mLANA virus compared with the wild type virus is similar in IFNγR$^{-/-}$ mice and 129Sv mice. (A) IFNγ R-/- mice (KO) and 129Sv (WT) mice were infected with 4×10^3pfu mLANA MHV-68 in 40μl sterile PBS intranasally. Spleen cells were harvested on day 16, 20, 28, 48. The percentage of mLANA-positive cells detected by flow cytometry within total spleen cells were shown in the figure. (B) shows the percentage of MHV-68 wild type virus genome carrying cells detected by limiting dilution-PCR assay (see figure 3.5). A and B show a very similar pattern of viral activity in IFNγR$^{-/-}$ mice (red) and 129Sv mice (blue).

4.2.3 Confirmation of infected cell isolation by qPCR

To further confirm that the β-lactamase positive cells detected by flow cytometry were actually infected, we sorted both positive and negative cells and carried out qPCR for viral gene transcripts. Four IFNγR$^{-/-}$ mice and 4 wild type mice were tested and for each individual there were 3 qPCR repeats. As expected, all of the β-lactamase-mLANA positive samples from both IFNγR$^{-/-}$ and wild type mice were expressing viral genes, whereas most of the β-lactamase-mLANA negative samples tested did not express viral genes. Using ORF73 as an example, all β-lactamase positive samples were found to be expressing mLANA (ORF73) (24 out of 24 reactions). Among the negative samples, although some reactions were found to be positive for expression in melt curve analysis (5 out of 24 reactions), their copy numbers were less than the detection limit of 5 copies/20μl reaction (24 out of 24 reactions). The results above show that the isolation of infected cells using the recombinant virus was successful. However, it also shows that a small proportion of the rest of the splenocytes still expressed ORF73, which is not detected by this system. It may be because of the incomplete reaction between β-lactamase and the substrate, or the sensitivity of the FACS facility. Based on the observation of the gross change of the spleen and viral load analysis and qPCR results, this method is a sensitive way to enrich and separate infected cells which express mLANA. Therefore we believe the mLANA virus is a good reporting system reflecting the nature of long-term infection in the spleen of IFNγR$^{-/-}$ mice and 129Sv mice.

4.2.4 mLANA-MHV-68 detection in macrophages

We concluded that the mLANA virus is a powerful tool to track the infected cells in IFNγR$^{-/-}$ mice. We then used this virus to detect the viral infection in the spleen-cell populations. Fluorescence conjugated antibodies were used in this series of experiments. As the β-lactamase detection system needs both blue and green channels, we could only choose

antibodies conjugated with red and far-red fluorophores. We first examined the infection in macrophages. CD11b-APC and Ly-6G-PE antibodies were used to identify macrophages and neutrophils. As the regular macrophage marker F4/80 is reported to be problematic in flow cytometry, we chose CD11b as the macrophage marker for spleen macrophages. CD11b is expressed mainly on macrophages and some granulocytes and dendritic cells. Neutrophil infiltration was also observed during infection; therefore we used Ly-6G to separate the neutrophils from the macrophages.

For every spleen sample, we stained $1x10^6$ cells to put through FACS. Very few events showing beta-lactamase positive in macrophages (less than 0.1% of total cells) and no positive events were detected in neutrophils. These events were checked again using FACS analysis software based on the cell size (forward scatter) and cellular granularity (side scatter), as well as the level of auto-fluorescence generated (data not shown), in which the results suggest that they were most likely debris or lymphocytes. Indeed, CD11b was also expressed in a low level on a small proportion of activated lymphocytes. Therefore we conclude that mLANA-MHV-68 is not detected in the macrophage/monocytes lineage in both IFNγR$^{-/-}$ and wild type mice. mLANA-positive cell population was not observed in the macrophage population. However, considering the limitation of techniques, there are three other possibilities. First, the number of infected macrophages was very low so that a much larger number of spleen cells needed to be analysed in order to get a recognisable population. Second, the virus infecting macrophages did not express ORF73 so that beta-lactamase was not expressed either. Some work *in vitro* and *in vivo,* based on other strains of mice supports this idea (Marques et al., 2003). Third, the macrophages were not infected between day 16 and day 35 post infection in both IFN γ R$^{-/-}$ and 129Sv (wild type) mice.

The percentage of macrophages and neutrophils within the total spleen cells through the time course of infection is shown in Figure 4.3 D: in the phase of splenomegaly (day 16 post infection), there were more macrophages in IFNγR$^{-/-}$ spleens than in the wild type. Then,

during fibrosis, both the number and the percentage of macrophages were reduced from 6% to 2% of total spleen cells. Moreover, considering that during the dramatic reduction the total number of spleen cells in IFNγR$^{-/-}$ mice dropped greatly, the loss of macrophages during fibrosis was more severe in terms of absolute numbers. In wild type mice, there was a similar but smaller reduction, from 4.5% to 2.5%; however, the percentage recovered to 3% on day 35 post infection. On day 20 and day 35 post infection, the percentage of macrophages in the spleen of IFNγR$^{-/-}$ mice was significantly lower than that in wild type mice (p<0.05). The results suggest a boosted macrophage activity on day 16 post infection in both types of mice; however, in IFNγR$^{-/-}$ mice there was an extra cell loss of macrophages during fibrosis. Neutrophils showed similar patterns, where there were no significant differences observed between the two strains of mice. These results add to the previous observation of cell loss in IFN γ R$^{-/-}$ spleens during fibrosis. Therefore, in the massive cell loss during fibrosis, not only lymphocytes but also macrophages are affected.

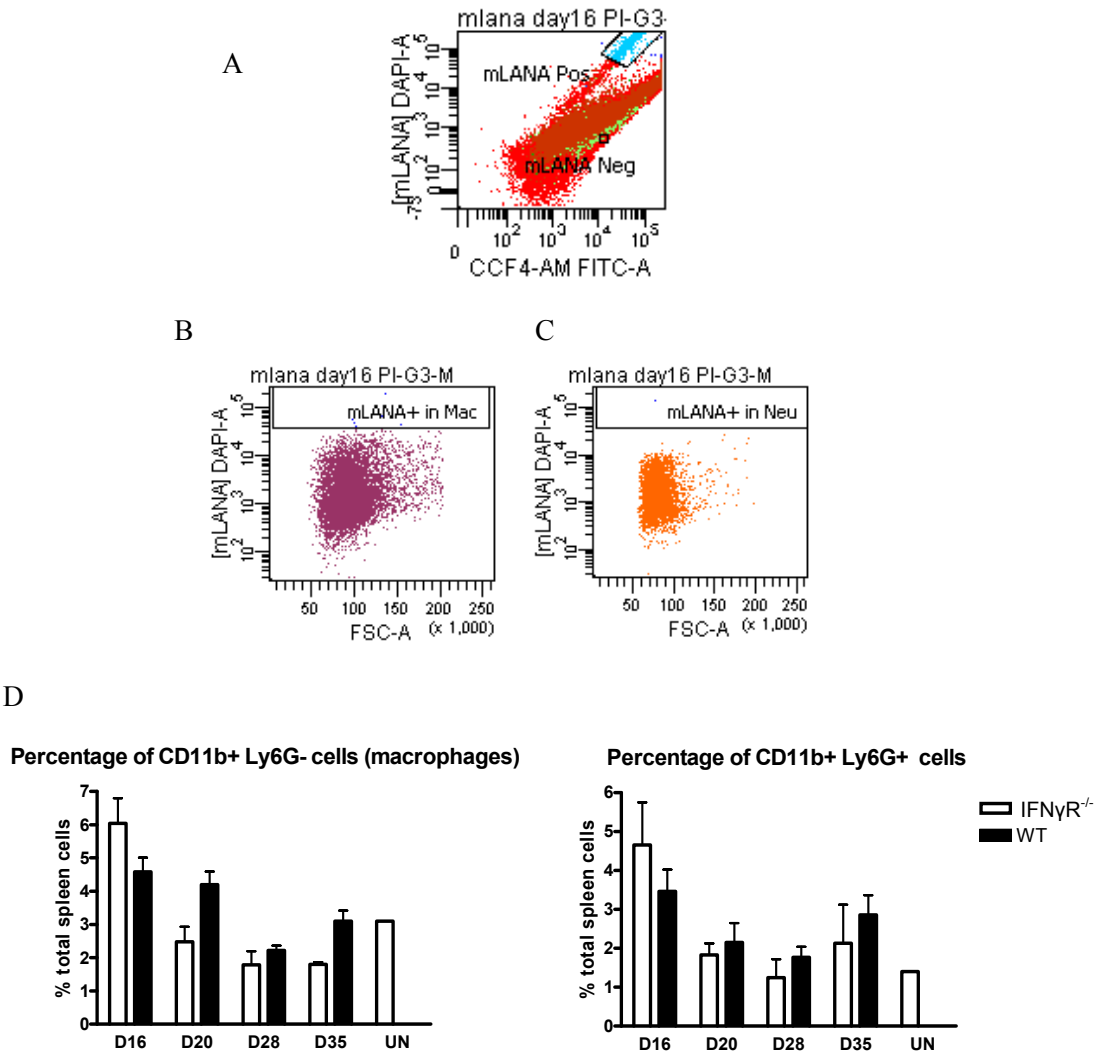

Figure 4.3 FACS analysis of multi-colour staining for macrophages/monocytes lineage subsets with β-lactamase detection. IFNγ $R^{-/-}$ mice and 129Sv mice were infected with 4×10^3pfu mLANA-MHV-68 in 40μl sterile PBS intranasally. Spleen cells were harvested on day 16, 20, 28, 35 and were stained as described in Chapter 2. (A) shows mLANA positive cell population (blue) in total spleen cells. (B) shows macrophages (CD11b-APC^+) and (C) shows granulocytes (CD11b-APC^+ Ly6G-PE^+). Very little mLANA positive cells were detected in macrophages and splenomegaly. (D) shows the percentage of macrophages and granulocytes populations in the spleen. Left: CD11b+Ly6G-; Right: CD11b+Ly6G+ (granulocytes, mostly neutrophils). KO: IFNγ $R^{-/-}$ mice; WT: 129Sv mice, UN: uninfected IFNγ $R^{-/-}$.

4.3 mLANA-MHV-68 infection in B-cell subsets

4.3.1 Distributions of B-cell subpopulations in the spleen during fibrosis

We then focused on changes in population of each B-cell subset and the infected cells within these subsets through the infection time course. Using FACS analysis we were able to observe how the population size of each subset of B cells changed over time. To identify B-cell subsets, CD19-APC-Cy7, CD38-APC, and IgD-PE were used. An example for the gating for B-cell subsets and β-lactamase reaction positive cells is shown in Figure 4.6. We were interested to see how the fibrosis in the spleen of IFNγ $R^{-/-}$ mice would affect these B-cell subpopulations, in comparison to that in wild type mice, which we consider to represent a normal MHV-68 infection. The total number of spleen cells recovered from IFNγ$R^{-/-}$ spleen was significantly reduced during fibrosis (from more than $1x10^8$ cells/spleen on day 12 post infection to $3x10^6$ cells/spleen on day 28 post infection), whereas in wild type mice there were around $1x10^8$ cells/spleen with a reduction of around 10% because of the resolving of splenomegaly (Figure 4.4 A). For each spleen, a similar number of total spleen cells were used for FACS analysis (around $2x10^6$ for most of the samples; however, in the cases of highly fibrotic spleen, fewer cells were analysed). The total number of B cells in IFNγ $R^{-/-}$ mice was reduced from 53% to 35% of total spleen cells analysed (Figure 4.4 B, top), while in wild type mice, the number dropped from 55% to 43% of total spleen cells. The decrease in wild type mice may be caused by resolution from splenomegaly. In IFNγ $R^{-/-}$ mice, due to the fibrosis, the spleen lost about 70% (estimated number) of its cells, consisting of B cells, T cells, and macrophages. The decreased percentage of B cells suggests that there was more cell loss in the B-cell population than in other cell types.

The changes of B-cell subsets showed different patterns between wild type mice and IFNγ$R^{-/-}$ mice (Figure 4.4 B and C). Generally, the proportion of naïve B cells in the spleen was

relatively stable, comprising more than 50% of the total number of B cells. The rest were germinal centre B cells and memory B cells, which vary according to the state of infection (Figure 4.4 C).

In WT mice, the percentage of naïve B cells was reduced while the number of germinal centre B cells and memory B cells increased from day 16 to day 35 post infection. The percentage of germinal centre B cells of total spleen cells was first reduced slightly from day 16 to day 20 post infection then return to the original level on day 35 post infection (Figure 4.4 B, left). In the case of memory B cells, the percentage reached the peak on day28 post infection and was only slightly reduced by day 35 post infection (Figure 4.4 B, middle). The percentage of naïve B cells in total spleen cells was reduced from day 16 to 20 post infection (Figure 4.4 B, right). The percentage of B-cell subsets in total B cells are shown in Figure 4.4 C; the germinal centre (GC) and memory B cells decreased from 25% to 18% of total B cells on day 20 post infection and then gradually increased to 35% from day 20 to day 35 post infection (Figure 4.4 C). The changes observed in WT mice pictured the activity of naïve B cells differentiating into germinal centre B cells and memory B cells in the spleen. The driving forces underlying this may include both virus-driven differentiation and host immune response against infection. However, according to the limiting dilution-qPCR assay (Chapter 3), the proportion of infected cells was very low in WT spleen throughout the time course (<0.005% in total spleen cells). Hence, the immune response, rather than virus activity, seems to be the main driving force of the B-cell differentiation.

In contrast to WT mice, IFNγR$^{-/-}$ mice, from day 20 to day 28 post infection, the germinal centre B cell population of IFNγR$^{-/-}$ mice was reduced significantly from 15% to less than 5% of total spleen cells (p=0.008, Figure 4.4 B, left), and the percentage of memory B cells reduced from 3% to 1% of total spleen cells (p=0.01, Figure 4.4 B, middle). The percentage of naïve B cells reduced from 35% to 30% of total spleen cells and there were no differences between IFNγR$^{-/-}$ mice and wild type mice (Figure 4.4 B, right). The result shows the

germinal centre B cells and memory B cells in IFNγR$^{-/-}$ mice suffered extra cell loss compared to primary B cells. In IFN ɣ R$^{-/-}$ mice, 33% of total B cells on day 20 post infection were under differentiation; this number kept dropping during the development of fibrosis and recovery phase (day 48 post infection), and remained less than 10% of total B cells (Figure 4.4 C). Interestingly, on day 35 post infection, 33% of B cells in wild type spleen were GC B cells and memory B cells, while these were only 10% in IFN ɣ R$^{-/-}$ spleen (noted in the rectangle in Figure 4.4 C). Moreover, this low level of GC and memory B cells remained so on day 48 post infection (Figure 4.4 C). Wild type mice on day 48 post infection were not tested, for it is generally accepted that there is little change in wild type spleen after day 35 post infection. To conclude, the populations of germinal centre B cells and memory B cells in IFN ɣ R$^{-/-}$ mice were reduced during fibrosis (day 20 to day 28 post infection, $p<0.05$), resulting in a significantly lower level than that in wild type mice at the same days post infection (day 28 and day 35 post infection, $p<0.05$). In the next section, we continue to discuss the viral infection in each population in order to further understand the nature of this significant change in IFNγR$^{-/-}$ mice.

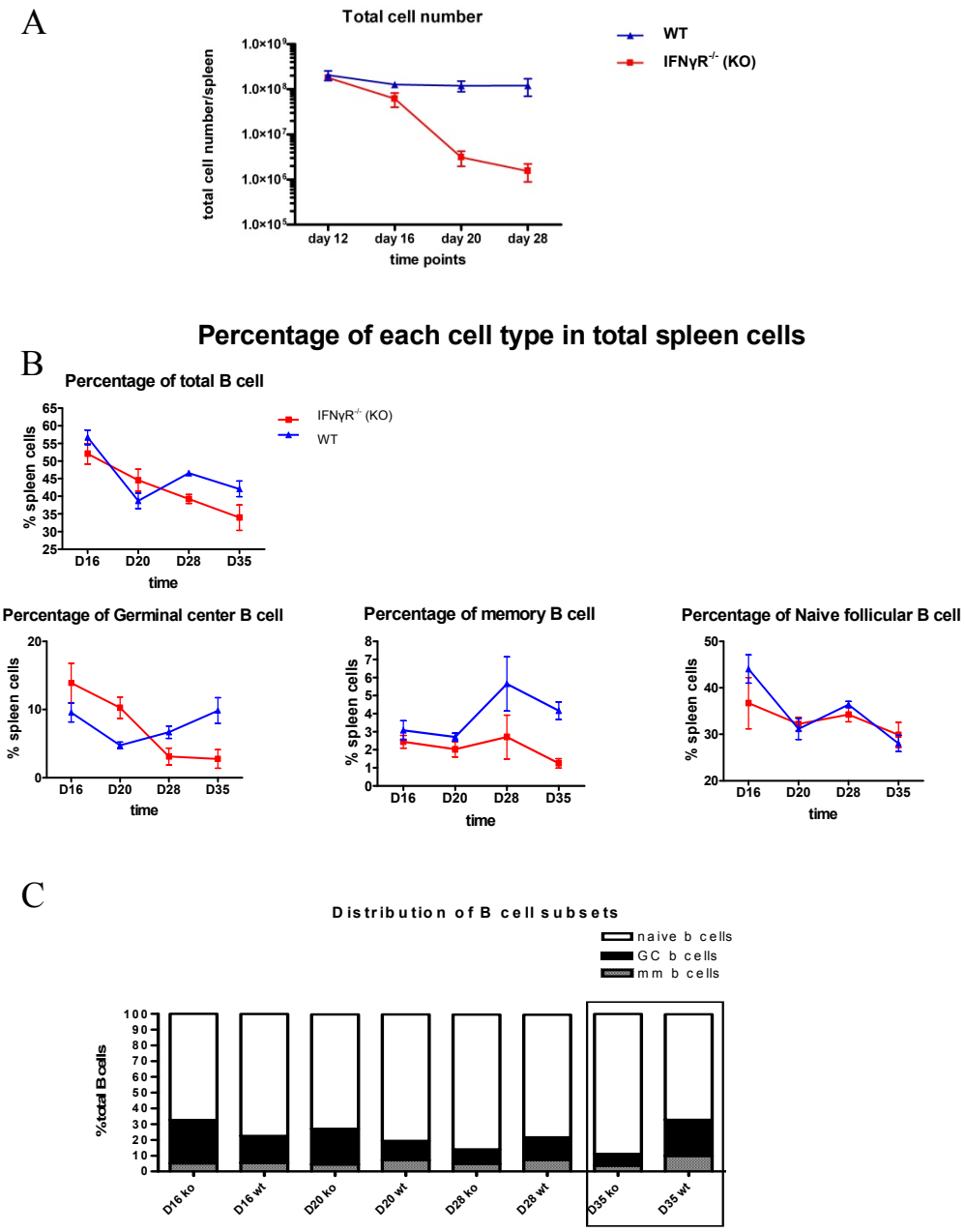

Figure 4.4 Percentage of B-cell subsets in the spleen of IFNγR$^{-/-}$ and wild type mice infected with mLANA-MHV-68. IFNγ R$^{-/-}$ mice (KO) and 129Sv (WT) mice were infected with 4×10^{3}pfu mLANA-MHV-68 in 40μl sterile PBS intranasally. Spleen cells were harvested on day 16, 20, 28, 35 and were stained as described in Chapter 2. (A) Changes of the number of total spleen cells recovered from IFNγR$^{-/-}$ and wild type mice. (B) Changes of total B cells (CD19$^+$), naïve B cells (CD19$^+$ IgD$^+$ CD38$^+$), germinal centre B cells (CD19$^+$ IgD$^-$ CD38$^-$), and memory B cells (CD19$^+$ IgD$^-$ CD38$^+$) within total B cells. (C) Distribution of B-cell subpopulations (total B cell in each group was considered 100%; value shown is an average of 4–5 individuals). The significant difference between IFNγR$^{-/-}$ and wild type mice on day 35 post infection is noted.

4.3.2 Distribution of infected B cells in subpopulations during fibrosis

Infected cells in each spleen cell sample were detected by flow cytometry and the distribution of these cells in each cell population was analysed. For all samples tested, over 95% of infected cells detected were B cells (defined as CD19 positive, Figure 4.5). The percentages of infected cells in different cell populations compared with total spleen numbers are shown in Figure 4.6, in which the infected cell populations were looked at in different ways: the percentage of infected cells within total spleen cells (Figure 4.6 C to E), the percentage of infected cells within each B-cell subpopulation (Figure 4.6 F to H), and the percentage of different types of B cells within the infected cell population (Figure 4.6 I).

Generally, in wild type mice, about 0.1% of total spleen cells and 0.2% of splenic B cells were infected, and this changed very little during the time course. In contrast, in IFNγ $R^{-/-}$ mice, there was a significantly higher viral load in IFNγ R-/- spleen, in which 0.4% of spleen cells (0.8% of B cells) were infected on day 16 post infection. Furthermore, this number kept increasing to 0.9% of spleen cells (2% of B cells) infected on day 20 post infection, which may be due to proliferation of latently infected B cells and low-level lytic virus from reactivation. As expected, a dramatic fall of viral load was observed during fibrosis (day 20 to day 35 post infection). On day 35 post infection very few infected cells were detected (Figure 4.6 A and B).

Interestingly, the infection of each B-cell subset showed differences between WT and IFNγR-/- mice throughout the time course. On day 16 post infection, germinal centre B cells contributed the most to the infection in both types of mice. In IFN ɣ $R^{-/-}$ mice, 2% of germinal centre B cells were infected, while 1% were infected in WT mice (Figure 4.6 F). In IFN ɣ $R^{-/-}$ mice 1.5% of memory B cells were infected, while in WT mice 1.5% of memory B cells were infected (Figure 4.6 G). However, germinal centre B cells contributed (about

70% in both types of mice) much more in the infected population than did memory B cells (about 15% in both types of mice) (Figure 4.6 I, D16ko and D16wt). This is because the population of germinal centre B cells (about 9% of total spleen cells) was larger than that of memory B cells (about 3% of total spleen cells) due to the expansion of germinal centres (Figure 4.4). On the other hand, naïve B cells, which make up 70% of the B-cell population, showed very little contribution to the infection. Only 0.1% of naïve B cells in IFN γ $R^{-/-}$ mice and 0.03% in wild type mice were infected (Figure 4.6 H). The low infection rate in naïve B cells agrees with previous studies (Flano et al., 2002; Willer and Speck, 2003).

On day 20 post infection, the viral load increased significantly compared to day 16 post infection ($p<0.05$) and reached its peak in IFN γ $R^{-/-}$ mice. Eight per cent of germinal centre B cells (Figure 4.6 F), 7% of memory B cells (Figure 4.6 G), and 0.45% of naïve B cells (Figure 4.6 H) were infected.

The distribution of infected cells between the B-cell populations had not changed since day 16 post infection. In wild type mice, 2.5% of germinal centre B cells, 4% of memory B cells, and 0.2% of naïve B cells were infected. Significant changes were observed in the distribution of infected cells between the B-cell populations compared to day 16 post infection (Figure 4.6 I, D20wt and D16wt), in which memory B cells accounted for about 40% of the infected population. This change indicates a shift of phenotype of infected B cells from day 16 to day 20, suggesting virus-driven B-cell differentiation from germinal centre B cells to memory B cells. Moreover, the percentage of memory B cells remained at a similar level, which suggests the population of infected memory B cells was maintained long term. Another possibility is that the percentage of germinal centre B cells in wild type mice from day 16 to day 20 was slightly reduced, which may have led to a reduction in percentage of infected germinal centre B cells, and subsequently an increased ratio of cells from the other two populations. Such changes were not observed in IFNγ$R^{-/-}$ mice from day 16 to day 20 post infection, but observed on day 20 to day 28 post infection (Figure 4.6 I).

Fibrosis persisted in IFNγR$^{-/-}$ spleen from day 20 to day 28 post infection, and resolution occurred from day 28 to day 35 post infection. During fibrosis, all cell populations were decreasing rapidly, especially the germinal centre B cells and memory B cells. This was concomitant with a reduction in the number of virus-infected (mLANA positive) cells. As discussed above, there was an increased contribution of memory B cells from day 20 to day 28 post infection, which occurred later than that in WT mice. Interestingly, this change occurred during the significant reduction of the percentages of germinal centre B cells in the spleen (Figure 4.6 C), which indicates the contraction of the germinal centre B subpopulation was responsible. The infection in naïve B cells on day 35 post infection of IFN ɣ R$^{-/-}$ mice was affected by the fibrosis less than any other populations during fibrosis (Figure 4.6 E and H). On day 35 post infection, the percentage of infected cells in naïve B cells in IFNγR$^{-/-}$ mice was significantly lower than that in WT mice ($p<0.05$), which indicates that in wild type mice, a proportion of infected primary B cells were maintained and renewed, while in IFNγR$^{-/-}$ spleen, this was blocked by fibrosis.

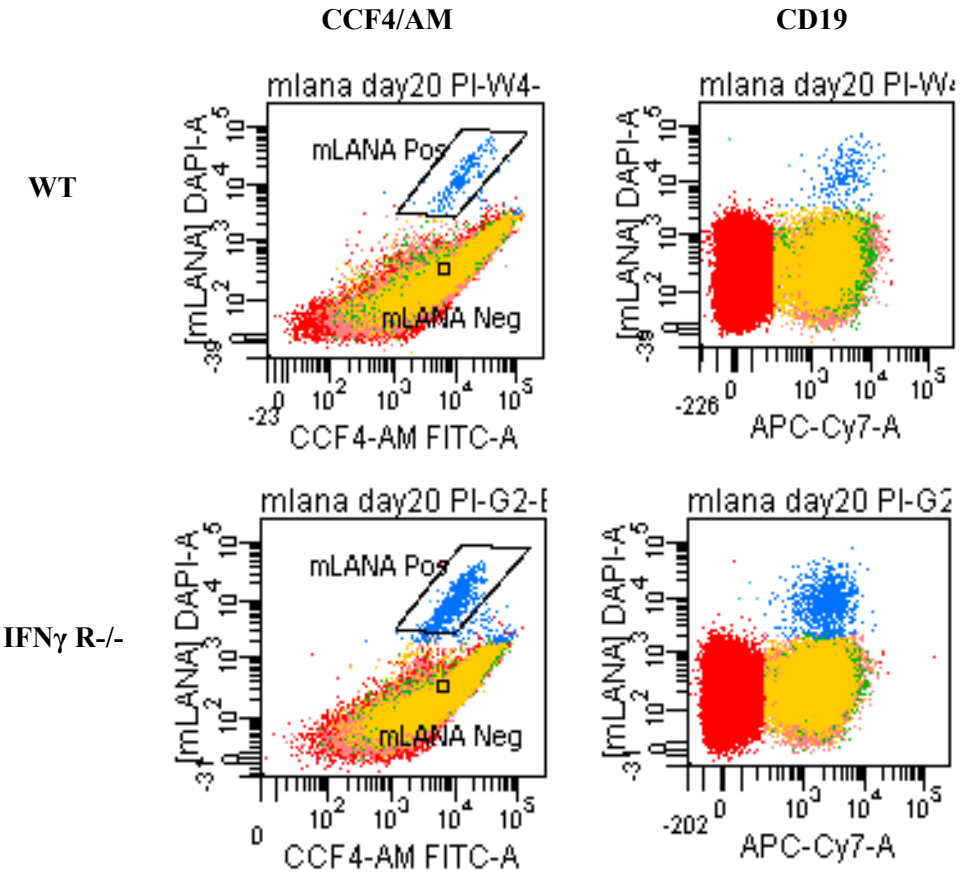

Figure 4.5 The majority of mLANA-positive cells (blue, gated as mLANA Pos) detected were B cells: IFNγ $R^{-/-}$ mice and 129Sv mice were infected with 4×10^3pfu mLANA-MHV-68 in 40μl sterile PBS intranasally. Spleen cells were harvested on day20 post infection, and were stained with Anti-CD19-APC-Cy7 antibody as described in Chapter 2. In the spleen of both IFNγ $R^{-/-}$ mice and 129Sv mice, the majority of mLANA positive cells were CD19 positive.

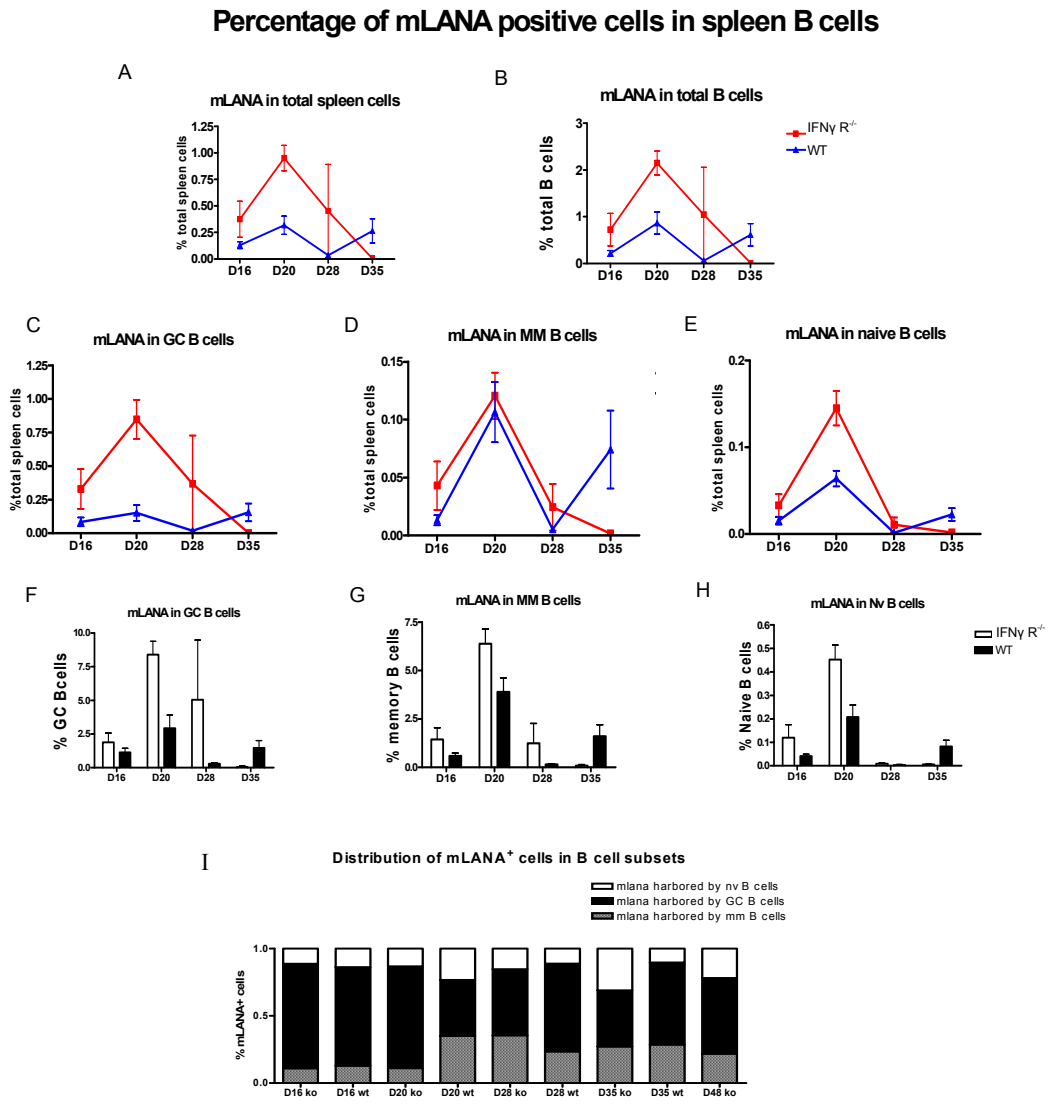

Figure 4.6 FACS analysis of virus positive cells in different splenic cells compartments through the time course post infection (See figure 4.4 legend). Infected cells were detected as β-lactamase-ORF73 (mLANA) positive by flow cytometry. (A) The percentage of infected cells within total spleen cells tested (about $2x10^6$ for each spleen). (B) The percentage of infected cells in total B cells. (C to E) The percentage of infected cells harboured by either naïve B cells, germinal centre B cells, or memory B cells in total spleen cells tested. (F to H) The percentage of infected cells harboured by naïve B cells, germinal centre B cells, or memory B cells within total B cell population. (I) Distribution of B-cell subpopulations (total infected cells in each group was considered 100%; value shown is an average of 4–5 individuals, IFNγ R-/-- KO; 129Sv-WT).

On day 35 post infection, although the spleen of IFNγR$^{-/-}$ mice had started to recover from fibrosis, the cell populations were not yet recovered (Figure 4.4 A and B). Meanwhile the infected cell population in IFNγR$^{-/-}$ spleen also reached its lowest point. Most interestingly, by comparing the FACS analysis result of uninfected mice and IFNγR$^{-/-}$ mice on day 35 post infection, we saw some similarities which indicate a recovery from infection (Appendix 3 A and C).

First, the IgD- population (GC and memory B cells) was very limited in IFNγR$^{-/-}$ mice and uninfected mice (Appendix 3 A and C), while a significant population was formed in WT mice (Appendix 3 B). In uninfected mice under specific pathogen-free conditions, the germinal centres were not developed in the spleen so that no GC and memory B cell populations were detected. However, in IFNγR$^{-/-}$ mice on day 35 post infection, the populations of GC and memory B cells were reduced during fibrosis. A significant difference was observed in the comparison of IFNγR$^{-/-}$ spleen before the development of fibrosis on day 20 post infection (Appendix 3 D) with that on day 35 (Appendix 3 A) post infection.

Second, the number of infected cells in B-cell subpopulations on day 35 post infection was significantly reduced and they were hardly detected in some individuals (Appendix 3 A, bottom lane), which is distinct from the situation on day 20 post infection (Appendix 3 D, bottom lane). In contrast, infected cells were detected in all three B-cell subpopulations in WT mice on day 35 post infection (Appendix 3 B, bottom lane). Such observations were repeatedly made in 6 out of 8 mice tested in 2 independent experiments.

Day 35 post infection signalled the recovery phase from fibrosis when the spleen started to rebuild its structure and the fibrosis was partially resolved. This result is particularly interesting to us, for we saw lower viral activity compared to wild type mice at the same time post infection. It appears that the infection was effectively controlled on day 35 post infection in IFN γ R$^{-/-}$ mice. Some individual IFNγR$^{-/-}$ mice had lost most of their germinal

centre B cells and memory B cells during fibrosis; therefore most of the viral load went with these cells, hence the lack of virus positive cells.

Although we already knew that there was a low viral load detected by PCR, we wanted to know if IFNγ $R^{-/-}$ mice could stay clear from infection. Therefore, we compared infection in IFNγ$R^{-/-}$ mice on day 35 and day 48 post infection (Figure 4.7). One mouse out of 5 showed a high viral load on day 48. Despite the individual variation, there was no significant increase in infection in the spleen from day 35 to day 48 post infection. However, on day 48 p.i. all 5 mice were positive. The results demonstrate that the infection in IFNγ$R^{-/-}$ spleen was controlled but not cleared, corresponding with the results from limiting dilution assay that there was viral DNA persistence in the spleen cells up to day 68 post infection (Chapter 3). The infection in the spleen may have reached the lowest point around day 35, and while the spleen was repopulated, the latently infected memory cells that circulated in the periphery may have re-seeded the spleen when fibrosis resolved. Another possibility is that very few infected cells remained in the spleen during fibrosis, so that the infection expanded from these cells.

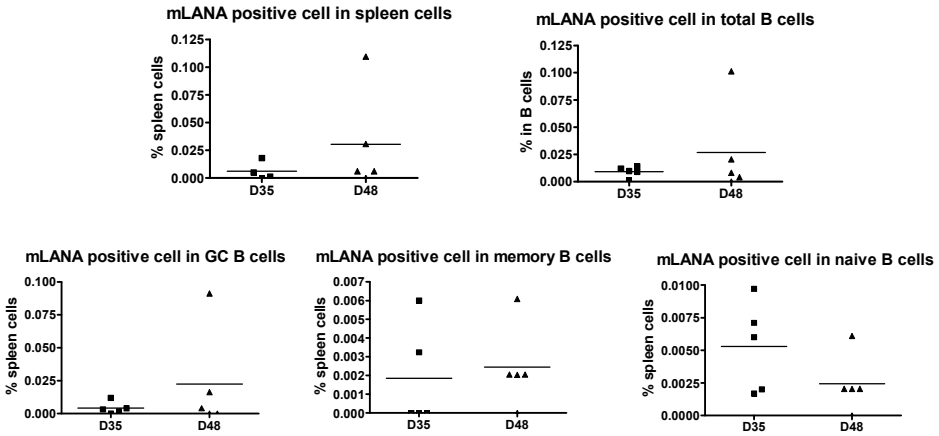

Figure 4.7 Comparison of viral load in IFNγR$^{-/-}$ spleens on days 35 and 48 post infection. IFNγ R$^{-/-}$ mice were infected with 4×10^{3}pfu mLANA-MHV-68 in 40μl sterile PBS intranasally. Spleen cells were harvested on day 35 and day48, and were stained as described in Chapter 2. There was no significant difference between day 35 and 48 p.i. in the terms of the percentage of mLANA positive cells in B cell subpopulations.

4.4 Viral gene expression in mLANA-positive cells

mLANA-positive and mLANA-negative cells were sorted using flow cytometry. There were many more negative cells than positive, so only a very small fraction of negative cells were collected for comparison. Total RNA was recovered from sorted mLANA-positive cells, followed by reverse transcription to generate first-strand cDNA which was followed by qPCR for selected viral genes. The aim of this experiment was to investigate the difference between IFNγR$^{-/-}$ mice and wild type mice and viral gene expression in infected spleen cells. We were mainly interested in lytic cycle genes because viral reactivation may result in cell loss, especially the loss of IgD-negative B cells in IFNγR$^{-/-}$ spleen. Therefore we chose RTA and viral DNA polymerase as target genes. Meanwhile, we also tested M1, which is a reactivation inhibitor which is also essential in triggering fibrosis in the spleen of IFNγR$^{-/-}$ mice (Clambey et al., 2000). ORF73 expression was also tested.

The gene expression profile shows the latency related genes ORF73 and M1 were highly expressed compared with lytic cycle genes (Figure 4.8 B) in IFNγR$^{-/-}$ mice and wild type mice on day 20 post infection. There was no statistically significant difference between IFNγR$^{-/-}$ mice and wild type mice for all 4 genes tested. However, M1 and ORF50 in IFNγR$^{-/-}$ mice were expressed at lower levels than in wild type mice. This suggests that on day 20 post infection, the infection in IFNγR$^{-/-}$ mice and wild type mice was mostly latent; there was no sign of viral reactivation in IFNγR$^{-/-}$ mice. Hence, the results suggest the massive loss of spleen cells was unlikely to be caused by lytic infection following viral reactivation. However, we chose day 20 in this experiment because the proportion of infected cells for sorting reached its peak at day 20 post infection. Attempts to recover total RNA from FACS sorted cells on other time points failed, as the cell number from each individual mouse was too low to generate enough RNA for reverse transcription using an RNA extraction kit. Therefore we were not able to profile the change of gene expression in IFNγR$^{-/-}$ mice in infected cells during a period of time. Also, this result was only normalised by the

expression of housekeeping gene YWHAZ; viral DNA was not measured, and therefore the possibility of one cell carrying different numbers of viral genome was not considered. These set-backs may affect the results.

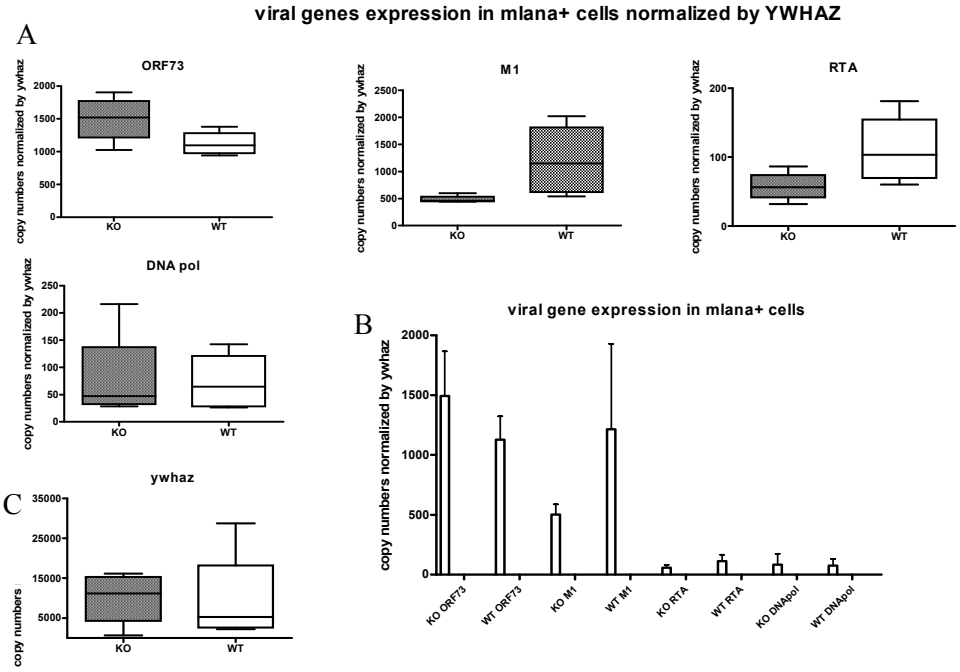

Figure 4.8 Viral gene expression in mLANA-positive cells. IFNγ $R^{-/-}$ mice and 129Sv mice were infected with 4×10^3pfu mLANA-MHV-68 in 40μl sterile PBS intranasally (IFNγ $R^{-/-}$-KO; 129Sv-WT). Spleen cells were harvested on day 20 and were stained as described in Chapter 2. Cells were sorted by FACS, and total RNA were extracted and reverse transcription-qPCR were performed for Viral genes ORF73, M1, RTA, and viral DNA polymerase. The results were normalised against copy numbers of housekeeping gene YWHAZ. (A) The expression of ORF73, M1, RTA, and DNApol in IFNγ$R^{-/-}$(KO) and WT (wild type) mice. (B) The comparison of viral genes expression. (C) The copy number of housekeeping gene YWHAZ for normalisation.

4.5 Viral gene expression profiling in spleen tissue

Finding it difficult to profile the viral gene expression in sorted cells, we had to compromise due to the limitation of RNA and DNA extraction. Moreover, we already knew that the infected cells do not express ORF73 and therefore could not be collected, so the gene profile on sorted infected cells may not reflect the general viral gene expression level of a whole spleen. Hence, viral gene expression profiling was performed using the whole spleen tissue preserved in RNAlater.

Viral genes tested were M1, ORF73, RTA, vDNA polymerase, and M11. We investigated the viral gene expression at a series of time points ranging from the establishment of latent infection (day 16) to the long-term latency (day 60). The important time points which mark the development of fibrosis and recovery in IFNγR$^{-/-}$ spleen, such as day 20, day 28, day 32, and day 40, were included.

Absolute quantification was performed and the results were normalised in two ways. First, the absolute copy numbers were normalised with housekeeping gene YWHAZ (Figure 4.9 left row), which shows the level of viral gene expression in the total RNA from the same amount of spleen tissue. The housekeeping gene YWHAZ was steadily expressed in the spleen of IFNγR$^{-/-}$ mice and wild type mice and therefore a valid gene to use for normalisation.

Although each qPCR reaction contained the same amount of mRNA from spleen tissue, the viral load in each sample varied according to mouse strain (e.g., IFNγR$^{-/-}$ mice carried more virus than WT mice) and time point post infection (e.g., IFNγR$^{-/-}$ mice carried more virus on day 16 than day 28 post infection). Therefore, as the second way to normalise the qPCR result, viral DNA was made as a normalisation factor to reflect the gene expression on the level of each viral genome (Figure 4.9 right row).

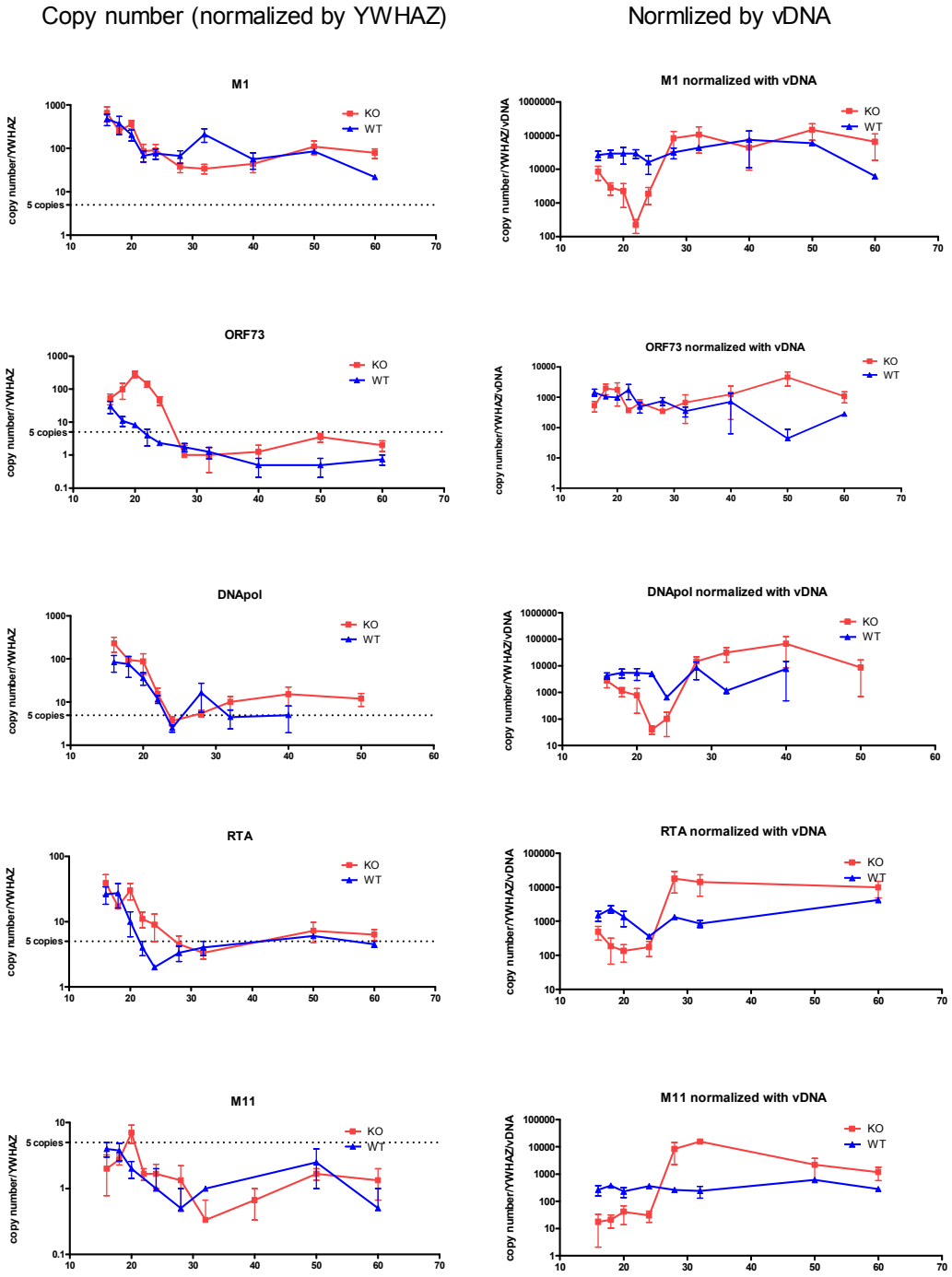

Figure 4.9 Result of gene profiling normalised by either YWHAZ or viral DNA. IFNγ $R^{-/-}$ mice (KO) and 129Sv (WT) mice were infected with 4×10^3pfu MHV-68 in 40μl sterile PBS intranasally. Spleen tissues were harvested on day 16, 18, 20, 22, 24, 28, 32, 40, 50 and 60, and were preserved in RNAlater. Total RNA was extracted, and reverse transcription-qPCR was performed. The left row shows copy numbers of genes of interest normalised with YWHAZ expression. Dot line represents the limitation of quantification, which is 5 copies; the right row shows copy number firstly normalised by YWHAZ expression factor, then normalised with vDNA factor. Viral genome DNA was quantified by qPCR on total DNA extracted from spleen tissue.

Generally, M1 and ORF73 were highly expressed, while vDNA polymerase, RTA, and M11 expression was low in both strains of mice. The results show different patterns of viral gene expression between IFNγR$^{-/-}$ mice and wild type mice.

In wild type mice the M1 gene was stably expressed during the time course, while the other four genes tested were expressed at low levels. After day 20 post infection, the copy number of RTA, ORF73, and viral DNApol was lower than the sensitivity limitation of the assay (5 copies, noted in the left row of Figure 4.9). Quantification of results that are below 5 copies is not considered to be accurate, although the amplicons can be confirmed by melt-curve analysis. The profile shows that from day 16 to day 24 post infection, there was a reduction in the expression of all viral genes tested, which remained low at later time points. The profile shows that the virus shut down gene transcription from day 16 to day 28, and remained latent in a long-term, on the same level as whole spleen tissue (Figure 4.9 left row). Interestingly, for each viral genome, expressions of all viral genes did not change from day 16 to day 24 post infection (Figure 4.9 right row). This suggests the down-regulation of viral gene transcripts may be due to the contraction of viral load, rather than the down-regulation on the mRNA level. Marques et al. (2003) have shown that viral gene expression on day 14 post infection in the spleen varies among macrophages and dendritic cells, and B-cell subpopulations. Therefore it is highly possible that in our case, the down-regulation of viral gene expression reflected a reduction of certain infected cell population(s) in the spleen, which may be a result of host immune responses.

On the other hand, in IFNγR$^{-/-}$ mice, the expression of ORF73 was increased during day 16 to day 28, corresponding to a boosted viral load in the spleen. The analysis also shows this increase was due to the expansion of viral load, for there was no difference between IFNγR$^{-/-}$ mice and wild type mice with respect to ORF73 expression normalized against viral genome (Figure 4.9 right row). Previous research has shown that the function of ORF73 encoded mLANA is as a tethering viral genome as an epitome when host cells undergo mitosis, so

that the viral genome can be replicated and persist in daughter cells. Research using mLANA-null virus showed that without mLANA, the virus was unable to maintain the episomal genome *in vivo* and could not reactivate from latency (Paden et al., 2010). With its essential role in viral infection, ORF73 is expressed through lytic and latent infection. Our results demonstrate that mRNA for ORF73 increased while the infected spleen cells proliferated, then reduced rapidly during the cell loss caused by fibrosis. ORF73 expression showed a different pattern from other genes tested. IFNγR$^{-/-}$ mice had significantly higher ORF73 expression from day 16 to day 24 post infection, peaking on day 20 post infection, and then dropping to a level similar to that of wild type mice during the fibrosis and recovery phase. However, the average level of expression of ORF73 per viral genome shows a similar trend in IFNγR$^{-/-}$ mice and wild type mice (Figure 4.9 lane 2). Hence, the change of ORF73 expression corresponded with the change of viral DNA load in both strains. Moreover, it is obvious that in IFNγR$^{-/-}$ spleen, ORF73 was steadily expressed in most of the infected cells.

However, the other four genes tested showed a different expression pattern compared to ORF73. Within the same spleen tissue, the expression of M1 was similar between IFNγR$^{-/-}$ mice and wild type mice, and it hardly changed through the time course (Figure 4.9 lane 1, left). However, after normalisation with viral DNA factor, M1 expression in IFNγR$^{-/-}$ spleen was first comparable to that of WT mice, then became lower during splenomegaly, and then back to a level similar to that of wild type mice again (Figure 4.9 lane 1, right). Although it is possible that the transcription level of M1 for each viral genome is first inhibited and then up-regulated, it is most likely that this change is caused by normalisation by vDNA, which suggests that the level of M1 transcripts remains at a similar level in spleen tissue although the viral DNA has changed greatly from day 16 to day 28.

Similar trends were also found in viral DNA polymerase, RTA, and M11 (Figure 4.9 lanes 3–5). Therefore, we conclude that the increase of infected cells in IFNγR$^{-/-}$ spleen during day

16 to day 20 post infection were expressing ORF73 but not M1, vDNA polymerase, RTA, and M11. On the level of the whole spleen, the expression of the productive infection/reactivation related genes was shutting down over the period from day 16 to day 28 and remained low in both IFNγR$^{-/-}$ and WT mice. Although there was a significant increase in ORF50 expression from day 20 to day 24 post infection which indicates an enhanced reactivation in the IFNγR$^{-/-}$ spleen (Figure 4.9 lane 4, left), it did not fit the trend of the changing viral load (Figure 4.9 lane 4, right). As discussed in section 4.3.2, on day 16 to day 20 post infection, the newly increased number of infected cells which expressed mLANA were mainly germinal centre B cells and memory B cells, and these two populations contributed the majority of B-cell loss as well as viral load reduction during fibrosis. There was no elevated expression of reactivation-associated genes corresponding to the change in these two B-cell subpopulations; hence, it is unlikely that the viral reactivation caused massive cell loss during fibrosis. However, this conclusion needs to be confirmed by examining the viral gene expression in enriched germinal centre B cells and memory B cells.

4.6 Discussion

In this chapter, we investigated the change of distribution of B-cell subpopulations, and the cells expressing viral ORF73 in IFNγR$^{-/-}$ mice during fibrosis in each subpopulation. Further, we examined viral transcripts in both spleen tissue and sorted ORF73 expressing cells for selected viral genes.

1. Reactivation-associated viral genes are not the main reason causing massive cell loss in IFNγR$^{-/-}$ mice

The expression of viral DNA polymerase, RTA, and M11 decreased throughout latent infection from day 16 to day 60 post infection in both IFNγR$^{-/-}$ and WT mice. The dramatic change of viral infection in IFNγR$^{-/-}$ mice does not contribute to the expression of vDNA pol, RTA, and M11. This result shows that an enhanced reactivation from latency is unlikely to be the main reason causing massive cell loss during fibrosis in IFNγR$^{-/-}$ spleen. Moreover, viral gene expressions in sorted mLANA-positive cells on day 20 post infection confirmed that these viral genes were expressed at very low levels in infected cells, and there was no significant difference (p>0.05) between IFNγR$^{-/-}$ mice and WT mice on the expression levels.

Evans et al. suggest that persistent reactivation from latency may cause tissue damage which subsequently leads to the occurrence and development of fibrosis in IFNγR$^{-/-}$ mice (Evans et al., 2008). The persistent infection includes both latent infection and a low level of reactivation from latency. During latency establishment, lytic infection is observed using immunohistochemistry method on day 16 to day 20 post infection (Gangadharan, 2006). Moreover, a majority of MHV-68 infected cells in the spleen which undergo reactivation were shown to be plasma cells (Collins et al., 2009; Liang et al., 2009). Therefore one of the possible explanations is that in IFNγR$^{-/-}$ mice, the increased virus-driven B-cell differentiation lead to increase in the plasma cell population which lead to an increased

reactivation. This enhanced reactivation caused cell death, but it is not the main reason for the rapid reduction of germinal centre B cells and memory B cells during fibrosis.

Our results have pointed out the importance of studying viral gene expression in different subtypes of infected cells in IFNγR$^{-/-}$ mice. However, currently, our techniques of cell separation and RNA extraction are not ideal. Further experiments and advanced methods are required.

2. M1 expression during fibrosis

In spleen tissue, the number of M1 transcripts remained steady despite the viral DNA load is increasing. This suggests the increased numbers of infected cells were not expressing M1 or expressed only a very low level of M1. In enriched mLANA-MHV-68 infected cells, the expression of M1 was only detected in infected cells, suggesting there are fewer M1 transcripts detected in IFNγR $^{-/-}$ mice and wild type mice on day 20 post infection. These results indicate that a proportion of ORF73 expressing cells are expressing M1 and other genes tested. However, this difference does not appear to be statistically significant (p>0.05). M1 has been proved to be essential for fibrosis forming in IFNγR$^{-/-}$ mice (Clambey et al., 2000; Dutia et al., 2004). Here we show that there was no increased M1 expression corresponding to the development of fibrosis. The work of Evans et al. suggests that M1 may trigger the expansion of Vβ4 CD8+ T cells as a super antigen, which leads to fibrosis. However, the role of M1 in the formation of fibrosis is still unclear. Investigations on a protein-level may help to understand the role of M1.

3. ORF73 expression during fibrosis

The core viral gene in this series of experiments is ORF73, which encodes the latency associated nuclear antigen of MHV-68 (mLANA). ORF73 expression was investigated in two ways in this chapter. First, we examined ORF73 transcripts in spleen tissue and sorted

mLANA cells by qPCR. Second, we utilised recombinant virus mLANA-MHV-68 to isolate latent infected virus.

The qPCR assay shows that IFNγ receptor deficiency had no direct effect on ORF73 expression on a mRNA level. Our results show that the increase of the crucial latent gene ORF73 in the spleen is correlated with the increase of viral genome DNA, which suggests there is no enhanced up-regulation of ORF73 expression. In the IFNγR$^{-/-}$ spleen after day 16 post infection, the significant increase of viral load was mainly due to the increased number of latently infected B cells (Gangadharan, 2006). Therefore, our results show that the change of ORF73 expression in spleen tissue corresponds to the dramatic increase and decrease of the number of latently infected B cells during fibrosis. As discussed before, these newly generated cells do not express RTA, DNApol, M11, and M1.

Using mLANA-MHV-68, Nealy et al. have identified the ORF73 expressing cells which comprise around 15% of viral genome positive cells in immune competent mice on day 16 post infection. On day 28 the percentage of genome positive cells which were labelled with the lactamase substrate reached its peak of 42% post infection (Nealy et al., 2010). The same studies have not been carried out with IFNγR$^{-/-}$ mice. A similar result was also found when identifying spliced mLANA *in vivo* using RACE analysis (Allen et al., 2006). Namely, although ORF73 is expressed throughout the time course post infection, only some of the viral DNA carrying cells express ORF73. Its expression may depend on cell type and/or cell cycle. ORF73 expression was not detected in follicular B cells and newly formed B cells or macrophages in the spleen on day 14 post infection, while it was expressed in germinal centre B cells and marginal zone B cells (Marques et al., 2003). Recent research also shows that ORF73 has the potential function to manipulate the host cell cycle: ORF73 has been shown to bind BET proteins which affect the activation of cell cyclin D1, D2, and E (Ottinger et al., 2009). Therefore it is possible that ORF73 is expressed in a certain subset and stage of the host cell. There is the low expression of reactivation-associated genes at this

stage, where there was also very little reactivation and lytic infection going on compared to a latent infection in which ORF73 is expressed. Hence it is likely that the proportion of the ORF73 expressing cells within infected cells is higher than that identified by Nealy et al. (Nealy et al., 2010). The infected cells not expressing ORF73 may be the cells not undergoing mitosis while viral gene expression is been shut down or under detection. Also, there may be other type of cells such as macrophages and dendritic cells infected which do not express ORF73 or only express it at a very low level (Marques et al., 2003). Therefore, although mLANA-MHV-68 is the best tool available so far to examine and isolate latent infected cells at late time points, it cannot detect all infected cells. The limitation of the system has to be noted before further discussion.

4. Change of distribution of B-cell subpopulations and infection within these subpopulations during fibrosis

Studies on EBV also show that sIgD-negative memory B cells are the main location of persistency (Babcock et al., 1998). Moreover, it has been reported that in long-term latency in the spleen after intranasal inoculation, the latent MHV-68 is mainly confined to the surface IgD-negative subset of B cells (Willer and Speck, 2003). Our results also show that the vast majority of mLANA-positive cells are from IgD-negative B-cell subsets (germinal centre and memory B cells) despite the fact that the population is much smaller than the naïve B cell population. A significant reduction of infection in naïve B cells was observed in IFN$\gamma R^{-/-}$ mice on day 35 post infection, suggesting the presence of fibrosis affected the maintenance of the population of infected naïve B cells. The infection of IgD+ naïve B cells has been shown to be inefficient (Jarousse et al., 2008; Liang et al., 2011). Therefore the infected naïve B cells may also come from infected B-cell progenitors from bone marrow. Recent studies indicate that immature B cells in the bone marrow are a site of latency (Coleman et al., 2010) and may possibly become the origin of infected cells which reseed

the spleen. The reseeding may occur once the fibrosis is resolved and the circulation of lymphocytes is unblocked.

A number of studies have suggested a model of MHV-68 using the B-cell life cycle in a germinal centre reaction to expand the pool of infected cells by driving B-cell proliferation and differentiation, therefore establishing long-term latency in memory B cells (reviewed in Barton et al., 2011). We have found that this crucial strategy for viral persistence seems to be disturbed in the spleen of IFNγR$^{-/-}$ mice. The Th2 dominated immune response triggers severe fibrosis around splenic follicles, in which the populations of germinal centre and memory B cells rapidly decrease, and these two populations account for about 80% of infected cells. Therefore on day 35, decreased infections were observed in IFNγR$^{-/-}$ spleens corresponding with the disappearance of GC B cells and memory B cells. Why the germinal centre B cells and memory B cells in IFNγR$^{-/-}$ spleen cannot survive in the spleen during fibrosis is still unknown. We have already known that these cells did not undergo accelerated Caspase3-dependent apoptosis; moreover, TUNEL assays show they were not elevation within the spleen during fibrosis. Moreover, the viral reactivation within these cells was not elevated during fibrosis. The possibility which remains is that the presence of fibrosis has blocked the signals such as cytokines and chemokines which are important in the survival and homing of the developing B cells. Therefore these cells either leave the spleen or undergo cell death which is independent from Caspase3 and does not cause significant DNA damage. Further discussion of the fate of B cells will continue in Chapter 6.

Chapter 5 Cellular events in the spleen during MHV-68-mediated fibrosis—the role of splenic macrophages

5.1 Introduction

MHV-68 induced lung fibrosis is intensively studied as a mouse model for human herpesvirus-related idiopathic pulmonary fibrosis (IPF); nevertheless, the fibrosis which occurs in the spleen is also of great interest. In MHV-68 infection, the spleen B cells are the major site of long-term viral persistence, and in IFNγR$^{-/-}$ mice, it is observed that fibrosis forms around follicles (Gangadharan et al., 2008). We have demonstrated in Chapter 4 that during fibrosis, germinal centre and memory B cells, which carry the majority of latent virus, suffered an extra cell loss, which is not due to viral reactivation. All this evidence suggests that fibrosis has an important role in controlling viral latency in the spleen of IFNγR$^{-/-}$ mice. However, the detailed cellular basis of fibrosis and its interaction with latent infected B cells in the spleen remains unclear. In this chapter, we observe the cellular events during MHV-68 mediated fibrosis, and we pay special attention to cells that may involve in the formation of fibrosis.

Gangadharan demonstrated a dramatic change of macrophage activities in IFNγR$^{-/-}$ mice by staining for different subsets of macrophages and observing their movement into the white pulp on days 12 to 16 post infection, where they exhibit signs of activation(Gangadharan, 2006). IFNγ signalling is one of the main features of Th1 immune response and the lack of the IFNγ receptor favours the induction of Th2 cytokines such as IL-4 and IL-13. Under such circumstances, alternative activation of macrophages (AAMφ) assumes a more dominant role in the immune response (Mills et al., 2000). Elevated expression of markers of AAMφ such as Arginase 1, Ym1/2, and FIZZ 1 suggests that AAMφ is associated with fibrosis in the spleen (Gangadharan et al., 2008), lung (Mora et al., 2006), liver, and bile duct (Gangadharan et al., 2009) in IFNγR$^{-/-}$ mice. In herpesvirus-infected patients, reactivation from latency is considered to be the main trigger/stimulus which lead to fibrosis—a disorder of wound repair. It has been reported that antiviral therapy which

controls reactivation helps to limit MHV-68 infection induced lung fibrosis in IFNγR$^{-/-}$ mice (Mora et al., 2007) on the C57BL/6 background. On the contrary, similar studies done in our lab on IFNγR$^{-/-}$ on the 129Sv/Ev background show that the inhibition of lytic infection does not limit fibrosis in the lung (Dutia et al., unpublished results). This is possibly because of the breed of mice, or because of the drug dose or different routes of infection. The mechanisms of MHV-68 infection causing splenic fibrosis are still unclear. There are two hypotheses: the persistent reactivation from latent infection, and/or tissue damage caused by immune response. Further discussion about both hypotheses continues in Chapter 6.

As introduced in Chapter 1, macrophages play a key role in generation and resolution of fibrosis. This is particularly true for hepatic fibrosis, in which macrophages are closely associated with the activity of the main ECM producing cells—myofibroblasts (Leicester et al., 2004; Wynn and Barron, 2010). In the MHV-68 model, Gangadharan found macrophage-like spleen cells stained positive for the myofibroblast marker α-smooth muscle actin (α-SMA) (Gangadharan, 2006). Moreover, Mooney et al. have observed CSF1R-EGFP positive cells co-expressing α-SMA, which suggests that macrophages may have the potential to trans-differentiate into myofibroblasts (Mooney et al., 2010). Based on these observations, we set out to investigate in our model whether macrophages contribute to the cellular basis of fibrosis by trans-differentiating into myofibroblasts.

To further explore the possible role of alternatively activated macrophages in the spleen of IFNγR$^{-/-}$ mice during MHV-68 induced fibrosis, immunofluorescent assay was carried out using mice in which EGFP is expressed in macrophage/monocytes lineage. Macgreen mice have a reporter gene EGFP insertion after the colony stimulation factor 1 receptor (CSF1R, also called c-fms) promoter (Sasmono et al., 2007; Sasmono et al., 2003). CSF1R is the receptor for cytokine CSF1 which regulates macrophage proliferation and differentiation. We crossed the Macgreen mice with IFNγR$^{-/-}$ mice to produce IFNγR$^{-/-}$ mice with EGPF +ve

macrophages (Macgreen × IFNγR$^{-/-}$). With visible macrophages, Macgreen × IFNγR$^{-/-}$ mice provide an excellent tool to study the role of macrophages in viral induced fibrosis.

There was a technical problem with traditional microscopy when used at high magnification to observe tissue samples: the view is too restricted to show the relationship of cell events with other components of the tissue. Pictures shown in this chapter were taken using tiled scan based on confocal microscopy, in which several pictures were taken at high magnification and then were stitched together to form a general view. With this technique, we were able to locate the events in the scale of the whole spleen, and at the same time have a very close look at each cell of interest at high resolution and magnification. In this chapter, we aimed to explore the role of alternatively activated macrophages in the development of the fibrosis. Particularly, we investigate if the α-SMA expressing cells observed by Gangadharan are co-expressing macrophage markers. To achieve this, we took high-resolution images showing the distribution of B cells, T cells, and macrophages by co-stained spleen frozen sections with α-SMA along with cell markers for B cells and T cells.

5.2 Optimisation of multi-colour immunofluorescent staining

5.2.1 α-SMA distribution in the spleen

Anti-α-smooth muscle actin (α-SMA) antibody was initially used to show the trans-differentiation of macrophages into myofibroblasts. However, using immunofluorescent staining we observed accumulation of α-SMA as extracellular material (Figure 5.1) as a component of fibrosis. The spleen structures, such as capsule, spleen trabecular, and blood vessel, were all α-SMA positive (Figure 5.1 A and C). The ECM accumulating around the germinal centres was also α-SMA positive (Figure 5.1 A), and stained positive for collagen in Masson's trichrome staining (Figure 5.1 B). Therefore we used this antibody not only as a marker for myofibroblasts, but also to show the distribution of ECM.

5.2.2 Single-staining (isotype) controls

Single-staining (isotype) controls were performed to detect the level of non-specific binding for each antibody, as well as to detect the spillover between channels. When compared to normal spleen tissue, the fibrotic spleen showed a high background of auto-fluorescence and non-specific binding. Therefore we used spleen from IFNγR$^{-/-}$ mice on day 28 post infection to see whether severe fibrosis affects single-cell staining with different cell markers including α-SMA. As expected, we detected green auto-fluorescence caused by Elastin . Also, a low level of non-specific binding of mouse IgG2b isotype control antibody was detected in yellow and red channels (data no shown). However, the non-specific staining can be distinguished from the positive staining and therefore is negligible.

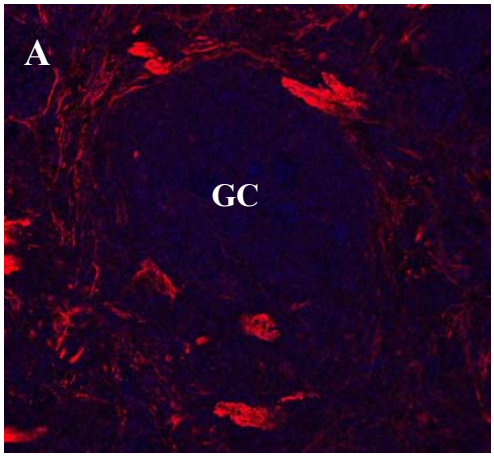

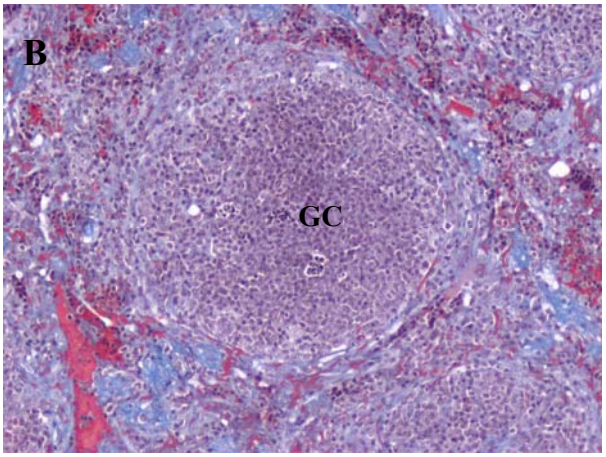

Day 16 P.I.

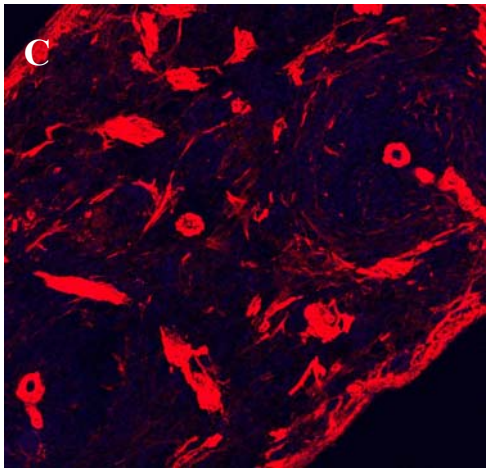

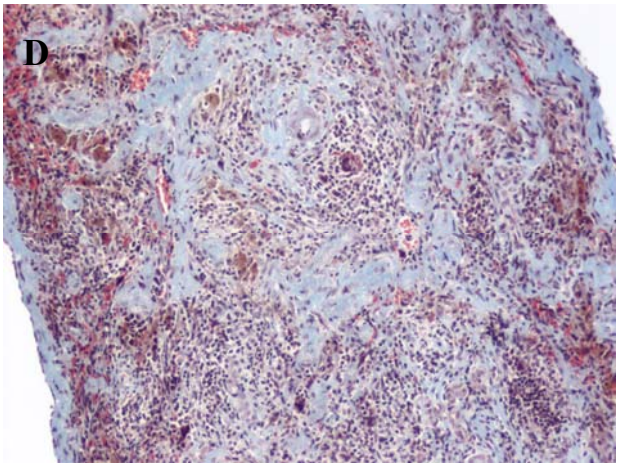

Day 26 P.I.

Figure 5.1 Comparison of immunostaining for α-SMA (A and C, red) and Masson's trichrome staining for collagen (B and D, blue) in the spleen of IFNγR$^{-/-}$ mice on day 16 (A and B) and day 26 (C and D). The patterns of distribution of α-SMA and that of collagen are very similar. Pictures were taken at 20x magnification.

5.3 Cellular events in the spleen during fibrosis: induction, appearance, and resolution

In this section, we demonstrate the cellular events which occur in the spleen of IFNγR$^{-/-}$ mice during the induction (day 12 post infection), appearance (days 16 and 28 post infection), and resolution (day 35 post infection) of fibrosis, and compare them with those in immune competent mice at the same stages of infection. Special attention is paid to the appearance of macrophages and ECM-producing cells in forming fibrosis. Each group had 3 to 4 mice of mixed age and sex.

5.3.1 Day 12 post infection: Fibrosis starts from peri-arteriolar lymph sheath (PALS)

In Macgreen × IFNγR$^{-/-}$ mice on day 12 post infection, mild accumulation of ECM was observed around lymphoid follicles (Figure 5.2 A), and more evidentlyobserved, in PALS (Figure 5.2 B). Interestingly, the α-SMA positive cells followed the distribution of the fibroblastic reticular cells (FRCs) network. In comparison to the B-cell zone, the T-cell zone (PALS) appeared to be more involved in fibrosis at this stage. Angiogenesis was observed in PALS where T cells interacted with macrophages.

In wild type mice on day 12 post infection there was no accumulation of ECM in the spleen. There was neither enhanced signal for α-SMA, nor sign of angiogenesis (Figure 5.2 D). Notably, there were two levels of expression of CSF1R-eGFP (Figure 5.2 C and D): macrophages with high expression of eGFP lining the red pulp and marginal zone; and cells morphologically distinguishable from macrophages with low eGFP expression scattered in both red pulp and white pulp. The identity of these cells is not known. A previous study has shown that there exists a CSF1R-eGFP^{low} CD11c^{low} CD45R (b220)$^{+}$ population defined as splenic plasmacytoid dendritic cells (MacDonald et al., 2005). Moreover, these eGFP low expressing cells were recently shown to be co-stained with Gr1 and Ly6C; therefore there

are possibly neutrophils and monocytes within this population (Mooney et al., 2010). Based on previous study, as well as our observation of cell morphology as size, cell shape, and nuclear shape, we believe the CSF1R-eGFP ^{low} CD45R(b220)$^{+}$ observed here were follicular dendritic cells (Figure 5.2 D, orange arrows), while the dim green cell within germinal centre but b220 negative was infiltrating neutrophils. The infiltration of neutrophils into germinal centres was observed in wild type mice and IFNγR$^{-/-}$ mice, but to a higher extent in wild type mice.

Compared with IFNγR$^{-/-}$ spleen, the expression of the eGFP is considerably higher in WT on day 12 post infection. This could be related to the macrophage function involved in the immune response against MHV-68 infection in immune-competent mice.

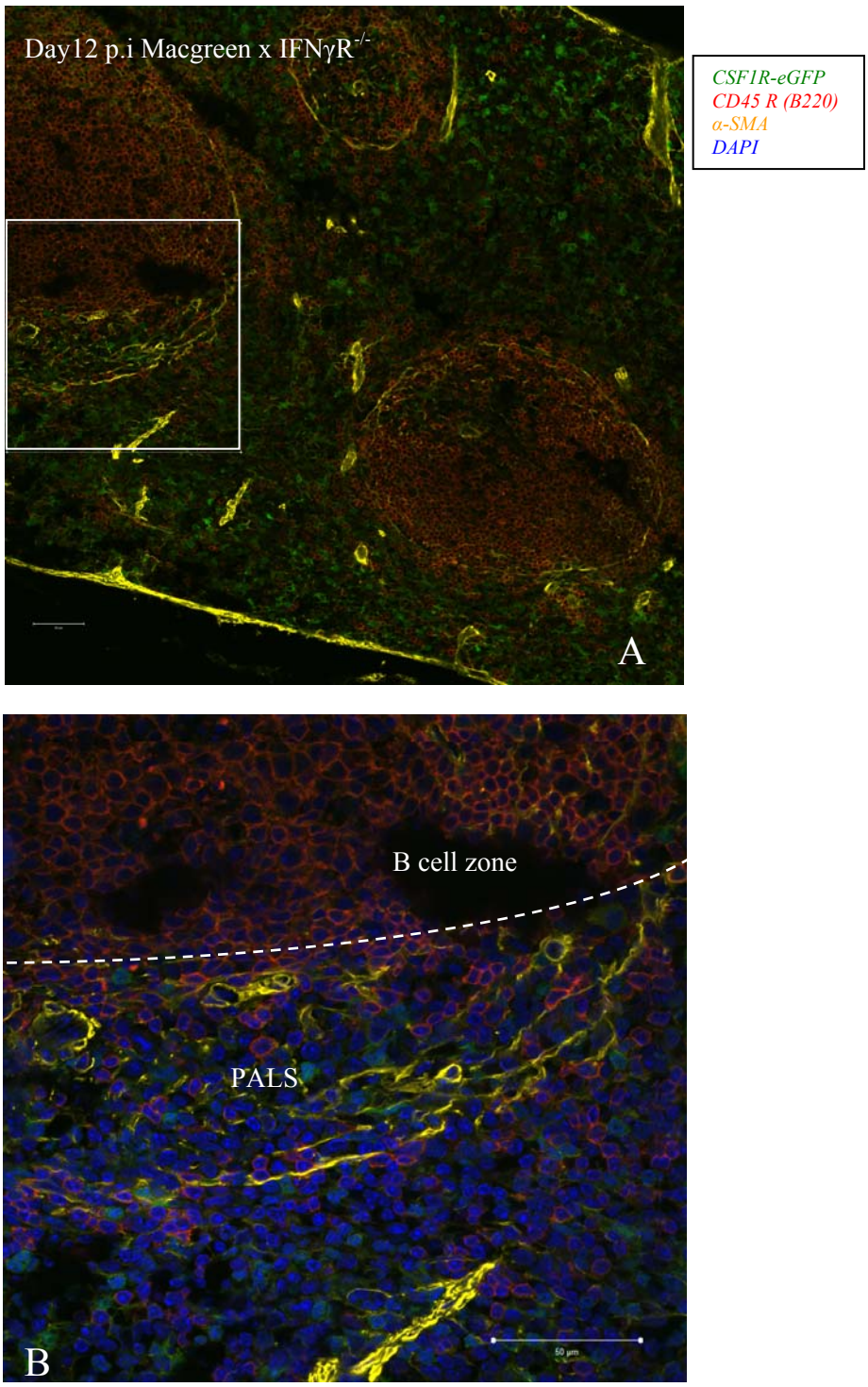

Figure 5.2 Spleen frozen section (Confocal microscopy tiled scan 63x magnification oil lens) of a Macgreen × IFNγR$^{-/-}$ mouse (A and B) and a macgreen mouse (WT, C and D, next page) infected with MHV-68 on day 12 post infection: All scale bars represent 50µm. Macrophages were marked by eGFP. Frozen sections were stained with anti-CD45R(B220)and anti-α-SMA antibodies, and counterstained with DAPI. (A): Macgreen × IFNγR$^{-/-}$ mouse: 3x3 tiled scan shows overview of spleen structure. (B): Amplified rectangular area from A. (C): Macgreen mouse: 3x3 tiled scan shows overview of spleen structure. (D): Amplified rectangular area from C; orange arrow shows follicular dendritic cell.

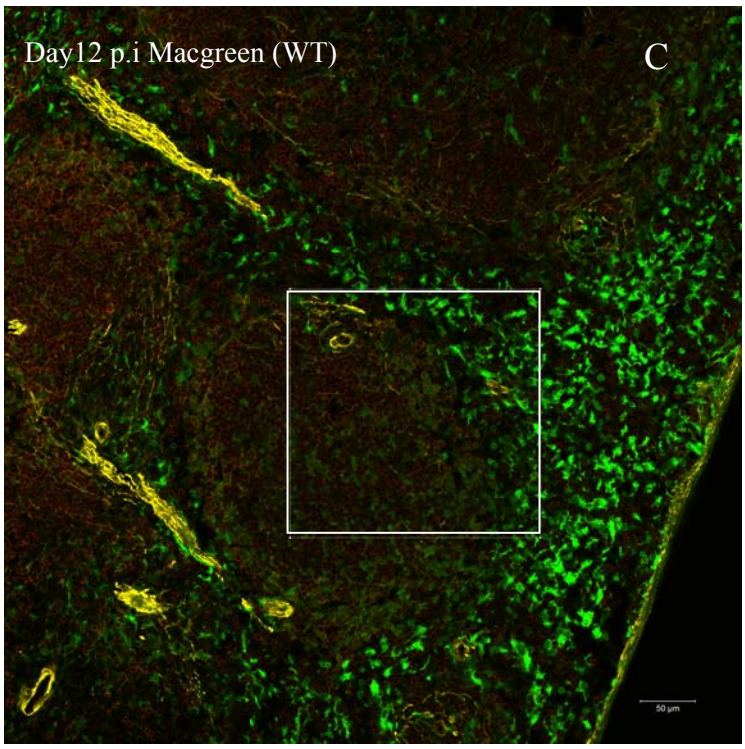
Day12 p.i Macgreen (WT)
C
CSF1R-eGFP
CD45 R (B220)
α-SMA
DAPI

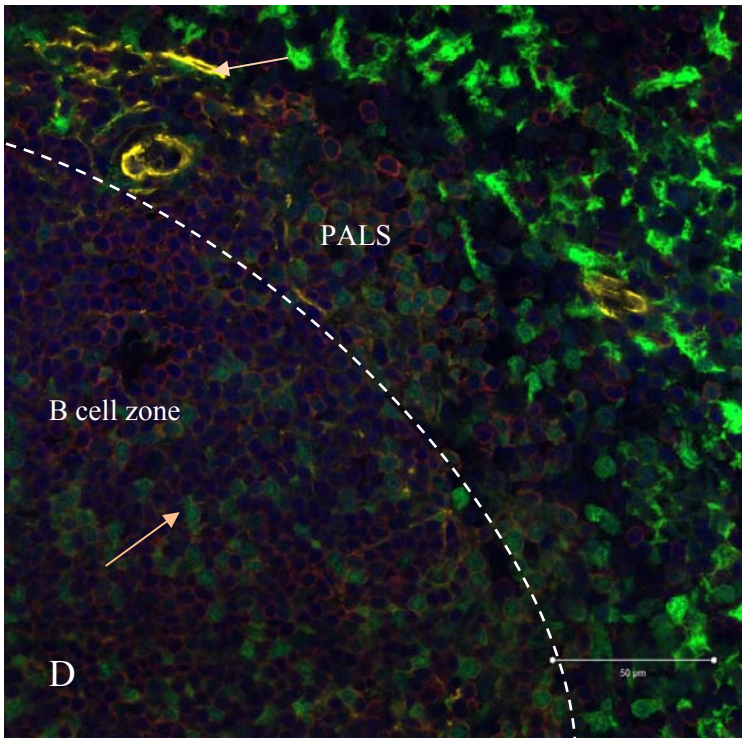
PALS
B cell zone
D

5.3.2 Increased Fibrosis and the destruction of splenic architecture: Day 16 and day 28 post infection

In Macgreen × IFNγR$^{-/-}$ mice on day 16 post infection, the spleen structure, capsule and trabecular, were thickened with enhanced α-SMA signal compared to that at day 12 p.i.. More angiogenesis and more elastin were produced. There was a higher density of eGFP signal compared to day 12 post infection. The cell density in red pulp and PALS had significantly increased. Patches of B cells were surrounded by ECM and green macrophages, resulting in a decrease in the size of the B-cell zone (Figure 5.3 A). More interestingly, we saw α-SMA positive staining in the cytoplasm within some eGFP positive cells in IFNγR$^{-/-}$ spleen (Figure 5.3 B, white arrows). It appears that these cells were either producing or engulfing ECM, or the yellow signal was caused by auto-fluorescence. However, such morphology could only be observed in fibrotic spleens. This may suggest a significant role played by macrophages in ECM accumulation. We also observed α-SMA positive cells, specifically in IFNγR$^{-/-}$ mice. They were located on the edge of the B-cell zone as well as the marginal zone (Figure 5.3 C, white arrows). These cells are myofibroblasts, which play the key role of producing ECM and lead to fibrosis. Their appearance around the B-cell zone explains how ECM forms around the infected B cell follicle.

In wild-type mice on day 16 post infection, no fibrosis developed. In the marginal zone, some cells expressed CD45R (b220) on the cell surface while CSF1R-eGFP was expressed in the cell cytoplasm (Figure 5.4 A). Infiltration of both macrophages and neutrophils into the B-cell zone was observed. Neither α-SMA positive-non-green cells, nor macrophages stained with α-SMA in the cell cytoplasm were observed in wild-type spleens (Figure 5.4 B).

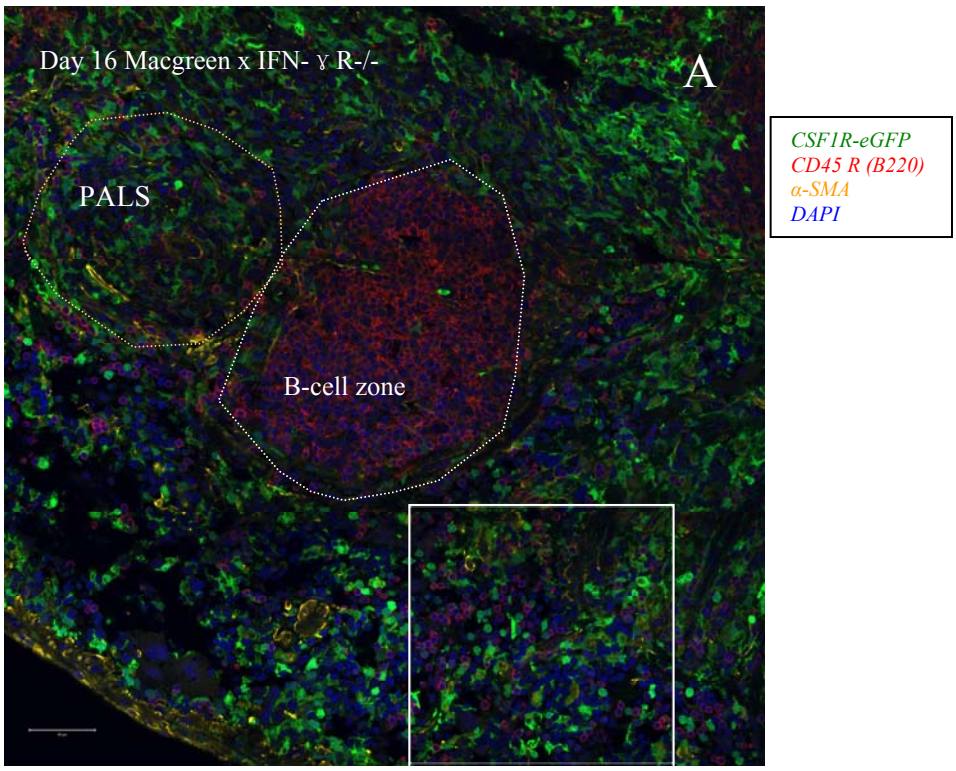
Day 16 Macgreen x IFN- γ R-/-
A
PALS
B-cell zone
CSF1R-eGFP
CD45 R (B220)
α-SMA
DAPI

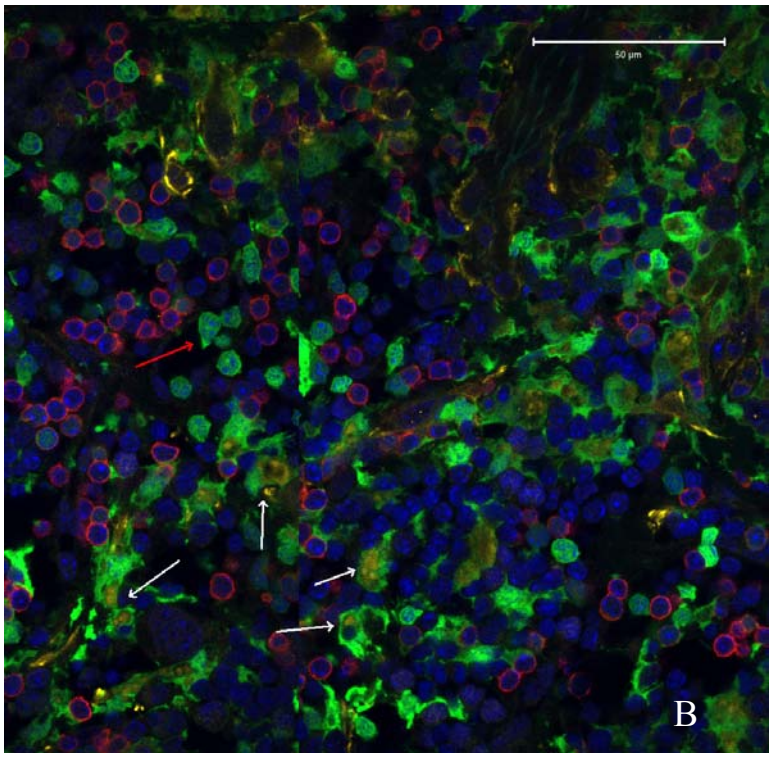
50 µm
B

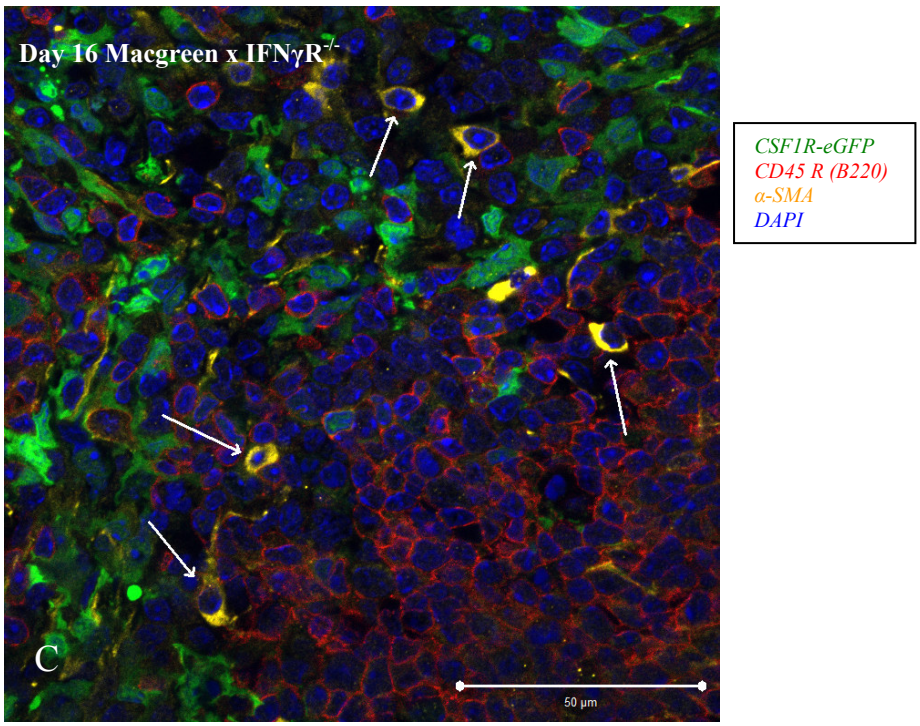

Figure 5.3 Spleen frozen sections (Confocal microscopy tiled scan 63x magnification oil lens) of a Macgreen × IFNγR$^{-/-}$ mouse infected with MHV-68 on day 16 post infection: All scale bars represent 50µm. Macrophages were marked by eGFP. Frozen sections were stained with anti-CD45R(B220)and anti-α-SMA antibodies, and counterstained with DAPI. (A): Macgreen × IFNγR$^{-/-}$ mouse: 3x3 tiled scan shows overview of spleen structure. (B): Amplified rectangular area from A. (C) shows α-SMA positive cells (arrows).

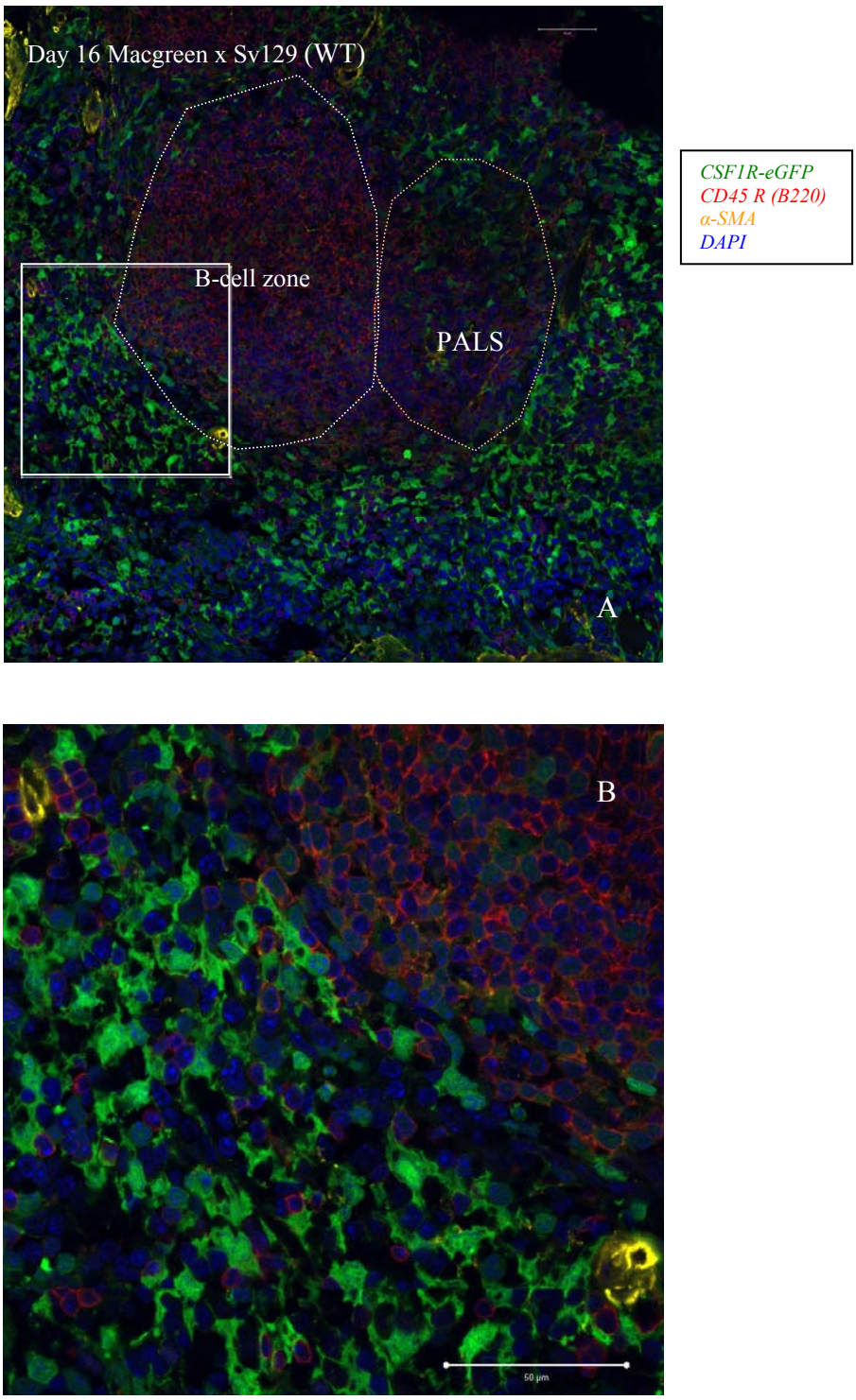

Figure 5.4 Spleen frozen sections (Confocal microscopy tiled scan 63x magnification oil lens) of a Macgreen × 129Sv mouse on day 16 post infection: All scale bars represent 50µm. (A): 5x5 tiled scan shows overview of spleen structure. (B): Amplified rectangular area from A.

In Macgreen × IFNγR$^{-/-}$ mice on day 28 post infection, the spleen had become highly fibrotic and the red pulp had collapsed. The size of PALS was greatly reduced and there was an increase in angiogenesis. The number of macrophages in the red pulp had greatly decreased and the rest remained in PALS (Figure 5.5 B). The thickened capsule had been padded with elastin, which increased the tension of the spleen and caused shrinking in size and lack of blood circulation. Overall the spleen structure had been destroyed: the B cells were greatly reduced in number, as were macrophages and T cells (Figure 5.5 A). Interestingly, there was a depletion of eGFP low expressing population within the B-cell zone, suggesting a depletion of dendritic cells (Figure 5.5 B).

In wild-type mice on day 28 post infection, the spleen had recovered from splenomegaly (Figure 5.5 C).

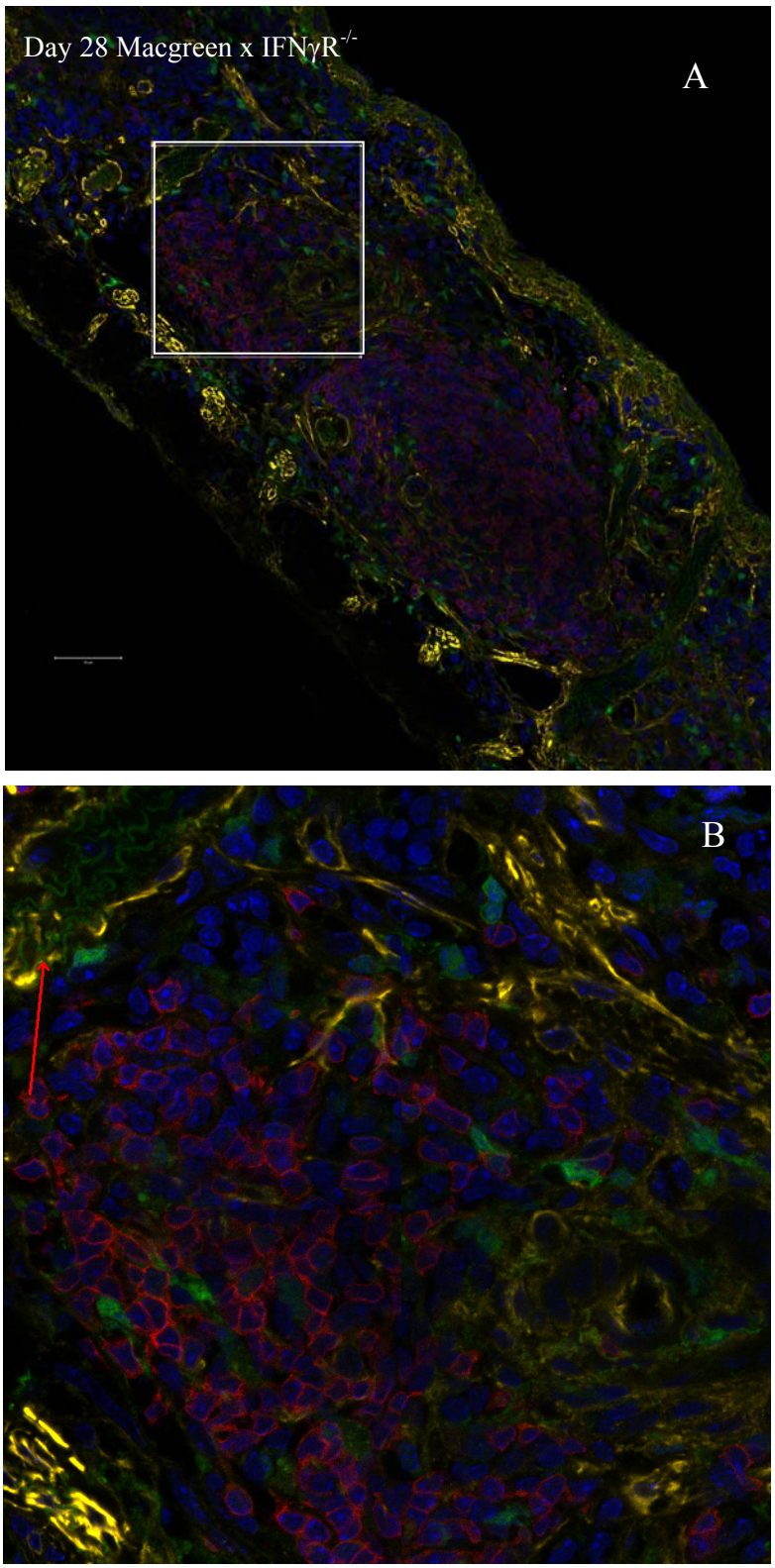
Day 28 Macgreen x IFNγR-/-
A
B
CSF1R-eGFP
CD45 R (B220)
α-SMA
DAPI

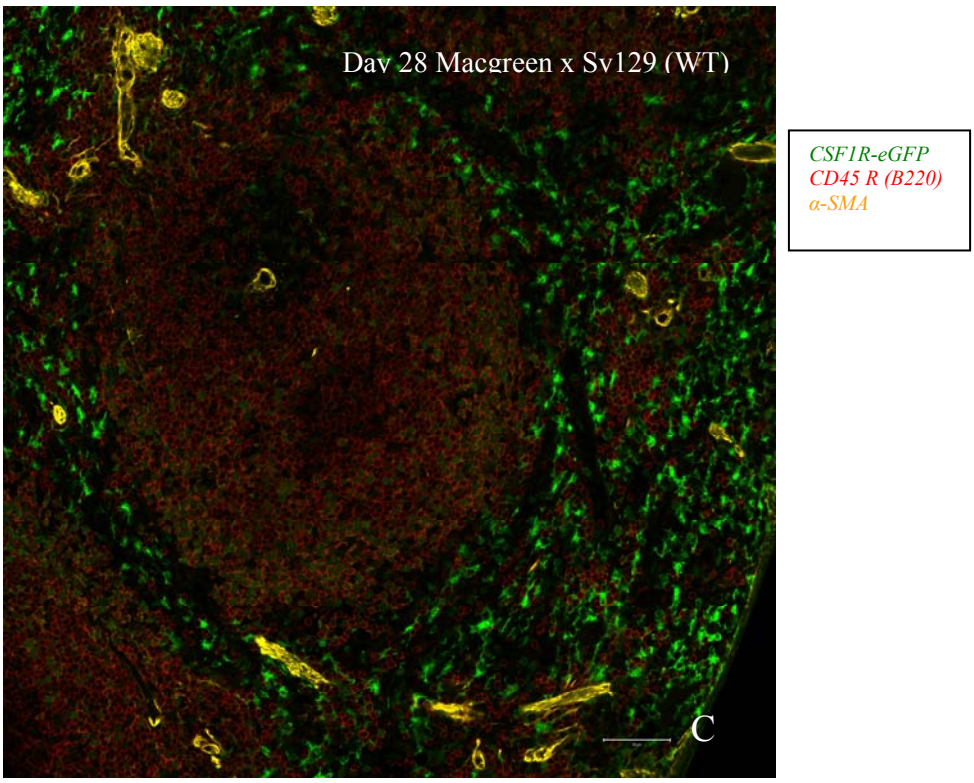

Figure 5.5 Spleen frozen section (Confocal microscopy tiled scan 63× magnification oil lens) of a Macgreen × IFNγR-/- mouse (A and B) and a Macgreen × 129Sv mouse (WT, C) infected with MHV-68 on day 28 post infection: All scale bars represent 50μm. Macrophages were marked by eGFP. Frozen sections were stained with anti-CD45R(B220)and anti-α-SMA antibodies, and counterstained with DAPI. (A): Macgreen × IFNγR-/- mice on day 28 post infection: 5×5 tiled scan shows overview of spleen structure. (B): Amplified rectangular area from A. (C): Macgreen on day 28 post infection: 3×3 tiled scan shows overview of spleen structure.

5.3.3 Resolution of fibrosis and rebuilding of follicle structure: Day 35

In the recovery phase of day 35 post infection IFNγR$^{-/-}$ spleen, the T-cell zone (PALS) was rebuilt and macrophages appeared again in the red pulp and PALS (Figure 5.6 A). Interestingly, green pigments appeared within the macrophages, and these cells were distributed very close to the tissue undergoing angiogenesis (Figure 5.6 B, white arrow).

In the wild-type spleen, the spleen structure was well kept and no sign of infection was observed (Figure 5.6 C).

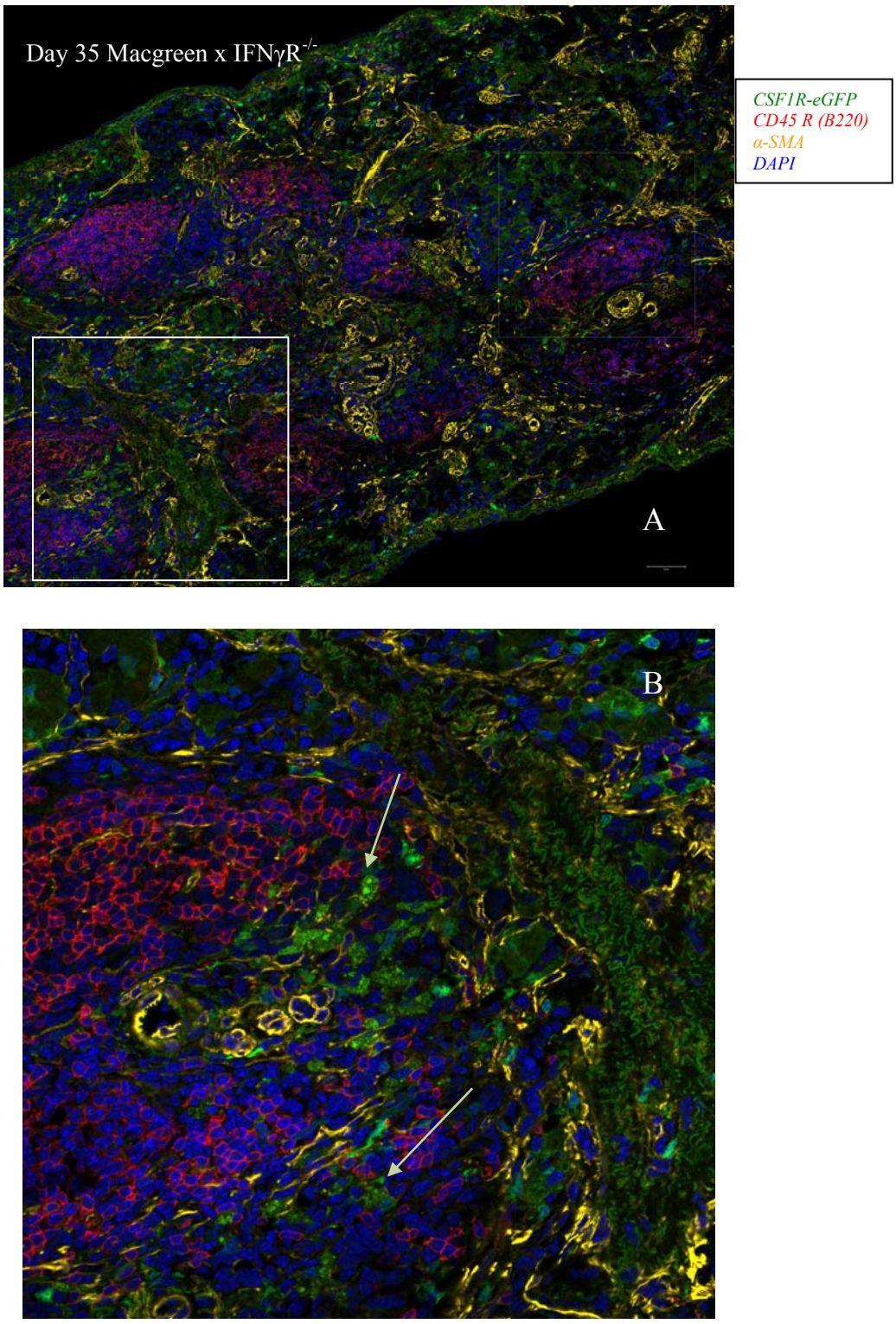
Day 35 Macgreen x IFNγR-/-
CSF1R-eGFP
CD45 R (B220)
α-SMA
DAPI
A
B

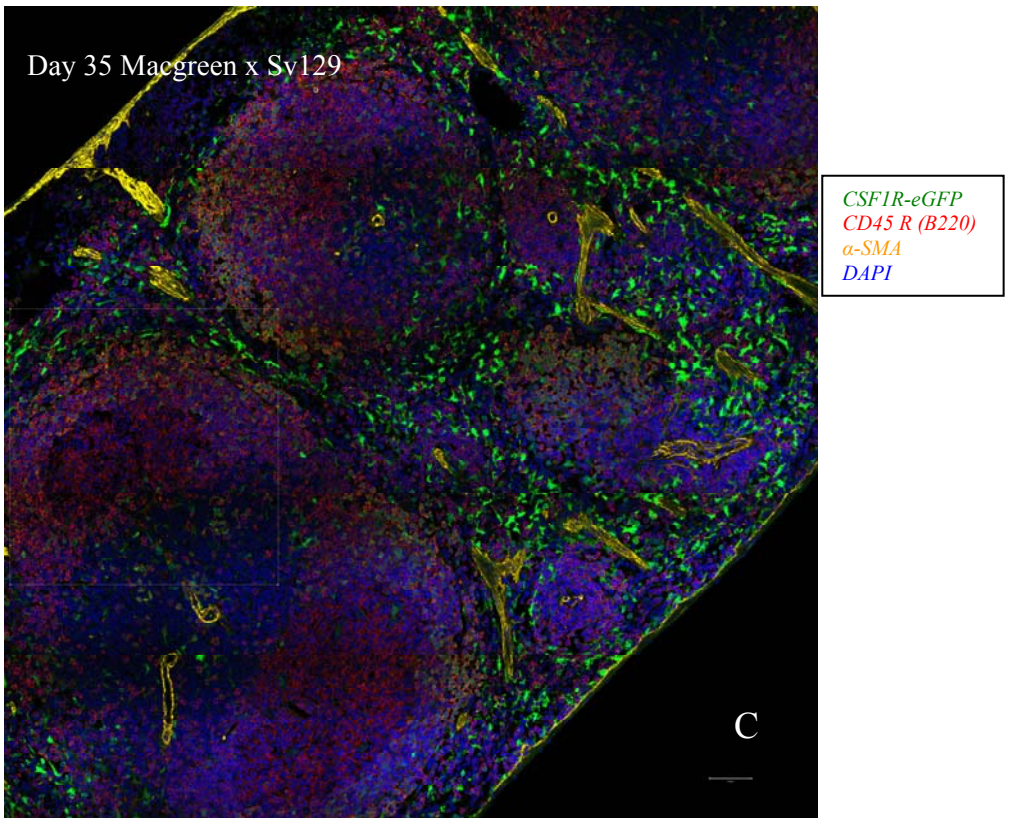

Figure 5.6 Spleen frozen section (Confocal microscopy tiled scan 63× magnification oil lens) of Macgreen × IFNγR-/- mouse (A and B) and Macgreen × 129Sv mouse (WT, C) infected with MHV-68 on day 35 post infection: All scale bars represent 50μm. Macrophages were marked by eGFP. Frozen sections were stained with anti-CD45R(B220)and anti-α-SMA antibodies, and counterstained with DAPI. (A): Macgreen × IFNγR-/- mice on day 35 post infection: 5×4 tiled scan shows overview of spleen structure. (B): Amplified rectangular area from A. (C): Macgreen × 129Sv on day 35 post infection: 5×5 tiled scan shows overview of spleen structure.

5.3.4 T-cell distribution during fibrosis

Gangadharan observed a change in the distribution of T cells during fibrosis: $CD3^+$ T cells were observed moving from PALS to germinal centres in the spleen of both $IFN\gamma R^{-/-}$ and wild-type mice before fibrosis. Once fibrosis had fully formed, T cells were no longer observed (Gangadharan, 2006). We confirmed his finding and, using the multi-colour system, we were able to observe in more details this process of T-cell trafficking.

There were 4 to 5 mice in each group aged 12 to 16 weeks. Using the pan-specific CD3 marker, we observed more infiltration of T cells from PALS to germinal centre in an $IFN\gamma R^{-/-}$ spleen than in wild-type spleen on day 16 post infection, when fibrosis had just begun (Figure 5.7). A large number of macrophages appeared in the area of PALS of $IFN\gamma R^{-/-}$ spleen.

On day 20 post infection, T cells in PALS in $IFN\gamma R^{-/-}$ mice were greatly reduced in number and their population was not restored during fibrosis (Figure 5.8).

On day 28 post infection, in a highly fibrotic spleen, patches of T cells were no longer observed, while there were still a number of B cells left. However, there were T cells scattered the B-cell zone and also in a shrunken PALS with a decreased number of macrophages (Figure 5.9).

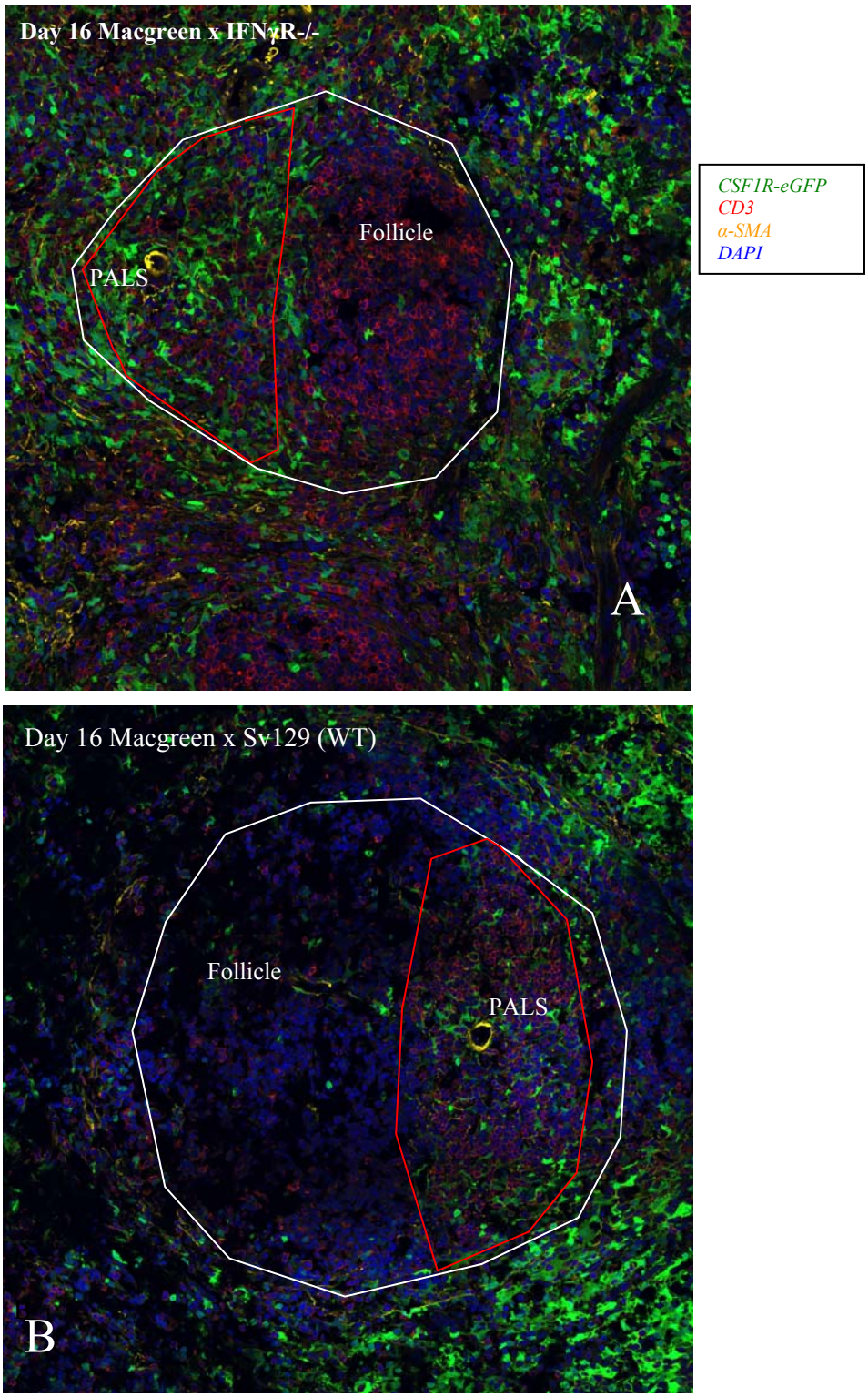

Figure 5.7 Distribution of splenic T cells during infection with MHV-68: Spleen frozen section (Confocal microscopy tiled scan 63× magnification oil lens) of a Macgreen × IFNγR-/- mouse (A and B) and a Macgreen × 129Sv mouse (WT, C) infected with MHV-68 on day 16 post infection: All scale bars represent 50µm. Macrophages were marked by eGFP. Frozen sections were stained with anti-CD3 and anti-α-SMA antibodies, and counterstained with DAPI. (A): Macgreen × IFNγR-/- mice on day16 post infection: 3×3 tiled scan shows overview of spleen structure. (B): Macgreen × 129Sv on day 16 post infection: 3×3 tiled scan shows overview of spleen structure.

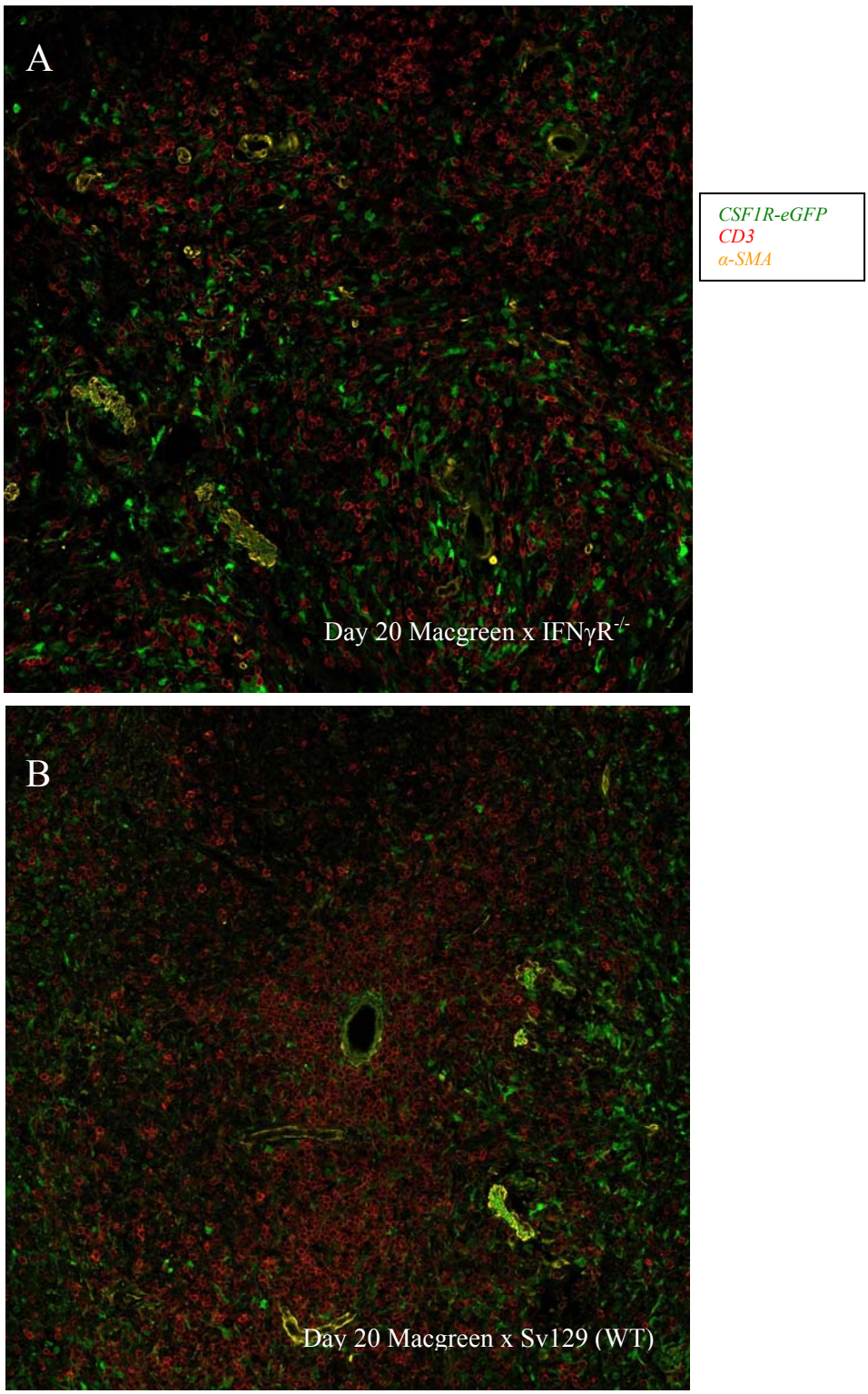

Figure 5.8 Distribution of splenic T cells during infection with MHV-68: Spleen frozen section (Confocal microscopy tiled scan 63× magnification oil lens) of a Macgreen × IFNγR-/- mouse (A and B) and a Macgreen × 129Sv mouse (WT, C) infected with MHV-68 on day 20 post infection: All scale bars represent 50µm. Macrophages were marked by eGFP. Frozen sections were stained with anti-CD3 and anti-α-SMA antibodies. (A): Macgreen × IFNγR-/- mice on day20 post infection: 3×3 tiled scan shows overview of spleen structure. (B): Macgreen × 129Sv on day 20 post infection: 3×3 tiled scan shows overview of spleen structure.

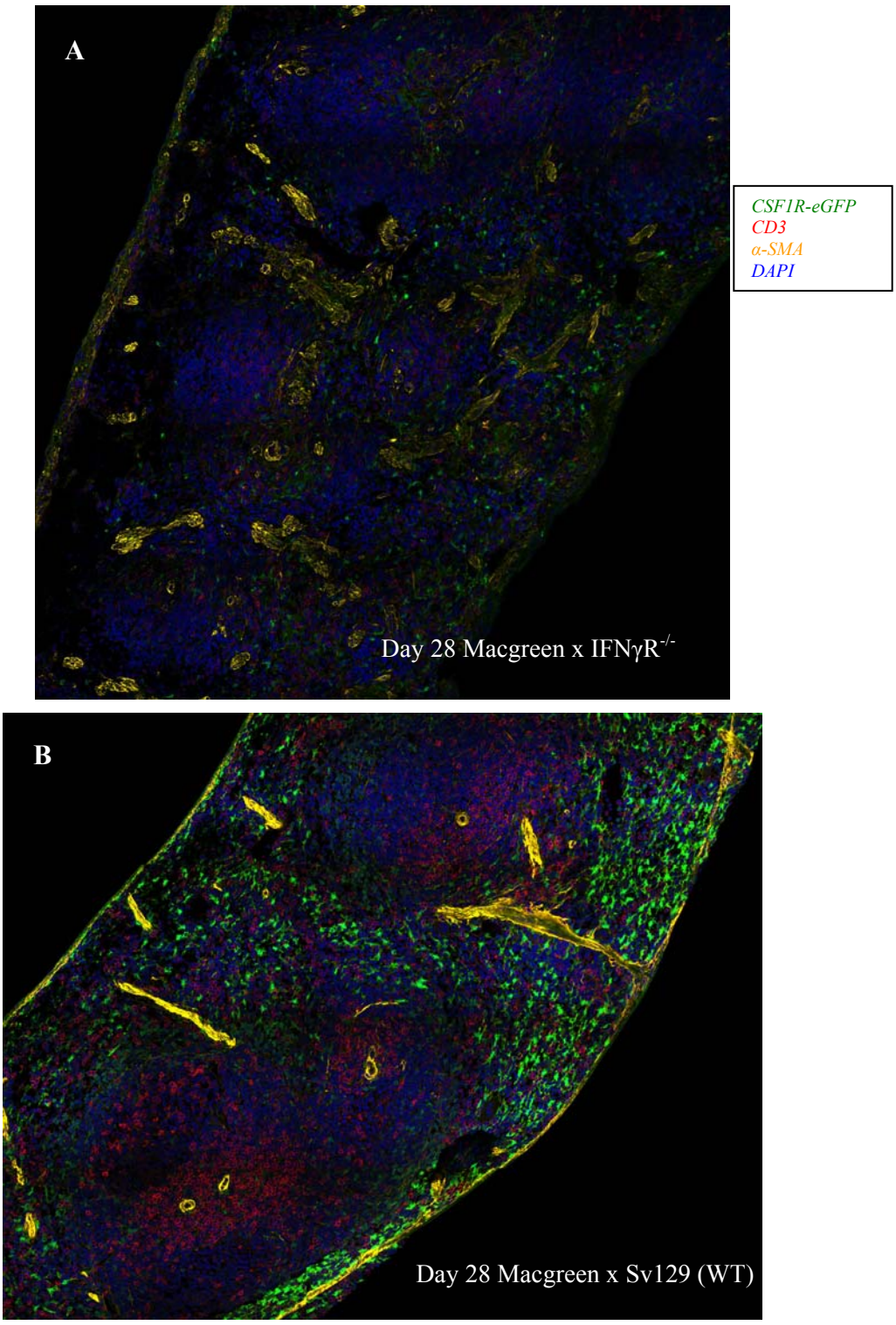

Figure 5.9 Distribution of splenic T cells during infection with MHV-68: Spleen frozen section (Confocal microscopy tiled scan 63× magnification oil lens) of a Macgreen × IFNγR-/- mouse (A and B) and a Macgreen × 129Sv mouse (WT, C) infected with MHV-68 on day 28 post infection: All scale bars represent 50µm. Macrophages were marked by eGFP. Frozen sections were stained with anti-CD3 and anti-α-SMA antibodies, and were counterstained with DAPI. (A): Macgreen × IFNγR-/- mice on day28 post infection: 5×5 tiled scan shows overview of spleen structure. (B): Macgreen × 129Sv on day 28 post infection: 5×4 tiled scan shows overview of spleen structure.

5.4 Discussion

The cellular events in the fibrotic spleen have been investigated by Gangadharan using the method of immunohistochemistry (Gangadharan, 2006). However, this method can only mark one type of cell at a time. The multi-colour system provides a tool to look at the interaction among T cells, B cells, macrophages, and FRCs. Moreover, confocal tiled scanning enables a wide overview of the whole spleen structure, as well as high resolution and magnification of events at the single-cell level. Using this technology we extended our understanding of the change of macrophages in number, location, and morphology during fibrosis. Moreover, some of our observations raise questions for further investigation.

In our model of spleen fibrosis induced by MHV-68, we hypothesised that these macrophages trans-differentiate into myofibroblasts. We examined this hypothesis by looking for green macrophages co-expressing α-SMA. On day 16 post infection, we observed many macrophages in the red pulp and that the areas which were close to spleen trabeculae had a dim staining for α-SMA in the cell cytoplasm. Mooney et al. (2010) describes the α-SMA expressing cell in the peritoneal cavity as ‘spindle-shaped’, and they express α-SMA on the cell surface. However, these cells which we observed seemed to be morphologically different from those observed by Mooney et al., and the staining of α-SMA was in the cell plasma. Moreover, in the same spleen section, we also observed myofibroblasts which were strongly positive for α-SMA, but non-green, located at the marginal zone where they produced ECM and formed fibrosis. Therefore, the macrophages we observed share little similarity with myofibroblasts, and they are also distinct from the trans-differentiating macrophages which have been described in previous studies.

We think the dim signal of α-SMA in green macrophages may be due to auto-fluorescence or other activity of macrophages—for example, engulfing dead cells or ECM—and there is

still the possibility that they are producing ECM, including α-SMA. Based on what has been observed, we conclude that although the macrophages may produce ECM which contributes to fibrosis, there is no evidence of macrophages trans-differentiating into myofibroblasts. There are two possible roles of macrophages in the generation of ECM in IFNγR$^{-/-}$ spleen: first, alternatively activated macrophages may regulate myofibroblasts producing ECM by secreting pro-fibrosis factors such as TGFβ1, PDGF, and TIMPs; and second, the macrophages may produce ECM; however, morphologically, they do not become myofibroblasts.

Since the myofibroblasts do not come from the macrophages, what is the origin of the myofibroblasts? One possibility is bone marrow-derived fibrocytes which circulate through the blood stream and contribute to fibrosis in multiple organs (Bucala et al., 1994; Direkze et al., 2003; Forbes et al., 2004).

Another potential origin of myofibroblasts could be the fibroblastic reticular cells (FRCs). The functions of the spleen largely depends on its architecture which is maintained by fibroblastic reticular cell (FRC) network which consists mainly of endothelial cells and fibroblast-like cells of mesenchyme origin (Cyster, 2005; Junt et al., 2008; Luther et al., 2011; Mueller and Germain, 2009). FRCs in the spleen include the marginal zone macrophages, sinus-lining endothelial cells of the marginal sinus, T cell zone FRCs within PALS, as well as FDCs and follicular FRC subsets (Mebius et al., 2004; Balogh et al., 2008). Accumulating evidence has shown that FRCs have multiple functions. As the scaffold of the spleen, FRCs enwrap ECM in a certain arrangement (reviewed in Balogh et al., 2008). Moreover, FRCs are involved in organ homeostasis and immune response and the function of each FRC subsets differs (Luther et al., 2011). Reticular cells in the marginal zone express a wide range of cytokines and chemokines such as CCL19, CCL21, and IL-7, suggesting a regulatory role in adaptive immunity and lymphocyte migration. Interestingly,

FRC cells co-express desmin and α-SMA, which form a conduit system which allows trafficking of small molecules such as antigens (Sixt et al., 2005).

FRCs in secondary lymph organs, especially those which reside in the T-cell zone and marginal zone, express markers for myofibroblasts and show similar morphology to myofibroblasts in cell culture. Moreover, by secreting extracellular materials, these cells are capable of providing contractile force, to the same extent as lung myofibroblasts (Link et al., 2007). These features indicate that fibroblastic reticular cells may share functions similar to those of myofibroblasts, which indicates a relation between FRCs and ECM deposition in the spleen.

Accumulated evidence has confirmed that the migration and survival of T cells, as well as the structure of the T-cell zone, are highly related to the microenvironment maintained by FRCs in PALS (Bajenoff et al., 2006; Link et al., 2007). Interestingly, HIV and SIV infection induced fibrosis causes T-cell apoptosis and depletion by disrupting the FRC network (Zeng et al., 2011). Zeng's work has shown that collagen deposition and loss of the FRC network lead to loss of contact between T cells and FRCs, which limits T-cell access to a major source of survival signal IL-7 and results in apoptosis and reduction of T cells. Loss of T cells also includes depletion of the LTβ-producing T-cell population, which in turn results in further destruction, for LTβ is necessary in maintaining the FRC network (Zeng et al., 2011).

In MHV-68 infected IFNγR$^{-/-}$ spleen, we first observed fibrosis starting from PALS, followed by disruption of the T-cell zone from which T cells disappeared. Therefore it is possible that fibroblastic cells in FRC network may differentiate into myofibroblasts, and subsequently they lose the function of maintaining T-cell zone structure. This hypothesis needs to be confirmed by further experiments by staining spleen sections with anti-IL-7 and LTβ, as well as markers for FRCs (Desmin and ER-TR-7) and FDCs (CD35 and CD21) in

the spleen during fibrosis. Also, profiling relevant cytokine expression in the host at both the mRNA and the protein levels may provide supportive evidence.

Interestingly, we observed that $EGFP^{low}$ CD45R $(B220)^{+}$ cells within B-cell follicles disappear during fibrosis, suggesting that they are affected by ECM accumulating around the follicle. However, we have not yet identified whether they are follicular dendritic cells on spleen sections. Co-staining with the dendritic cell marker CD11c and granulocyte marker GR-1, as well as neutrophil marker Ly6G may further identify these cells. Another possibility would be the infiltration of neutrophils or other granulocytes in the early stage which was resolved later.

Due to the limitations of our technique, we were unable to visualise the latently infected cells in the system. We tried infecting mice with two MHV-68 recombinant viruses with insertion of GFP gene but neither showed a signal after day 24 post infection. So far, many reporter gene-labelled MHV-68 viruses have been generated; however, the vast majority show attenuation at late time points. There are two explanations for this: first, the production of reporter proteins may elicit a host immune response; second, the viral gene expression may be affected by the insertion so that it cannot establish a latent infection like a 'normal' virus. Although mLANA-MHV-68 does not show attenuation within 90 days post infection, it is not suitable for multi-colour staining as the β-lactamase substrate leaves all cells with high green fluorescence. Moreover, as discussed in Chapter 4, there are considerable populations of infected cells which do not express ORF73 and therefore cannot be detected.

Although there are no ideal method to track virus in long-term latency, staining for lytic infected cells on spleen sections by Gangadharan demonstrated that on days 12 to 20 post infection, lytic infected cells appear in the area around lymphoid follicles in $IFN\gamma R^{-/-}$ mice (Gangadharan, 2006). This finding suggests the lytic infection may occur in marginal zone macrophages, so that cell death becomes the continuous trigger/stimulus for the generation of fibrosis. On the other hand, the work of Speck's group suggests that a considerable

proportion of the lytic infection in the spleen occurs in plasma cells, and that the virus drives B-cell differentiation into plasma cells (Collins et al., 2009; Liang et al., 2009). Moreover, plasma cells stay in the marginal zone before they enter red pulp and release antibodies, which suggest the lytic infection observed by Gangadharan may be in plasma cells. Therefore, it is also possible that plasma cells are responsible for the majority of lytic infection but not macrophages. Lytic infection is considered as one of the possible reason triggering fibrosis, so it would be very interesting to define the lytic infection using anti-MHV-68 antibody.

To examine whether the macrophages were infected, we tried detecting mLANA-MHV-68 in CD11b+ cells and we found no infection in CD11b+ populations. However, it is quite possible that ORF73 is not expressed in infected macrophages. Therefore, a PCR for viral genome would be a better way of testing whether macrophages are infected. However, subsets of macrophages express different markers, causing difficulty to distinguish them. Moreover, the population of macrophages is relatively small in the spleen, so that it would be costly to use antibodies such as CD11b-Ab. These problems can be solved by using Macgreen and Macgreen × IFNγR$^{-/-}$ mice.

Chapter 6 Discussion

In this project, we explored the cellular events and viral activities in splenic fibrosis induced by MHV-68 infection in mice that lack an IFNγ response. First, we investigated the possible mechanisms that may cause massive cell loss in the spleen. We concluded that excessive apoptosis and viral reactivation are not responsible for the cell loss. Second, we examined mLANA-expressing cells during latent infection using recombinant virus. We have observed a loss of latently infected B cells caused by the removal of germinal centre and memory B cell subsets. Finally, we investigated splenic macrophages using Macgreen mice during fibrosis which show significant changes in number and the pattern of distribution in time course, in which we found no evidence of macrophages trans-differentiate into myofibroblasts.

Mechanisms of reducing the number of latently infected B cells

As discussed in Chapter 4, we have observed a significant reduction of germinal centre B cells and memory B cells in IFNγR$^{-/-}$ spleen, whereas the IgD+ B cells (naïve B cells) maintained a certain population. Subsequently, on day 35 post infection, the B cells which remained in the spleen of IFNγR$^{-/-}$ mice were mostly naïve B cells. Germinal centre B cells and memory B cells were carrying the majority of the virus, while naïve B cells showed least level of MHV-68 infection. These observations suggest that the significant reduction of latently infected B cells is possibly caused by the removal of the subpopulations of germinal centre B cells and memory B cells. The low infection rate in naïve B cells is possibly due to two reasons: first, naïve B cells are less susceptible; or, once a naïve B cell is infected, it becomes activated and become a germinal centre B cell. Furthermore, we hypothesise that one possible reason for the reduction of germinal centre B cells and memory B cells is that ECM deposition blocked the interaction between B cells and follicular dendritic cells, and the interaction between B cells and T cells. Therefore, naïve B cells could not undergo somatic hypermutation and class-switching, whereas the germinal centre B cells underwent activated apoptosis without survival signals and hence they could not differentiate into

memory B cells and plasma cells. However, we did not observe significant elevated apoptosis in the spleen during the reduction of B cells. Current study investigating the fate of splenic B cells during fibrosis showed no evidence of enhanced cell death caused by Caspase 3-dependent apoptosis from day 16 to day 24 post infection. It has been shown using the method of TUNEL assay that the reduction of B cells was not due to increased cell death from day 4 to day 16 post infection (Ebrahimi et al., 2001). Hence, it is possible that the fibrosis may block cell recruitment, and the cells may leave the spleen at the same time. However, these studies were carried out using total spleen cells, which may not be sensitive enough to reflect the potential cell death in B cells subsets. FACS analysis using a combination of apoptosis marker and B cell markers may be a better method with less sensitivity issue. Moreover, there are still possibilities that the B cell may undergo accelerated cell death which cannot be detected by either TUNEL or caspase 3.

If the spleen cells do not die during fibrosis, they may leave the spleen and contribute to the leucocytosis in the peripheral blood. The development of fibrosis leads to accumulation of ECM in structural scaffolding such as the capsule, resulting in high pressure inside of the spleen. Together with the observation that fibrosis formed around follicles, the lesion leads to blockage of peripheral blood and leukocytes passing though the spleen (Ebrahimi et al., 2001). Ebrahimi et.al have demonstrated that a leucocytosis peaking at day 23 post infection, corresponding to the development of fibrosis. In the same study, injected labelled leukocytes could be observed in the spleen of wild type mice but not in IFNγR$^{-/-}$ mice, which suggests the recruitment of lymphocytes from the blood into the spleen is blocked because of fibrosis (Ebrahimi et al., 2001). However, we do not know to what extent this blockage of cell recruitment contributes to the cell loss. One possible way of studying the contribution of cell recruitment to maintaining the splenic cell numbers during fibrosis may be transplanting bone marrow cells from male mice into female mice (both 129Sv and IFNγR$^{-/-}$ mice), then detecting the number of Y chromosomes in newly generated lymphocytes within the fibrotic

spleen and wild type spleen. By comparing the percentage of Y chromosome positive cells within the IFNγR$^{-/-}$ and wild type spleen, one could figure out how many cells are newly recruited in the spleen. Also, the percentage of non-Y chromosome-positive leukocytes in the blood in the IFNγR$^{-/-}$ and wild type spleen may indicate the female cells which leave the spleen and enter the circulation during splenic fibrosis.

Apoptosis is the most widely recognised mechanism for programmed cell death. However, several forms of cell death which are distinct from apoptosis have been identified recently. Among them, pryoptosis and autophagy have been associated to chronic infection. Therefore it would be very interesting to investigate their potential roles in reducing the number of latently infected B cells in the spleen during MHV-68 infection of IFNγR$^{-/-}$ spleen.

Pryoptosis, also termed Caspase1-dependent cell death, is distinct from apoptosis morphologically and mechanistically. Caspase1 (also called IL-1β-converting enzyme) is essential for pryoptosis but dispensable to apoptosis (Kuida et al., 1995; Li et al., 1995), whereas the apoptosis-associated, caspases such as Caspase 3 and Caspase 8, are not involved in pryoptosis (Bergsbaken and Cookson, 2007; Brennan and Cookson, 2000; Jesenberger et al., 2000). Also, pryoptosis is suggested to be a conserved process of cell death which can be activated by different stimuli through diverted pathways (Fink et al., 2008). So far, the mechanism of pryoptosis has mostly been demonstrated using a parasite infection model in macrophages. Cell death through pryoptosis is characterised by rapid plasma-membrane rupture and release of pro-inflammatory intracellular contents, which is in contrast to the features of apoptosis, which include condensed cellular contents and non-inflammatory phagocytes clearing apoptotic bodies (Albert, 2004). Furthermore, DNA cleavage, which is considered as the hallmark of apoptotic cell death, also occurs, but is not required in cell lysis by pryoptosis (Fink and Cookson, 2006). Interestingly, in MHV-68 infection, Caspase3-dependent apoptosis and DNA damage (examined by TUNEL) were not elevated; however, the number of membrane-compromised cells in IFNγR$^{-/-}$ mice was higher

compared to that in wild-type mice (Chapter 4). Moreover, Caspase1 activation during pryoptosis also involves the production of inflammatory cytokines IL-1β and IL-18 (Fantuzzi et al., 1999). Elevated IL-1β is observed in the spleen of IFNγR$^{-/-}$ mice from day 10 to day 14 post infection (Ebrahimi et al., 2001). Although IL-18 production has never been tested, a slight increase in TNFα and TNFβ has also been observed in IFNγR$^{-/-}$ mice (Ebrahimi et al., 2001). Consistently, TNF secretion by Caspase1-deficient mice in response to pryoptosis stimulation is significantly reduced (Li et al., 1995; Miggin et al., 2007), which suggests that Caspase1 activation is also related to the secretion of TNFs. Caspase1, together with IL-12 and IL-18, is reported to stimulate Th1 cell proliferation and enhance IFNγ production (Fantuzzi and Dinarello, 1999; Nakanishi et al., 2001). However, stimulation of Caspase1 has also been reported to promote Th2 response and humoural immunity (Eisenbarth et al., 2008; Kool et al., 2008). The regulatory roles of Caspase1 activation in both innate and adaptive immunity still need to be elucidated. Interestingly, in IFNγR$^{-/-}$ mice, IFNγ production is highly elevated (Dutia et al., 1999; Dutia et al., 1997; Ebrahimi et al., 2001), suggesting a feedback mechanism in the response of IFNγ receptor deficiency which may be regulated by Caspase1-associated cytokines such as IL18. Therefore, pryoptosis can be a possible mechanism which results in the significant reduction of B cells during fibrosis in MHV-68 infected IFNγR$^{-/-}$ mice. One possible method of investigating pryoptosis would be staining for the activated form of Caspase1.

In cell biology, autophagy is a catabolic process in which the cell degrades its own components through the lysosomal machinery. It is a major mechanism by which a starving cell reallocates nutrients from unnecessary processes to more essential processes. Autophagy has recently been linked to the progression of several diseases, such as cancer and chronic infection. For example, autophagy has been shown to play a role in detection of ssRNA virus infection in dendritic cells through pattern recognition receptors (PRR), which are part of the innate immune system (Lee et al., 2007). Although it used to be considered as another

form of programmed cell death in addition to apoptosis, autophagy does not necessarily lead to cell death (reviewed in Rubinsztein et al., 2005). Recently, it is more and more seen as a survival mechanism rather than a means of cell death. Moreover, autophagy and apoptosis appear to have negative regulation of each other (Gordy and He, 2012). Cellular Bcl-2 has been demonstrated to not only inhibit apoptosis, but also prevent autophagy through binding to Beclin-1 (Sinha et al., 2008). Gammaherpesvirus encoded vBcl-2 also interacts with Beclin-1a; moreover, this binding has higher affinity than the interaction with apoptotic proteins. It has been hypothesised that vBcl-2 is an antagonist which frees Beclin-1 from cellular Bcl-2 (Ku et al., 2008). Moreover, recent study has been performed using mutant MHV-68 whose vBcl-2 cannot prevent autophagy but still retains the ability to inhibit apoptosis. This virus showed no difference in acute infection and acute latent infection in the spleen; however, it exhibited decreased latent viral load during long-term latency around days 28 to 42 post infection (E et al., 2009). The same study also demonstrated another mutant virus to lack the anti-apoptotic function of vBcl-2 but maintain the anti-autophagy function to establish long-term latency as a wild-type virus, but with compromised reactivation. Therefore, this suggests that autophagy may play an important role which is different from the role of apoptosis in controlling maintenance of MHV-68 latency. In the spleen of IFNγR$^{-/-}$ mice infected with MHV-68, the microenvironment of fibrosis may possibly lead to cell starvation, and may induce autophagy of spleen cells. Moreover, as an anti-viral infection mechanism, the infected cells may also undergo autophagy. However, it is not known if the vBcl-2 expression co-relates with the state of the cell which undergoes autophagy. Our experiment shows that the expression of vBcl-2 (M11) was very low and that there was no up-regulation in IFNγR$^{-/-}$ mice while the significant reduction of B cells occurred. Thus, further experiments are needed to examine whether autophagy actually contributes to the reduction of B cells.

IFNγ response suppresses viral reactivation in macrophages but not B cells following intraperitoneal inoculation (Steed et al., 2006). Moreover, in primary bone-marrow derived macrophages, IFNγ can inhibit the activity of ORF50 (Rta) promoters through STAT1 and subsequently inhibit lytic replication/reactivation (Goodwin et al., 2010). We have ruled out the possibility of viral reactivation leading to cell death by measuring the transcription of important lytic viral genes, M11, vDNApol, and Rta in spleen tissue. Furthermore, we have confirmed that these lytic genes are not up-regulated in ORF-73-expressing infected cells (which are mainly B cells).

MHV-68 mediated splenic fibrosis — protective or pathological?

In IFN γ $R^{-/-}$ mice, the immune response is dominated by Th2 cytokines such as IL-4 and IL-13, both of which have the function of promoting fibrosis. In chronic parasite infection, fibrosis acts as a part of the Th2 immune response in isolating the non-self-pathogen. In the case of MHV-68 infection, lacking of IFNγ response results in poor control of latently infected cells at early stage, followed by high viral load then rapidly decreased, corresponding with a drop in the number of spleen cells. Moreover, during the severe fibrosis (around day 20 to day28), the viral load and spleen cell number kept dropping until day 28, when they reached the lowest point and the fibrosis started to resolve. Seemingly, the pathological changes of fibrosis were accompanied by the control of the number of latently infected cells. Using mLANA-MHV-68, we show that germinal centre B cells and memory B cells suffered extra cell loss, which is responsible for the removal of latently infected cells (Chapter 4). This may suggest that fibrosis which formed around the follicle, is a part of Th2-biased immune response, and is the main force of clearing the latently infected B cells.

Fibrosis is generally considered to be a disordered wound-repair process triggered by tissue damage. To understand the nature of fibrosis, one of the important questions addressed is: what causes tissue damage during MHV-68 infection in the spleen of IFNγ $R^{-/-}$ mice? Generally, there are two existing hypotheses: persistent lytic infection and/or host immune response caused tissue damage.

Persistent viral replication will cause cell death and is believed to be a trigger of splenic fibrosis: inhibition of persistent viral replication has been reported to ameliorate MHV-68 induced pulmonary fibrosis (Mora et al., 2007). Therefore, it seems that the trigger of lung fibrosis induced by MHV-68 followed intranasal inoculation is depending on productive infection. However, it seems not the case in the spleen fibrosis: inhibition using anti-viral drug 4'-S-EtdU which can effectively clear lytic virus but not latent virus from day 6 p.i., fails to prevent the pathologies observed on day 15 post infection (Dutia et al., 1997). Indeed, the inhibition observed in pulmonary fibrosis may not reflect the changes that may happen in the spleen. The lung is the location of primary lytic infection, and the latency and reactivation is occurred in epithelial cells. Whereas in the spleen, the latent infection is mostly established in B cells, and reactivation is largely from plasma cells. The terminal of virus-driven B cell differentiation is either long-term latency in memory B cells or reactivation in plasma cells (Ottinger et al., 2009). Normally, plasma cells stay in marginal zone of the spleen for a short time before they move into PALS and red pulp where they secrete antibody into the blood, which corresponds with the observation of lytic infected cells are mostly located in the marginal zone which is around the follicle from day 12 to day 16 post infection (Ehtisham et al., 1993; Gangadharan, 2006). These findings indicate a link between lytic infection and fibrosis.

However, there is another possibility that the tissue damage is caused by immune responses, such as inflammatory infiltration and CTL targeting infected cells. A significantly higher rate of neutrophil infiltration was observed in IFNγ$R^{-/-}$ mice at the early stage of spleen

infection, suggesting an elevated inflammation and exacerbated tissue damage (Ebrahimi et al., 2001). Depletion of CD8+ T cells by injecting specific antibodies prevent the occurrence of splenic fibrosis in IFNγR$^{-/-}$ mice while there were no enhanced lytic infection detected in the spleen on day 17 p.i. (Dutia et al., 1997). This result shows that CD8 T cells are essential for the formation of fibrosis. Moreover, Gangadharan has observed infiltration of CD8+ T cells at the start of fibrosis but not in advanced fibrosis (Gangadharan, 2006). These observations are consistent with our data using CD3 antibody detecting T cells during fibrosis, in which we found T cells leaving PALS and moving into follicles on day 16 and hardly saw them in the spleen on day 28. Indeed, the studies on the role of CD8+ T cells emphasise that CD8+ T cells are crucial in clearing lytic infection rather than controlling latent infection. The depletion of CD8 T cells has to be carried out after the productive infection because mice have IFNγ and CTL response double knockout cannot survive (Tsai et al., 2011). Further studies are required to dissect the role of CD8 T cells in latent infection without the effect from viral replication. Peritoneal inoculation may offer a route of infection in which the influences of lytic infection and associated immune responses raised in the lung can be avoided.

Another question to ask is that if the fibrosis specifically targets the latent infection. From day 16 to day 28 post infection, all types of cells in the spleen decreased in number, including B cells, CD4 T cells, CD8 T cells, dendritic cells and macrophages. Although fibrosis formed around the follicles, appearing to be specifically walling off the infected cells, as discussed previousely, this special formation may merely be because of the biological feature of the spleen. First, reactivation causes tissue damage to occur mostly in the marginal zone where fibroblasts from fibroblastic reticular cell network may differentiate into myofibroblasts, or the recruited fibrocytes may also contribute. Second, the shape of fibrosis observed might be because of the anatomy of the spleen, in which FRC network exists in the T cell zone and marginal zone, but not the compact B cell zone. Third, the virus

may drive cellular proliferation in order to exploit the germinal centre reaction to increase the number of latently infected cells, which would explains why patches of infected cells that we observed in *in situ* hybridisation for vtRNA like molecules were surrounded by collagen.

On the other hand, Clambey et al have shown that IFNγR$^{-/-}$ mice exhibit 50% mortality within 100 days post infection (Clambey et al., 2000). Consistently, we have observed higher death rate in IFNγR$^{-/-}$ mice than wild type mice between day 80 and day 90 post infection (data not shown). IFNγR$^{-/-}$ mice infected with the virus with interrupted expression of M1 protein survived up to 100 days post infection. These mice did not develop pathology such as splenomegaly, Vβ4 CD8+ T cell expansion in the periphery and splenic fibrosis (Clambey et al., 2000), in which Vβ4 CD8+ T cell expansion is closely related to splenic fibrosis (Evans et al., 2008). It has been reported that in IFNγR$^{-/-}$ mice, MHV-68 attack the smooth muscle cells in vascular system therefore the mice may die from large-vessel panarteritis (Weck et al., 1997), which indicates the death is not simply caused by the pathology occurred in the lung and the spleen. These findings suggest that although in short term, the viral load is controlled efficiently without IFNγ response, however, splenic fibrosis is more pathological rather than protective. Due to the complexity of the host-virus interaction, it is very difficult to define the role of fibrosis without the influence from other part of the immune system. Thus whether MHV-68 mediated fibrosis is protective or pathological to the host is still under debate.

Role of Macrophages in MHV-68 induced fibrosis

Macrophages have been proved to be a location for persistent infection (Weck et al., 1999). Moreover, IFNγ response can inhibit viral reactivation from latency in peritoneal macrophages but not B cells (Steed et al., 2007). However, splenic macrophages are only infected following intraperitoneal inoculation, and they are not infected in immune-

competent mice following MHV-68 intranasal infection. The high viral load detected in the spleen of IFNγR$^{-/-}$ mice implies a poor control of viral infection which may amplify the pathogenesis which is undetectable in normal mice. Hence, we were interested in the state of MHV-68 infection in the macrophages in IFNγR$^{-/-}$ spleen.

Using mLANA recombinant virus, we failed to detect a considerable population of infected cells within CD11b+ spleen cells. This is consistent with the work of Marques et al., who have shown that infected macrophages and dendritic cells do not express ORF73 (Marques et al., 2003). Therefore, mLANA is not suitable as a marker for detecting infected macrophages. More recently, infecting mice with a recombinant virus which was labelled at another site of the genome showed signal in splenic macrophages following neither intranasal nor intraperitoneal inoculation, whereas viral infection was observed in germinal centre B cells (Collins and Speck, 2012). This suggests that the failure of detecting infected spleen macrophages is not caused by the marker which has been chosen. However, it is also possible that the infection of macrophages requires different machinery of the virus compared to that of B cells. There are two possible explanations: first, both of the recombinant viruses fail to infect macrophages as a wild type virus; second, the conclusion of the splenic macrophages is questionable.

Alternatively activated macrophages used to be considered as 'pro-fibrotic', for their ability to produce fibrosis mediators such as TGFβ and PDGF and many other regulative functions. One of our main goals was to investigate the possible role of macrophages in the splenic pathogenesis of MHV-68 infection in IFNγR$^{-/-}$ mice, and we hypothesised that they may contribute to the myofibroblast population through differentiation so that they directly produce ECM. However, our data show no evidence of macrophages being potential origins of myofibroblasts. Therefore it suggests alternative roles of macrophages in Th2 biased immune response. On the other hand, it was recently suggested that Arginase-1-expressing macrophages suppressed fibrosis by competing with L-arginine which is required to sustain

Th2 CD4+ T cell responses (Pesce et al., 2009a). In addition, IL-10 and Fizz1 produced by alternatively activated macrophages were also shown to be anti-fibrotic (Pesce et al., 2009b; Wilson et al., 2007). Moreover, macrophages have functions of engulfing and digesting ECM components, stimulating other inflammatory cells such as myofibroblasts and neutrophils to produce MMPs to degrade collagen (reviewed in Murray and Wynn, 2011; Wynn, 2008). Interestingly, we have observed macrophages which appear to be 'engulfing' ECM during the development of fibrosis, which were no longer observed in the most severe fibrosis. In addition, these macrophages came back again during the phase of resolution and recovery. These findings suggest a role of macrophages in recovery from fibrosis and the rebuilding of spleen structure. Therefore the splenic fibrosis mediated by MHV-68 infection can be a model to study the resolution of virus-induced fibrosis.

References

Ackermann, M. (2004). Herpesviruses: a brief overview. Methods Mol Biol *256*, 199-219.

Ackermann, M. (2006). Pathogenesis of gammaherpesvirus infections. Veterinary microbiology *113*, 211-222.

Adler, H., Messerle, M., Wagner, M., and Koszinowski, U.H. (2000). Cloning and mutagenesis of the murine gammaherpesvirus 68 genome as an infectious bacterial artificial chromosome. Journal of virology *74*, 6964-6974.

Albert, M.L. (2004). Death-defying immunity: do apoptotic cells influence antigen processing and presentation? Nature reviews *4*, 223-231.

Allen, R.D., 3rd, Dickerson, S., and Speck, S.H. (2006). Identification of spliced gammaherpesvirus 68 LANA and v-cyclin transcripts and analysis of their expression in vivo during latent infection. Journal of virology *80*, 2055-2062.

Altmann, M., Pich, D., Ruiss, R., Wang, J., Sugden, B., and Hammerschmidt, W. (2006). Transcriptional activation by EBV nuclear antigen 1 is essential for the expression of EBV's transforming genes. Proceedings of the National Academy of Sciences of the United States of America *103*, 14188-14193.

Andrae, J., Gallini, R., and Betsholtz, C. (2008). Role of platelet-derived growth factors in physiology and medicine. Genes & development *22*, 1276-1312.

Arase, Y., Suzuki, F., Suzuki, Y., Akuta, N., Kobayashi, M., Kawamura, Y., Yatsuji, H., Sezaki, H., Hosaka, T., Hirakawa, M.*, et al.* (2008). Hepatitis C virus enhances incidence of idiopathic pulmonary fibrosis. World journal of gastroenterology : WJG *14*, 5880-5886.

Arvanitakis, L., Mesri, E.A., Nador, R.G., Said, J.W., Asch, A.S., Knowles, D.M., and Cesarman, E. (1996). Establishment and characterization of a primary effusion (body cavity-based) lymphoma cell line (BC-3) harboring kaposi's sarcoma-associated herpesvirus (KSHV/HHV-8) in the absence of Epstein-Barr virus. Blood *88*, 2648-2654.

Atanasiu, D., Whitbeck, J.C., Cairns, T.M., Reilly, B., Cohen, G.H., and Eisenberg, R.J. (2007). Bimolecular complementation reveals that glycoproteins gB and gH/gL of herpes simplex virus interact with each other during cell fusion. Proceedings of the National Academy of Sciences of the United States of America *104*, 18718-18723.

Babcock, G.J., Decker, L.L., Volk, M., and Thorley-Lawson, D.A. (1998). EBV persistence in memory B cells in vivo. Immunity *9*, 395-404.

Bach, E.A., Aguet, M., and Schreiber, R.D. (1997). The IFN gamma receptor: a paradigm for cytokine receptor signaling. Annual review of immunology *15*, 563-591.

Badovinac, V.P., Tvinnereim, A.R., and Harty, J.T. (2000). Regulation of antigen-specific CD8+ T cell homeostasis by perforin and interferon-gamma. Science *290*, 1354-1358.

Baer, R., Bankier, A.T., Biggin, M.D., Deininger, P.L., Farrell, P.J., Gibson, T.J., Hatfull, G., Hudson, G.S., Satchwell, S.C., Seguin, C.*, et al.* (1984). DNA sequence and expression of the B95-8 Epstein-Barr virus genome. Nature *310*, 207-211.

Bajenoff, M., Egen, J.G., Koo, L.Y., Laugier, J.P., Brau, F., Glaichenhaus, N., and Germain, R.N. (2006). Stromal cell networks regulate lymphocyte entry, migration, and territoriality in lymph nodes. Immunity *25*, 989-1001.

Balogh, P., Fisi, V., and Szakal, A.K. (2008). Fibroblastic reticular cells of the peripheral lymphoid organs: unique features of a ubiquitous cell type. Molecular immunology *46*, 1-7.

Barbas-Filho, J.V., Ferreira, M.A., Sesso, A., Kairalla, R.A., Carvalho, C.R., and Capelozzi, V.L. (2001). Evidence of type II pneumocyte apoptosis in the pathogenesis of idiopathic pulmonary fibrosis (IFP)/usual interstitial pneumonia (UIP). Journal of clinical pathology *54*, 132-138.

Baroni, G.S., D'Ambrosio, L., Curto, P., Casini, A., Mancini, R., Jezequel, A.M., and Benedetti, A. (1996). Interferon gamma decreases hepatic stellate cell activation and extracellular matrix deposition in rat liver fibrosis. Hepatology *23*, 1189-1199.

Barozzi, P., Luppi, M., Facchetti, F., Mecucci, C., Alu, M., Sarid, R., Rasini, V., Ravazzini, L., Rossi, E., Festa, S.*, et al.* (2003). Post-transplant Kaposi sarcoma originates from the seeding of donor-derived progenitors. Nature medicine *9*, 554-561.

Barton, E., Mandal, P., and Speck, S.H. (2011). Pathogenesis and host control of gammaherpesviruses: lessons from the mouse. Annual review of immunology *29*, 351-397.

Bataller, R., and Brenner, D.A. (2005). Liver fibrosis. The Journal of clinical investigation *115*, 209-218.

Beckstead, J.H., Wood, G.S., and Fletcher, V. (1985). Evidence for the origin of Kaposi's sarcoma from lymphatic endothelium. The American journal of pathology *119*, 294-300.

Belz, G.T., Stevenson, P.G., Castrucci, M.R., Altman, J.D., and Doherty, P.C. (2000). Postexposure vaccination massively increases the prevalence of gamma-herpesvirus-specific CD8+ T cells but confers minimal survival advantage on CD4-deficient mice. Proceedings of the National Academy of Sciences of the United States of America *97*, 2725-2730.

Bergsbaken, T., and Cookson, B.T. (2007). Macrophage activation redirects yersinia-infected host cell death from apoptosis to caspase-1-dependent pyroptosis. PLoS pathogens *3*, e161.

Bernabei, P., Coccia, E.M., Rigamonti, L., Bosticardo, M., Forni, G., Pestka, S., Krause, C.D., Battistini, A., and Novelli, F. (2001). Interferon-gamma receptor 2 expression as the deciding factor in human T, B, and myeloid cell proliferation or death. Journal of leukocyte biology *70*, 950-960.

Blaskovic, D., Stancekova, M., Svobodova, J., and Mistrikova, J. (1980). Isolation of five strains of herpesviruses from two species of free living small rodents. Acta virologica *24*, 468.

Boname, J.M., and Stevenson, P.G. (2001). MHC class I ubiquitination by a viral PHD/LAP finger protein. Immunity *15*, 627-636.

Bonner, J.C. (2004). Regulation of PDGF and its receptors in fibrotic diseases. Cytokine & growth factor reviews *15*, 255-273.

Bonner, J.C., Osornio-Vargas, A.R., Badgett, A., and Brody, A.R. (1991). Differential proliferation of rat lung fibroblasts induced by the platelet-derived growth factor-AA, -AB, and -BB isoforms secreted by rat alveolar macrophages. American journal of respiratory cell and molecular biology *5*, 539-547.

Borchers, A.T., Chang, C., Keen, C.L., and Gershwin, M.E. (2011). Idiopathic pulmonary fibrosis-an epidemiological and pathological review. Clinical reviews in allergy & immunology *40*, 117-134.

Bornkamm, G.W., Delius, H., Fleckenstein, B., Werner, F.J., and Mulder, C. (1976). Structure of Herpesvirus saimiri genomes: arrangement of heavy and light sequences in the M genome. Journal of virology *19*, 154-161.

Bowden, R.J., Simas, J.P., Davis, A.J., and Efstathiou, S. (1997). Murine gammaherpesvirus 68 encodes tRNA-like sequences which are expressed during latency. The Journal of general virology *78 (Pt 7)*, 1675-1687.

Braaten, D.C., McClellan, J.S., Messaoudi, I., Tibbetts, S.A., McClellan, K.B., Nikolich-Zugich, J., and Virgin, H.W. (2006). Effective control of chronic gamma-herpesvirus infection by unconventional MHC Class Ia-independent CD8 T cells. PLoS pathogens *2*, e37.

Brennan, M.A., and Cookson, B.T. (2000). Salmonella induces macrophage death by caspase-1-dependent necrosis. Molecular microbiology *38*, 31-40.

Bridgeman, A., Stevenson, P.G., Simas, J.P., and Efstathiou, S. (2001). A secreted chemokine binding protein encoded by murine gammaherpesvirus-68 is necessary for the establishment of a normal latent load. The Journal of experimental medicine *194*, 301-312.

Brownstein, D.G. (1998). Comparative genetics of resistance to viruses. Am J Hum Genet *62*, 211-214.

Bucala, R., Spiegel, L.A., Chesney, J., Hogan, M., and Cerami, A. (1994). Circulating fibrocytes define a new leukocyte subpopulation that mediates tissue repair. Mol Med *1*, 71-81.

Buxton, D., Jacoby, R.O., Reid, H.W., and Goodall, P.A. (1988). The pathology of "sheep-associated" malignant catarrhal fever in the hamster. Journal of comparative pathology *98*, 155-166.

Cai, X., and Cullen, B.R. (2006). Transcriptional origin of Kaposi's sarcoma-associated herpesvirus microRNAs. Journal of virology *80*, 2234-2242.

Cai, X., Lu, S., Zhang, Z., Gonzalez, C.M., Damania, B., and Cullen, B.R. (2005). Kaposi's sarcoma-associated herpesvirus expresses an array of viral microRNAs in latently infected cells. Proceedings of the National Academy of Sciences of the United States of America *102*, 5570-5575.

Campadelli-Fiume, G., Amasio, M., Avitabile, E., Cerretani, A., Forghieri, C., Gianni, T., and Menotti, L. (2007). The multipartite system that mediates entry of herpes simplex virus into the cell. Reviews in medical virology *17*, 313-326.

Campbell, M.E., and Preston, C.M. (1987). DNA sequences which regulate the expression of the pseudorabies virus major immediate early gene. Virology *157*, 307-316.

Card, G.L., Knowles, P., Laman, H., Jones, N., and McDonald, N.Q. (2000). Crystal structure of a gamma-herpesvirus cyclin-cdk complex. The EMBO journal *19*, 2877-2888.

Cardin, R.D., Brooks, J.W., Sarawar, S.R., and Doherty, P.C. (1996). Progressive loss of CD8+ T cell-mediated control of a gamma-herpesvirus in the absence of CD4+ T cells. The Journal of experimental medicine *184*, 863-871.

Casper, C., and Wald, A. (2007). The use of antiviral drugs in the prevention and treatment of Kaposi sarcoma, multicentric Castleman disease and primary effusion lymphoma. Current topics in microbiology and immunology *312*, 289-307.

Castleman, B., Iverson, L., and Menendez, V.P. (1956). Localized mediastinal lymphnode hyperplasia resembling thymoma. Cancer *9*, 822-830.

Cesarman, E., Chang, Y., Moore, P.S., Said, J.W., and Knowles, D.M. (1995a). Kaposi's sarcoma-associated herpesvirus-like DNA sequences in AIDS-related body-cavity-based lymphomas. The New England journal of medicine *332*, 1186-1191.

Cesarman, E., Moore, P.S., Rao, P.H., Inghirami, G., Knowles, D.M., and Chang, Y. (1995b). In vitro establishment and characterization of two acquired immunodeficiency syndrome-related lymphoma cell lines (BC-1 and BC-2) containing Kaposi's sarcoma-associated herpesvirus-like (KSHV) DNA sequences. Blood *86*, 2708-2714.

Chang, C.H., and Flavell, R.A. (1995). Class II transactivator regulates the expression of multiple genes involved in antigen presentation. The Journal of experimental medicine *181*, 765-767.

Chang, W., Wei, K., Jacobs, S.S., Upadhyay, D., Weill, D., and Rosen, G.D. (2010). SPARC suppresses apoptosis of idiopathic pulmonary fibrosis fibroblasts through constitutive activation of beta-catenin. The Journal of biological chemistry *285*, 8196-8206.

Chang, Y., Cesarman, E., Pessin, M.S., Lee, F., Culpepper, J., Knowles, D.M., and Moore, P.S. (1994). Identification of herpesvirus-like DNA sequences in AIDS-associated Kaposi's sarcoma. Science *266*, 1865-1869.

Cheever, A.W., Williams, M.E., Wynn, T.A., Finkelman, F.D., Seder, R.A., Cox, T.M., Hieny, S., Caspar, P., and Sher, A. (1994). Anti-IL-4 treatment of Schistosoma mansoni-infected mice inhibits development of T cells and non-B, non-T cells expressing Th2 cytokines while decreasing egg-induced hepatic fibrosis. J Immunol *153*, 753-759.

Chiang, A.K., Tao, Q., Srivastava, G., and Ho, F.C. (1996). Nasal NK- and T-cell lymphomas share the same type of Epstein-Barr virus latency as nasopharyngeal carcinoma and Hodgkin's disease. International journal of cancer Journal international du cancer *68*, 285-290.

Chiaramonte, M.G., Donaldson, D.D., Cheever, A.W., and Wynn, T.A. (1999). An IL-13 inhibitor blocks the development of hepatic fibrosis during a T-helper type 2-dominated inflammatory response. The Journal of clinical investigation *104*, 777-785.

Chin, Y.E., Kitagawa, M., Kuida, K., Flavell, R.A., and Fu, X.Y. (1997). Activation of the STAT signaling pathway can cause expression of caspase 1 and apoptosis. Molecular and cellular biology *17*, 5328-5337.

Christensen, J.P., Cardin, R.D., Branum, K.C., and Doherty, P.C. (1999). CD4(+) T cell-mediated control of a gamma-herpesvirus in B cell-deficient mice is mediated by IFN-gamma. Proceedings of the National Academy of Sciences of the United States of America *96*, 5135-5140.

Christensen, J.P., and Doherty, P.C. (1999). Quantitative analysis of the acute and long-term CD4(+) T-cell response to a persistent gammaherpesvirus. Journal of virology *73*, 4279-4283.

Clambey, E.T., Virgin, H.W.t., and Speck, S.H. (2000). Disruption of the murine gammaherpesvirus 68 M1 open reading frame leads to enhanced reactivation from latency. Journal of virology *74*, 1973-1984.

Coleman, C.B., Nealy, M.S., and Tibbetts, S.A. (2010). Immature and transitional B cells are latency reservoirs for a gammaherpesvirus. Journal of virology *84*, 13045-13052.

Collins, C.M., Boss, J.M., and Speck, S.H. (2009). Identification of infected B-cell populations by using a recombinant murine gammaherpesvirus 68 expressing a fluorescent protein. Journal of virology *83*, 6484-6493.

Collins, C.M., and Speck, S.H. (2012). Tracking murine gammaherpesvirus 68 infection of germinal center B cells in vivo. PloS one *7*, e33230.

Coulter, L.J., Wright, H., and Reid, H.W. (2001). Molecular genomic characterization of the viruses of malignant catarrhal fever. Journal of comparative pathology *124*, 2-19.

Cyster, J.G. (2005). Chemokines, sphingosine-1-phosphate, and cell migration in secondary lymphoid organs. Annual review of immunology *23*, 127-159.

Damania, B. (2004). Oncogenic gamma-herpesviruses: comparison of viral proteins involved in tumorigenesis. Nature reviews Microbiology *2*, 656-668.

Darnell, J.E., Jr., Kerr, I.M., and Stark, G.R. (1994). Jak-STAT pathways and transcriptional activation in response to IFNs and other extracellular signaling proteins. Science *264*, 1415-1421.

Davison, A.J., Eberle, R., Ehlers, B., Hayward, G.S., McGeoch, D.J., Minson, A.C., Pellett, P.E., Roizman, B., Studdert, M.J., and Thiry, E. (2009). The order Herpesvirales. Archives of virology *154*, 171-177.

de Lima, B.D., May, J.S., Marques, S., Simas, J.P., and Stevenson, P.G. (2005). Murine gammaherpesvirus 68 bcl-2 homologue contributes to latency establishment in vivo. The Journal of general virology *86*, 31-40.

de Lima, B.D., May, J.S., and Stevenson, P.G. (2004). Murine gammaherpesvirus 68 lacking gp150 shows defective virion release but establishes normal latency in vivo. Journal of virology *78*, 5103-5112.

Deiss, L.P., Feinstein, E., Berissi, H., Cohen, O., and Kimchi, A. (1995). Identification of a novel serine/threonine kinase and a novel 15-kD protein as potential mediators of the gamma interferon-induced cell death. Genes & development *9*, 15-30.

Deiss, L.P., Galinka, H., Berissi, H., Cohen, O., and Kimchi, A. (1996). Cathepsin D protease mediates programmed cell death induced by interferon-gamma, Fas/APO-1 and TNF-alpha. The EMBO journal *15*, 3861-3870.

Dighe, A.S., Richards, E., Old, L.J., and Schreiber, R.D. (1994). Enhanced in vivo growth and resistance to rejection of tumor cells expressing dominant negative IFN gamma receptors. Immunity *1*, 447-456.

Direkze, N.C., Forbes, S.J., Brittan, M., Hunt, T., Jeffery, R., Preston, S.L., Poulsom, R., Hodivala-Dilke, K., Alison, M.R., and Wright, N.A. (2003). Multiple organ engraftment by bone-marrow-derived myofibroblasts and fibroblasts in bone-marrow-transplanted mice. Stem Cells *21*, 514-520.

Dittmer, D., Stoddart, C., Renne, R., Linquist-Stepps, V., Moreno, M.E., Bare, C., McCune, J.M., and Ganem, D. (1999). Experimental transmission of Kaposi's sarcoma-associated herpesvirus (KSHV/HHV-8) to SCID-hu Thy/Liv mice. The Journal of experimental medicine *190*, 1857-1868.

Doherty, P.C., Tripp, R.A., Hamilton-Easton, A.M., Cardin, R.D., Woodland, D.L., and Blackman, M.A. (1997). Tuning into immunological dissonance: an experimental model for infectious mononucleosis. Current opinion in immunology *9*, 477-483.

Doucet, C., Brouty-Boye, D., Pottin-Clemenceau, C., Jasmin, C., Canonica, G.W., and Azzarone, B. (1998). IL-4 and IL-13 specifically increase adhesion molecule and inflammatory cytokine expression in human lung fibroblasts. International immunology *10*, 1421-1433.

Duffield, J.S., Forbes, S.J., Constandinou, C.M., Clay, S., Partolina, M., Vuthoori, S., Wu, S., Lang, R., and Iredale, J.P. (2005). Selective depletion of macrophages reveals distinct, opposing roles during liver injury and repair. The Journal of clinical investigation *115*, 56-65.

Dupin, N., Diss, T.L., Kellam, P., Tulliez, M., Du, M.Q., Sicard, D., Weiss, R.A., Isaacson, P.G., and Boshoff, C. (2000). HHV-8 is associated with a plasmablastic variant of Castleman disease that is linked to HHV-8-positive plasmablastic lymphoma. Blood *95*, 1406-1412.

Dupin, N., Fisher, C., Kellam, P., Ariad, S., Tulliez, M., Franck, N., van Marck, E., Salmon, D., Gorin, I., Escande, J.P.*, et al.* (1999). Distribution of human herpesvirus-8 latently infected cells in Kaposi's sarcoma, multicentric Castleman's disease, and primary effusion lymphoma. Proceedings of the National Academy of Sciences of the United States of America *96*, 4546-4551.

Dutia, B.M., Allen, D.J., Dyson, H., and Nash, A.A. (1999). Type I interferons and IRF-1 play a critical role in the control of a gammaherpesvirus infection. Virology *261*, 173-179.

Dutia, B.M., Clarke, C.J., Allen, D.J., and Nash, A.A. (1997). Pathological changes in the spleens of gamma interferon receptor-deficient mice infected with murine gammaherpesvirus: a role for CD8 T cells. Journal of virology *71*, 4278-4283.

Dutia, B.M., Roy, D.J., Ebrahimi, B., Gangadharan, B., Efstathiou, S., Stewart, J.P., and Nash, A.A. (2004). Identification of a region of the virus genome involved in murine gammaherpesvirus 68-induced splenic pathology. The Journal of general virology *85*, 1393-1400.

E, X., Hwang, S., Oh, S., Lee, J.S., Jeong, J.H., Gwack, Y., Kowalik, T.F., Sun, R., Jung, J.U., and Liang, C. (2009). Viral Bcl-2-mediated evasion of autophagy aids chronic infection of gammaherpesvirus 68. PLoS pathogens *5*, e1000609.

Ebrahimi, B., Dutia, B.M., Brownstein, D.G., and Nash, A.A. (2001). Murine gammaherpesvirus-68 infection causes multi-organ fibrosis and alters leukocyte trafficking in interferon-gamma receptor knockout mice. The American journal of pathology *158*, 2117-2125.

Ebrahimi, B., Dutia, B.M., Roberts, K.L., Garcia-Ramirez, J.J., Dickinson, P., Stewart, J.P., Ghazal, P., Roy, D.J., and Nash, A.A. (2003). Transcriptome profile of murine gammaherpesvirus-68 lytic infection. The Journal of general virology *84*, 99-109.

Eddy, A.A. (2005). Can renal fibrosis be reversed? Pediatr Nephrol *20*, 1369-1375.

Efstathiou, S., Ho, Y.M., Hall, S., Styles, C.J., Scott, S.D., and Gompels, U.A. (1990a). Murine herpesvirus 68 is genetically related to the gammaherpesviruses Epstein-Barr virus and herpesvirus saimiri. The Journal of general virology *71 (Pt 6)*, 1365-1372.

Efstathiou, S., Ho, Y.M., and Minson, A.C. (1990b). Cloning and molecular characterization of the murine herpesvirus 68 genome. The Journal of general virology *71 (Pt 6)*, 1355-1364.

Egan, J.J., Stewart, J.P., Hasleton, P.S., Arrand, J.R., Carroll, K.B., and Woodcock, A.A. (1995). Epstein-Barr virus replication within pulmonary epithelial cells in cryptogenic fibrosing alveolitis. Thorax *50*, 1234-1239.

Ehtisham, S., Sunil-Chandra, N.P., and Nash, A.A. (1993). Pathogenesis of murine gammaherpesvirus infection in mice deficient in CD4 and CD8 T cells. Journal of virology *67*, 5247-5252.

Eisenbarth, S.C., Colegio, O.R., O'Connor, W., Sutterwala, F.S., and Flavell, R.A. (2008). Crucial role for the Nalp3 inflammasome in the immunostimulatory properties of aluminium adjuvants. Nature *453*, 1122-1126.

Elgadi, M.M., Hayes, C.E., and Smiley, J.R. (1999). The herpes simplex virus vhs protein induces endoribonucleolytic cleavage of target RNAs in cell extracts. Journal of virology *73*, 7153-7164.

Elsharkawy, A.M., Oakley, F., and Mann, D.A. (2005). The role and regulation of hepatic stellate cell apoptosis in reversal of liver fibrosis. Apoptosis : an international journal on programmed cell death *10*, 927-939.

Eltom, M.A., Jemal, A., Mbulaiteye, S.M., Devesa, S.S., and Biggar, R.J. (2002). Trends in Kaposi's sarcoma and non-Hodgkin's lymphoma incidence in the United States from 1973 through 1998. Journal of the National Cancer Institute *94*, 1204-1210.

Emini, E.A., Luka, J., Armstrong, M.E., Banker, F.S., Provost, P.J., and Pearson, G.R. (1986). Establishment and characterization of a chronic infectious mononucleosislike syndrome in common marmosets. Journal of medical virology *18*, 369-379.

Emura, M., Nagai, S., Takeuchi, M., Kitaichi, M., and Izumi, T. (1990). In vitro production of B cell growth factor and B cell differentiation factor by peripheral blood mononuclear cells and bronchoalveolar lavage T lymphocytes from patients with idiopathic pulmonary fibrosis. Clinical and experimental immunology *82*, 133-139.

Ensser, A., Pflanz, R., and Fleckenstein, B. (1997). Primary structure of the alcelaphine herpesvirus 1 genome. Journal of virology *71*, 6517-6525.

Epstein, M.A., Achong, B.G., and Barr, Y.M. (1964). Virus Particles in Cultured Lymphoblasts from Burkitt's Lymphoma. Lancet *1*, 702-703.

Epstein, M.A., Morgan, A.J., Finerty, S., Randle, B.J., and Kirkwood, J.K. (1985). Protection of cottontop tamarins against Epstein-Barr virus-induced malignant lymphoma by a prototype subunit vaccine. Nature *318*, 287-289.

Evans, A.G., Moorman, N.J., Willer, D.O., and Speck, S.H. (2006). The M4 gene of gammaHV68 encodes a secreted glycoprotein and is required for the efficient establishment of splenic latency. Virology *344*, 520-531.

Evans, A.G., Moser, J.M., Krug, L.T., Pozharskaya, V., Mora, A.L., and Speck, S.H. (2008). A gammaherpesvirus-secreted activator of Vbeta4+ CD8+ T cells regulates chronic infection and immunopathology. The Journal of experimental medicine *205*, 669-684.

Fahraeus, R., Fu, H.L., Ernberg, I., Finke, J., Rowe, M., Klein, G., Falk, K., Nilsson, E., Yadav, M., Busson, P*., et al.* (1988). Expression of Epstein-Barr virus-encoded proteins in nasopharyngeal carcinoma. International journal of cancer Journal international du cancer *42*, 329-338.

Fantuzzi, G., and Dinarello, C.A. (1999). Interleukin-18 and interleukin-1 beta: two cytokine substrates for ICE (caspase-1). Journal of clinical immunology *19*, 1-11.

Fantuzzi, G., Reed, D.A., and Dinarello, C.A. (1999). IL-12-induced IFN-gamma is dependent on caspase-1 processing of the IL-18 precursor. The Journal of clinical investigation *104*, 761-767.

Farrar, W.L., Birchenall-Sparks, M.C., and Young, H.B. (1986). Interleukin 2 induction of interferon-gamma mRNA synthesis. J Immunol *137*, 3836-3840.

Farrell, P.J., Hollyoake, M., Niedobitek, G., Agathanggelou, A., Morgan, A., and Wedderburn, N. (1997). Direct demonstration of persistent Epstein-Barr virus gene expression in peripheral blood of infected common marmosets and analysis of virus-infected tissues in vivo. The Journal of general virology *78 (Pt 6)*, 1417-1424.

Feng, W., Li, W., Liu, W., Wang, F., Li, Y., and Yan, W. (2009). IL-17 induces myocardial fibrosis and enhances RANKL/OPG and MMP/TIMP signaling in isoproterenol-induced heart failure. Experimental and molecular pathology *87*, 212-218.

Fertin, C., Nicolas, J.F., Gillery, P., Kalis, B., Banchereau, J., and Maquart, F.X. (1991). Interleukin-4 stimulates collagen synthesis by normal and scleroderma fibroblasts in dermal equivalents. Cellular and molecular biology *37*, 823-829.

Fink, S.L., Bergsbaken, T., and Cookson, B.T. (2008). Anthrax lethal toxin and Salmonella elicit the common cell death pathway of caspase-1-dependent pyroptosis via distinct mechanisms. Proceedings of the National Academy of Sciences of the United States of America *105*, 4312-4317.

Fink, S.L., and Cookson, B.T. (2006). Caspase-1-dependent pore formation during pyroptosis leads to osmotic lysis of infected host macrophages. Cellular microbiology *8*, 1812-1825.

Flano, E., Hardy, C.L., Kim, I.J., Frankling, C., Coppola, M.A., Nguyen, P., Woodland, D.L., and Blackman, M.A. (2004). T cell reactivity during infectious mononucleosis and persistent gammaherpesvirus infection in mice. J Immunol *172*, 3078-3085.

Flano, E., Husain, S.M., Sample, J.T., Woodland, D.L., and Blackman, M.A. (2000). Latent murine gamma-herpesvirus infection is established in activated B cells, dendritic cells, and macrophages. J Immunol *165*, 1074-1081.

Flano, E., Kim, I.J., Woodland, D.L., and Blackman, M.A. (2002). Gamma-herpesvirus latency is preferentially maintained in splenic germinal center and memory B cells. The Journal of experimental medicine *196*, 1363-1372.

Forbes, S.J., Russo, F.P., Rey, V., Burra, P., Rugge, M., Wright, N.A., and Alison, M.R. (2004). A significant proportion of myofibroblasts are of bone marrow origin in human liver fibrosis. Gastroenterology *126*, 955-963.

Forrest, J.C., Paden, C.R., Allen, R.D., 3rd, Collins, J., and Speck, S.H. (2007). ORF73-null murine gammaherpesvirus 68 reveals roles for mLANA and p53 in virus replication. Journal of virology *81*, 11957-11971.

Fowler, P., Marques, S., Simas, J.P., and Efstathiou, S. (2003). ORF73 of murine herpesvirus-68 is critical for the establishment and maintenance of latency. The Journal of general virology *84*, 3405-3416.

Francois, S., Vidick, S., Sarlet, M., Michaux, J., Koteja, P., Desmecht, D., Stevenson, P.G., Vanderplasschen, A., and Gillet, L. (2010). Comparative study of murid gammaherpesvirus 4 infection in mice and in a natural host, bank voles. The Journal of general virology *91*, 2553-2563.

Friborg, J., Jr., Kong, W., Hottiger, M.O., and Nabel, G.J. (1999). p53 inhibition by the LANA protein of KSHV protects against cell death. Nature *402*, 889-894.

Friedman, S.L. (2008). Hepatic stellate cells: protean, multifunctional, and enigmatic cells of the liver. Physiological reviews *88*, 125-172.

Friedman, S.L., and Arthur, M.J. (1989). Activation of cultured rat hepatic lipocytes by Kupffer cell conditioned medium. Direct enhancement of matrix synthesis and stimulation of cell proliferation via induction of platelet-derived growth factor receptors. The Journal of clinical investigation *84*, 1780-1785.

Frucht, D.M., Fukao, T., Bogdan, C., Schindler, H., O'Shea, J.J., and Koyasu, S. (2001). IFN-gamma production by antigen-presenting cells: mechanisms emerge. Trends in immunology *22*, 556-560.

Fujimoto, M., Naka, T., Nakagawa, R., Kawazoe, Y., Morita, Y., Tateishi, A., Okumura, K., Narazaki, M., and Kishimoto, T. (2000). Defective thymocyte development and perturbed homeostasis of T cells in STAT-induced STAT inhibitor-1/suppressors of cytokine signaling-1 transgenic mice. J Immunol *165*, 1799-1806.

Gahn, T.A., and Schildkraut, C.L. (1989). The Epstein-Barr virus origin of plasmid replication, oriP, contains both the initiation and termination sites of DNA replication. Cell *58*, 527-535.

Gahn, T.A., and Sugden, B. (1995). An EBNA-1-dependent enhancer acts from a distance of 10 kilobase pairs to increase expression of the Epstein-Barr virus LMP gene. Journal of virology *69*, 2633-2636.

Gangadharan, B. (2006). Role of gamma interferon in the pathogenesis of Murine gannaherpesvirus-68 (University of Edinburgh).

Gangadharan, B., Dutia, B.M., Rhind, S.M., and Nash, A.A. (2009). Murid herpesvirus-4 induces chronic inflammation of intrahepatic bile ducts in mice deficient in gamma-interferon signalling. Hepatol Res *39*, 187-194.

Gangadharan, B., Hoeve, M.A., Allen, J.E., Ebrahimi, B., Rhind, S.M., Dutia, B.M., and Nash, A.A. (2008). Murine gammaherpesvirus-induced fibrosis is associated with the development of alternatively activated macrophages. Journal of leukocyte biology *84*, 50-58.

Gangappa, S., van Dyk, L.F., Jewett, T.J., Speck, S.H., and Virgin, H.W.t. (2002). Identification of the in vivo role of a viral bcl-2. The Journal of experimental medicine *195*, 931-940.

Gao, S.J., Kingsley, L., Hoover, D.R., Spira, T.J., Rinaldo, C.R., Saah, A., Phair, J., Detels, R., Parry, P., Chang, Y.*, et al.* (1996). Seroconversion to antibodies against Kaposi's sarcoma-associated herpesvirus-related latent nuclear antigens before the development of Kaposi's sarcoma. The New England journal of medicine *335*, 233-241.

Garber, D.A., Schaffer, P.A., and Knipe, D.M. (1997). A LAT-associated function reduces productive-cycle gene expression during acute infection of murine sensory neurons with herpes simplex virus type 1. Journal of virology *71*, 5885-5893.

Gaspar, M., May, J.S., Sukla, S., Frederico, B., Gill, M.B., Smith, C.M., Belz, G.T., and Stevenson, P.G. (2011). Murid herpesvirus-4 exploits dendritic cells to infect B cells. PLoS pathogens *7*, e1002346.

Geere, H.M., Ligertwood, Y., Templeton, K.M., Bennet, I., Gangadharan, B., Rhind, S.M., Nash, A.A., and Dutia, B.M. (2006). The M4 gene of murine gammaherpesvirus 68 modulates latent infection. The Journal of general virology *87*, 803-807.

Gessain, A., and Duprez, R. (2005). Spindle cells and their role in Kaposi's sarcoma. The international journal of biochemistry & cell biology *37*, 2457-2465.

Gillet, L., May, J.S., Colaco, S., and Stevenson, P.G. (2007). Glycoprotein L disruption reveals two functional forms of the murine gammaherpesvirus 68 glycoprotein H. Journal of virology *81*, 280-291.

Goding, C.R., and O'Hare, P. (1989). Herpes simplex virus Vmw65-octamer binding protein interaction: a paradigm for combinatorial control of transcription. Virology *173*, 363-367.

Goodwin, M.M., Canny, S., Steed, A., and Virgin, H.W. (2010). Murine gammaherpesvirus 68 has evolved gamma interferon and stat1-repressible promoters for the lytic switch gene 50. Journal of virology *84*, 3711-3717.

Gordon, S., and Taylor, P.R. (2005). Monocyte and macrophage heterogeneity. Nature reviews *5*, 953-964.

Gordy, C., and He, Y.W. (2012). The crosstalk between autophagy and apoptosis: where does this lead? Protein & cell *3*, 17-27.

Gorelik, L., and Flavell, R.A. (2002). Transforming growth factor-beta in T-cell biology. Nature reviews *2*, 46-53.

Gray, P.W., and Goeddel, D.V. (1983). Cloning and expression of murine immune interferon cDNA. Proceedings of the National Academy of Sciences of the United States of America *80*, 5842-5846.

Griffiths, P.D., Clark, D.A., and Emery, V.C. (2000). Betaherpesviruses in transplant recipients. The Journal of antimicrobial chemotherapy *45 Suppl T3*, 29-34.

Gurujeyalakshmi, G., and Giri, S.N. (1995). Molecular mechanisms of antifibrotic effect of interferon gamma in bleomycin-mouse model of lung fibrosis: downregulation of TGF-beta and procollagen I and III gene expression. Experimental lung research *21*, 791-808.

Hair, J.R., Lyons, P.A., Smith, K.G., and Efstathiou, S. (2007). Control of Rta expression critically determines transcription of viral and cellular genes following gammaherpesvirus infection. The Journal of general virology *88*, 1689-1697.

Hardy, C.L., Silins, S.L., Woodland, D.L., and Blackman, M.A. (2000). Murine gamma-herpesvirus infection causes V(beta)4-specific CDR3-restricted clonal expansions within CD8(+) peripheral blood T lymphocytes. International immunology *12*, 1193-1204.

Hauser, A.E., Junt, T., Mempel, T.R., Sneddon, M.W., Kleinstein, S.H., Henrickson, S.E., von Andrian, U.H., Shlomchik, M.J., and Haberman, A.M. (2007). Definition of germinal-center B cell migration in vivo reveals predominant intrazonal circulation patterns. Immunity *26*, 655-667.

Hayashi, H., and Sakai, T. (2011). Animal models for the study of liver fibrosis: new insights from knockout mouse models. American journal of physiology Gastrointestinal and liver physiology *300*, G729-738.

Heidaran, M.A., Pierce, J.H., Yu, J.C., Lombardi, D., Artrip, J.E., Fleming, T.P., Thomason, A., and Aaronson, S.A. (1991). Role of alpha beta receptor heterodimer formation in beta platelet-derived growth factor (PDGF) receptor activation by PDGF-AB. The Journal of biological chemistry *266*, 20232-20237.

Heldwein, E.E., Lou, H., Bender, F.C., Cohen, G.H., Eisenberg, R.J., and Harrison, S.C. (2006). Crystal structure of glycoprotein B from herpes simplex virus 1. Science *313*, 217-220.

Henle, G., Henle, W., Clifford, P., Diehl, V., Kafuko, G.W., Kirya, B.G., Klein, G., Morrow, R.H., Munube, G.M., Pike, P.*, et al.* (1969). Antibodies to Epstein-Barr virus in Burkitt's lymphoma and control groups. Journal of the National Cancer Institute *43*, 1147-1157.

Henle, G., Henle, W., and Diehl, V. (1968). Relation of Burkitt's tumor-associated herpes-ytpe virus to infectious mononucleosis. Proceedings of the National Academy of Sciences of the United States of America *59*, 94-101.

Henle, W., Diehl, V., Kohn, G., Zur Hausen, H., and Henle, G. (1967). Herpes-type virus and chromosome marker in normal leukocytes after growth with irradiated Burkitt cells. Science *157*, 1064-1065.

Herbert, D.R., Holscher, C., Mohrs, M., Arendse, B., Schwegmann, A., Radwanska, M., Leeto, M., Kirsch, R., Hall, P., Mossmann, H.*, et al.* (2004). Alternative macrophage activation is essential for survival during schistosomiasis and downmodulates T helper 1 responses and immunopathology. Immunity *20*, 623-635.

Herskowitz, J.H., Jacoby, M.A., and Speck, S.H. (2005). The murine gammaherpesvirus 68 M2 gene is required for efficient reactivation from latently infected B cells. Journal of virology *79*, 2261-2273.

Herskowitz, J.H., Siegel, A.M., Jacoby, M.A., and Speck, S.H. (2008). Systematic mutagenesis of the murine gammaherpesvirus 68 M2 protein identifies domains important for chronic infection. Journal of virology *82*, 3295-3310.

Hesse, M., Modolell, M., La Flamme, A.C., Schito, M., Fuentes, J.M., Cheever, A.W., Pearce, E.J., and Wynn, T.A. (2001). Differential regulation of nitric oxide synthase-2 and arginase-1 by type 1/type 2 cytokines in vivo: granulomatous pathology is shaped by the pattern of L-arginine metabolism. J Immunol *167*, 6533-6544.

Hetzel, M., Bachem, M., Anders, D., Trischler, G., and Faehling, M. (2005). Different effects of growth factors on proliferation and matrix production of normal and fibrotic human lung fibroblasts. Lung *183*, 225-237.

Hoge, A.T., Hendrickson, S.B., and Burns, W.H. (2000). Murine gammaherpesvirus 68 cyclin D homologue is required for efficient reactivation from latency. Journal of virology *74*, 7016-7023.

Hovanessian, A.G. (1991). Interferon-induced and double-stranded RNA-activated enzymes: a specific protein kinase and 2',5'-oligoadenylate synthetases. Journal of interferon research *11*, 199-205.

Hovanessian, A.G., and Galabru, J. (1987). The double-stranded RNA-dependent protein kinase is also activated by heparin. European journal of biochemistry / FEBS *167*, 467-473.

Huang, S., Hendriks, W., Althage, A., Hemmi, S., Bluethmann, H., Kamijo, R., Vilcek, J., Zinkernagel, R.M., and Aguet, M. (1993). Immune response in mice that lack the interferon-gamma receptor. Science *259*, 1742-1745.

Huaux, F., Liu, T., McGarry, B., Ullenbruch, M., Xing, Z., and Phan, S.H. (2003). Eosinophils and T lymphocytes possess distinct roles in bleomycin-induced lung injury and fibrosis. J Immunol *171*, 5470-5481.

Hughes, D.J., Kipar, A., Leeming, G.H., Bennett, E., Howarth, D., Cummerson, J.A., Papoula-Pereira, R., Flanagan, B.F., Sample, J.T., and Stewart, J.P. (2011). Chemokine binding protein M3 of murine gammaherpesvirus 68 modulates the host response to infection in a natural host. PLoS pathogens *7*, e1001321.

Hughes, D.J., Kipar, A., Sample, J.T., and Stewart, J.P. (2010). Pathogenesis of a model gammaherpesvirus in a natural host. Journal of virology *84*, 3949-3961.

Husain, S.M., Usherwood, E.J., Dyson, H., Coleclough, C., Coppola, M.A., Woodland, D.L., Blackman, M.A., Stewart, J.P., and Sample, J.T. (1999). Murine gammaherpesvirus M2 gene is latency-associated and its protein a target for CD8(+) T lymphocytes. Proceedings of the National Academy of Sciences of the United States of America *96*, 7508-7513.

Hutt-Fletcher, L.M. (2007). Epstein-Barr virus entry. Journal of virology *81*, 7825-7832.

Iredale, J.P., Benyon, R.C., Pickering, J., McCullen, M., Northrop, M., Pawley, S., Hovell, C., and Arthur, M.J. (1998). Mechanisms of spontaneous resolution of rat liver fibrosis. Hepatic stellate cell apoptosis and reduced hepatic expression of metalloproteinase inhibitors. The Journal of clinical investigation *102*, 538-549.

Irving, W.L., Day, S., and Johnston, I.D. (1993). Idiopathic pulmonary fibrosis and hepatitis C virus infection. The American review of respiratory disease *148*, 1683-1684.

Issa, R., Williams, E., Trim, N., Kendall, T., Arthur, M.J., Reichen, J., Benyon, R.C., and Iredale, J.P. (2001). Apoptosis of hepatic stellate cells: involvement in resolution of biliary fibrosis and regulation by soluble growth factors. Gut *48*, 548-557.

Issa, R., Zhou, X., Constandinou, C.M., Fallowfield, J., Millward-Sadler, H., Gaca, M.D., Sands, E., Suliman, I., Trim, N., Knorr, A.*, et al.* (2004). Spontaneous recovery from micronodular cirrhosis: evidence for incomplete resolution associated with matrix cross-linking. Gastroenterology *126*, 1795-1808.

Jacoby, M.A., Virgin, H.W.t., and Speck, S.H. (2002). Disruption of the M2 gene of murine gammaherpesvirus 68 alters splenic latency following intranasal, but not intraperitoneal, inoculation. Journal of virology *76*, 1790-1801.

Jacoby, R.O., Buxton, D., and Reid, H.W. (1988a). The pathology of wildebeest-associated malignant catarrhal fever in hamsters, rats and guinea-pigs. Journal of comparative pathology *98*, 99-109.

Jacoby, R.O., Reid, H.W., Buxton, D., and Pow, I. (1988b). Transmission of wildebeest-associated and sheep-associated malignant catarrhal fever to hamsters, rats and guinea-pigs. Journal of comparative pathology *98*, 91-98.

Jarousse, N., Chandran, B., and Coscoy, L. (2008). Lack of heparan sulfate expression in B-cell lines: implications for Kaposi's sarcoma-associated herpesvirus and murine gammaherpesvirus 68 infections. Journal of virology *82*, 12591-12597.

Jeong, W.I., Park, O., and Gao, B. (2008). Abrogation of the antifibrotic effects of natural killer cells/interferon-gamma contributes to alcohol acceleration of liver fibrosis. Gastroenterology *134*, 248-258.

Jesenberger, V., Procyk, K.J., Yuan, J., Reipert, S., and Baccarini, M. (2000). Salmonella-induced caspase-2 activation in macrophages: a novel mechanism in pathogen-mediated apoptosis. The Journal of experimental medicine *192*, 1035-1046.

Johannessen, I., and Crawford, D.H. (1999). In vivo models for Epstein-Barr virus (EBV)-associated B cell lymphoproliferative disease (BLPD). Reviews in medical virology *9*, 263-277.

Johannsen, E., Koh, E., Mosialos, G., Tong, X., Kieff, E., and Grossman, S.R. (1995). Epstein-Barr virus nuclear protein 2 transactivation of the latent membrane protein 1 promoter is mediated by J kappa and PU.1. Journal of virology *69*, 253-262.

Johnson, H.M., Russell, J.K., and Torres, B.A. (1986). Second messenger role of arachidonic acid and its metabolites in interferon-gamma production. J Immunol *137*, 3053-3056.

Johnson, H.M., and Torres, B.A. (1984). Leukotrienes: positive signals for regulation of gamma-interferon production. J Immunol *132*, 413-416.

Junt, T., Scandella, E., and Ludewig, B. (2008). Form follows function: lymphoid tissue microarchitecture in antimicrobial immune defence. Nature reviews *8*, 764-775.

Kapadia, S.B., Levine, B., Speck, S.H., and Virgin, H.W.t. (2002). Critical role of complement and viral evasion of complement in acute, persistent, and latent gamma-herpesvirus infection. Immunity *17*, 143-155.

Kaplan, D.H., Shankaran, V., Dighe, A.S., Stockert, E., Aguet, M., Old, L.J., and Schreiber, R.D. (1998). Demonstration of an interferon gamma-dependent tumor surveillance system in immunocompetent mice. Proceedings of the National Academy of Sciences of the United States of America *95*, 7556-7561.

Kapoor, P., and Frappier, L. (2003). EBNA1 partitions Epstein-Barr virus plasmids in yeast cells by attaching to human EBNA1-binding protein 2 on mitotic chromosomes. Journal of virology *77*, 6946-6956.

Kapoor, P., and Frappier, L. (2005). Methods for measuring the replication and segregation of Epstein-Barr virus-based plasmids. Methods Mol Biol *292*, 247-266.

Kaviratne, M., Hesse, M., Leusink, M., Cheever, A.W., Davies, S.J., McKerrow, J.H., Wakefield, L.M., Letterio, J.J., and Wynn, T.A. (2004). IL-13 activates a mechanism of tissue fibrosis that is completely TGF-beta independent. J Immunol *173*, 4020-4029.

Kedes, D.H., Operskalski, E., Busch, M., Kohn, R., Flood, J., and Ganem, D. (1996). The seroepidemiology of human herpesvirus 8 (Kaposi's sarcoma-associated herpesvirus): distribution of infection in KS risk groups and evidence for sexual transmission. Nature medicine *2*, 918-924.

Kim, I.J., Flano, E., Woodland, D.L., and Blackman, M.A. (2002). Antibody-mediated control of persistent gamma-herpesvirus infection. J Immunol *168*, 3958-3964.

Kim, J.H., Kim, H.Y., Kim, S., Chung, J.H., Park, W.S., and Chung, D.H. (2005). Natural killer T (NKT) cells attenuate bleomycin-induced pulmonary fibrosis by producing interferon-gamma. The American journal of pathology *167*, 1231-1241.

Kool, M., Soullie, T., van Nimwegen, M., Willart, M.A., Muskens, F., Jung, S., Hoogsteden, H.C., Hammad, H., and Lambrecht, B.N. (2008). Alum adjuvant boosts adaptive immunity by inducing uric acid and activating inflammatory dendritic cells. The Journal of experimental medicine *205*, 869-882.

Krug, L.T., Collins, C.M., Gargano, L.M., and Speck, S.H. (2009). NF-kappaB p50 plays distinct roles in the establishment and control of murine gammaherpesvirus 68 latency. Journal of virology *83*, 4732-4748.

Ku, B., Woo, J.S., Liang, C., Lee, K.H., Hong, H.S., E, X., Kim, K.S., Jung, J.U., and Oh, B.H. (2008). Structural and biochemical bases for the inhibition of autophagy and apoptosis by viral BCL-2 of murine gamma-herpesvirus 68. PLoS pathogens *4*, e25.

Kuida, K., Lippke, J.A., Ku, G., Harding, M.W., Livingston, D.J., Su, M.S., and Flavell, R.A. (1995). Altered cytokine export and apoptosis in mice deficient in interleukin-1 beta converting enzyme. Science *267*, 2000-2003.

Kuwano, K., Miyazaki, H., Hagimoto, N., Kawasaki, M., Fujita, M., Kunitake, R., Kaneko, Y., and Hara, N. (1999). The involvement of Fas-Fas ligand pathway in fibrosing lung diseases. American journal of respiratory cell and molecular biology *20*, 53-60.

Lan, K., Kuppers, D.A., Verma, S.C., and Robertson, E.S. (2004). Kaposi's sarcoma-associated herpesvirus-encoded latency-associated nuclear antigen inhibits lytic replication by targeting Rta: a potential mechanism for virus-mediated control of latency. Journal of virology *78*, 6585-6594.

Lan, K., Kuppers, D.A., Verma, S.C., Sharma, N., Murakami, M., and Robertson, E.S. (2005). Induction of Kaposi's sarcoma-associated herpesvirus latency-associated nuclear antigen by the lytic transactivator RTA: a novel mechanism for establishment of latency. Journal of virology *79*, 7453-7465.

Laquerre, S., Argnani, R., Anderson, D.B., Zucchini, S., Manservigi, R., and Glorioso, J.C. (1998). Heparan sulfate proteoglycan binding by herpes simplex virus type 1 glycoproteins B and C, which differ in their contributions to virus attachment, penetration, and cell-to-cell spread. Journal of virology *72*, 6119-6130.

Larsson, O., Diebold, D., Fan, D., Peterson, M., Nho, R.S., Bitterman, P.B., and Henke, C.A. (2008). Fibrotic myofibroblasts manifest genome-wide derangements of translational control. PloS one *3*, e3220.

Lee, A., Rana, B.K., Schiffer, H.H., Schork, N.J., Brann, M.R., Insel, P.A., and Weiner, D.M. (2003). Distribution analysis of nonsynonymous polymorphisms within the G-protein-coupled receptor gene family. Genomics *81*, 245-248.

Lee, C.G., Homer, R.J., Zhu, Z., Lanone, S., Wang, X., Koteliansky, V., Shipley, J.M., Gotwals, P., Noble, P., Chen, Q.*, et al.* (2001a). Interleukin-13 induces tissue fibrosis by selectively stimulating and activating transforming growth factor beta(1). The Journal of experimental medicine *194*, 809-821.

Lee, H.K., Lund, J.M., Ramanathan, B., Mizushima, N., and Iwasaki, A. (2007). Autophagy-dependent viral recognition by plasmacytoid dendritic cells. Science *315*, 1398-1401.

Lee, J.H., Kaminski, N., Dolganov, G., Grunig, G., Koth, L., Solomon, C., Erle, D.J., and Sheppard, D. (2001b). Interleukin-13 induces dramatically different transcriptional programs in three human airway cell types. American journal of respiratory cell and molecular biology *25*, 474-485.

Lee, K.S., Cool, C.D., and van Dyk, L.F. (2009). Murine gammaherpesvirus 68 infection of gamma interferon-deficient mice on a BALB/c background results in acute lethal pneumonia that is dependent on specific viral genes. Journal of virology *83*, 11397-11401.

Lee, M.A., Diamond, M.E., and Yates, J.L. (1999). Genetic evidence that EBNA-1 is needed for efficient, stable latent infection by Epstein-Barr virus. Journal of virology *73*, 2974-2982.

Leicester, K.L., Olynyk, J.K., Brunt, E.M., Britton, R.S., and Bacon, B.R. (2004). CD14-positive hepatic monocytes/macrophages increase in hereditary hemochromatosis. Liver international : official journal of the International Association for the Study of the Liver *24*, 446-451.

Lepparanta, O., Pulkkinen, V., Koli, K., Vahatalo, R., Salmenkivi, K., Kinnula, V.L., Heikinheimo, M., and Myllarniemi, M. (2010). Transcription factor GATA-6 is expressed in quiescent myofibroblasts in idiopathic pulmonary fibrosis. American journal of respiratory cell and molecular biology *42*, 626-632.

Letterio, J.J., and Roberts, A.B. (1998). Regulation of immune responses by TGF-beta. Annual review of immunology *16*, 137-161.

Levine, A.J. (1997). p53, the cellular gatekeeper for growth and division. Cell *88*, 323-331.

Li, P., Allen, H., Banerjee, S., Franklin, S., Herzog, L., Johnston, C., McDowell, J., Paskind, M., Rodman, L., Salfeld, J.*, et al.* (1995). Mice deficient in IL-1 beta-converting enzyme are defective in production of mature IL-1 beta and resistant to endotoxic shock. Cell *80*, 401-411.

Li, Q., Zhou, F., Ye, F., and Gao, S.J. (2008). Genetic disruption of KSHV major latent nuclear antigen LANA enhances viral lytic transcriptional program. Virology *379*, 234-244.

Liang, X., Collins, C.M., Mendel, J.B., Iwakoshi, N.N., and Speck, S.H. (2009). Gammaherpesvirus-driven plasma cell differentiation regulates virus reactivation from latently infected B lymphocytes. PLoS pathogens *5*, e1000677.

Liang, X., Paden, C.R., Morales, F.M., Powers, R.P., Jacob, J., and Speck, S.H. (2011). Murine gamma-herpesvirus immortalization of fetal liver-derived B cells requires both the viral cyclin D homolog and latency-associated nuclear antigen. PLoS pathogens *7*, e1002220.

Liang, X., Shin, Y.C., Means, R.E., and Jung, J.U. (2004). Inhibition of interferon-mediated antiviral activity by murine gammaherpesvirus 68 latency-associated M2 protein. Journal of virology *78*, 12416-12427.

Link, A., Vogt, T.K., Favre, S., Britschgi, M.R., Acha-Orbea, H., Hinz, B., Cyster, J.G., and Luther, S.A. (2007). Fibroblastic reticular cells in lymph nodes regulate the homeostasis of naive T cells. Nature immunology *8*, 1255-1265.

Liu, L., Flano, E., Usherwood, E.J., Surman, S., Blackman, M.A., and Woodland, D.L. (1999). Lytic cycle T cell epitopes are expressed in two distinct phases during MHV-68 infection. J Immunol *163*, 868-874.

Liu, Y., Meyer, C., Muller, A., Herweck, F., Li, Q., Mullenbach, R., Mertens, P.R., Dooley, S., and Weng, H.L. (2011). IL-13 induces connective tissue growth factor in rat hepatic stellate cells via TGF-beta-independent Smad signaling. J Immunol *187*, 2814-2823.

Loh, J., Huang, Q., Petros, A.M., Nettesheim, D., van Dyk, L.F., Labrada, L., Speck, S.H., Levine, B., Olejniczak, E.T., and Virgin, H.W.t. (2005). A surface groove essential for viral Bcl-2 function during chronic infection in vivo. PLoS pathogens *1*, e10.

Loh, J., Thomas, D.A., Revell, P.A., Ley, T.J., and Virgin, H.W.t. (2004). Granzymes and caspase 3 play important roles in control of gammaherpesvirus latency. Journal of virology *78*, 12519-12528.

Lok, S.S., Smith, E., Doran, H.M., Sawyer, R., Yonan, N., and Egan, J.J. (1998). Idiopathic pulmonary fibrosis and cyclosporine: a lesson from single-lung transplantation. Chest *114*, 1478-1481.

Longnecker, R., and Neipel, F. (2007). Introduction to the human gamma-herpesviruses. In Human Herpesviruses: Biology, Therapy, and Immunoprophylaxis, A. Arvin, G. Campadelli-Fiume, E. Mocarski, P.S. Moore, B. Roizman, R. Whitley, and K. Yamanishi, eds. (Cambridge).

Luppi, M., Barozzi, P., Rasini, V., and Torelli, G. (2002). HHV-8 infection in the transplantation setting: a concern only for solid organ transplant patients? Leukemia & lymphoma *43*, 517-522.

Luther, S.A., Vogt, T.K., and Siegert, S. (2011). Guiding blind T cells and dendritic cells: A closer look at fibroblastic reticular cells found within lymph node T zones. Immunology letters *138*, 9-11.

MacDonald, K.P., Rowe, V., Bofinger, H.M., Thomas, R., Sasmono, T., Hume, D.A., and Hill, G.R. (2005). The colony-stimulating factor 1 receptor is expressed on dendritic cells during differentiation and regulates their expansion. J Immunol *175*, 1399-1405.

MacLennan, I.C. (1994). Germinal centers. Annual review of immunology *12*, 117-139.

Macpherson, I., and Stoker, M. (1962). Polyoma transformation of hamster cell clones--an investigation of genetic factors affecting cell competence. Virology *16*, 147-151.

Macrae, A.I., Dutia, B.M., Milligan, S., Brownstein, D.G., Allen, D.J., Mistrikova, J., Davison, A.J., Nash, A.A., and Stewart, J.P. (2001). Analysis of a novel strain of murine gammaherpesvirus reveals a genomic locus important for acute pathogenesis. Journal of virology *75*, 5315-5327.

Macrae, A.I., Usherwood, E.J., Husain, S.M., Flano, E., Kim, I.J., Woodland, D.L., Nash, A.A., Blackman, M.A., Sample, J.T., and Stewart, J.P. (2003). Murid herpesvirus 4 strain 68 M2 protein is a B-cell-associated antigen important for latency but not lymphocytosis. Journal of virology *77*, 9700-9709.

Madala, S.K., Pesce, J.T., Ramalingam, T.R., Wilson, M.S., Minnicozzi, S., Cheever, A.W., Thompson, R.W., Mentink-Kane, M.M., and Wynn, T.A. (2010). Matrix metalloproteinase 12-deficiency augments extracellular matrix degrading metalloproteinases and attenuates IL-13-dependent fibrosis. J Immunol *184*, 3955-3963.

Maeyama, T., Kuwano, K., Kawasaki, M., Kunitake, R., Hagimoto, N., Matsuba, T., Yoshimi, M., Inoshima, I., Yoshida, K., and Hara, N. (2001). Upregulation of Fas-signalling molecules in lung epithelial cells from patients with idiopathic pulmonary fibrosis. The European respiratory journal : official journal of the European Society for Clinical Respiratory Physiology *17*, 180-189.

Mahboubi, K., and Pober, J.S. (2002). Activation of signal transducer and activator of transcription 1 (STAT1) is not sufficient for the induction of STAT1-dependent genes in endothelial cells. Comparison of interferon-gamma and oncostatin M. The Journal of biological chemistry *277*, 8012-8021.

Malizia, A.P., Keating, D.T., Smith, S.M., Walls, D., Doran, P.P., and Egan, J.J. (2008). Alveolar epithelial cell injury with Epstein-Barr virus upregulates TGFbeta1 expression. American journal of physiology Lung cellular and molecular physiology *295*, L451-460.

Marcelin, A.G., Roque-Afonso, A.M., Hurtova, M., Dupin, N., Tulliez, M., Sebagh, M., Arkoub, Z.A., Guettier, C., Samuel, D., Calvez, V.*, et al.* (2004). Fatal disseminated Kaposi's sarcoma following human herpesvirus 8 primary infections in liver-transplant recipients. Liver transplantation : official publication of the American Association for the Study of Liver Diseases and the International Liver Transplantation Society *10*, 295-300.

Marques, S., Efstathiou, S., Smith, K.G., Haury, M., and Simas, J.P. (2003). Selective gene expression of latent murine gammaherpesvirus 68 in B lymphocytes. Journal of virology *77*, 7308-7318.

Martro, E., Bulterys, M., Stewart, J.A., Spira, T.J., Cannon, M.J., Thacher, T.D., Bruns, R., Pellett, P.E., and Dollard, S.C. (2004). Comparison of human herpesvirus 8 and Epstein-Barr virus seropositivity among children in areas endemic and non-endemic for Kaposi's sarcoma. Journal of medical virology *72*, 126-131.

Masucci, M.G., Torsteindottir, S., Colombani, J., Brautbar, C., Klein, E., and Klein, G. (1987). Down-regulation of class I HLA antigens and of the Epstein-Barr virus-encoded latent membrane protein in Burkitt lymphoma lines. Proceedings of the National Academy of Sciences of the United States of America *84*, 4567-4571.

Matsui, T., Heidaran, M., Miki, T., Popescu, N., La Rochelle, W., Kraus, M., Pierce, J., and Aaronson, S. (1989). Isolation of a novel receptor cDNA establishes the existence of two PDGF receptor genes. Science *243*, 800-804.

May, J.S., de Lima, B.D., Colaco, S., and Stevenson, P.G. (2005a). Intercellular gamma-herpesvirus dissemination involves co-ordinated intracellular membrane protein transport. Traffic *6*, 780-793.

May, J.S., Walker, J., Colaco, S., and Stevenson, P.G. (2005b). The murine gammaherpesvirus 68 ORF27 gene product contributes to intercellular viral spread. Journal of virology *79*, 5059-5068.

McMillan, T.R., Moore, B.B., Weinberg, J.B., Vannella, K.M., Fields, W.B., Christensen, P.J., van Dyk, L.F., and Toews, G.B. (2008). Exacerbation of established pulmonary fibrosis in a murine model by gammaherpesvirus. American journal of respiratory and critical care medicine *177*, 771-780.

Mebius, R.E., Nolte, M.A., and Kraal, G. (2004). Development and function of the splenic marginal zone. Critical reviews in immunology *24*, 449-464.

Mehrad, B., Burdick, M.D., Zisman, D.A., Keane, M.P., Belperio, J.A., and Strieter, R.M. (2007). Circulating peripheral blood fibrocytes in human fibrotic interstitial lung disease. Biochemical and biophysical research communications *353*, 104-108.

Meliconi, R., Andreone, P., Fasano, L., Galli, S., Pacilli, A., Miniero, R., Fabbri, M., Solforosi, L., and Bernardi, M. (1996). Incidence of hepatitis C virus infection in Italian patients with idiopathic pulmonary fibrosis. Thorax *51*, 315-317.

Meurs, E., Chong, K., Galabru, J., Thomas, N.S., Kerr, I.M., Williams, B.R., and Hovanessian, A.G. (1990). Molecular cloning and characterization of the human double-stranded RNA-activated protein kinase induced by interferon. Cell *62*, 379-390.

Miggin, S.M., Palsson-McDermott, E., Dunne, A., Jefferies, C., Pinteaux, E., Banahan, K., Murphy, C., Moynagh, P., Yamamoto, M., Akira, S*., et al.* (2007). NF-kappaB activation by the Toll-IL-1 receptor domain protein MyD88 adapter-like is regulated by caspase-1. Proceedings of the National Academy of Sciences of the United States of America *104*, 3372-3377.

Milho, R., Smith, C.M., Marques, S., Alenquer, M., May, J.S., Gillet, L., Gaspar, M., Efstathiou, S., Simas, J.P., and Stevenson, P.G. (2009). In vivo imaging of murid herpesvirus-4 infection. The Journal of general virology *90*, 21-32.

Mills, C.D., Kincaid, K., Alt, J.M., Heilman, M.J., and Hill, A.M. (2000). M-1/M-2 macrophages and the Th1/Th2 paradigm. Journal of Immunology *164*, 6166-6173.

Miyazaki, H., Kuwano, K., Yoshida, K., Maeyama, T., Yoshimi, M., Fujita, M., Hagimoto, N., Yoshida, R., and Nakanishi, Y. (2004). The perforin mediated apoptotic pathway in lung injury and fibrosis. Journal of clinical pathology *57*, 1292-1298.

Mizuno, S., Matsumoto, K., Li, M.Y., and Nakamura, T. (2005). HGF reduces advancing lung fibrosis in mice: a potential role for MMP-dependent myofibroblast apoptosis. FASEB journal : official publication of the Federation of American Societies for Experimental Biology *19*, 580-582.

Moeller, A., Gilpin, S.E., Ask, K., Cox, G., Cook, D., Gauldie, J., Margetts, P.J., Farkas, L., Dobranowski, J., Boylan, C*., et al.* (2009). Circulating fibrocytes are an indicator of poor prognosis in idiopathic pulmonary fibrosis. American journal of respiratory and critical care medicine *179*, 588-594.

Moghaddam, A., Koch, J., Annis, B., and Wang, F. (1998). Infection of human B lymphocytes with lymphocryptoviruses related to Epstein-Barr virus. Journal of virology *72*, 3205-3212.

Molesworth, S.J., Lake, C.M., Borza, C.M., Turk, S.M., and Hutt-Fletcher, L.M. (2000). Epstein-Barr virus gH is essential for penetration of B cells but also plays a role in attachment of virus to epithelial cells. Journal of virology *74*, 6324-6332.

Moodley, Y.P., Caterina, P., Scaffidi, A.K., Misso, N.L., Papadimitriou, J.M., McAnulty, R.J., Laurent, G.J., Thompson, P.J., and Knight, D.A. (2004). Comparison of the morphological and biochemical changes in normal human lung fibroblasts and fibroblasts derived from lungs of patients with idiopathic pulmonary fibrosis during FasL-induced apoptosis. The Journal of pathology *202*, 486-495.

Mooney, J.E., Rolfe, B.E., Osborne, G.W., Sester, D.P., van Rooijen, N., Campbell, G.R., Hume, D.A., and Campbell, J.H. (2010). Cellular Plasticity of Inflammatory Myeloid Cells in the Peritoneal Foreign Body Response. American Journal of Pathology *176*, 369-380.

Moore, B.B., and Hogaboam, C.M. (2008). Murine models of pulmonary fibrosis. American journal of physiology Lung cellular and molecular physiology *294*, L152-160.

Moorman, N.J., Lin, C.Y., and Speck, S.H. (2004). Identification of candidate gammaherpesvirus 68 genes required for virus replication by signature-tagged transposon mutagenesis. Journal of virology *78*, 10282-10290.

Moorman, N.J., Virgin, H.W.t., and Speck, S.H. (2003a). Disruption of the gene encoding the gammaHV68 v-GPCR leads to decreased efficiency of reactivation from latency. Virology *307*, 179-190.

Moorman, N.J., Willer, D.O., and Speck, S.H. (2003b). The gammaherpesvirus 68 latency-associated nuclear antigen homolog is critical for the establishment of splenic latency. Journal of virology *77*, 10295-10303.

Mora, A.L., Torres-Gonzalez, E., Rojas, M., Corredor, C., Ritzenthaler, J., Xu, J., Roman, J., Brigham, K., and Stecenko, A. (2006). Activation of alveolar macrophages via the alternative pathway in herpesvirus-induced lung fibrosis. American journal of respiratory cell and molecular biology *35*, 466-473.

Mora, A.L., Torres-Gonzalez, E., Rojas, M., Xu, J., Ritzenthaler, J., Speck, S.H., Roman, J., Brigham, K., and Stecenko, A. (2007). Control of virus reactivation arrests pulmonary herpesvirus-induced fibrosis in IFN-gamma receptor-deficient mice. American journal of respiratory and critical care medicine *175*, 1139-1150.

Mora, A.L., Woods, C.R., Garcia, A., Xu, J., Rojas, M., Speck, S.H., Roman, J., Brigham, K.L., and Stecenko, A.A. (2005). Lung infection with gamma-herpesvirus induces progressive pulmonary fibrosis in Th2-biased mice. American journal of physiology Lung cellular and molecular physiology *289*, L711-721.

Mueller, S.N., and Germain, R.N. (2009). Stromal cell contributions to the homeostasis and functionality of the immune system. Nature reviews *9*, 618-629.

Muller, U., Steinhoff, U., Reis, L.F., Hemmi, S., Pavlovic, J., Zinkernagel, R.M., and Aguet, M. (1994). Functional role of type I and type II interferons in antiviral defense. Science *264*, 1918-1921.

Munger, J.S., Huang, X., Kawakatsu, H., Griffiths, M.J., Dalton, S.L., Wu, J., Pittet, J.F., Kaminski, N., Garat, C., Matthay, M.A.*, et al.* (1999). The integrin alpha v beta 6 binds and

activates latent TGF beta 1: a mechanism for regulating pulmonary inflammation and fibrosis. Cell *96*, 319-328.

Murphy, E., Vanicek, J., Robins, H., Shenk, T., and Levine, A.J. (2008). Suppression of immediate-early viral gene expression by herpesvirus-coded microRNAs: implications for latency. Proceedings of the National Academy of Sciences of the United States of America *105*, 5453-5458.

Murray, L.A., Argentieri, R.L., Farrell, F.X., Bracht, M., Sheng, H., Whitaker, B., Beck, H., Tsui, P., Cochlin, K., Evanoff, H.L.*, et al.* (2008). Hyper-responsiveness of IPF/UIP fibroblasts: interplay between TGFbeta1, IL-13 and CCL2. The international journal of biochemistry & cell biology *40*, 2174-2182.

Murray, P.J., and Wynn, T.A. (2011). Protective and pathogenic functions of macrophage subsets. Nature reviews *11*, 723-737.

Nador, R.G., Cesarman, E., Chadburn, A., Dawson, D.B., Ansari, M.Q., Sald, J., and Knowles, D.M. (1996). Primary effusion lymphoma: a distinct clinicopathologic entity associated with the Kaposi's sarcoma-associated herpes virus. Blood *88*, 645-656.

Nakamura, H., Lu, M., Gwack, Y., Souvlis, J., Zeichner, S.L., and Jung, J.U. (2003). Global changes in Kaposi's sarcoma-associated virus gene expression patterns following expression of a tetracycline-inducible Rta transactivator. Journal of virology *77*, 4205-4220.

Nakanishi, K., Yoshimoto, T., Tsutsui, H., and Okamura, H. (2001). Interleukin-18 regulates both Th1 and Th2 responses. Annual review of immunology *19*, 423-474.

Nash, A.A., Dutia, B.M., Stewart, J.P., and Davison, A.J. (2001). Natural history of murine gamma-herpesvirus infection. Philosophical transactions of the Royal Society of London Series B, Biological sciences *356*, 569-579.

Nayyar, V.K., Shire, K., and Frappier, L. (2009). Mitotic chromosome interactions of Epstein-Barr nuclear antigen 1 (EBNA1) and human EBNA1-binding protein 2 (EBP2). Journal of cell science *122*, 4341-4350.

Nealy, M.S., Coleman, C.B., Li, H., and Tibbetts, S.A. (2010). Use of a virus-encoded enzymatic marker reveals that a stable fraction of memory B cells expresses latency-associated nuclear antigen throughout chronic gammaherpesvirus infection. Journal of virology *84*, 7523-7534.

Neipel, F., Albrecht, J.C., and Fleckenstein, B. (1998). Human herpesvirus 8--the first human Rhadinovirus. Journal of the National Cancer Institute Monographs, 73-77.

Niedobitek, G., Deacon, E.M., Young, L.S., Herbst, H., Hamilton-Dutoit, S.J., and Pallesen, G. (1991). Epstein-Barr virus gene expression in Hodgkin's disease. Blood *78*, 1628-1630.

Nonn, R.A., and Garrity, E.R., Jr. (1998). Lung transplantation for fibrotic lung diseases. The American journal of the medical sciences *315*, 146-154.

Oldroyd, S.D., Thomas, G.L., Gabbiani, G., and El Nahas, A.M. (1999). Interferon-gamma inhibits experimental renal fibrosis. Kidney international *56*, 2116-2127.

Ong, C., Wong, C., Roberts, C.R., Teh, H.S., and Jirik, F.R. (1998). Anti-IL-4 treatment prevents dermal collagen deposition in the tight-skin mouse model of scleroderma. European journal of immunology *28*, 2619-2629.

Ostendorf, T., Eitner, F., and Floege, J. (2012). The PDGF family in renal fibrosis. Pediatr Nephrol *27*, 1041-1050.

Osterrieder, N., Kamil, J.P., Schumacher, D., Tischer, B.K., and Trapp, S. (2006). Marek's disease virus: from miasma to model. Nature reviews Microbiology *4*, 283-294.

Ottinger, M., Pliquet, D., Christalla, T., Frank, R., Stewart, J.P., and Schulz, T.F. (2009). The interaction of the gammaherpesvirus 68 orf73 protein with cellular BET proteins affects the activation of cell cycle promoters. Journal of virology *83*, 4423-4434.

Paden, C.R., Forrest, J.C., Moorman, N.J., and Speck, S.H. (2010). Murine gammaherpesvirus 68 LANA is essential for virus reactivation from splenocytes but not long-term carriage of viral genome. Journal of virology *84*, 7214-7224.

Pallesen, G., Sandvej, K., Hamilton-Dutoit, S.J., Rowe, M., and Young, L.S. (1991). Activation of Epstein-Barr virus replication in Hodgkin and Reed-Sternberg cells. Blood *78*, 1162-1165.

Parker, B.D., Bankier, A., Satchwell, S., Barrell, B., and Farrell, P.J. (1990). Sequence and transcription of Raji Epstein-Barr virus DNA spanning the B95-8 deletion region. Virology *179*, 339-346.

Parry, C.M., Simas, J.P., Smith, V.P., Stewart, C.A., Minson, A.C., Efstathiou, S., and Alcami, A. (2000). A broad spectrum secreted chemokine binding protein encoded by a herpesvirus. The Journal of experimental medicine *191*, 573-578.

Patterson, J.B., Thomis, D.C., Hans, S.L., and Samuel, C.E. (1995). Mechanism of interferon action: double-stranded RNA-specific adenosine deaminase from human cells is inducible by alpha and gamma interferons. Virology *210*, 508-511.

Pearce, M., Matsumura, S., and Wilson, A.C. (2005). Transcripts encoding K12, v-FLIP, v-cyclin, and the microRNA cluster of Kaposi's sarcoma-associated herpesvirus originate from a common promoter. Journal of virology *79*, 14457-14464.

Pearl, J.E., Saunders, B., Ehlers, S., Orme, I.M., and Cooper, A.M. (2001). Inflammation and lymphocyte activation during mycobacterial infection in the interferon-gamma-deficient mouse. Cellular immunology *211*, 43-50.

Perng, G.C., Jones, C., Ciacci-Zanella, J., Stone, M., Henderson, G., Yukht, A., Slanina, S.M., Hofman, F.M., Ghiasi, H., Nesburn, A.B.*, et al.* (2000). Virus-induced neuronal apoptosis blocked by the herpes simplex virus latency-associated transcript. Science *287*, 1500-1503.

Pesce, J.T., Ramalingam, T.R., Mentink-Kane, M.M., Wilson, M.S., El Kasmi, K.C., Smith, A.M., Thompson, R.W., Cheever, A.W., Murray, P.J., and Wynn, T.A. (2009a). Arginase-1-expressing macrophages suppress Th2 cytokine-driven inflammation and fibrosis. PLoS pathogens *5*, e1000371.

Pesce, J.T., Ramalingam, T.R., Wilson, M.S., Mentink-Kane, M.M., Thompson, R.W., Cheever, A.W., Urban, J.F., Jr., and Wynn, T.A. (2009b). Retnla (relmalpha/fizz1) suppresses helminth-induced Th2-type immunity. PLoS pathogens *5*, e1000393.

Pfeffer, S., Sewer, A., Lagos-Quintana, M., Sheridan, R., Sander, C., Grasser, F.A., van Dyk, L.F., Ho, C.K., Shuman, S., Chien, M.*, et al.* (2005). Identification of microRNAs of the herpesvirus family. Nature methods *2*, 269-276.

Pierce, E.M., Carpenter, K., Jakubzick, C., Kunkel, S.L., Evanoff, H., Flaherty, K.R., Martinez, F.J., Toews, G.B., and Hogaboam, C.M. (2007). Idiopathic pulmonary fibrosis fibroblasts migrate and proliferate to CC chemokine ligand 21. The European respiratory journal : official journal of the European Society for Clinical Respiratory Physiology *29*, 1082-1093.

Pires de Miranda, M., Alenquer, M., Marques, S., Rodrigues, L., Lopes, F., Bustelo, X.R., and Simas, J.P. (2008). The Gammaherpesvirus m2 protein manipulates the Fyn/Vav pathway through a multidocking mechanism of assembly. PloS one *3*, e1654.

Plataki, M., Koutsopoulos, A.V., Darivianaki, K., Delides, G., Siafakas, N.M., and Bouros, D. (2005). Expression of apoptotic and antiapoptotic markers in epithelial cells in idiopathic pulmonary fibrosis. Chest *127*, 266-274.

Poynard, T., Yuen, M.F., Ratziu, V., and Lai, C.L. (2003). Viral hepatitis C. Lancet *362*, 2095-2100.

Prota, A.E., Sage, D.R., Stehle, T., and Fingeroth, J.D. (2002). The crystal structure of human CD21: Implications for Epstein-Barr virus and C3d binding. Proceedings of the National Academy of Sciences of the United States of America *99*, 10641-10646.

Renne, R., Lagunoff, M., Zhong, W., and Ganem, D. (1996a). The size and conformation of Kaposi's sarcoma-associated herpesvirus (human herpesvirus 8) DNA in infected cells and virions. Journal of virology *70*, 8151-8154.

Renne, R., Zhong, W., Herndier, B., McGrath, M., Abbey, N., Kedes, D., and Ganem, D. (1996b). Lytic growth of Kaposi's sarcoma-associated herpesvirus (human herpesvirus 8) in culture. Nature medicine *2*, 342-346.

Rickinson, A. (2002). Epstein-Barr virus. Virus research *82*, 109-113.

Roberts, A.B., Russo, A., Felici, A., and Flanders, K.C. (2003). Smad3: a key player in pathogenetic mechanisms dependent on TGF-beta. Annals of the New York Academy of Sciences *995*, 1-10.

Roizman, B., Carmichael, L.E., Deinhardt, F., de-The, G., Nahmias, A.J., Plowright, W., Rapp, F., Sheldrick, P., Takahashi, M., and Wolf, K. (1981). Herpesviridae. Definition, provisional nomenclature, and taxonomy. The Herpesvirus Study Group, the International Committee on Taxonomy of Viruses. Intervirology *16*, 201-217.

Roizman, B., and Pellett, P.E. (2001). The family *Herpesviridae*: a brief introduction. Philadelphia: Lippincott, Williams and Wilkins, 2381-2397.

Rosa, G.T., Gillet, L., Smith, C.M., de Lima, B.D., and Stevenson, P.G. (2007). IgG fc receptors provide an alternative infection route for murine gamma-herpesvirus-68. PloS one *2*, e560.

Rosbottom, J. (2003). The molecular pathogenesis of Ovine Herpesvirus 2 (University of Edinburgh).

Rouyez, M.C., Lestingi, M., Charon, M., Fichelson, S., Buzyn, A., and Dusanter-Fourt, I. (2005). IFN regulatory factor-2 cooperates with STAT1 to regulate transporter associated with antigen processing-1 promoter activity. J Immunol *174*, 3948-3958.

Rowe, D.T., Rowe, M., Evan, G.I., Wallace, L.E., Farrell, P.J., and Rickinson, A.B. (1986). Restricted expression of EBV latent genes and T-lymphocyte-detected membrane antigen in Burkitt's lymphoma cells. The EMBO journal *5*, 2599-2607.

Rowe, M., Kelly, G.L., Bell, A.I., and Rickinson, A.B. (2009). Burkitt's lymphoma: the Rosetta Stone deciphering Epstein-Barr virus biology. Seminars in cancer biology *19*, 377-388.

Rowe, M., Lear, A.L., Croom-Carter, D., Davies, A.H., and Rickinson, A.B. (1992). Three pathways of Epstein-Barr virus gene activation from EBNA1-positive latency in B lymphocytes. Journal of virology *66*, 122-131.

Roy, D.J., Ebrahimi, B.C., Dutia, B.M., Nash, A.A., and Stewart, J.P. (2000). Murine gammaherpesvirus M11 gene product inhibits apoptosis and is expressed during virus persistence. Archives of virology *145*, 2411-2420.

Rubinsztein, D.C., DiFiglia, M., Heintz, N., Nixon, R.A., Qin, Z.H., Ravikumar, B., Stefanis, L., and Tolkovsky, A. (2005). Autophagy and its possible roles in nervous system diseases, damage and repair. Autophagy *1*, 11-22.

Russo, F.P., Alison, M.R., Bigger, B.W., Amofah, E., Florou, A., Amin, F., Bou-Gharios, G., Jeffery, R., Iredale, J.P., and Forbes, S.J. (2006). The bone marrow functionally contributes to liver fibrosis. Gastroenterology *130*, 1807-1821.

Russo, J.J., Bohenzky, R.A., Chien, M.C., Chen, J., Yan, M., Maddalena, D., Parry, J.P., Peruzzi, D., Edelman, I.S., Chang, Y.*, et al.* (1996). Nucleotide sequence of the Kaposi sarcoma-associated herpesvirus (HHV8). Proceedings of the National Academy of Sciences of the United States of America *93*, 14862-14867.

Sakamoto, H., Yasukawa, H., Masuhara, M., Tanimura, S., Sasaki, A., Yuge, K., Ohtsubo, M., Ohtsuka, A., Fujita, T., Ohta, T.*, et al.* (1998). A Janus kinase inhibitor, JAB, is an interferon-gamma-inducible gene and confers resistance to interferons. Blood *92*, 1668-1676.

Samols, M.A., Hu, J., Skalsky, R.L., and Renne, R. (2005). Cloning and identification of a microRNA cluster within the latency-associated region of Kaposi's sarcoma-associated herpesvirus. Journal of virology *79*, 9301-9305.

Samols, M.A., Skalsky, R.L., Maldonado, A.M., Riva, A., Lopez, M.C., Baker, H.V., and Renne, R. (2007). Identification of cellular genes targeted by KSHV-encoded microRNAs. PLoS pathogens *3*, e65.

Sangster, M.Y., Topham, D.J., D'Costa, S., Cardin, R.D., Marion, T.N., Myers, L.K., and Doherty, P.C. (2000). Analysis of the virus-specific and nonspecific B cell response to a persistent B-lymphotropic gammaherpesvirus. J Immunol *164*, 1820-1828.

Sarawar, S.R., Cardin, R.D., Brooks, J.W., Mehrpooya, M., Hamilton-Easton, A.M., Mo, X.Y., and Doherty, P.C. (1997). Gamma interferon is not essential for recovery from acute infection with murine gammaherpesvirus 68. Journal of virology *71*, 3916-3921.

Sarawar, S.R., Cardin, R.D., Brooks, J.W., Mehrpooya, M., Tripp, R.A., and Doherty, P.C. (1996). Cytokine production in the immune response to murine gammaherpesvirus 68. Journal of virology *70*, 3264-3268.

Sarawar, S.R., Lee, B.J., Reiter, S.K., and Schoenberger, S.P. (2001). Stimulation via CD40 can substitute for CD4 T cell function in preventing reactivation of a latent herpesvirus. Proceedings of the National Academy of Sciences of the United States of America *98*, 6325-6329.

Sasmono, R.T., Ehrnsperger, A., Cronau, S.L., Ravasi, T., Kandane, R., Hickey, M.J., Cook, A.D., Himes, S.R., Hamilton, J.A., and Hume, D.A. (2007). Mouse neutrophilic granulocytes express mRNA encoding the macrophage colony-stimulating factor receptor (CSF-1R) as well as many other macrophage-specific transcripts and can transdifferentiate into macrophages in vitro in response to CSF-1. Journal of leukocyte biology *82*, 111-123.

Sasmono, R.T., Oceandy, D., Pollard, J.W., Tong, W., Pavli, P., Wainwright, B.J., Ostrowski, M.C., Himes, S.R., and Hume, D.A. (2003). A macrophage colony-stimulating factor receptor-green fluorescent protein transgene is expressed throughout the mononuclear phagocyte system of the mouse. Blood *101*, 1155-1163.

Schaefer, B.C., Strominger, J.L., and Speck, S.H. (1995). Redefining the Epstein-Barr virus-encoded nuclear antigen EBNA-1 gene promoter and transcription initiation site in group I Burkitt lymphoma cell lines. Proceedings of the National Academy of Sciences of the United States of America *92*, 10565-10569.

Schafer, A., Lengenfelder, D., Grillhosl, C., Wieser, C., Fleckenstein, B., and Ensser, A. (2003). The latency-associated nuclear antigen homolog of herpesvirus saimiri inhibits lytic virus replication. Journal of virology *77*, 5911-5925.

Schoenborn, J.R., and Wilson, C.B. (2007). Regulation of interferon-gamma during innate and adaptive immune responses. Advances in immunology *96*, 41-101.

Schroder, K., Hertzog, P.J., Ravasi, T., and Hume, D.A. (2004). Interferon-gamma: an overview of signals, mechanisms and functions. Journal of leukocyte biology *75*, 163-189.

Schwam, D.R., Luciano, R.L., Mahajan, S.S., Wong, L., and Wilson, A.C. (2000). Carboxy terminus of human herpesvirus 8 latency-associated nuclear antigen mediates dimerization, transcriptional repression, and targeting to nuclear bodies. Journal of virology *74*, 8532-8540.

Schwickert, T.A., Lindquist, R.L., Shakhar, G., Livshits, G., Skokos, D., Kosco-Vilbois, M.H., Dustin, M.L., and Nussenzweig, M.C. (2007). In vivo imaging of germinal centres reveals a dynamic open structure. Nature *446*, 83-87.

Selvarajah, S. (2001). Early events following murine gammaherpesvirus (MHV-68) infection (University of Edinburgh).

Sempowski, G.D., Beckmann, M.P., Derdak, S., and Phipps, R.P. (1994). Subsets of murine lung fibroblasts express membrane-bound and soluble IL-4 receptors. Role of IL-4 in enhancing fibroblast proliferation and collagen synthesis. J Immunol *152*, 3606-3614.

Sen, G.C. (2001). Viruses and interferons. Annual review of microbiology *55*, 255-281.

Shao, D.D., Suresh, R., Vakil, V., Gomer, R.H., and Pilling, D. (2008). Pivotal Advance: Th-1 cytokines inhibit, and Th-2 cytokines promote fibrocyte differentiation. Journal of leukocyte biology *83*, 1323-1333.

Shimokado, K., Raines, E.W., Madtes, D.K., Barrett, T.B., Benditt, E.P., and Ross, R. (1985). A significant part of macrophage-derived growth factor consists of at least two forms of PDGF. Cell *43*, 277-286.

Shire, K., Ceccarelli, D.F., Avolio-Hunter, T.M., and Frappier, L. (1999). EBP2, a human protein that interacts with sequences of the Epstein-Barr virus nuclear antigen 1 important for plasmid maintenance. Journal of virology *73*, 2587-2595.

Shukla, D., Liu, J., Blaiklock, P., Shworak, N.W., Bai, X., Esko, J.D., Cohen, G.H., Eisenberg, R.J., Rosenberg, R.D., and Spear, P.G. (1999). A novel role for 3-O-sulfated heparan sulfate in herpes simplex virus 1 entry. Cell *99*, 13-22.

Shukla, D., and Spear, P.G. (2001). Herpesviruses and heparan sulfate: an intimate relationship in aid of viral entry. The Journal of clinical investigation *108*, 503-510.

Si, H., and Robertson, E.S. (2006). Kaposi's sarcoma-associated herpesvirus-encoded latency-associated nuclear antigen induces chromosomal instability through inhibition of p53 function. Journal of virology *80*, 697-709.

Siegel, A.M., Herskowitz, J.H., and Speck, S.H. (2008). The MHV68 M2 protein drives IL-10 dependent B cell proliferation and differentiation. PLoS pathogens *4*, e1000039.

Siegel, A.M., Rangaswamy, U.S., Napier, R.J., and Speck, S.H. (2010). Blimp-1-dependent plasma cell differentiation is required for efficient maintenance of murine gammaherpesvirus latency and antiviral antibody responses. Journal of virology *84*, 674-685.

Simas, J.P., and Efstathiou, S. (1998). Murine gammaherpesvirus 68: a model for the study of gammaherpesvirus pathogenesis. Trends in microbiology *6*, 276-282.

Simas, J.P., Marques, S., Bridgeman, A., Efstathiou, S., and Adler, H. (2004). The M2 gene product of murine gammaherpesvirus 68 is required for efficient colonization of splenic follicles but is not necessary for expansion of latently infected germinal centre B cells. The Journal of general virology *85*, 2789-2797.

Simas, J.P., Swann, D., Bowden, R., and Efstathiou, S. (1999). Analysis of murine gammaherpesvirus-68 transcription during lytic and latent infection. The Journal of general virology *80 (Pt 1)*, 75-82.

Simpson, G.R., Schulz, T.F., Whitby, D., Cook, P.M., Boshoff, C., Rainbow, L., Howard, M.R., Gao, S.J., Bohenzky, R.A., Simmonds, P.*, et al.* (1996). Prevalence of Kaposi's sarcoma associated herpesvirus infection measured by antibodies to recombinant capsid protein and latent immunofluorescence antigen. Lancet *348*, 1133-1138.

Sinha, S., Colbert, C.L., Becker, N., Wei, Y., and Levine, B. (2008). Molecular basis of the regulation of Beclin 1-dependent autophagy by the gamma-herpesvirus 68 Bcl-2 homolog M11. Autophagy *4*, 989-997.

Sixt, M., Kanazawa, N., Selg, M., Samson, T., Roos, G., Reinhardt, D.P., Pabst, R., Lutz, M.B., and Sorokin, L. (2005). The conduit system transports soluble antigens from the afferent lymph to resident dendritic cells in the T cell area of the lymph node. Immunity *22*, 19-29.

Smith, R.E., Strieter, R.M., Zhang, K., Phan, S.H., Standiford, T.J., Lukacs, N.W., and Kunkel, S.L. (1995). A role for C-C chemokines in fibrotic lung disease. Journal of leukocyte biology *57*, 782-787.

Song, E., Ouyang, N., Horbelt, M., Antus, B., Wang, M., and Exton, M.S. (2000). Influence of alternatively and classically activated macrophages on fibrogenic activities of human fibroblasts. Cellular immunology *204*, 19-28.

Song, M.J., Hwang, S., Wong, W.H., Wu, T.T., Lee, S., Liao, H.I., and Sun, R. (2005). Identification of viral genes essential for replication of murine gamma-herpesvirus 68 using signature-tagged mutagenesis. Proceedings of the National Academy of Sciences of the United States of America *102*, 3805-3810.

Soulier, J., Grollet, L., Oksenhendler, E., Miclea, J.M., Cacoub, P., Baruchel, A., Brice, P., Clauvel, J.P., d'Agay, M.F., Raphael, M.*, et al.* (1995). Molecular analysis of clonality in Castleman's disease. Blood *86*, 1131-1138.

Spear, P.G. (2004). Herpes simplex virus: receptors and ligands for cell entry. Cellular microbiology *6*, 401-410.

Spriggs, M.K., Armitage, R.J., Comeau, M.R., Strockbine, L., Farrah, T., Macduff, B., Ulrich, D., Alderson, M.R., Mullberg, J., and Cohen, J.I. (1996). The extracellular domain of the Epstein-Barr virus BZLF2 protein binds the HLA-DR beta chain and inhibits antigen presentation. Journal of virology *70*, 5557-5563.

Staudt, M.R., Kanan, Y., Jeong, J.H., Papin, J.F., Hines-Boykin, R., and Dittmer, D.P. (2004). The tumor microenvironment controls primary effusion lymphoma growth in vivo. Cancer research *64*, 4790-4799.

Steed, A., Buch, T., Waisman, A., and Virgin, H.W.t. (2007). Gamma interferon blocks gammaherpesvirus reactivation from latency in a cell type-specific manner. Journal of virology *81*, 6134-6140.

Steed, A.L., Barton, E.S., Tibbetts, S.A., Popkin, D.L., Lutzke, M.L., Rochford, R., and Virgin, H.W.t. (2006). Gamma interferon blocks gammaherpesvirus reactivation from latency. Journal of virology *80*, 192-200.

Stevenson, P.G. (2004). Immune evasion by gamma-herpesviruses. Current opinion in immunology *16*, 456-462.

Stevenson, P.G., Belz, G.T., Castrucci, M.R., Altman, J.D., and Doherty, P.C. (1999a). A gamma-herpesvirus sneaks through a CD8(+) T cell response primed to a lytic-phase epitope. Proceedings of the National Academy of Sciences of the United States of America *96*, 9281-9286.

Stevenson, P.G., Boname, J.M., de Lima, B., and Efstathiou, S. (2002a). A battle for survival: immune control and immune evasion in murine gamma-herpesvirus-68 infection. Microbes and infection / Institut Pasteur *4*, 1177-1182.

Stevenson, P.G., Cardin, R.D., Christensen, J.P., and Doherty, P.C. (1999b). Immunological control of a murine gammaherpesvirus independent of CD8+ T cells. The Journal of general virology *80 (Pt 2)*, 477-483.

Stevenson, P.G., and Doherty, P.C. (1998). Kinetic analysis of the specific host response to a murine gammaherpesvirus. Journal of virology *72*, 943-949.

Stevenson, P.G., Efstathiou, S., Doherty, P.C., and Lehner, P.J. (2000). Inhibition of MHC class I-restricted antigen presentation by gamma 2-herpesviruses. Proceedings of the National Academy of Sciences of the United States of America *97*, 8455-8460.

Stevenson, P.G., May, J.S., Smith, X.G., Marques, S., Adler, H., Koszinowski, U.H., Simas, J.P., and Efstathiou, S. (2002b). K3-mediated evasion of CD8(+) T cells aids amplification of a latent gamma-herpesvirus. Nature immunology *3*, 733-740.

Stewart, J.P., Silvia, O.J., Atkin, I.M., Hughes, D.J., Ebrahimi, B., and Adler, H. (2004). In vivo function of a gammaherpesvirus virion glycoprotein: influence on B-cell infection and mononucleosis. Journal of virology *78*, 10449-10459.

Stewart, J.P., Usherwood, E.J., Ross, A., Dyson, H., and Nash, T. (1998). Lung epithelial cells are a major site of murine gammaherpesvirus persistence. The Journal of experimental medicine *187*, 1941-1951.

Stuller, K.A., Cush, S.S., and Flano, E. (2010). Persistent gamma-herpesvirus infection induces a CD4 T cell response containing functionally distinct effector populations. J Immunol *184*, 3850-3856.

Sunil-Chandra, N.P., Efstathiou, S., Arno, J., and Nash, A.A. (1992a). Virological and pathological features of mice infected with murine gamma-herpesvirus 68. The Journal of general virology *73 (Pt 9)*, 2347-2356.

Sunil-Chandra, N.P., Efstathiou, S., and Nash, A.A. (1992b). Murine gammaherpesvirus 68 establishes a latent infection in mouse B lymphocytes in vivo. The Journal of general virology *73 (Pt 12)*, 3275-3279.

Sunil-Chandra, N.P., Efstathiou, S., and Nash, A.A. (1993). Interactions of murine gammaherpesvirus 68 with B and T cell lines. Virology *193*, 825-833.

Sutkowski, N., Conrad, B., Thorley-Lawson, D.A., and Huber, B.T. (2001). Epstein-Barr virus transactivates the human endogenous retrovirus HERV-K18 that encodes a superantigen. Immunity *15*, 579-589.

Svobodova, J., Blaskovic, D., and Mistrikova, J. (1982). Growth characteristics of herpesviruses isolated from free living small rodents. Acta virologica *26*, 256-263.

Swanton, C., Card, G.L., Mann, D., McDonald, N., and Jones, N. (1999). Overcoming inhibitions: subversion of CKI function by viral cyclins. Trends in biochemical sciences *24*, 116-120.

Tam, H.K., Zhang, Z.F., Jacobson, L.P., Margolick, J.B., Chmiel, J.S., Rinaldo, C., and Detels, R. (2002). Effect of highly active antiretroviral therapy on survival among HIV-infected men with Kaposi sarcoma or non-Hodgkin lymphoma. International journal of cancer Journal international du cancer *98*, 916-922.

Tannenbaum, C.S., and Hamilton, T.A. (2000). Immune-inflammatory mechanisms in IFNgamma-mediated anti-tumor activity. Seminars in cancer biology *10*, 113-123.

Tanner, J.E., and Alfieri, C. (2001). The Epstein-Barr virus and post-transplant lymphoproliferative disease: interplay of immunosuppression, EBV, and the immune system in disease pathogenesis. Transplant infectious disease : an official journal of the Transplantation Society *3*, 60-69.

Tau, G., and Rothman, P. (1999). Biologic functions of the IFN-gamma receptors. Allergy *54*, 1233-1251.

Taylor, T.J., Brockman, M.A., McNamee, E.E., and Knipe, D.M. (2002). Herpes simplex virus. Frontiers in bioscience : a journal and virtual library *7*, d752-764.

Telford, E.A., Watson, M.S., Aird, H.C., Perry, J., and Davison, A.J. (1995). The DNA sequence of equine herpesvirus 2. Journal of molecular biology *249*, 520-528.

Tempera, I., and Lieberman, P.M. (2010). Chromatin organization of gammaherpesvirus latent genomes. Biochimica et biophysica acta *1799*, 236-245.

Tibbetts, S.A., McClellan, J.S., Gangappa, S., Speck, S.H., and Virgin, H.W.t. (2003). Effective vaccination against long-term gammaherpesvirus latency. Journal of virology *77*, 2522-2529.

Tibbetts, S.A., van Dyk, L.F., Speck, S.H., and Virgin, H.W.t. (2002). Immune control of the number and reactivation phenotype of cells latently infected with a gammaherpesvirus. Journal of virology *76*, 7125-7132.

Topham, D.J., Cardin, R.C., Christensen, J.P., Brooks, J.W., Belz, G.T., and Doherty, P.C. (2001). Perforin and Fas in murine gammaherpesvirus-specific CD8(+) T cell control and morbidity. The Journal of general virology *82*, 1971-1981.

Townsley, A.C., Dutia, B.M., and Nash, A.A. (2004). The m4 gene of murine gammaherpesvirus modulates productive and latent infection in vivo. Journal of virology *78*, 758-767.

Tripp, R.A., Hamilton-Easton, A.M., Cardin, R.D., Nguyen, P., Behm, F.G., Woodland, D.L., Doherty, P.C., and Blackman, M.A. (1997). Pathogenesis of an infectious mononucleosis-like disease induced by a murine gamma-herpesvirus: role for a viral superantigen? The Journal of experimental medicine *185*, 1641-1650.

Tsai, C.Y., Hu, Z., Zhang, W., and Usherwood, E.J. (2011). Strain-dependent requirement for IFN-gamma for respiratory control and immunotherapy in murine gammaherpesvirus infection. Viral immunology *24*, 273-280.

Tzouvelekis, A., Harokopos, V., Paparountas, T., Oikonomou, N., Chatziioannou, A., Vilaras, G., Tsiambas, E., Karameris, A., Bouros, D., and Aidinis, V. (2007). Comparative expression profiling in pulmonary fibrosis suggests a role of hypoxia-inducible factor-1alpha

in disease pathogenesis. American journal of respiratory and critical care medicine *176*, 1108-1119.

Ueda, T., Ohta, K., Suzuki, N., Yamaguchi, M., Hirai, K., Horiuchi, T., Watanabe, J., Miyamoto, T., and Ito, K. (1992). Idiopathic pulmonary fibrosis and high prevalence of serum antibodies to hepatitis C virus. The American review of respiratory disease *146*, 266-268.

Uhal, B.D., Joshi, I., Hughes, W.F., Ramos, C., Pardo, A., and Selman, M. (1998). Alveolar epithelial cell death adjacent to underlying myofibroblasts in advanced fibrotic human lung. The American journal of physiology *275*, L1192-1199.

Upton, J.W., and Speck, S.H. (2006). Evidence for CDK-dependent and CDK-independent functions of the murine gammaherpesvirus 68 v-cyclin. Journal of virology *80*, 11946-11959.

Usherwood, E.J., Brooks, J.W., Sarawar, S.R., Cardin, R.D., Young, W.D., Allen, D.J., Doherty, P.C., and Nash, A.A. (1997). Immunological control of murine gammaherpesvirus infection is independent of perforin. The Journal of general virology *78 (Pt 8)*, 2025-2030.

Usherwood, E.J., Ross, A.J., Allen, D.J., and Nash, A.A. (1996a). Murine gammaherpesvirus-induced splenomegaly: a critical role for CD4 T cells. The Journal of general virology *77 (Pt 4)*, 627-630.

Usherwood, E.J., Stewart, J.P., and Nash, A.A. (1996b). Characterization of tumor cell lines derived from murine gammaherpesvirus-68-infected mice. Journal of virology *70*, 6516-6518.

Usherwood, E.J., Stewart, J.P., Robertson, K., Allen, D.J., and Nash, A.A. (1996c). Absence of splenic latency in murine gammaherpesvirus 68-infected B cell-deficient mice. The Journal of general virology *77 (Pt 11)*, 2819-2825.

van Berkel, V., Levine, B., Kapadia, S.B., Goldman, J.E., Speck, S.H., and Virgin, H.W.t. (2002). Critical role for a high-affinity chemokine-binding protein in gamma-herpesvirus-induced lethal meningitis. The Journal of clinical investigation *109*, 905-914.

van Berkel, V., Barrett, J., Tiffany, H.L., Fremont, D.H., Murphy, P.M., McFadden, G., Speck, S.H., and Virgin, H.I. (2000). Identification of a gammaherpesvirus selective chemokine binding protein that inhibits chemokine action. Journal of virology *74*, 6741-6747.

van Berkel, V., Preiter, K., Virgin, H.W.t., and Speck, S.H. (1999). Identification and initial characterization of the murine gammaherpesvirus 68 gene M3, encoding an abundantly secreted protein. Journal of virology *73*, 4524-4529.

van den Broek, M.F., Muller, U., Huang, S., Zinkernagel, R.M., and Aguet, M. (1995). Immune defence in mice lacking type I and/or type II interferon receptors. Immunological reviews *148*, 5-18.

van Dyk, L.F., Hess, J.L., Katz, J.D., Jacoby, M., Speck, S.H., and Virgin, H.I. (1999). The murine gammaherpesvirus 68 v-cyclin gene is an oncogene that promotes cell cycle progression in primary lymphocytes. Journal of virology *73*, 5110-5122.

van Dyk, L.F., Virgin, H.W.t., and Speck, S.H. (2003). Maintenance of gammaherpesvirus latency requires viral cyclin in the absence of B lymphocytes. Journal of virology *77*, 5118-5126.

Vannella, K.M., Luckhardt, T.R., Wilke, C.A., van Dyk, L.F., Toews, G.B., and Moore, B.B. (2010). Latent herpesvirus infection augments experimental pulmonary fibrosis. American journal of respiratory and critical care medicine *181*, 465-477.

Vergnon, J.M., Vincent, M., de The, G., Mornex, J.F., Weynants, P., and Brune, J. (1984). Cryptogenic fibrosing alveolitis and Epstein-Barr virus: an association? Lancet *2*, 768-771.

Verma, S.C., Lan, K., and Robertson, E. (2007). Structure and function of latency-associated nuclear antigen. Current topics in microbiology and immunology *312*, 101-136.

Verzijl, D., Fitzsimons, C.P., Van Dijk, M., Stewart, J.P., Timmerman, H., Smit, M.J., and Leurs, R. (2004). Differential activation of murine herpesvirus 68- and Kaposi's sarcoma-associated herpesvirus-encoded ORF74 G protein-coupled receptors by human and murine chemokines. Journal of virology *78*, 3343-3351.

Victora, G.D., Dominguez-Sola, D., Holmes, A.B., Deroubaix, S., Dalla-Favera, R., and Nussenzweig, M.C. (2012). Identification of human germinal center light and dark zone cells and their relationship to human B cell lymphomas. Blood.

Victora, G.D., and Nussenzweig, M.C. (2012). Germinal centers. Annual review of immunology *30*, 429-457.

Vilcek, J., Henriksen-Destefano, D., Siegel, D., Klion, A., Robb, R.J., and Le, J. (1985). Regulation of IFN-gamma induction in human peripheral blood cells by exogenous and endogenously produced interleukin 2. J Immunol *135*, 1851-1856.

Virgin, H.W.t., Latreille, P., Wamsley, P., Hallsworth, K., Weck, K.E., Dal Canto, A.J., and Speck, S.H. (1997). Complete sequence and genomic analysis of murine gammaherpesvirus 68. Journal of virology *71*, 5894-5904.

Wahl, S.M., McCartney-Francis, N., Allen, J.B., Dougherty, E.B., and Dougherty, S.F. (1990). Macrophage production of TGF-beta and regulation by TGF-beta. Annals of the New York Academy of Sciences *593*, 188-196.

Waisberg, D.R., Barbas-Filho, J.V., Parra, E.R., Fernezlian, S., de Carvalho, C.R., Kairalla, R.A., and Capelozzi, V.L. (2010). Abnormal expression of telomerase/apoptosis limits type II alveolar epithelial cell replication in the early remodeling of usual interstitial pneumonia/idiopathic pulmonary fibrosis. Human pathology *41*, 385-391.

Wakeling, M.N., Roy, D.J., Nash, A.A., and Stewart, J.P. (2001). Characterization of the murine gammaherpesvirus 68 ORF74 product: a novel oncogenic G protein-coupled receptor. The Journal of general virology *82*, 1187-1197.

Wallace, K., Burt, A.D., and Wright, M.C. (2008). Liver fibrosis. The Biochemical journal *411*, 1-18.

Wallace, W.A., Ramage, E.A., Lamb, D., and Howie, S.E. (1995). A type 2 (Th2-like) pattern of immune response predominates in the pulmonary interstitium of patients with cryptogenic fibrosing alveolitis (CFA). Clinical and experimental immunology *101*, 436-441.

Wang, F., Rivailler, P., Rao, P., and Cho, Y. (2001). Simian homologues of Epstein-Barr virus. Philosophical transactions of the Royal Society of London Series B, Biological sciences *356*, 489-497.

Wang, F., Tsang, S.F., Kurilla, M.G., Cohen, J.I., and Kieff, E. (1990). Epstein-Barr virus nuclear antigen 2 transactivates latent membrane protein LMP1. Journal of virology *64*, 3407-3416.

Wang, G.H., Garvey, T.L., and Cohen, J.I. (1999). The murine gammaherpesvirus-68 M11 protein inhibits Fas- and TNF-induced apoptosis. The Journal of general virology *80 (Pt 10)*, 2737-2740.

Wang, H.W., Trotter, M.W., Lagos, D., Bourboulia, D., Henderson, S., Makinen, T., Elliman, S., Flanagan, A.M., Alitalo, K., and Boshoff, C. (2004). Kaposi sarcoma herpesvirus-induced cellular reprogramming contributes to the lymphatic endothelial gene expression in Kaposi sarcoma. Nature genetics *36*, 687-693.

Wang, L., Chen, S., and Xu, K. (2011). IL-17 expression is correlated with hepatitis Brelated liver diseases and fibrosis. International journal of molecular medicine *27*, 385-392.

Weck, K.E., Barkon, M.L., Yoo, L.I., Speck, S.H., and Virgin, H.I. (1996). Mature B cells are required for acute splenic infection, but not for establishment of latency, by murine gammaherpesvirus 68. Journal of virology *70*, 6775-6780.

Weck, K.E., Dal Canto, A.J., Gould, J.D., O'Guin, A.K., Roth, K.A., Saffitz, J.E., Speck, S.H., and Virgin, H.W. (1997). Murine gamma-herpesvirus 68 causes severe large-vessel arteritis in mice lacking interferon-gamma responsiveness: a new model for virus-induced vascular disease. Nature medicine *3*, 1346-1353.

Weck, K.E., Kim, S.S., Virgin, H.I., and Speck, S.H. (1999). Macrophages are the major reservoir of latent murine gammaherpesvirus 68 in peritoneal cells. Journal of virology *73*, 3273-3283.

Wedderburn, N., Edwards, J.M., Desgranges, C., Fontaine, C., Cohen, B., and de The, G. (1984). Infectious mononucleosis-like response in common marmosets infected with Epstein-Barr virus. The Journal of infectious diseases *150*, 878-882.

Weinberg, J.B., Lutzke, M.L., Alfinito, R., and Rochford, R. (2004). Mouse strain differences in the chemokine response to acute lung infection with a murine gammaherpesvirus. Viral immunology *17*, 69-77.

Wen, K.W., and Damania, B. (2010). Kaposi sarcoma-associated herpesvirus (KSHV): molecular biology and oncogenesis. Cancer letters *289*, 140-150.

Wen, K.W., Dittmer, D.P., and Damania, B. (2009). Disruption of LANA in rhesus rhadinovirus generates a highly lytic recombinant virus. Journal of virology *83*, 9786-9802.

Wenner, C.A., Guler, M.L., Macatonia, S.E., O'Garra, A., and Murphy, K.M. (1996). Roles of IFN-gamma and IFN-alpha in IL-12-induced T helper cell-1 development. J Immunol *156*, 1442-1447.

Whitley, R.J., and Roizman, B. (2001). Herpes simplex virus infections. Lancet *357*, 1513-1518.

Whitmire, J.K., Eam, B., Benning, N., and Whitton, J.L. (2007). Direct interferon-gamma signaling dramatically enhances CD4+ and CD8+ T cell memory. J Immunol *179*, 1190-1197.

Willer, D.O., and Speck, S.H. (2003). Long-term latent murine Gammaherpesvirus 68 infection is preferentially found within the surface immunoglobulin D-negative subset of splenic B cells in vivo. Journal of virology *77*, 8310-8321.

Willis, B.C., duBois, R.M., and Borok, Z. (2006). Epithelial origin of myofibroblasts during fibrosis in the lung. Proceedings of the American Thoracic Society *3*, 377-382.

Wilson, M.S., Elnekave, E., Mentink-Kane, M.M., Hodges, M.G., Pesce, J.T., Ramalingam, T.R., Thompson, R.W., Kamanaka, M., Flavell, R.A., Keane-Myers, A.*, et al.* (2007). IL-13Ralpha2 and IL-10 coordinately suppress airway inflammation, airway-hyperreactivity, and fibrosis in mice. The Journal of clinical investigation *117*, 2941-2951.

Wilson, M.S., Madala, S.K., Ramalingam, T.R., Gochuico, B.R., Rosas, I.O., Cheever, A.W., and Wynn, T.A. (2010). Bleomycin and IL-1beta-mediated pulmonary fibrosis is IL-17A dependent. The Journal of experimental medicine *207*, 535-552.

Woisetschlaeger, M., Yandava, C.N., Furmanski, L.A., Strominger, J.L., and Speck, S.H. (1990). Promoter switching in Epstein-Barr virus during the initial stages of infection of B lymphocytes. Proceedings of the National Academy of Sciences of the United States of America *87*, 1725-1729.

Wu, H., Ceccarelli, D.F., and Frappier, L. (2000). The DNA segregation mechanism of Epstein-Barr virus nuclear antigen 1. EMBO reports *1*, 140-144.

Wynn, T.A. (2004). Fibrotic disease and the T(H)1/T(H)2 paradigm. Nature reviews *4*, 583-594.

Wynn, T.A. (2008). Cellular and molecular mechanisms of fibrosis. The Journal of pathology *214*, 199-210.

Wynn, T.A., and Barron, L. (2010). Macrophages: master regulators of inflammation and fibrosis. Seminars in liver disease *30*, 245-257.

Wynn, T.A., and Ramalingam, T.R. (2012). Mechanisms of fibrosis: therapeutic translation for fibrotic disease. Nature medicine *18*, 1028-1040.

Xu, X., Fu, X.Y., Plate, J., and Chong, A.S. (1998). IFN-gamma induces cell growth inhibition by Fas-mediated apoptosis: requirement of STAT1 protein for up-regulation of Fas and FasL expression. Cancer research *58*, 2832-2837.

Yao, Z., Maraskovsky, E., Spriggs, M.K., Cohen, J.I., Armitage, R.J., and Alderson, M.R. (1996). Herpesvirus saimiri open reading frame 14, a protein encoded by T lymphotropic herpesvirus, binds to MHC class II molecules and stimulates T cell proliferation. J Immunol *156*, 3260-3266.

Yates, J., Warren, N., Reisman, D., and Sugden, B. (1984). A cis-acting element from the Epstein-Barr viral genome that permits stable replication of recombinant plasmids in latently infected cells. Proceedings of the National Academy of Sciences of the United States of America *81*, 3806-3810.

Yi, E.S., Lee, H., Yin, S., Piguet, P., Sarosi, I., Kaufmann, S., Tarpley, J., Wang, N.S., and Ulich, T.R. (1996). Platelet-derived growth factor causes pulmonary cell proliferation and collagen deposition in vivo. The American journal of pathology *149*, 539-548.

Yin, Y., Manoury, B., and Fahraeus, R. (2003). Self-inhibition of synthesis and antigen presentation by Epstein-Barr virus-encoded EBNA1. Science *301*, 1371-1374.

Yoshiji, H., Kuriyama, S., Yoshii, J., Ikenaka, Y., Noguchi, R., Nakatani, T., Tsujinoue, H., Yanase, K., Namisaki, T., Imazu, H.*, et al.* (2002). Tissue inhibitor of metalloproteinases-1 attenuates spontaneous liver fibrosis resolution in the transgenic mouse. Hepatology *36*, 850-860.

Young, L.S., Dawson, C.W., Clark, D., Rupani, H., Busson, P., Tursz, T., Johnson, A., and Rickinson, A.B. (1988). Epstein-Barr virus gene expression in nasopharyngeal carcinoma. The Journal of general virology *69 (Pt 5)*, 1051-1065.

Yu, Y.Y., Harris, M.R., Lybarger, L., Kimpler, L.A., Myers, N.B., Virgin, H.W.t., and Hansen, T.H. (2002). Physical association of the K3 protein of gamma-2 herpesvirus 68 with major histocompatibility complex class I molecules with impaired peptide and beta(2)-microglobulin assembly. Journal of virology *76*, 2796-2803.

Zeisberg, E.M., Potenta, S., Xie, L., Zeisberg, M., and Kalluri, R. (2007). Discovery of endothelial to mesenchymal transition as a source for carcinoma-associated fibroblasts. Cancer research *67*, 10123-10128.

Zeng, M., Smith, A.J., Wietgrefe, S.W., Southern, P.J., Schacker, T.W., Reilly, C.S., Estes, J.D., Burton, G.F., Silvestri, G., Lifson, J.D.*, et al.* (2011). Cumulative mechanisms of lymphoid tissue fibrosis and T cell depletion in HIV-1 and SIV infections. The Journal of clinical investigation *121*, 998-1008.

Zhou, X., Murphy, F.R., Gehdu, N., Zhang, J., Iredale, J.P., and Benyon, R.C. (2004). Engagement of alphavbeta3 integrin regulates proliferation and apoptosis of hepatic stellate cells. The Journal of biological chemistry *279*, 23996-24006.

Zhu, J.Y., Strehle, M., Frohn, A., Kremmer, E., Hofig, K.P., Meister, G., and Adler, H. (2010). Identification and analysis of expression of novel microRNAs of murine gammaherpesvirus 68. Journal of virology *84*, 10266-10275.

Zurawski, S.M., Vega, F., Jr., Huyghe, B., and Zurawski, G. (1993). Receptors for interleukin-13 and interleukin-4 are complex and share a novel component that functions in signal transduction. The EMBO journal *12*, 2663-2670.

Appendix 1

The components of a PCR reaction:

Component	*Amount per reaction (μl added/50μl reaction)*
Distilled water (dH_2O)	*40.6*
10× cloned Pfu DNA polymerase reaction buffer	*5.0*
dNTPs (2mM each dNTP)	*0.4*
DNA template	*50–200ng per reaction*
Primers (100ng/μl)	*1.0 each*
PfuTurbo DNA polymerase (2.5U/μl)	*1.0*

A PCR reaction was performed as follows:

1. 95°C for 2 minutes

2. 95°C for 30 seconds

3. Anneal temperature (according to primers, normally start with Tm -5°C) for 30 seconds

4. 72°C extension for 1 minute for targets up to 1kb and 1 minute per kb for targets longer than 1kb (30 cycles of step 2 through step 4)

5. 72°C for 10 minutes

Appendix 2

Primers used in qPCR assay

Sense (For) Antisense (Rev)	Sequence	Annealing Temperature (°C)
M1 qPCR -For M1 qPCR -For	5'-CCTTTGCTGGATTCTTATTTGC-3' 5'-CTTGAAACGATAACACTGG-3'	60
Ywhaz-For Ywhaz-Rev	5'-AGACGGAAGGGTGCTGAG-3' 5'-GGTATGCTTGCTGTGACTG-3'	60
DNA Pol qPCR-For DNA Pol qPCR-Rev	5'-AGAGTGTTTGGGTGAATGTGG-3' 5'-GCTTGGAGATGGAGTTGGTG-3'	63
RTA qPCR-For RTA qPCR-Rev	5'-CAAAGTCCATAACAGGCATCC-3' 5'-GCCAGAGGTTGAGGTAGC-3'	60
M11 qPCR-For M11 qPCR-Rev	5'-AACTGGATTGTGTTGATTCTGC-3' 5'-CGGTAAACGCTGTCATAGTGC-3'	62
ORF73-For ORF73-Rev	5'- CGTCTGTCTCTCCTACATCTAAACC-3' 5'- CACCAACACTTCCCTCATCC-3'	62

Appendix 3

FACS analysis of MHV-68 infection in spleen B-cell subsets. Each panel is 1 example representative of a group of 5 mice.

A Day 35 IFN ɣ $R^{-/-}$

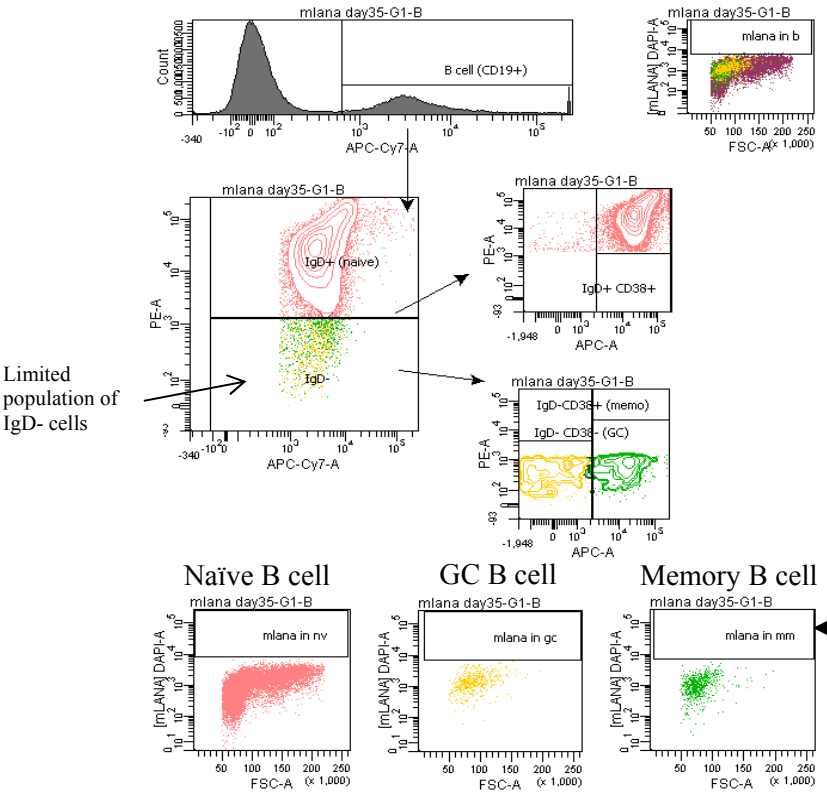

B Day 35 WT

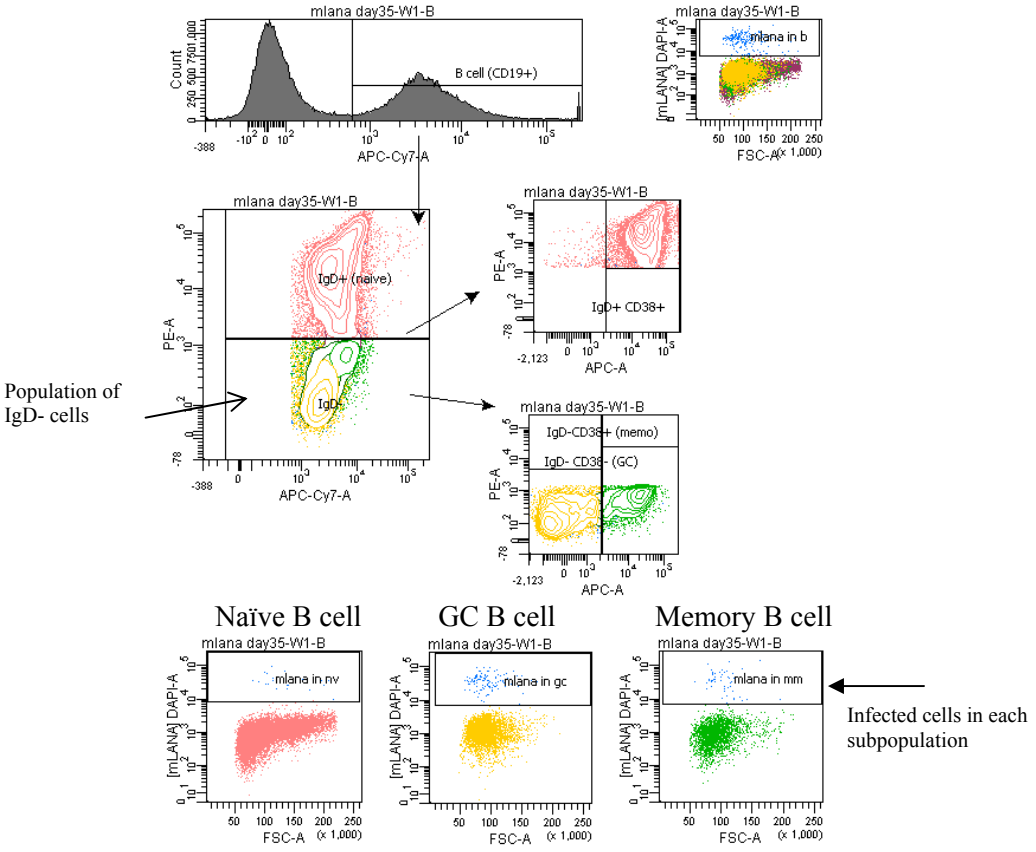

C Uninfected

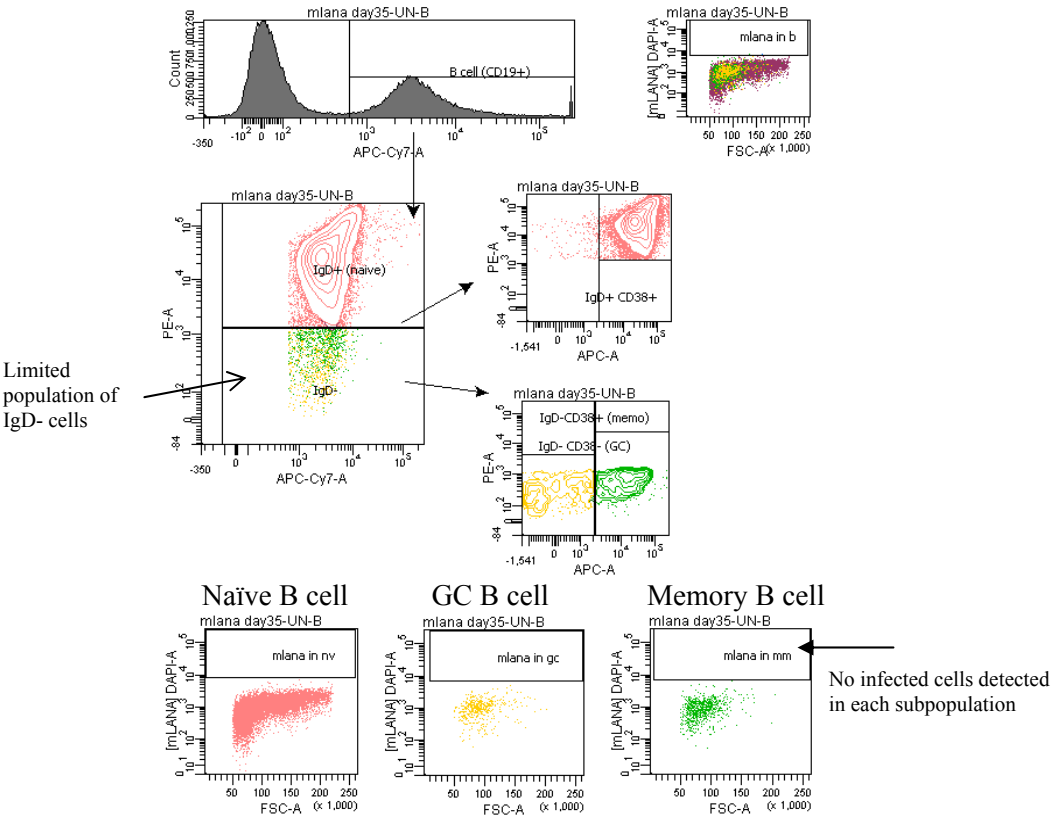

D Day 20 IFN γ $R^{-/-}$